

**Design, Synthesis and Biological Evaluation of Ring-constrained and
Biphenyl Derivatives as Hsp90 C-terminal Inhibitors**

By

Gaurav Garg

Submitted to the graduate degree program in Medicinal Chemistry and the Graduate Faculty of
The University of Kansas in partial fulfillment of the requirements for
the degree of Master of Science.

Committee Members:

Brian S. J. Blagg, Ph.D.
Chairperson

Apurba Dutta, Ph.D.

Paul Hanson, Ph.D.

Date Defended: March 07, 2014

The Thesis Committee for Gaurav Garg
certifies that this is the approved version of the following dissertation:

**Design, Synthesis and Biological Evaluation of Ring-constrained and
Biphenyl Derivatives as Hsp90 C-terminal Inhibitors**

Brian S. J. Blagg, Ph.D.
Chairperson

Date approved:.....

Abstract

Heat shock protein 90 (Hsp90) is an ATP-dependent molecular chaperone that plays a pivotal role in protein homeostasis in responses to cellular stress. Hsp90 regulates the conformational maturation, activation, and integrity of a wide array of client proteins, including oncogenic proteins (Her2, Raf1, Akt, CDK4 etc.) associated with all six hallmarks of cancer. Consequently, Hsp90 inhibition offers a unique opportunity for the simultaneous degradation of multiple anti-cancer targets and hence, for the development of cancer chemotherapeutics.

Hsp90 exists as a homodimer with each monomer consisting of a druggable domain; the N-terminal domain, the middle domain, and the C-terminus. The majority of research has focused on development of Hsp90 N-terminal inhibitors. In fact, all Hsp90 inhibitors in clinical trials belong to this class. One of the major drawbacks associated with N-terminal inhibitors is the concomitant induction of the pro-survival response, which results in an upregulation of Hsp's and affects the dosing schedule. As a result, alternative strategies are sought for the development of future Hsp90 inhibitors.

Over the last decade, Hsp90 C-terminal inhibitors have emerged an attractive alternative for Hsp90 modulation. These inhibitors exhibit similar inhibitory activity to N-terminal inhibitors, but do not induce the pro-survival response and could potentially circumvent the clinical limitations imposed on N-terminal Inhibitors.

Presented herein are the design, synthesis and biological evaluation of ring-constrained novobiocin analogues that provide new insights into the Hsp90 C-terminal binding pocket and SAR's that can be used for future analog development. In addition, identification of a novel class of Hsp90 inhibitors is discussed. These new agents provide a platform upon which future Hsp90 inhibitors can be built upon.

Acknowledgments

During my research work, I have been supported and guided by many people and now it's time to acknowledge their valuable contributions.

First of all, I would like to express my deep sense of gratitude to my advisor, Dr. Brian S. J. Blagg, for believing in my capabilities and providing me an opportunity to nurture my career. I greatly appreciate his suggestions and constructive criticism that helped me throughout my research work here at KU. He is an inspiring source filled with immense ideas and suggestions.

I am also grateful to the other members of the Blagg's group who enlighten me with their suggestions at the time of need. Especially, I would like to thank Dr. Zhao, Dr. Anyika, Dr. Liu, and Sanket for their help in shaping up this thesis.

I will take this opportunity to express my love towards my family for their continuous support and care.

It is privilege to express my gratitude to my committee members Dr. Apurba Dutta and Dr. Paul Hanson for their guidance.

Finally, I would like to thank the Department of Medicinal Chemistry and the funding agencies for providing me resources to complete my research work.

Table of Contents

List of Sections:

Chapter 1

Hsp90 Structure, Function, and Therapeutic Potential

1. Introduction.....	2
2. Hsp90 Structure.....	3
3. Hsp90 Function.....	4
4. Therapeutic Potentials of Hsp90.....	7
A. Therapeutic opportunities.....	7
A.1. Cancer.....	7
A.2. Neurodegenerative diseases.....	9
A.3. Infectious diseases.....	11
B. Hsp90 Inhibitors and their implications.....	12
B.1. N-terminal Inhibitors.....	12
B.1.1. Geldanamycin and Related Analogues.....	12
B.1.2. Radicol and Related Analogues.....	13
B.1.3. Synthetic small molecule inhibitors.....	14
B.2. C-terminal Inhibitors.....	16
B.2.1 Novobiocin and Related Natural Products.....	16
B.2.2 Epigallocatechin-3-Gallate.....	18
B.2.3 Cisplatin.....	19
B.3. Miscellaneous Inhibitors.....	19
5. Conclusion and Future Directions.....	20
6. References.....	22

Chapter 2

Identification of Arylbiphenylamides as Hsp90 Inhibitors

1. Introduction.....	29
2. Design, Synthesis and Evaluation of Ring-constrained Novobiocin Analogues.....	32
3. Conclusion and Future Directions.....	47
4. Experimental Section.....	49
5. References.....	78

Chapter 3

Development of Ring-constrained Novobiocin analogues as Hsp90 Inhibitors

1. Introduction.....	81
2. Design, Synthesis and Biological Evaluation of Arylbiphenylamides.....	83
A. Rationale for design of Arylbiphenylamides.....	84
B. Synthesis and Evaluation of Arylbiphenylamides.....	87
3. Conclusion and Future Directions.....	100
4. Experimental Section.....	101
5. References.....	153

List of Figures:

Chapter 1

Hsp90 Structure, Function, and Therapeutic Potential

Figure 1.1. The Crystal structure of yeast Hsp90; PDB 2CG9.....	3
Figure 1.2. The Hsp90-mediated protein folding mechanism.....	5
Figure 1.3. Proposed mechanism of Hsp90 inhibition for the cancer treatment.....	8
Figure 1.4. Proposed mechanism of Hsp90 modulation for the treatment of neurodegenerative diseases.....	10
Figure 1.5. Structures of geldanamycin and related analogues.....	13
Figure 1.6. Structure of radicicol and related analogues.....	14
Figure 1.7. Structures of purine analogues.....	14
Figure 1.8. Structures of pyrazole and isoxazole derivatives.....	16
Figure 1.9. Novobiocin and other natural inhibitors of Hsp90 C-terminus.....	17
Figure 1.10. Structures of A4, KU32, DHN1 and DHN2.....	18
Figure 1.11. Structures of EGCG, cisplatin, celastrol and gedunin.....	19

Chapter 2

Identification of Arylbiphenylamides as Hsp90 Inhibitors

Figure 2.1. Structures of Novobiocin, A4, DHN1 and DHN2.....	31
Figure 2.2. A1 SAR and structures of KU174, KU135 and KU292.....	32
Figure 3.3. Rationale for proposed ring-constrained novobiocin analogues.....	34
Figure 2.4. Docked structures of KU174 and investigational molecule 9	35
Figure 2.5. Docked structure of compound 17a in the Hsp90 C-terminal binding site.....	42
Figure 2.6. Western blot analyses of lactams.....	47

Chapter 3

Development of Ring-constrained Novobiocin analogues as Hsp90 Inhibitors

Figure 3.1. Structures of DHN1, DHN2, A4 and KU32.....	83
Figure 3.2. Hsp90 C-terminus inhibitors-containing coumarin scaffold.....	84
Figure 3.3. Rationale for proposed arylbiphenylamides analogues.....	86
Figure 3.4. Molecular overlay of arylbiphenylamides to coumarin derivatives in the putative Hsp90 C-terminal binding site.....	87
Figure 3.5. Western blot analyses of biphenyl analogues 8a and 8c	91
Figure 3.6. Western blot analyses of biphenyl analogues 20c , 20j , and 20m	100

List of Schemes:

Chapter 2

Identification of Arylbiphenylamides as Hsp90 Inhibitors

Scheme 2.1. Retrosynthetic analysis of lactamized novobiocin analogue 9	36
Scheme 2.2. Synthesis of pyrrolidine-containing lactam 9	37
Scheme 2.3. Synthesis of aromatic-containing lactams.....	39
Scheme 2.4. Synthesis of amine-containing lactams.....	39
Scheme 2.5. Synthesis of ethylene-containing lactams.....	43
Scheme 2.6. Synthesis of propylene-containing lactams.....	45

Chapter 3

Development of Ring-constrained Novobiocin analogues as Hsp90 Inhibitors

Scheme 3.1. Retrosynthetic analysis of arylbiphenylamides.....	88
Scheme 3.2. Synthesis of biphenyl analogues.....	89
Scheme 3.3. Synthesis of substituted biphenyl analogues.....	93
Scheme 3.4. Synthesis of substituted biphenyl analogue.....	94
Scheme 3.5. Synthesis of substituted biphenyl analogues.....	95
Scheme 3.6. Synthesis of biphenyl analogues with a modified benzamide side chain.....	98

List of Tables:

Chapter 1

Hsp90 Structure, Function, and Therapeutic Potential

Table 1.1. Co-chaperones and Co-activators that comprise the Hsp90 protein folding cycle..6

Table-1.2. Hsp90 client proteins associated with the six hallmarks of cancer.....9

Chapter 2

Identification of Arylbiphenylamides as Hsp90 Inhibitors

Table 2.1. Anti-proliferative activity of pyrrolidine-containing lactam **9**.....38

Table 2.2. Anti-proliferative activity of aromatic- and amine-containing lactams.....40

Table 2.3. Anti-proliferative activity of ethylene-containing lactams.....44

Table 2.4. Anti-proliferative activity of propylene-containing lactams.....46

Chapter 3

Development of Ring-constrained Novobiocin analogues as Hsp90 Inhibitors

Table 3.1. Anti-proliferative activity of novobiocin mimics.....90

Table 3.2. Anti-proliferative activity of substituted biphenyl analogues.....96

Table 3.3. Anti-proliferative activity of biphenyl analogues with a modified benzamide side chain.....99

Abbreviations:

17-AAG = 17-allylamino-17-demethoxygeldanamycin
17-DMAG = 17-dimethylamino-17-demethoxygeldanamycin
ACN = acetonitrile
ADP = adenosine diphosphate
Aha1 = activator of Hsp90 ATPase homologue-1
Akt = serine/threonine protein kinase
ATP = adenosine triphosphate
CDK4 = cyclin-dependent kinase-4
CHIP = carboxy terminus of Hsp70 interacting protein
DCM = dichloromethane
DHN = 4-deshydroxy novobiocin
DIPEA = *N,N*-diisopropylethylamine
DMAP = 4-dimethylaminopyridine
DMF = dimethylformamide
DNA = deoxyribonucleic acid
EGCG = epigallocatechin-3-gallate
EtOAc = ethyl acetate
GDA = geldanamycin
GHKL = Family of ATPases consisting of DNA Gyrase, Hsp90, Histidine Kinase, and Mut L
Grp = glucose regulated protein (endoplasmic reticulum Hsp90 isoform)
Her2 = human epidermal growth factor receptor-2 (erbB2 synonym)
HOP = Hsp70/Hsp90 organizing protein
Hsc70 = Heat shock cognate isoform of Hsp70
HSF1 = Heat shock factor 1 (Hsp transcription factor)
Hsp = Heat shock protein
HTS = highthroughput screen
MCF-7 = Michigan Cancer Foundation – 7 (breast cancer cell line)
MeOH = methanol
NaBH₄ = sodium borohydride
NAH = sodium hydride
NB = novobiocin
p23 = chaperone associated protein 23 kDa
p53 = tumor protein 53
RM = reaction mixture
RT = room temperature
SKBr3 = Sloan-Kettering breast cancer cell line
RAD = radicicol
TFA = trifluoroacetic acid
THF = tetrahydrofuran

**Design, Synthesis and Biological Evaluation of Ring-
constrained and Biphenyl Derivatives as Hsp90
C-terminal Inhibitors**

Chapter 1

Hsp90 Structure, Function and Therapeutic Potential

1. Introduction

The 90 kDa heat shock proteins 90 (Hsp90) are molecular chaperones responsible for the conformational maturation, activation and stability of a wide-range of proteins, referred to as “client proteins”.^{1, 2} More than 200 clients have been identified that depend upon the Hsp90 protein folding machinery to produce active conformations.³ Hsp90 is one of the most abundant proteins in eukaryotic cells and is overexpressed under cellular stress, including elevated temperature, abnormal pH, or nutrient deprivation.⁴ In humans, Hsp90 exists in four isoforms: Hsp90 α (inducible form) and Hsp90 β (constitutive form) are primarily localized in the cytosol, whereas the 94kDa glucose-regulated protein (GRP94) and Hsp75/tumor necrosis factor receptor associated protein 1 (TRAP-1) reside in the endoplasmic reticulum and mitochondria, respectively.⁵

Hsp90 client proteins regulate a wide range of cellular functions, including signal transduction, chromatin remodeling, protein trafficking, cell proliferation and survival.⁶ A large number of these client proteins are often mutated and/or overexpressed in cancer and are actively pursued as individual therapeutic targets for the treatment of cancer.⁷ Therefore, Hsp90 inhibition offers a unique opportunity for the simultaneous degradation of multiple anti-cancer targets and hence, for the development of cancer chemotherapeutics. In addition to its potential for cancer treatment, Hsp90 inhibition has been found to induce a pro-survival response that results in increased level of molecular chaperones.⁸ Molecular chaperones protect cells by redirecting protein aggregation, a major attribute to the etiology of neurodegenerative diseases including Alzheimer’s and Parkinson disease. Consequently, Hsp90 has emerged as a promising therapeutic target for the development of several diseases.

2. Hsp90 Structure

The Hsp90 molecular chaperone belongs to the GHKL (Gyrase, Hsp90, Histidine Kinase and MutL) superfamily and shares structural homology with other ATPase members.⁹ Like other members, eukaryotic Hsp90 exists as a homodimer with each monomer consisting of three highly conserved domains: A 25 kDa N-terminal ATP-binding domain (NTD), a 35 kDa middle domain (MD), and a 12 kDa C-terminal dimerization domain (CTD) (Figure 1.1).⁴

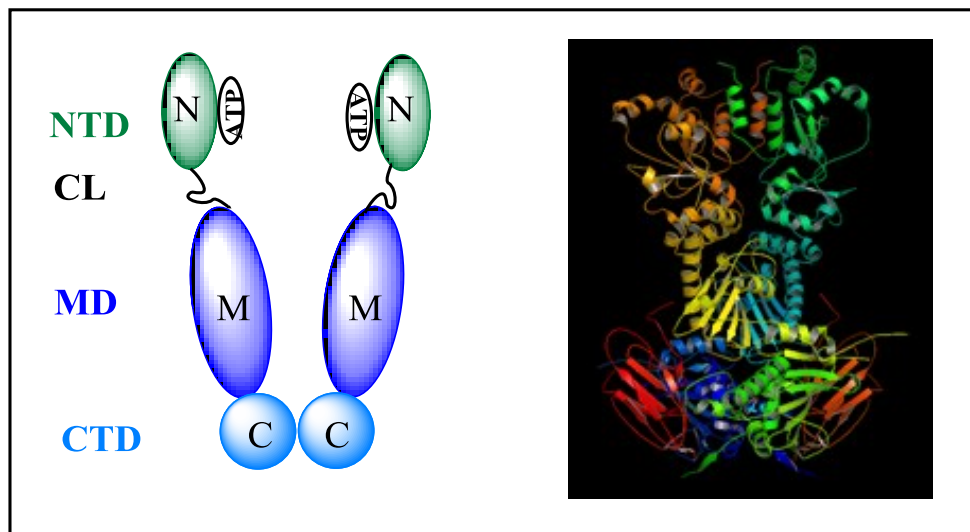


Figure 1.1. The Crystal structure of yeast Hsp90; PDB 2CG9.

The NTD contains an ATP-binding site wherein ATP binds in a unique, bent conformation, a characteristic feature shared by members of GHKL superfamily.⁹ Co-crystal structures of this domain revealed that the ATP-binding motif comprises four-interstranded β -sheets and three α -helices with an ATP-binding pocket located in the middle.¹⁰⁻¹² The NTD is responsible for Hsp90 ATPase activity and represents a major binding site for the development of Hsp90 inhibitors.

The MD of Hsp90 is connected to the NTD by a flexible, highly charged linker (CL). This domain plays a key role in modulating Hsp90 ATPase activity by binding to the γ -phosphate of ATP when bound to the N-terminus.¹³ Structural and functional analyses

suggest that it is a major site for recognition and binding of several client proteins and co-chaperones (e.g. Aha1).¹⁴

The CTD is responsible for Hsp90 homodimerization.¹⁰ This domain comprises of a dimer consisting of a mixed α/β domain and features a conserved MEEVD sequence that recognizes TPR (tetratricopeptide-containing repeats) domains that bind with co-chaperones, such as Hsp70-Hsp90 organizing protein (HOP), immunophilins etc. The CTD also contains a second ATP-binding site that modulates N-terminal ATPase activity in an allosteric manner.^{15, 16} Natural products such as novobiocin and EGCG have been found to bind this site and disrupt Hsp90 function.¹⁷⁻¹⁹

3. Hsp90 Function

Hsp90 is a versatile protein that is responsible for the maintenance of protein homeostasis as well as the stress response.²⁰ Hsp90 comprises about 1-2% of total protein present in the cytoplasm of unstressed cells and can become significantly overexpressed (4-6%) under hostile conditions to buffer proteotoxic stresses.²¹ Hsp90 performs a wide range of cellular functions, including conformational maturation of the nascent polypeptides, solubilizing and refolding of aggregated or denatured proteins, protein disposition and degradation.²²

Although the mechanism of the Hsp90-mediated protein folding cycle remains elusive, accumulating evidence suggests that a multi-protein complex containing a variety of co-chaperones, immunophilins and partner proteins, is involved in the folding process.²³ During the chaperone cycle, a nascent polypeptide is relayed through various multiprotein complexes before gaining conformational maturity (Figure 1.2).

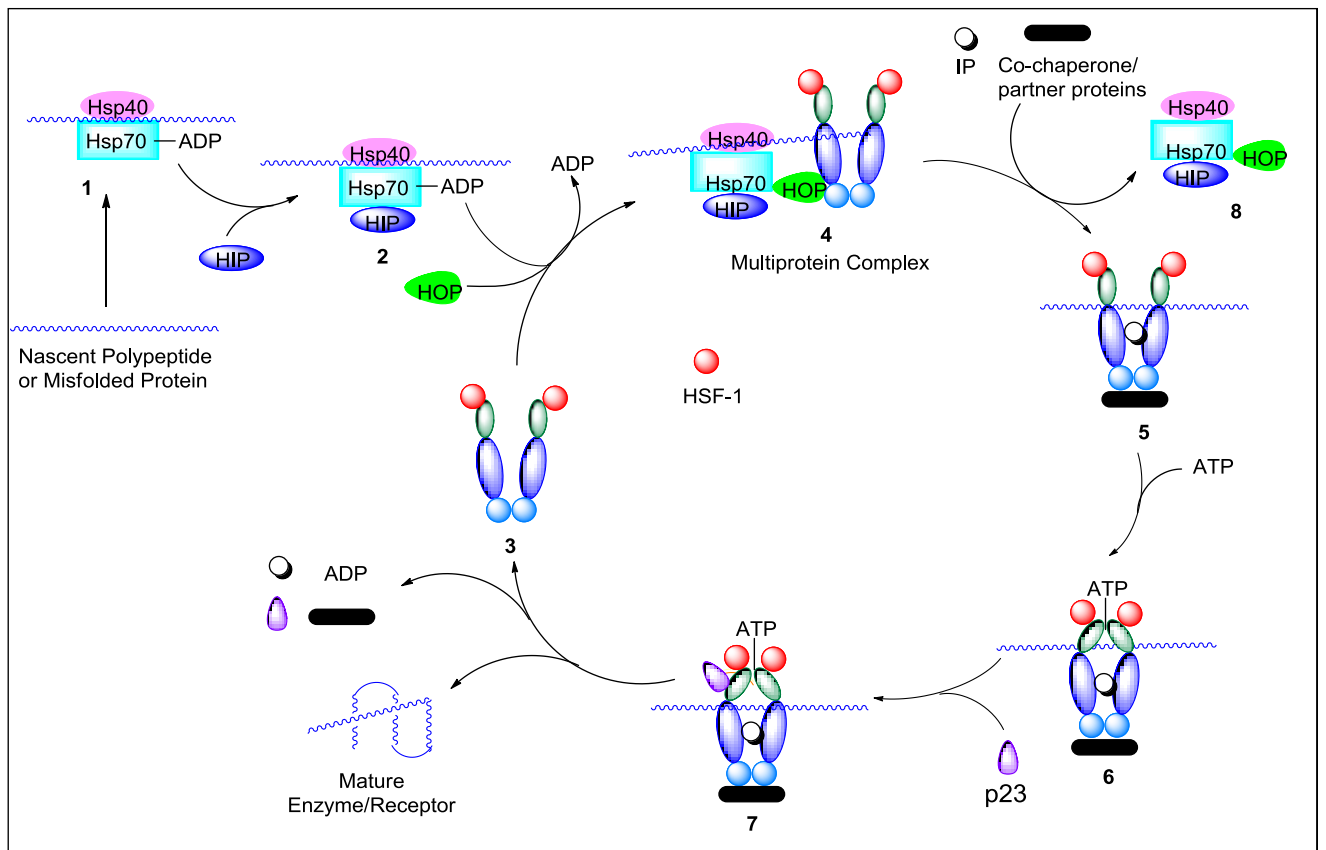


Figure 1.2. The Hsp90-mediated protein folding mechanism.

Proteins are synthesized as linear polypeptides by the ribosome. As nascent polypeptides exit the ribosome, they have the propensity to aggregate via hydrophobic interactions between amino acid side chains. Molecular chaperones stabilize these polypeptides from aggregation and facilitate their folding into biologically active structures.²⁴ The chaperone cycle begins by binding nascent polypeptides with the molecular chaperone, Hsp70, in conjunction with Hsp40 and ATP. Bound ATP is then hydrolyzed to ADP, which prevents the aggregation of polypeptides.²⁵ Hsp70 interacting protein (HIP) then binds to and stabilizes this complex. Alternatively, Bcl2 associated athanogene (BAG) homologs can bind to this complex and exchange ATP for ADP, resulting in polypeptide release and dissociation of the complex.²⁶ Hsp90-Hsp70 organizing protein (HOP), which contains a TPR domain recognized by both Hsp90 and Hsp70, coordinates association of the Hsp70-protein complex and Hsp90, transferring the unfolded protein from Hsp70 to the Hsp90.²⁷ Subsequently,

immunophilins (FKBP51, FKBP52), co-chaperones and partner proteins bind the Hsp90 homodimer to form an activated multiprotein complex with concomitant release of Hsp70, Hip and HOP.²⁸ ATP binds the Hsp90 multiprotein complex at the N-terminus and promotes the clamping of Hsp90 around the bound client protein, resulting in a closed clamp conformation.²⁹ At this stage, Hsp90 inhibitors can compete with ATP at the N-terminal binding site and prevent formation of the closed clamp conformation, leading to the degradation of the client through the ubiquitin-proteasome pathway.⁴ In the absence of inhibition, the co-chaperone p23 is recruited to the complex and assists in the folding of client proteins into biologically active structures through an ATP-driven process.³⁰ Finally, the mature protein is released from the complex along with the dissociation of immunophilins and co-chaperones from Hsp90.

The folding process is regulated by a number of co-chaperones and post-translational modifications.³ Many co-chaperones and co-activators work in conjunction with Hsp90 by modulating the protein folding machinery (Table 1.1).^{6, 23} Numerous post-translational modifications including acetylation, phosphorylation, and S-nitrosylation control Hsp90 chaperone activity by modulating its affinity for co-chaperones or client proteins.³

Table 1.1. Co-chaperones and Co-activators that comprise the Hsp90 protein folding cycle.^{6, 23}

Co-chaperone or Co-activator	Description
Aha1	Stimulates ATPase activity
Cdc37	Mediates activation of protein kinase substrates
CHIP	Involved in degradation of unfolded client proteins
Cyclophilin-40	Peptidyl propyl isomerase
FKBP51 and 52	Peptidyl propyl isomerase
Hop	Mediates interaction between Hsp90 and Hsp70
Hsp40	Stabilizes and delivers client proteins to Hsp90 complex
Hsp70	Stabilizes and delivers client proteins to Hsp90 complex

p23	Stabilizes closed, clamped substrate bound conformation
HIP	Inhibits ATPase activity of Hsp70
PP5	Protein phosphatase 5
Sgt1	Client adaptor, involved in client recruitment
Tom70	Facilitates translocation of pre-proteins into mitochondrial matrix
WISp39	Regulates p21 stability

4. Therapeutic Potentials of Hsp90

A. Therapeutic opportunities

Hsp90 plays an integral role in the stability and function of a wide range of client proteins including signaling kinases, steroid hormones receptors, and telomerase.³¹ A large number of these client proteins contribute to the development, maintenance and progression of human diseases including cancer, neurodegenerative diseases, and infections.³² In cancer, malignant cells depend upon the Hsp90 chaperone machinery for the folding of mutated and over-activated oncoproteins. As a result, inhibition of Hsp90 by a small molecule provides an excellent opportunity for the treatment of cancer.³³ In contrast to its role in oncoprotein degradation, Hsp90 inhibition can also induce the pro-survival heat shock response, which in turn, causes the upregulation of heat shock proteins (Hsps). Although detrimental for cancer treatment, upregulation of Hsps could be beneficial for neurodegenerative diseases, where Hsps protects cells from the accumulation of neurotoxic proteins.³⁴ As a consequence, non-toxic molecules manifesting such activities could be potential candidates for the treatment of neurodegenerative disorders.

A.1. Cancer

Cancer is a group of diseases involving uncontrolled cell growth and is one of the leading causes of disease-related deaths worldwide. Cancer results from the de-regulation of signaling pathways essential for cell proliferation and survival.² Conventional therapeutic

strategies have focused on the inhibition of a specific enzyme and/or receptor associated with signaling pathways, but often become ineffective due to the development of resistance. As our understanding of cancer physiology advances, it has become apparent that malignant transformations result from multiple interconnected dysregulated pathways. Consequently, combinatorial therapy has evolved as a new paradigm for cancer treatment. As an alternative approach, Hsp90 inhibition has shown potential to simultaneously disrupt multiple signaling pathways through a single target.³⁵ Figure 1.3 represents the proposed mechanism of Hsp90 inhibition for cancer treatment. Hsp90 inhibitors bind to the Hsp90 multiprotein complex and halt the protein folding process. Consequently, the complex is directed to the ubiquitin-proteasome pathway, which leads to the degradation of client proteins.

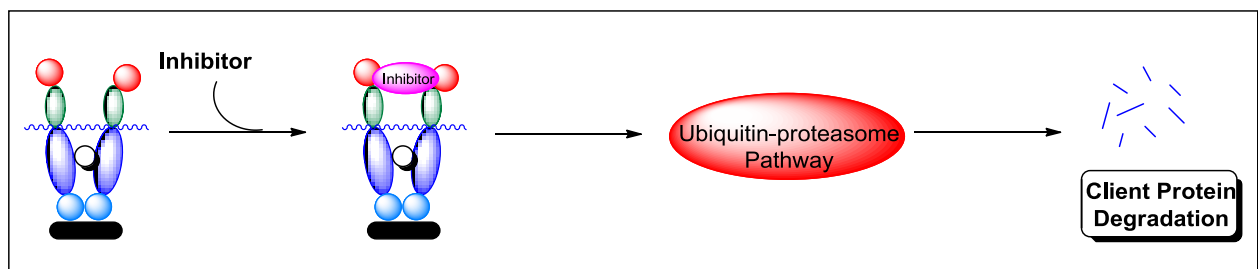


Figure 1.3. Proposed mechanism of Hsp90 inhibition for the cancer treatment.

Clientele of Hsp90 include several oncogenic proteins such as Her2, Raf1, Akt, and CDK4, which are distributed among all the six hallmarks of cancer (Table-1.2).^{5, 33} Hsp90 client proteins protect cancer cells through regulation of various oncogenic cellular processes including signal transduction, anti-apoptosis, proliferation, angiogenesis and metastasis.³⁵

Table-1.2. Hsp90 client proteins associated with the six hallmarks of cancer.⁵

Hallmarks of Cancer	Hsp90 Client Protein(s)
1. Self-sufficiency in growth signals	Raf-1, AKT, Her2, MEK, Bcr-Abl
2. Insensitivity to anti-growth signals	Plk, Wee1, Myc1, CDK4, CDK6, Myt1
3. Evasion of apoptosis	RIP, AKT, p53, c-MET, Apaf-1, Survivin
4. Limitless replicative potential	Telomerase (h-Tert)
5. Sustained angiogenesis	FAK, AKT, Hif-1 α , VEGFR, flt-3
6. Tissue invasion and Metastasis	C-MET

Since Hsp90 is abundantly expressed in both normal and cancer cells, there has been some apprehension about the therapeutic selectivity manifested by Hsp90 inhibitors. However, growing evidence suggests that Hsp90 inhibitors show significant differential selectivity towards cancer cells compared to normal cells and can therefore exhibit a large therapeutic window.³⁶⁻³⁹ Hsp90 inhibitors have been found to accumulate to a greater extent in tumors than in normal tissues.³⁶ Kamal and co-workers demonstrated that the increased concentration of Hsp90 inhibitors in tumor cells originates from the altered conformation of Hsp90 in cancer vs normal cells.³⁷ In cancer cells, Hsp90 exists in an activated multiprotein complex with enhanced ATPase activity and higher affinity for Hsp90 inhibitors, compared to latent complex found in normal cells. As a proof-of-concept for Hsp90 inhibition with therapeutic benefit, first Hsp90 inhibitor 17-AAG has shown encouraging results in phase I and II studies with HER2+ breast cancer patients.^{40, 41} Consequently, Hsp90 has become a promising target for the development of cancer chemotherapeutics.

A.2. Neurodegenerative diseases

Neurodegenerative diseases, including Alzheimer's disease (AD), Parkinson disease (PD), Huntington disease (HD), Polyglutamine disease (PGD) and Prion disease, are chronic and progressive diseases that arise from dysfunction or loss of neurons in the central nervous

system.^{34, 42} Although, there could be multiple causes for the development of neurodegenerative diseases, the most common characteristic shared is accumulation of misfolded/aberrant proteins, which eventually leads to neuronal toxicity.⁴³ Therefore, the prevention of neurotoxic aggregates represents a therapeutic strategy for the treatment of neurodegenerative diseases. It has been observed that inhibition of Hsp90 results in the release of a transcription factor, heat shock factor-1 (HSF-1).⁸ Upon release, HSF-1 is trimerized, phosphorylated and translocated to nucleus, wherein it causes overexpression of molecular chaperones, including Hsp27, Hsp40, Hsp70 and Hsp90 (Figure 1.4).⁴⁴ These molecular chaperones provide neuroprotection by preventing protein aggregation, solubilizing aggregated proteins, and promoting the clearance of the misfolded and aggregated proteins that are difficult to degrade through other mechanisms.^{26, 45}

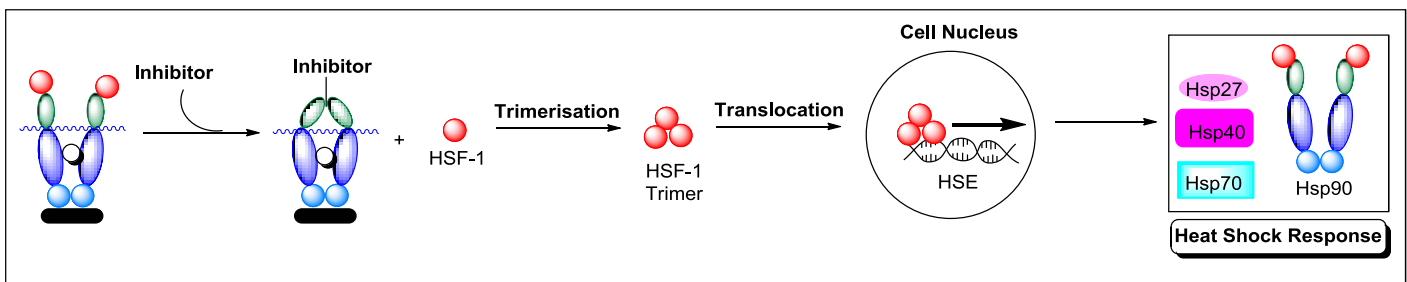


Figure 1.4. Proposed mechanism of Hsp90 modulation for the treatment of neurodegenerative diseases.

In addition to its indirect role via induction of the pro-survival response, Hsp90 inhibition causes degradation of many aberrant proteins, including TauP301L and α -synuclein that form neurotoxic aggregates.^{46, 47} This approach is important in the treatment of neurodegenerative diseases, such as AD and PD, where aberrant protein is responsible for progression and the maintenance of the diseased condition.

AD is a protein misfolding disease (proteopathy), caused by formation of β -amyloid ($A\beta$) plaques and neurofibrillary tangles in the brain.⁴⁷ In AD, hyperphosphorylation of the

Tau protein results in aggregation of filamentous structures that lead to neurofibrillary tangles.⁴⁸ A study conducted by Chiosis and co-workers revealed that Hsp90 client proteins, including cyclin-dependent protein kinase 5 (Cdk5) and glycogen synthase kinase-3 β (GSK3 β) are dysregulated in AD and cause hyperphosphorylation of the *Tau* protein, leading to neuronal death.⁴⁶ Furthermore, the study showed that suppression of Hsp90 client proteins p35 (activator of Cdk5) and TauP301L (most common mutant in AD) led to reduction in neuronal loss and functional improvement. Another Hsp90 client protein α -synuclein has been found to be associated with the pathogenesis of PD and its suppression by the Hsp90 inhibitor, GDA, was shown to alleviate PD-like symptoms in a transgenic mouse model.⁴⁹ Collectively, these findings highlight the role of Hsp90 in the pathogenesis of neurodegenerative diseases. Consequently, Hsp90 inhibitors are emerging as chemotherapeutics for the treatment of neurodegenerative diseases as they offer dual therapeutic advantages by inhibiting the maturation of client proteins implicated in disease and by induction of the protective heat shock response.

A.3. Infectious diseases

Hsp90 plays a central role in the pathogenesis of many infectious diseases such as viral replication, bacterial, and fungal infection.^{32, 50} Hsp90 folds clients that are essential for the replication of many viruses including hepatitis B, hepatitis C, polio, herpes simplex and influenza viruses.²⁰ So, inhibition of Hsp90 can provide an alternative strategy for the treatment of viral diseases. Similar to viral infection, Hsp90 client proteins have been directly linked with virulence of various fungal pathogens including *Candida albicans*, *Aspergillus fumigatus* and *teereus* and hence could be targeted for development of antifungal agents.⁵¹ Recently, Novartis developed a recombinant antibody Mycograb that binds Hsp90 and sensitizes fungal pathogens to antifungal agents.⁵²

B. Hsp90 Inhibitors and their implications

Hsp90 inhibitors represent a unique class of therapeutic agents for the treatment of a variety of human diseases through a single target. Small molecules belonging to a wide range of chemical classes have been identified, that disrupt Hsp90 chaperone activity via various mechanisms. Hsp90 chaperone function can be inhibited by small molecules that either compete with ATP for the binding pocket or interfere with the C-terminal or middle region of Hsp90.⁵³ Hsp90 inhibitors can be broadly divided into three main categories; (1) N-terminal inhibitors, (2) C-terminal inhibitors, or (3) other inhibitors, which will be discussed in detail below.

B.1. N-terminal Inhibitors

B.1.1. Geldanamycin and Related Analogues

Geldanamycin (GDA), a naturally occurring ansamycin, was originally isolated in cell culture screening for antimicrobial agents from the broth of *Streptomyces hygroscopicus* in 1970s.⁵⁴ Later, GDA was shown to manifest anti-proliferative activity against v-Src oncogene transformed cells.⁵⁵ Further studies by Whitesell and Neckers revealed that GDA exerted its activity through inhibition of Hsp90.⁵⁶ Finally, crystal structure analysis of the human and yeast Hsp90 N-terminus established that GDA competes with ATP for binding pocket to the N-terminus of Hsp90, resulting in the disruption of the chaperone cycle and degradation of client proteins.^{11, 12} Since the discovery of GDA as an Hsp90 inhibitor, it has been used a standard probe for the identification of additional Hsp90 client proteins and to explore the role of Hsp90 in malignant transformations. Although GDA showed promising antitumor activities against various cell lines, its clinical utility was limited by poor solubility, poor *in vivo* stability, and high hepatotoxicity.³⁸ Subsequent structure-activity relationship studies resulted in the identification of 17-(allylamino)-17-demethoxygeldanamycin (17-AAG) and 17-(2-dimethylaminoethylamino)-17-desmethoxygeldanamycin (17-DMAG), which

demonstrated an improved toxicity profile and are currently under investigation in clinical trials.^{57, 58}

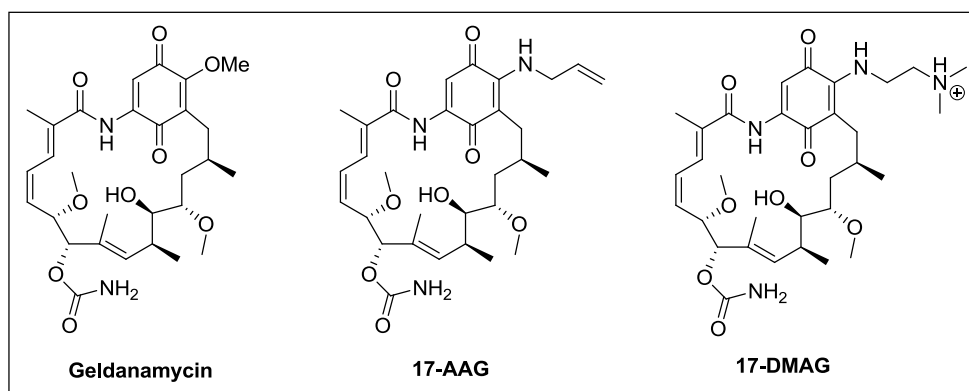


Figure 1.5. Structures of geldanamycin and related analogues.

B.1.2. Radicol and Related Analogues

Radicol (RDC), a natural resorcylic lactone, was originally isolated from *Monosporium bonorden* in 1953 as an antifungal agent.⁵⁹ Like GDA, RDC was found to be a competitive inhibitor of the Hsp90 N-terminus ($K_d = 14\text{nM}$).^{60, 61} Although RDC exhibits promising *in vitro* affinity, it is inactive *in vivo*, likely due to the presence of an electrophilic $\alpha,\beta,\gamma,\delta$ -unsaturated ketone and an epoxide, which make it prone to rapid metabolism.⁶² Therefore, SAR studies have focused on the identification of analogues with better *in vivo* stability profile. Various oxime derivatives of RDC have been reported that manifest potent inhibitory activity both in whole cell assays and human tumor xenograft models.⁶³ Furthermore, it was observed that the labile allylic epoxide could be replaced with a cyclopropyl ring (cycloproparadicol, c-RDC) without compromising inhibitory activity.⁶⁴ Currently, this class of compounds has been the subject of extensive research for the development of potent Hsp90 inhibitors.⁶⁵

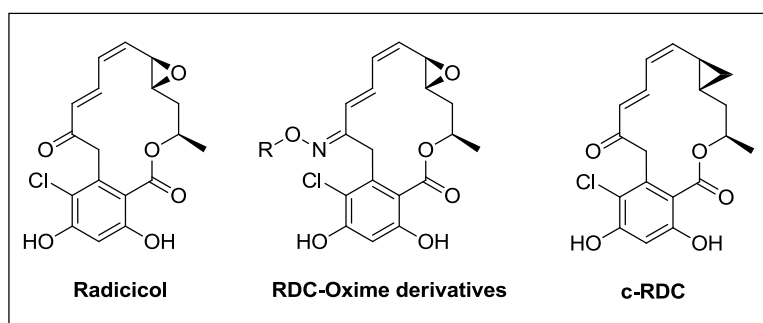


Figure 1.6. Structure of radicol and related analogues.

B.1.3. Synthetic small molecule inhibitors

Limited synthetic accessibility and potential toxicity of natural products and their derivatives promoted a search for small molecule inhibitors of Hsp90 that exhibit improved drug-like features. Chiosis and co-workers used X-ray crystallographic analysis and molecular modeling to identify PU3, a purine analog, which showed low micromolar affinity ($K_d = 15\text{--}20\ \mu\text{M}$) for the N-terminus of Hsp90 and moderate anti-proliferative activity ($IC_{50} = 50$) against the MCF-7 breast cancer cell line.⁶⁶ Further improvement of this class led to identification of PU24FC1, which manifested better antitumor activities both in *in vitro* and *in vivo* models of cancer.⁶⁷ Finally, an optimized purine-based molecule BIIB021 was identified in 2005 and is currently under investigation for the treatment of advanced solid tumors.⁶⁸

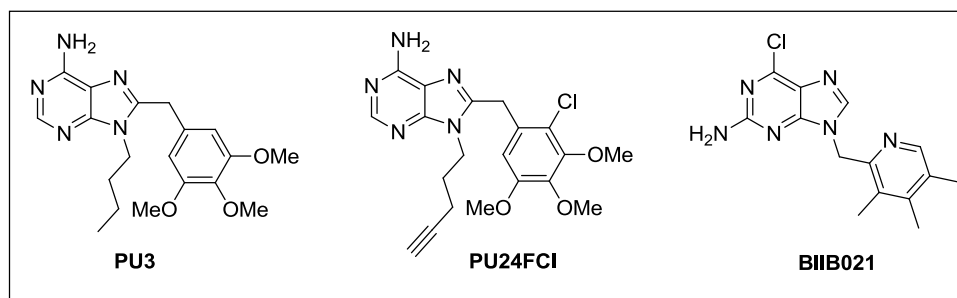


Figure 1.7. Structures of purine analogues.

In 2004, high throughput screening (HTS) of a library of 60,000 compounds led to identification of 3,4-diarylpyrazole CCT018159, which showed potent ATPase inhibition activity against yeast Hsp90 ($IC_{50} = 7.1 \mu M$).⁶⁹ Later, protein crystallographic studies revealed that CCT018159 binds deep into the ATP pocket of the Hsp90 N-terminal domain and that the resorcinol groups and pyrazole nitrogen form water-mediated hydrogen bonding interactions.⁷⁰ In another HTS, the Novartis Research Foundation screened a library of 1,000,000 compounds and identified two lead compounds G3129 and G3130. Co-crystal structures of G3129 and G3130 bound to Hsp90 suggested that both compounds bind the N-terminus of human Hsp90 α and the resorcinol ring bind Hsp90 α similar to that of RDC.⁷¹ Building on this information, Dymock and co-workers identified a highly potent analog of CCT018159, VER49009 (ATPase $IC_{50} = 0.14 \mu M$), which contains an amide group that formed an additional interaction with Gly97 of the Hsp90 N-domain.⁷² Subsequent structural optimization involved replacement of the pyrazole with an isoxazole and produced VER50589, which exhibits higher affinity and good cellular uptake ($K_d = 4.5 \text{ nM}$).^{73, 74} Finally, an optimized isoxazole analog, VER52296/NVP-AUY922, entered clinical trials in 2008 and is currently being investigated in phase I/II for the treatment of solid malignancies.^{75, 76}

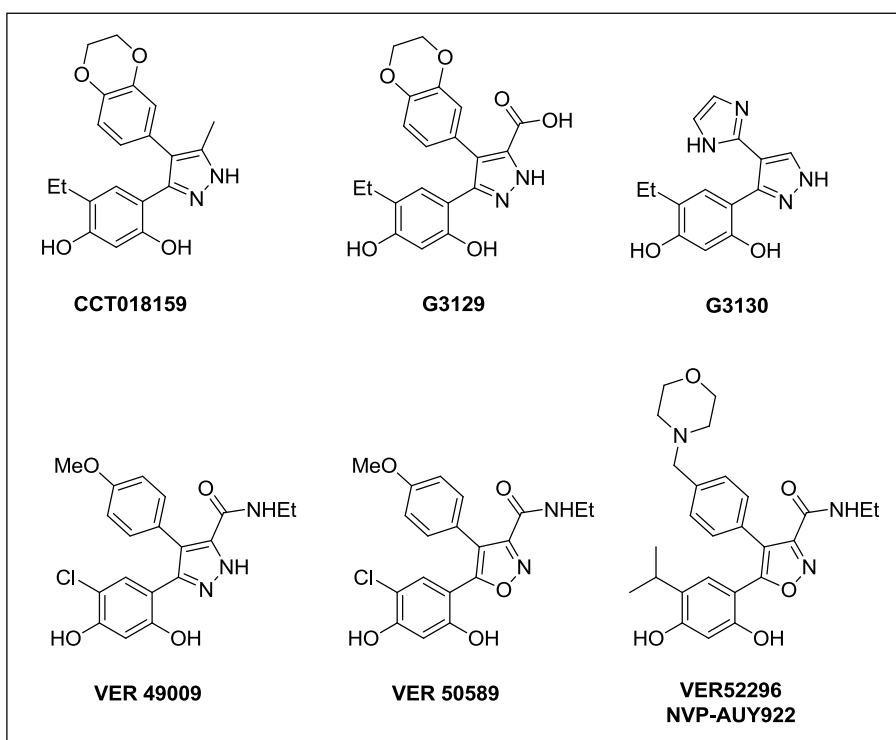


Figure 1.8. Structures of pyrazole and isoxazole derivatives.

B.2. C-terminal Inhibitors

B.2.1. Novobiocin and Related Natural Products

The coumarin antibiotics including Novobiocin (NB), chlorobiocin and coumermycin A1, are potent inhibitors of DNA gyrase and have been used extensively for the treatment of infections caused by multi-resistant gram-positive bacteria.⁷⁷ In 2000, Neckers and co-workers reported that NB bound weakly to a previously unrecognized Hsp90 C-terminal nucleotide binding site ($IC_{50} = 700 \mu\text{M}$ in SKBr3 cells) and caused the degradation of Hsp90 client proteins including v-src, Raf-1 and Erb2.^{17, 78} Interestingly, NB did not induce a pro-survival heat shock response, which is a major drawback associated with N-terminal inhibition.

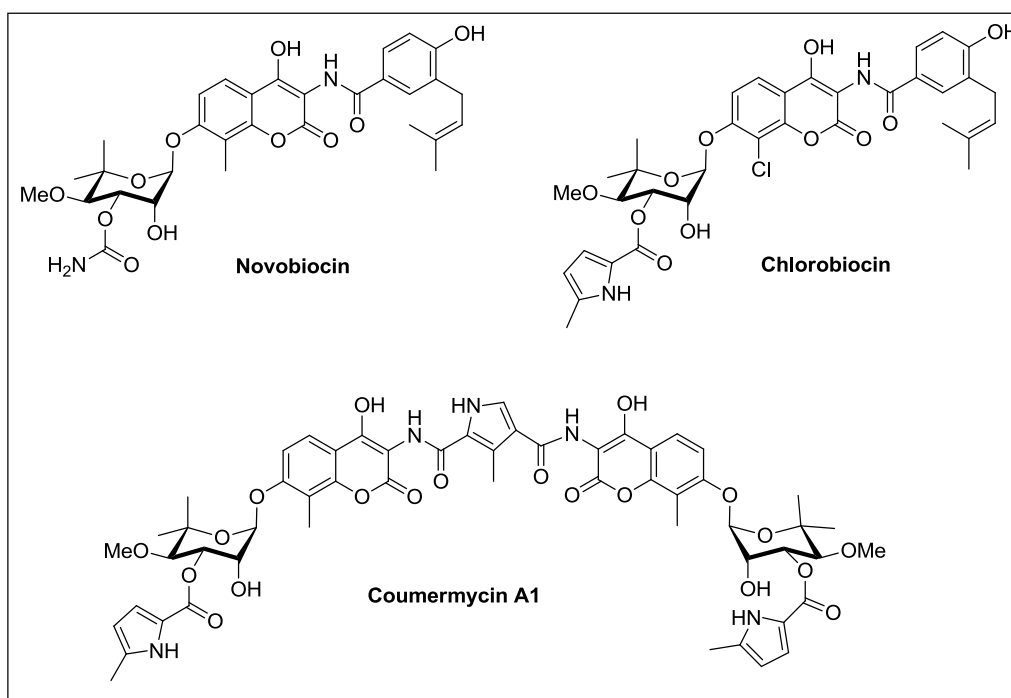


Figure 1.9. Novobiocin and other natural inhibitors of Hsp90 C-terminus.

Encouraged by the initial findings, attempts were made to improve the inhibitory activity of NB. Initial SAR studies done by Blagg and co-workers revealed key structural features of NB required for the observed activities.⁷⁹ Compound A4, lacking both the 4-hydroxy substituent and the carbamoyl group, and containing an N-acyl side chain was found to induce Hsp90 client protein degradation at ~70 fold lower concentrations than NB ($IC_{50} = 10 \mu\text{M}$). Surprisingly, compound A4 also induced Hsp90 levels at much lower concentrations (1000-1000 fold) than that required for client protein degradation and showed the potential of being a neuroprotective agent. KU32, a variant of compound A4 is currently under investigation for the treatment of neurodegenerative diseases.⁸⁰ Further studies highlighted the role of the benzamide side chain in the paradoxical activities observed with Hsp90 C-terminal inhibitors.⁸¹ Incorporation of a benzamide side chain was shown to restore the anti-proliferative activity without induction of the heat shock response and subsequently resulted in identification of two potent compounds, DHN1 and DHN2. The improved activities manifested by both compounds reiterated the detrimental effect of 4-hydroxy substituent and

carbamoyl group for Hsp90 inhibition and marked the first selective Hsp90 C-terminal inhibitors. Further SAR studies on this class of compounds resulted in highly potent compounds with mid nanomolar activities in anti-proliferative assays against various cancer cell lines.⁸²⁻⁸⁴

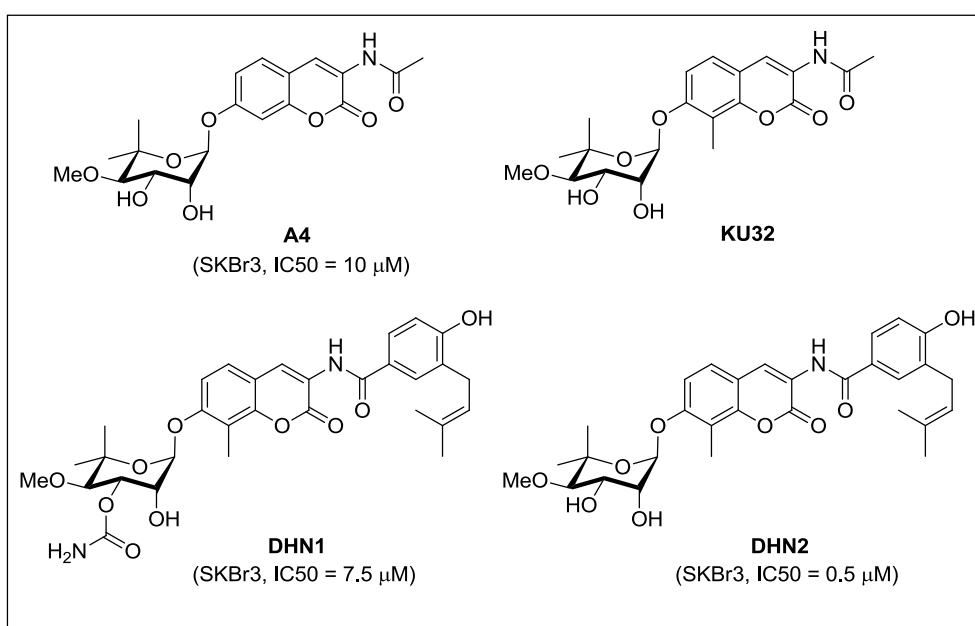


Figure 1.10. Structures of A4, KU32, DHN1 and DHN2.

B.2.2. Epigallocatechin-3-Gallate (EGCG)

EGCG is a polyphenolic compound found in green tea. EGCG has been shown to inhibit the activity of a wide range of proteins including telomerase, aryl hydrocarbons receptor (AhR), several kinases and transcription factors, all of which are well known Hsp90 client proteins.¹⁸ In 2005, Palermo and co-workers showed that EGCG exhibits its antagonistic behavior against AhR through Hsp90 inhibition.⁸⁵ Subsequent SAR studies revealed the essential role of phenols for anti-proliferative activity. Studies are currently underway to improve the inhibitory activity of EGCG analogues.

B.2.3. Cisplatin

Cisplatin is a platinum-containing chemotherapeutic agent used to treat bladder, cervical, testicular, ovarian, and other solid tumors.⁸⁶ Cisplatin binds DNA and induces intrastrand and/or interstrand adducts, which ultimately triggers apoptosis.⁸⁷ Additionally, cisplatin has been found to bind Hsp90 and interfere with its chaperone activity.⁸⁸ Subsequent studies suggested that cisplatin is a selective C-terminal inhibitor that binds near the C-terminal ATP-binding site.⁸⁹

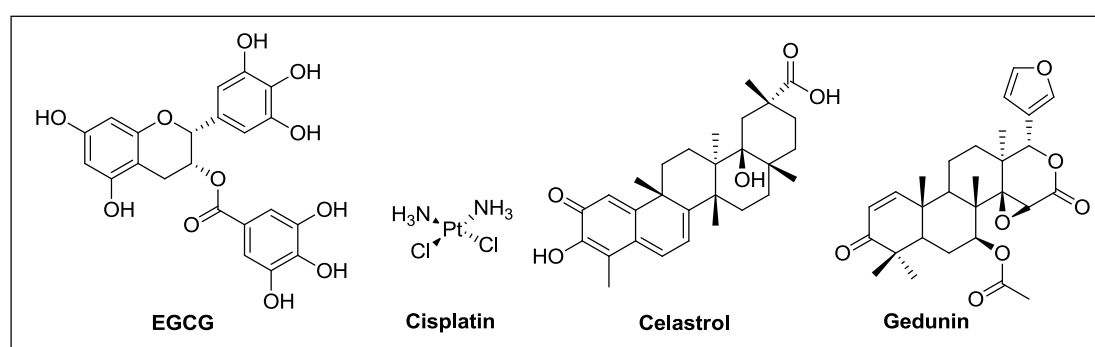


Figure 1.11. Structures of EGCG, cisplatin, celastrol and gedunin.

B.3. Miscellaneous Inhibitors

A third class of Hsp90 inhibitors includes compounds that disrupt protein-protein interactions between Hsp90 and its co-chaperones such as Cdc37 and p23.⁹⁰ Natural products such as celastrol and gedunin, have been identified that disrupt these interactions.^{91, 92} Celastrol is a natural product that disrupts the Hsp90-cdc37 complex formation, thus inhibiting Hsp90 chaperone activity.⁹¹ The co-chaperone Cdc37 is required for the recruitment and maturation of several oncoproteins kinases such as BRAF and EGFRvIII and hence, disruption of this interaction provides a potential opportunity against malignant cells.⁹³ Gedunin, a tetranortriterpenoid natural product, has traditionally been used for the treatment of malaria and other infectious diseases.⁹² In addition, gedunin exhibits potent anti-proliferative activity against various cancer cell lines. Patwardhan and co-workers determined

that geldunin manifests its inhibitory activity via disruption of Hsp90-p23 interactions and causes cell death through the activation of caspase 7.⁹⁴ In the light of these results, this class of compounds is now gaining importance as powerful pharmacological tools to selectively block one set of Hsp90 client proteins and to limit off-target effects.

5. Conclusion and Future Directions

The recognition of Hsp90 as a crucial mediator of oncogene addiction in the laboratory and the translation of these findings into clinically useful interventions have created a new dimension in cancer chemotherapeutics. Natural products and their derivatives have been developed as Hsp90 inhibitors that show encouraging results against a variety of cancers. As the potential use of Hsp90 inhibitors has extended beyond cancer, new opportunities for use in non-oncological diseases such as neurodegenerative, aberrant inflammation, viral, and bacterial infections are being pursued.

Although initial success with Hsp90 inhibitors generated significant interest, clinical challenges are emerging from clinical trials. Currently, all administered agents are Hsp90 N-terminal inhibitors. One of the major issues with N-terminal inhibitors is induction of the pro-survival heat shock response, which increases Hsp90 levels and directly affects the dosing schedule. In addition, all Hsp90 inhibitors in clinical trials are pan-inhibitors and exhibit unanticipated side effects. Several toxicities such as cardiotoxicity and hepatotoxicity, have been observed during clinical evaluation of these agents. As a consequence, alternative strategies are desired for the future development of Hsp90 inhibitors.

Recently, Hsp90 C-terminal inhibitors have emerged as an attractive alternative for Hsp90 modulation. These agents manifest similar, and in some cases, even superior inhibitory activity without induction of the pro-survival heat shock response and may potentially overcome the clinical limitations attributed to N-terminal inhibitors. Alternatively, isoform-selective agents that target a specific isoform of Hsp90, could provide a new avenue

for the development of future Hsp90 inhibitors. Another potential strategy includes the development of therapeutic agents that inhibit protein-protein interactions between Hsp90 and co-chaperones, leading to degradation of a subset of client proteins with fewer side-effects. In conclusion, as we gain a better insight into the biology of Hsp90 and its client proteins, it is likely that a more rational approach to drug design can be implemented and that drugs of superior therapeutic benefits will emerge.

6. References

1. Taipale, M.; Jarosz, D. F.; Lindquist, S., HSP90 at the hub of protein homeostasis: emerging mechanistic insights. *Nat. Rev. Mol. Cell Biol.* **2010**, *11*, 515-528.
2. Neckers, L.; Workman, P., Hsp90 Molecular Chaperone Inhibitors: Are We There Yet? *Clin. Cancer Res.* **2012**, *18*, 64-76.
3. Trepel, J.; Mollapour, M.; Giaccone, G.; Neckers, L., Targeting the dynamic HSP90 complex in cancer. *Nat. Rev. Cancer* **2010**, *10*, 537-549.
4. Donnelly, A.; Blagg, B. S. J., Novobiocin and Additional Inhibitors of the Hsp90 C-Terminal Nucleotide-binding Pocket. *Curr. Med. Chem.* **2008**, *15*, 2702-2717.
5. Blagg, B. S. J.; Kerr, T. D., Hsp90 inhibitors: Small molecules that transform the Hsp90 protein folding machinery into a catalyst for protein degradation. *Med. Res. Rev.* **2006**, *26*, 310-338.
6. Zuehlke, A.; Johnson, J. L., Hsp90 and co-chaperones twist the functions of diverse client proteins. *Biopolymers* **2010**, *93*, 211-217.
7. Whitesell, L.; Lindquist, S. L., HSP90 and the chaperoning of cancer. *Nat. Rev. Cancer* **2005**, *5*, 761-772.
8. Luo, W.; Sun, W.; Taldone, T.; Rodina, A.; Chiosis, G., Heat shock protein 90 in neurodegenerative diseases. *Mol. Neurodegeneration* **2010**, *5*, 24.
9. Dutta, R.; Inouye, M., GHKL, an emergent ATPase/kinase superfamily. *Tren. biochem. sci.* **2000**, *25*, 24-28.
10. Pearl, L. H.; Prodromou, C., Structure and Mechanism of the Hsp90 Molecular Chaperone Machinery. *Annu. Rev. Biochem.* **2006**, *75*, 271-294.
11. Prodromou, C.; Roe, S. M.; O'Brien, R.; Ladbury, J. E.; Piper, P. W.; Pearl, L. H., Identification and Structural Characterization of the ATP/ADP-Binding Site in the Hsp90 Molecular Chaperone. *Cell* **1997**, *90*, 65-75.
12. Stebbins, C. E.; Russo, A. A.; Schneider, C.; Rosen, N.; Hartl, F. U.; Pavletich, N. P., Crystal Structure of an Hsp90 Geldanamycin Complex: Targeting of a Protein Chaperone by an Antitumor Agent. *Cell* **1997**, *89*, 239-250.
13. Meyer, P.; Prodromou, C.; Hu, B.; Vaughan, C.; Roe, S. M.; Panaretou, B.; Piper, P. W.; Pearl, L. H., Structural and Functional Analysis of the Middle Segment of Hsp90: Implications for ATP Hydrolysis and Client Protein and Cochaperone Interactions. *Molecular Cell* **2003**, *11*, 647-658.
14. Huai, Q.; Wang, H.; Liu, Y.; Kim, H.-Y.; Toft, D.; Ke, H., Structures of the N-Terminal and Middle Domains of *E. coli* Hsp90 and Conformation Changes upon ADP Binding. *Structure* **2005**, *13*, 579-590.
15. So'ti, C.; Vermes, Á.; Haystead, T. A. J.; Csermely, P., Comparative analysis of the ATP-binding sites of Hsp90 by nucleotide affinity cleavage: a distinct nucleotide specificity of the C-terminal ATP-binding site. *Euro. J. Biochem.* **2003**, *270*, 2421-2428.
16. Prodromou, C.; Siligardi, G.; O'Brien, R.; Woolfson, D. N.; Regan, L.; Panaretou, B.; Ladbury, J. E.; Piper, P. W.; Pearl, L. H., Regulation of Hsp90 ATPase activity by tetratricopeptide repeat (TPR)-domain co-chaperones. *EMBO J* **1999**, *18*, 754-62.
17. Marcu, M. G.; Chadli, A.; Bouhouche, I.; Catelli, M.; Neckers, L. M., The Heat Shock Protein 90 Antagonist Novobiocin Interacts with a Previously Unrecognized ATP-binding Domain in the Carboxyl Terminus of the Chaperone. *J. Biol. Chem.* **2000**, *275*, 37181-37186.
18. Yin, Z.; Henry, E. C.; Gasiewicz, T. A., (-)-Epigallocatechin-3-gallate Is a Novel Hsp90 Inhibitor†. *Biochemistry* **2008**, *48*, 336-345.
19. Byrd, C. A.; Bornmann, W.; Erdjument-Bromage, H.; Tempst, P.; Pavletich, N.; Rosen, N.; Nathan, C. F.; Ding, A., Heat shock protein 90 mediates macrophage

- activation by Taxol and bacterial lipopolysaccharide. *Proc. Natl. Acad. Sci. USA* **1999**, *96*, 5645-5650.
20. Pearl, L. H.; Prodromou, C.; Workman, P., The Hsp90 molecular chaperone: an open and shut case for treatment. *Biochem. J.* **2008**, *410*, 439-453.
 21. Picard, D., Heat-shock protein 90, a chaperone for folding and regulation. *CMLS, Cell. Mol. Life Sci.* **2002**, *59*, 1640-1648.
 22. Sidera, K.; Patsavoudi, E., Extracellular HSP90: An Emerging Target for Cancer Therapy. *Curr. Signal Transd. T.* **2009**, *4*, 51-58.
 23. Peterson, L. B.; Blagg, B. S. J., To fold or not to fold: modulation and consequences of Hsp90 inhibition. *Future Med. Chem.* **2009**, *1*, 267-283.
 24. Walter, S.; Buchner, J., Molecular Chaperones—Cellular Machines for Protein Folding. *Angew. Chem. Int. Ed. Engl.* **2002**, *41*, 1098-1113.
 25. Söti, C.; Nagy, E.; Giricz, Z.; Vigh, L.; Csermely, P.; Ferdinandy, P., Heat shock proteins as emerging therapeutic targets. *Brit. J. Pharmacol.* **2005**, *146*, 769-780.
 26. Chaudhury, S.; Welch, T. R.; Blagg, B. S. J., Hsp90 as a Target for Drug Development. *ChemMedChem* **2006**, *1*, 1331-1340.
 27. Murphy, P. J. M.; Kanelakis, K. C.; Galigniana, M. D.; Morishima, Y.; Pratt, W. B., Stoichiometry, Abundance, and Functional Significance of the hsp90/hsp70-based Multiprotein Chaperone Machinery in Reticulocyte Lysate. *J. Biol. Chem.* **2001**, *276*, 30092-30098.
 28. Kosano, H.; Stensgard, B.; Charlesworth, M. C.; McMahon, N.; Toft, D., The Assembly of Progesterone Receptor-hsp90 Complexes Using Purified Proteins. *J. Biol. Chem.* **1998**, *273*, 32973-32979.
 29. Prodromou, C.; Panaretou, B.; Chohan, S.; Siligardi, G.; Brien, R.; Ladbury, J. E.; Roe, S. M.; Piper, P. W.; Pearl, L. H., The ATPase cycle of Hsp90 drives a molecular 'clamp' via transient dimerization of the N-terminal domains. *EMBO J.* **2000**, *19*, 4383-4392.
 30. Ali, M. M. U.; Roe, S. M.; Vaughan, C. K.; Meyer, P.; Panaretou, B.; Piper, P. W.; Prodromou, C.; Pearl, L. H., Crystal structure of an Hsp90–nucleotide–p23/Sba1 closed chaperone complex. *Nature* **2006**, *440*, 1013-1017.
 31. Miyata, Y.; Nakamoto, H.; Neckers, L., The therapeutic target Hsp90 and cancer hallmarks. *Curr. pharmaceu. desi.* **2013**, *19*, 347-65.
 32. Solit, D. B.; Chiosis, G., Development and application of Hsp90 inhibitors. *Drug Discovery Today* **2008**, *13*, 38-43.
 33. KOGA, F.; KIHARA, K.; NECKERS, L., Inhibition of Cancer Invasion and Metastasis by Targeting the Molecular Chaperone Heat-shock Protein 90. *Anticancer Res.* **2009**, *29*, 797-807.
 34. Paul, S.; Mahanta, S., Association of heat-shock proteins in various neurodegenerative disorders: is it a master key to open the therapeutic door? *Mol. Cell Biochem.* **2014**, *386*, 45-61.
 35. Xu, W.; Neckers, L., Targeting the Molecular Chaperone Heat Shock Protein 90 Provides a Multifaceted Effect on Diverse Cell Signaling Pathways of Cancer Cells. *Clin. Cancer Res.* **2007**, *13*, 1625-1629.
 36. Chiosis, G.; Huez, H.; Rosen, N.; Mimnaugh, E.; Whitesell, L.; Neckers, L., 17AAG: Low Target Binding Affinity and Potent Cell Activity—Finding an Explanation. *Mol. Cancer Ther.* **2003**, *2*, 123-129.
 37. Kamal, A.; Thao, L.; Sensintaffar, J.; Zhang, L.; Boehm, M. F.; Fritz, L. C.; Burrows, F. J., A high-affinity conformation of Hsp90 confers tumour selectivity on Hsp90 inhibitors. *Nature* **2003**, *425*, 407-410.
 38. Chiosis, G.; Neckers, L., Tumor Selectivity of Hsp90 Inhibitors: The Explanation Remains Elusive. *ACS Chem. Biol.* **2006**, *1*, 279-284.

39. Workman, P., Altered states: selectively drugging the Hsp90 cancer chaperone. *Trends mol. med.* **2004**, *10*, 47-51.
40. Modi, S.; Stopeck, A. T.; Gordon, M. S.; Mendelson, D.; Solit, D. B.; Bagatell, R.; Ma, W.; Wheler, J.; Rosen, N.; Norton, L.; Cropp, G. F.; Johnson, R. G.; Hannah, A. L.; Hudis, C. A., Combination of Trastuzumab and Tanespimycin (17-AAG, KOS-953) Is Safe and Active in Trastuzumab-Refractory HER-2–Overexpressing Breast Cancer: A Phase I Dose-Escalation Study. *J. Clin. Onco.* **2007**, *25*, 5410-5417.
41. Modi, S.; Stopeck, A.; Linden, H.; Solit, D.; Chandarlapaty, S.; Rosen, N.; D'Andrea, G.; Dickler, M.; Moynahan, M. E.; Sugarman, S.; Ma, W.; Patil, S.; Norton, L.; Hannah, A. L.; Hudis, C., HSP90 Inhibition Is Effective in Breast Cancer: A Phase II Trial of Tanespimycin (17-AAG) Plus Trastuzumab in Patients with HER2-Positive Metastatic Breast Cancer Progressing on Trastuzumab. *Clin. Cancer Res.* **2011**, *17*, 5132-5139.
42. Ross, C. A.; Poirier, M. A., Protein aggregation and neurodegenerative disease. *Nat. Med.* **2004**, *10 Suppl*, S10-7.
43. Meriin, A. B.; Sherman, M. Y., Role of molecular chaperones in neurodegenerative disorders. *Int. J. Hyperthermia* **2005**, *21*, 403-419.
44. Dickey, C. A.; Eriksen, J.; Kamal, A.; Burrows, F.; Kasibhatla, S.; Eckman, C. B.; Hutton, M.; Petrucelli, L., Development of a high throughput drug screening assay for the detection of changes in tau levels -- proof of concept with HSP90 inhibitors. *Curr. Alzheimer res.* **2005**, *2*, 231-8.
45. Muchowski, P. J.; Wacker, J. L., Modulation of neurodegeneration by molecular chaperones. *Nat. Rev. Neurosci.* **2005**, *6*, 11-22.
46. Luo, W.; Dou, F.; Rodina, A.; Chip, S.; Kim, J.; Zhao, Q.; Moulick, K.; Aguirre, J.; Wu, N.; Greengard, P.; Chiosis, G., Roles of heat-shock protein 90 in maintaining and facilitating the neurodegenerative phenotype in tauopathies. *Proc. Natl. Acad. Sci. USA* **2007**, *104*, 9511-9516.
47. Hashimoto, M.; Rockenstein, E.; Crews, L.; Masliah, E., Role of protein aggregation in mitochondrial dysfunction and neurodegeneration in Alzheimer's and Parkinson's diseases. *Neuromol. Med.* **2003**, *4*, 21-35.
48. Alonso, A. d. C.; Zaidi, T.; Novak, M.; Grundke-Iqbal, I.; Iqbal, K., Hyperphosphorylation induces self-assembly of τ into tangles of paired helical filaments/straight filaments. *Proc. Natl. Acad. Sci. USA* **2001**, *98*, 6923-6928.
49. Kim, H.-Y.; Heise, H.; Fernandez, C. O.; Baldus, M.; Zweckstetter, M., Correlation of Amyloid Fibril β -Structure with the Unfolded State of α -Synuclein. *ChemBioChem* **2007**, *8*, 1671-1674.
50. Neckers, L.; Tatu, U., Molecular Chaperones in Pathogen Virulence: Emerging New Targets for Therapy. *Cell host & microbe* **2008**, *4*, 519-527.
51. Cowen, L. E.; Lindquist, S., Hsp90 Potentiates the Rapid Evolution of New Traits: Drug Resistance in Diverse Fungi. *Science* **2005**, *309*, 2185-2189.
52. Casadevall, A., The Third Age of Antimicrobial Therapy. *Clin. Infect. Diseases* **2006**, *42*, 1414-1416.
53. Messaoudi, S.; Peyrat, J. F.; Brion, J. D.; Alami, M., Recent advances in Hsp90 inhibitors as antitumor agents. *Anti-cancer agents med. chem.* **2008**, *8*, 761-82.
54. DeBoer, C.; Meulman, P. A.; Wnuk, R. J.; Peterson, D. H., Geldanamycin, a new antibiotic. *J. antibiot.* **1970**, *23*, 442-7.
55. Jove, R.; Hanafusa, H., Cell transformation by the viral src oncogene. *Annu. rev. cell biol.* **1987**, *3*, 31-56.
56. Whitesell, L.; Mimnaugh, E. G.; De Costa, B.; Myers, C. E.; Neckers, L. M., Inhibition of heat shock protein HSP90-pp60v-src heteroprotein complex formation

- by benzoquinone ansamycins: essential role for stress proteins in oncogenic transformation. *Proc. Natl. Acad. Sci. USA* **1994**, *91*, 8324-8.
57. Schulte, T. W.; Neckers, L. M., The benzoquinone ansamycin 17-allylamino-17-demethoxygeldanamycin binds to HSP90 and shares important biologic activities with geldanamycin. *Cancer Chemother. Pharmacol.* **1998**, *42*, 273-279.
 58. Tian, Z.-Q.; Liu, Y.; Zhang, D.; Wang, Z.; Dong, S. D.; Carreras, C. W.; Zhou, Y.; Rastelli, G.; Santi, D. V.; Myles, D. C., Synthesis and biological activities of novel 17-aminogeldanamycin derivatives. *Bioorg. Med. Chem.* **2004**, *12*, 5317-5329.
 59. Delmotte, P.; Delmotte-Plaquee, J., A New Antifungal Substance of Fungal Origin. *Nature* **1953**, *171*, 344-344.
 60. Schulte, T. W.; Akinaga, S.; Soga, S.; Sullivan, W.; Stensgard, B.; Toft, D.; Neckers, L. M., Antibiotic Radicicol Binds to the N-Terminal Domain of Hsp90 and Shares Important Biologic Activities with Geldanamycin. *Cell Stress & Chaperones* **1998**, *3*, 100-108.
 61. Roe, S. M.; Prodromou, C.; O'Brien, R.; Ladbury, J. E.; Piper, P. W.; Pearl, L. H., Structural Basis for Inhibition of the Hsp90 Molecular Chaperone by the Antitumor Antibiotics Radicicol and Geldanamycin. *J. Med. Chem.* **1999**, *42*, 260-266.
 62. Xudong, G.; Zhi-Qiang, Y.; Samuel, J. D., Synthetic Development of Radicicol and Cycloproparadicicol: Highly Promising Anticancer Agents Targeting Hsp90. *ChemInform* **2004**, *35*.
 63. Soga, S.; Shiotsu, Y.; Akinaga, S.; Sharma, S. V., Development of radicicol analogues. *Curr. cancer drug targets* **2003**, *3*, 359-69.
 64. Yang, Z.-Q.; Geng, X.; Solit, D.; Pratilas, C. A.; Rosen, N.; Danishefsky, S. J., New Efficient Synthesis of Resorcinylic Macrolides via Ynolides: Establishment of Cycloproparadicicol as Synthetically Feasible Preclinical Anticancer Agent Based on Hsp90 as the Target. *J. Am. Chem. Soc.* **2004**, *126*, 7881-7889.
 65. Duerfeldt, A. S.; Peterson, L. B.; Maynard, J. C.; Ng, C. L.; Eletto, D.; Ostrovsky, O.; Shinogle, H. E.; Moore, D. S.; Argon, Y.; Nicchitta, C. V.; Blagg, B. S. J., Development of a Grp94 inhibitor. *J. Am. Chem. Soc.* **2012**, *134*, 9796-9804.
 66. Chiosis, G.; Timaul, M. N.; Lucas, B.; Munster, P. N.; Zheng, F. F.; Sepp-Lorenzino, L.; Rosen, N., A small molecule designed to bind to the adenine nucleotide pocket of Hsp90 causes Her2 degradation and the growth arrest and differentiation of breast cancer cells. *Chem. Biol.* **2001**, *8*, 289-299.
 67. Chiosis, G.; Lucas, B.; Shtil, A.; Huezo, H.; Rosen, N., Development of a Purine-Scaffold Novel Class of Hsp90 Binders that Inhibit the Proliferation of Cancer Cells and Induce the Degradation of Her2 Tyrosine Kinase. *Bioorg. Med. Chem.* **2002**, *10*, 3555-3564.
 68. Kasibhatla, S. R.; Hong, K.; Biamonte, M. A.; Busch, D. J.; Karjian, P. L.; Sensintaffar, J. L.; Kamal, A.; Lough, R. E.; Brekken, J.; Lundgren, K.; Grecko, R.; Timony, G. A.; Ran, Y.; Mansfield, R.; Fritz, L. C.; Ulm, E.; Burrows, F. J.; Boehm, M. F., Rationally Designed High-Affinity 2-Amino-6-halopurine Heat Shock Protein 90 Inhibitors That Exhibit Potent Antitumor Activity. *J. Med. Chem.* **2007**, *50*, 2767-2778.
 69. Rowlands, M. G.; Newbatt, Y. M.; Prodromou, C.; Pearl, L. H.; Workman, P.; Aherne, W., High-throughput screening assay for inhibitors of heat-shock protein 90 ATPase activity. *Anal. Biochem.* **2004**, *327*, 176-183.
 70. Cheung, K.-M. J.; Matthews, T. P.; James, K.; Rowlands, M. G.; Boxall, K. J.; Sharp, S. Y.; Maloney, A.; Roe, S. M.; Prodromou, C.; Pearl, L. H.; Aherne, G. W.; McDonald, E.; Workman, P., The identification, synthesis, protein crystal structure and in vitro biochemical evaluation of a new 3,4-diarylpyrazole class of Hsp90 inhibitors. *Bioorg. Med. Chem. Lett.* **2005**, *15*, 3338-3343.

71. Kreuzsch, A.; Han, S.; Brinker, A.; Zhou, V.; Choi, H.-s.; He, Y.; Lesley, S. A.; Caldwell, J.; Gu, X.-j., Crystal structures of human HSP90 α -complexed with dihydroxyphenylpyrazoles. *Bioorg. Med. Chem. Lett.* **2005**, *15*, 1475-1478.
72. Dymock, B. W.; Barril, X.; Brough, P. A.; Cansfield, J. E.; Massey, A.; McDonald, E.; Hubbard, R. E.; Surgenor, A.; Roughley, S. D.; Webb, P.; Workman, P.; Wright, L.; Drysdale, M. J., Novel, Potent Small-Molecule Inhibitors of the Molecular Chaperone Hsp90 Discovered through Structure-Based Design. *J. Med. Chem.* **2005**, *48*, 4212-4215.
73. Sharp, S. Y.; Prodromou, C.; Boxall, K.; Powers, M. V.; Holmes, J. L.; Box, G.; Matthews, T. P.; Cheung, K.-M. J.; Kalusa, A.; James, K.; Hayes, A.; Hardcastle, A.; Dymock, B.; Brough, P. A.; Barril, X.; Cansfield, J. E.; Wright, L.; Surgenor, A.; Foloppe, N.; Hubbard, R. E.; Aherne, W.; Pearl, L.; Jones, K.; McDonald, E.; Raynaud, F.; Eccles, S.; Drysdale, M.; Workman, P., Inhibition of the heat shock protein 90 molecular chaperone in vitro and in vivo by novel, synthetic, potent resorcinyl pyrazole/isoxazole amide analogues. *Mol. Cancer Ther.* **2007**, *6*, 1198-1211.
74. Eccles, S. A.; Massey, A.; Raynaud, F. I.; Sharp, S. Y.; Box, G.; Valenti, M.; Patterson, L.; de Haven Brandon, A.; Gowan, S.; Boxall, F.; Aherne, W.; Rowlands, M.; Hayes, A.; Martins, V.; Urban, F.; Boxall, K.; Prodromou, C.; Pearl, L.; James, K.; Matthews, T. P.; Cheung, K.-M.; Kalusa, A.; Jones, K.; McDonald, E.; Barril, X.; Brough, P. A.; Cansfield, J. E.; Dymock, B.; Drysdale, M. J.; Finch, H.; Howes, R.; Hubbard, R. E.; Surgenor, A.; Webb, P.; Wood, M.; Wright, L.; Workman, P., NVP-AUY922: A Novel Heat Shock Protein 90 Inhibitor Active against Xenograft Tumor Growth, Angiogenesis, and Metastasis. *Cancer Res.* **2008**, *68*, 2850-2860.
75. Hong, D. S.; Banerji, U.; Tavana, B.; George, G. C.; Aaron, J.; Kurzrock, R., Targeting the molecular chaperone heat shock protein 90 (HSP90): Lessons learned and future directions. *Cancer Treat. Rev.* **2013**, *39*, 375-387.
76. Brough, P. A.; Aherne, W.; Barril, X.; Borgognoni, J.; Boxall, K.; Cansfield, J. E.; Cheung, K.-M. J.; Collins, I.; Davies, N. G. M.; Drysdale, M. J.; Dymock, B.; Eccles, S. A.; Finch, H.; Fink, A.; Hayes, A.; Howes, R.; Hubbard, R. E.; James, K.; Jordan, A. M.; Lockie, A.; Martins, V.; Massey, A.; Matthews, T. P.; McDonald, E.; Northfield, C. J.; Pearl, L. H.; Prodromou, C.; Ray, S.; Raynaud, F. I.; Roughley, S. D.; Sharp, S. Y.; Surgenor, A.; Walmsley, D. L.; Webb, P.; Wood, M.; Workman, P.; Wright, L., 4,5-Diarylisoaxazole Hsp90 Chaperone Inhibitors: Potential Therapeutic Agents for the Treatment of Cancer. *J. Med. Chem.* **2007**, *51*, 196-218.
77. Yu, X. M.; Shen, G.; Blagg, B. S. J., Synthesis of (-)-Noviose from 2,3-O-Isopropylidene-d-erythronolactol. *J. Org. Chem.* **2004**, *69*, 7375-7378.
78. Marcu, M. G.; Schulte, T. W.; Neckers, L., Novobiocin and Related Coumarins and Depletion of Heat Shock Protein 90-Dependent Signaling Proteins. *J. Natl. Cancer Inst.* **2000**, *92*, 242-248.
79. Yu, X. M.; Shen, G.; Neckers, L.; Blake, H.; Holzbeierlein, J.; Cronk, B.; Blagg, B. S. J., Hsp90 Inhibitors Identified from a Library of Novobiocin Analogues. *J. Am. Chem. Soc.* **2005**, *127*, 12778-12779.
80. Farmer, K.; Williams, S. J.; Novikova, L.; Ramachandran, K.; Rawal, S.; Blagg, B. S. J.; Dobrowsky, R.; Stehno-Bittel, L., KU-32, a Novel Drug for Diabetic Neuropathy, Is Safe for Human Islets and Improves In Vitro Insulin Secretion and Viability. *Exp. Diabetes Res.* **2012**, *2012*, 11.
81. Burlison, J. A.; Neckers, L.; Smith, A. B.; Maxwell, A.; Blagg, B. S. J., Novobiocin: Redesigning a DNA Gyrase Inhibitor for Selective Inhibition of Hsp90. *J. Am. Chem. Soc.* **2006**, *128*, 15529-15536.

82. Zhao, H.; Donnelly, A. C.; Kusuma, B. R.; Brandt, G. E. L.; Brown, D.; Rajewski, R. A.; Vielhauer, G.; Holzbeierlein, J.; Cohen, M. S.; Blagg, B. S. J., Engineering an Antibiotic to Fight Cancer: Optimization of the Novobiocin Scaffold to Produce Antiproliferative Agents. *J. Med. Chem.* **2011**, *54*, 3839-3853.
83. Donnelly, A. C.; Mays, J. R.; Burlison, J. A.; Nelson, J. T.; Vielhauer, G.; Holzbeierlein, J.; Blagg, B. S. J., The Design, Synthesis, and Evaluation of Coumarin Ring Derivatives of the Novobiocin Scaffold that Exhibit Antiproliferative Activity. *J. Org. Chem.* **2008**, *73*, 8901-8920.
84. Zhao, H.; Reddy Kusuma, B.; Blagg, B. S. J., Synthesis and Evaluation of Noviose Replacements on Novobiocin That Manifest Antiproliferative Activity. *ACS Med. Chem. Lett.* **2010**, *1*, 311-315.
85. Palermo, C. M.; Westlake, C. A.; Gasiewicz, T. A., Epigallocatechin Gallate Inhibits Aryl Hydrocarbon Receptor Gene Transcription through an Indirect Mechanism Involving Binding to a 90 kDa Heat Shock Protein†. *Biochemistry* **2005**, *44*, 5041-5052.
86. Galanski, M., Recent developments in the field of anticancer platinum complexes. *Recent pat. anti-cancer drug discovery* **2006**, *1*, 285-95.
87. Jordan, P.; Carmo-Fonseca*, M., Molecular mechanisms involved in cisplatin cytotoxicity. *CMLS, Cell. Mol. Life Sci.* **2000**, *57*, 1229-1235.
88. Sreedhar, A. S.; So"ti, C.; Csermely, P., Inhibition of Hsp90: a new strategy for inhibiting protein kinases. *Biochimica et Biophysica Acta (BBA) - Prot. Proteo.* **2004**, *1697*, 233-242.
89. Söti, C.; Rácz, A.; Csermely, P., A Nucleotide-dependent Molecular Switch Controls ATP Binding at the C-terminal Domain of Hsp90: N-TERMINAL NUCLEOTIDE BINDING UNMASKS A C-TERMINAL BINDING POCKET. *J. Biol. Chem.* **2002**, *277*, 7066-7075.
90. Brandt, G. E.; Blagg, B. S., Alternate strategies of Hsp90 modulation for the treatment of cancer and other diseases. *Curr. Top. Med. Chem.* **2009**, *9*, 1447-61.
91. Sreeramulu, S.; Gande, S. L.; Göbel, M.; Schwalbe, H., Molecular Mechanism of Inhibition of the Human Protein Complex Hsp90–Cdc37, a Kinome Chaperone–Cochaperone, by Triterpene Celastrol. *Angew. Chem. Int. Ed. Engl.* **2009**, *48*, 5853-5855.
92. Brandt, G. E. L.; Schmidt, M. D.; Prisinzano, T. E.; Blagg, B. S. J., Gedunin, a Novel Hsp90 Inhibitor: Semisynthesis of Derivatives and Preliminary Structure–Activity Relationships. *J. Med. Chem.* **2008**, *51*, 6495-6502.
93. Roe, S. M.; Ali, M. M. U.; Meyer, P.; Vaughan, C. K.; Panaretou, B.; Piper, P. W.; Prodromou, C.; Pearl, L. H., The Mechanism of Hsp90 Regulation by the Protein Kinase-Specific Cochaperone p50cdc37. *Cell* **2004**, *116*, 87-98.
94. Patwardhan, C. A.; Fauq, A.; Peterson, L. B.; Miller, C.; Blagg, B. S. J.; Chadli, A., Gedunin Inactivates the Co-chaperone p23 Protein Causing Cancer Cell Death by Apoptosis. *J. Biol. Chem.* **2013**, *288*, 7313-7325.

**Design, Synthesis and Biological Evaluation of Ring-
constrained Hsp90 C-Terminal Inhibitors**

Chapter 2

Development of Ring-constrained Novobiocin Analogues as Hsp90 Inhibitors

1. Introduction

Heat shock protein 90 (Hsp90) is an ATP-dependent molecular chaperone responsible for the maintenance of protein homeostasis.¹⁻³ It is the key component of a protein folding machinery that regulates the conformational maturation, activation and stability of a vast array of client proteins, including protein kinases, steroid receptors, telomerase, and transcription factors.⁴ These client proteins perform several housekeeping functions, such as signal transduction, protein trafficking, cell proliferation and survival.³ However, in cancer cells, many of these client proteins are frequently mutated and/or over-expressed and are believed to be critical for transformation and the maintenance of oncogenic phenotypes.⁵ Approximately 50 Hsp90 client proteins (e.g., Her2, Raf1, Akt, MET, Src, CDK4 etc.) are known to be directly associated with all six hallmarks of cancer, which are actively pursued as individual therapeutic targets for cancer treatment.^{6, 7} Consequently, Hsp90 inhibition provides an attractive opportunity for the simultaneous disruption of multiple oncogenic pathways and hence, for the development of anti-cancer agents.

The Hsp90 protein function can be inhibited by small molecules that competitively displace ATP from the Hsp90 nucleotide-binding site and halt the protein folding cycle.⁸ Over past two decades, a large number of small molecules have been developed that competitively block ATP from binding to the Hsp90 N-terminus, leading to the degradation of client proteins.⁹ In fact, 17 such inhibitors of Hsp90 are currently in clinical trials for the treatment of cancer.² Although there has been great interest in the development of this class of Hsp90 inhibitors, challenges such as concomitant induction of the pro-survival response,

hepatotoxicity and multidrug resistance, have raised serious concerns about their clinical utility.⁵

In 2000, Neckers and co-workers demonstrated that the coumarin antibiotics, such as novobiocin (a DNA gyrase inhibitor), bound to a previously unrecognized ATP binding site at the Hsp90 C-terminus and induced a concentration-dependent degradation of Hsp90 client proteins.¹⁰ In addition, it was found that the Hsp90 C-terminal binding site allosterically modulates ligand binding to the N-terminus. Unlike N-terminal inhibitors, novobiocin and other C-terminal inhibitors do not induce Hsp levels and thus, present an attractive alternative to modulation of the Hsp90 folding machinery.¹¹ However, novobiocin exhibits low affinity for Hsp90 (~700 μ M against SKBr3) and therefore has limited therapeutic application.

In an effort to improve its efficacy, Yu and co-workers developed a small library of novobiocin analogues and elucidated the first structure-activity relationships for this molecule.¹² Their study revealed that the 4-hydroxy substituent and the carbamoyl group were detrimental towards Hsp90 inhibitory activity and removal of both substituents resulted in the identification of the compound **A4** (Figure 1), which induced Hsp90 client protein degradation at ~70 fold lower concentrations than novobiocin ($IC_{50} = 10 \mu$ M). Additional SAR studies, aimed at elucidating functionality responsible for Hsp90 inhibition vs DNA gyrase, led to the development of two novobiocin analogues DHNI and DHN2 (Figure 1), which transformed this DNA gyrase inhibitor (novobiocin) into a selective Hsp90 inhibitor.¹³

In 2008, Donnelly and co-workers explored the coumarin core and benzamide side chain of novobiocin and revealed structure-activity relationships for these moieties.¹⁴ Inspired by activity manifested by **A4** and its dimer¹⁵, derivatives of **A4** with variations to the coumarin core and the benzamide chain were designed and then evaluated for anti-proliferative activity. Their studies demonstrated that substitutions at the 6- and 8-position of the coumarin core were tolerable and that incorporation of a hydrogen-bond acceptor (e.g. OMe) at these locations improved inhibitory activity (Figure 2.1). In addition, replacement of

the acetamide side chain with benzamide led to development of KU174, which manifests sub-micromolar to mid nanomolar activity in cell proliferation assay against various cancer cell lines. Unlike N-terminal inhibitors, KU174 exhibits potent cytotoxicity without induction of the heat shock response.¹⁶ Furthermore, it induces apoptosis within 24 hours, which is consistent with clinical administration protocols.

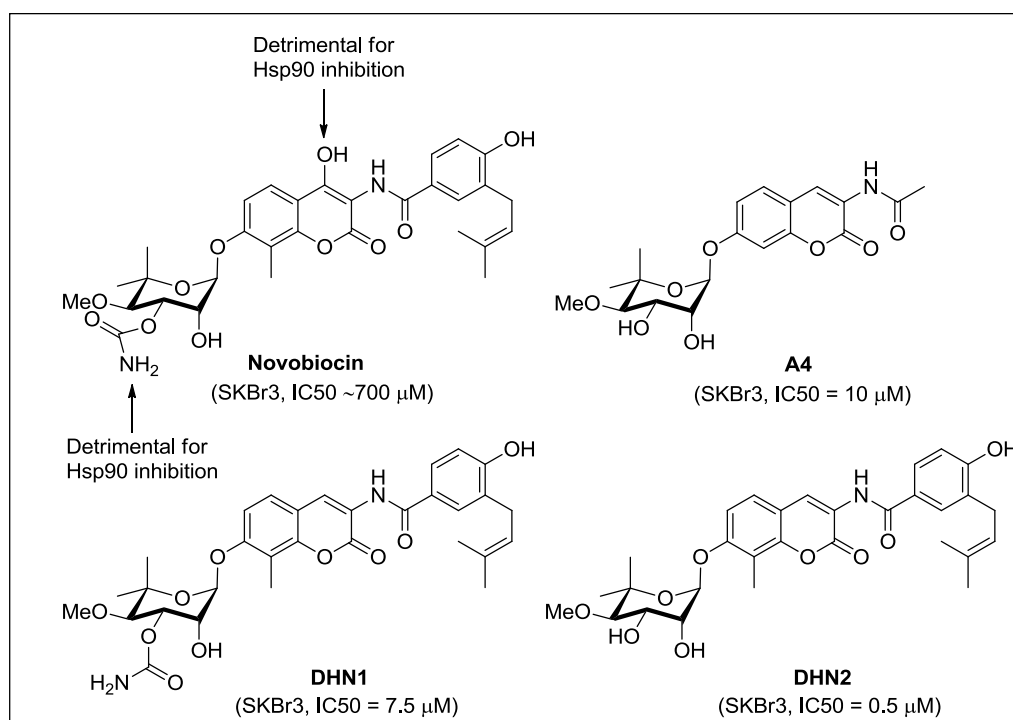


Figure 2.1. Structures of Novobiocin, A4, DHN1 and DHN2.

Recently, the role of the noviose sugar was explored and SAR revealed.¹⁷⁻¹⁹ These SAR studies demonstrated that the sugar moiety, although important for enhancing solubility (and hence efficacy), could be replaced with other sugars or sugar surrogates without compromising inhibitory activity. These SAR studies led to development of several promising lead molecules such as KU135 and KU292 (Figure 2.2), which manifest anti-proliferative activity against multiple cancer cell lines.

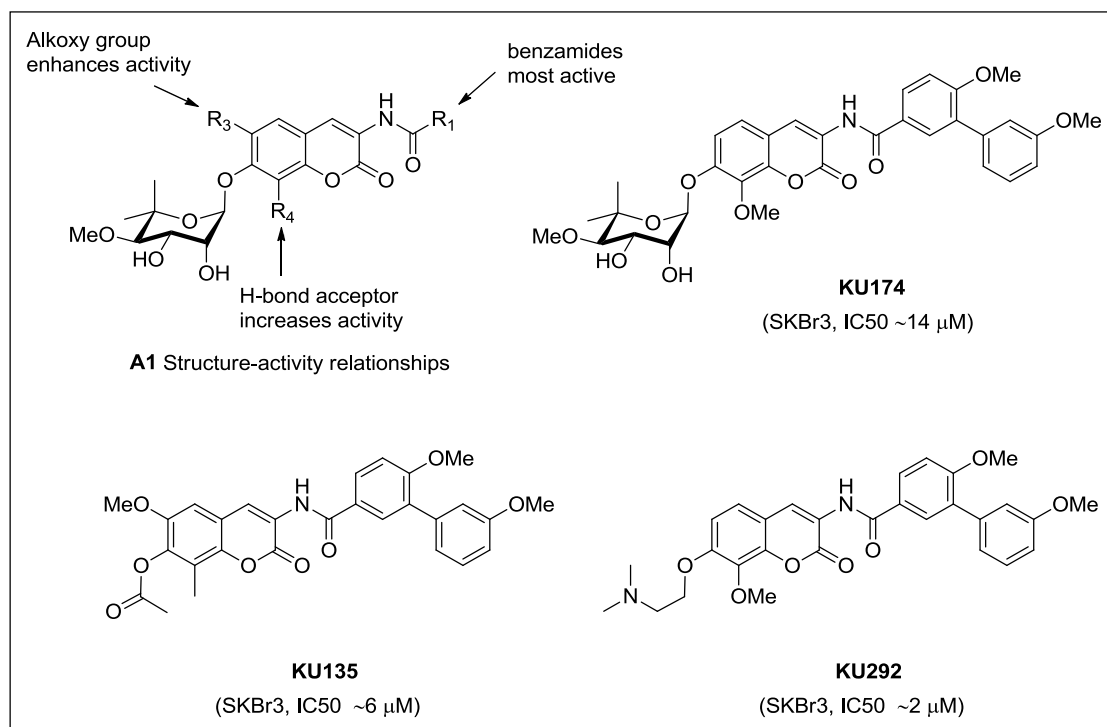


Figure 2.2. A1 SAR and structures of KU174, KU135 and KU292.

2. Design, Synthesis and Biological Evaluation of Ring-constrained Novobiocin Analogues

Since the discovery of novobiocin as the first Hsp90 C-terminal inhibitor, intense investigations for the development of more efficacious Hsp90 inhibitors have been pursued.^{10, 13, 14, 19} Extensive structural modifications to novobiocin led to identification of several efficacious analogues (e.g., KU174, KU135) that manifest potent anti-proliferative activity against multiple cancer cell lines.^{14, 16, 18, 19} Recently, it was shown that replacement of the sugar with amines improve inhibitory activity and several analogues such as KU292 were identified.¹⁹ These SAR studies led to elucidation of the following structure-activity relationships: 1) The biaryl side chain appears optimal compared to other side chains; 2) the amide linker provides hydrogen bonding interactions with the binding pocket; 3) incorporation of a hydrogen-bond acceptor at the 8-position improves inhibitory activity; and

4) modification to the phenolic ether are tolerated and allows for replacement of the sugar with other moieties without compromising inhibitory activity.

Based on these structure-activity relationships as well as molecular docking studies²⁰, it was hypothesized that compounds containing lactams and substituents at the α -position in lieu of the sugar moiety would provide ring-constrained analogues containing all these features (Figure 2.3). Furthermore, as a consequence of ring constraint, the analogues would exhibit less entropic penalty compared to their freely rotating counterparts, and would therefore project the side chain into the region occupied by the noiose sugar. In addition, replacement of hydrolytically sensitive ether linkage with a lactam would result in analogues with improved metabolic stability.

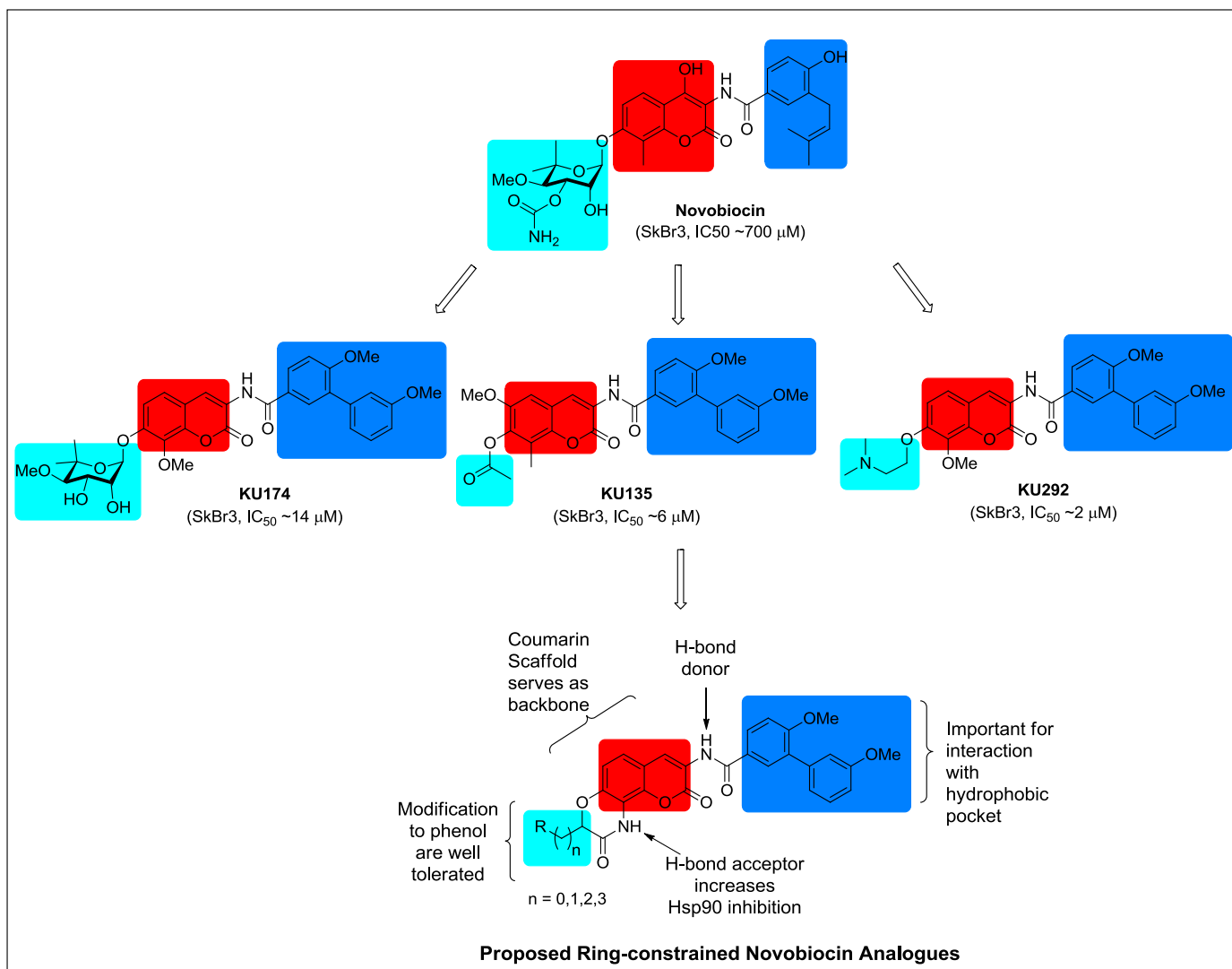


Figure 2.3. Rationale for proposed ring-constrained novobiocin analogues.

To evaluate this hypothesis, the design of investigational molecules commenced that would contain a sugar surrogate at the α -position of the lactam and would project into the region usually occupied by the sugar moiety and establish interactions with the binding pocket. Earlier SAR studies revealed that the incorporation of solubilizing moieties such as amines, in sugar-binding region of Hsp90, improves both solubility and efficacy.^{19, 21} In addition, recent QSAR studies by Huang and co-workers suggested that modification to these amines can produce more efficacious inhibitors.²⁰ Therefore, the amines were selected as sugar surrogate for these investigational molecules. Using our earlier reported molecular

docking strategy,²² compound **9** (Scheme 2.1), which contains the physiologically ionizable pyrrolidine moiety appended to the α -position of the lactam was designed and docked into our Hsp90 C-terminal docking model. As shown in Figure 2.4B, compound **9** showed a strong structural alignment with the lead compound, KU174.

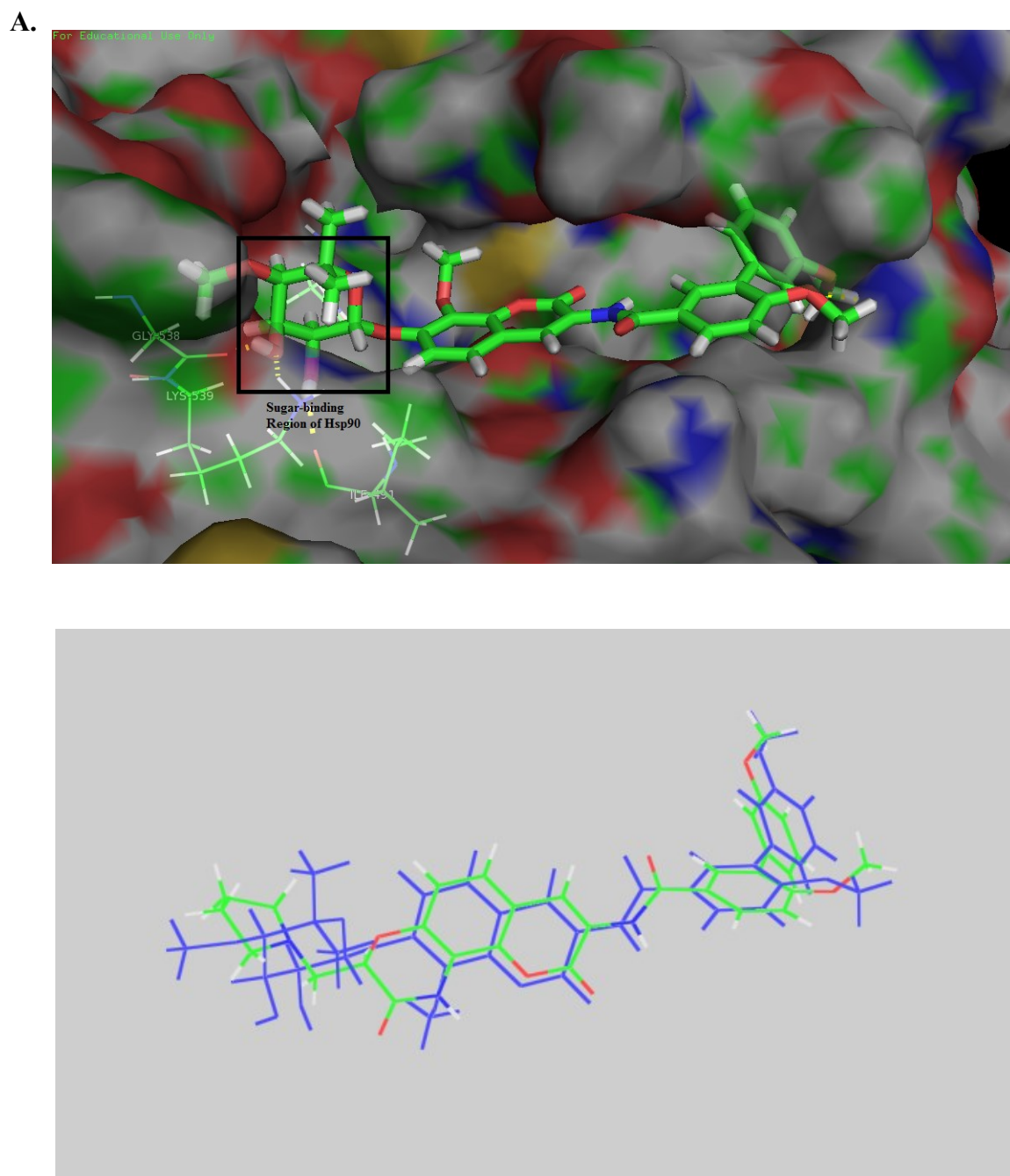
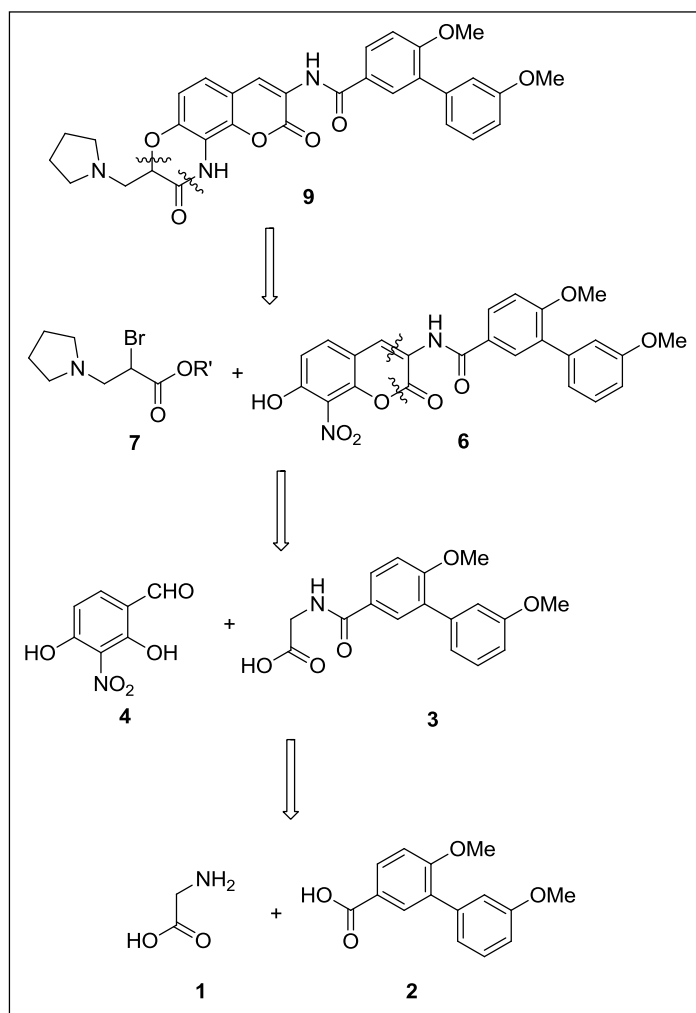


Figure 2.4. **A.** Docked structure of KU174 in the putative Hsp90 C-terminal binding site. **B.** Molecular overlay of KU174 (blue) and investigational molecule **9** (green).

Retrosynthetically, we envisioned construction of **9** from *O*-alkylation of phenol **6** with α -bromo ester **7**, followed by a tandem reduction/ring closing reaction catalyzed by Pd hydrogenolysis (Scheme 2.1). Phenol **6** was proposed to result from an Aldol condensation between aldehyde **4** and acid **3**. Aldehyde **4** could be obtained by the formylation of commercially available nitro resorcinol.²³ Synthesis of acid **3** could be achieved via an amide coupling reaction between the glycine ester and the previously reported biaryl acid,²⁴ followed by base-catalyzed hydrolysis.

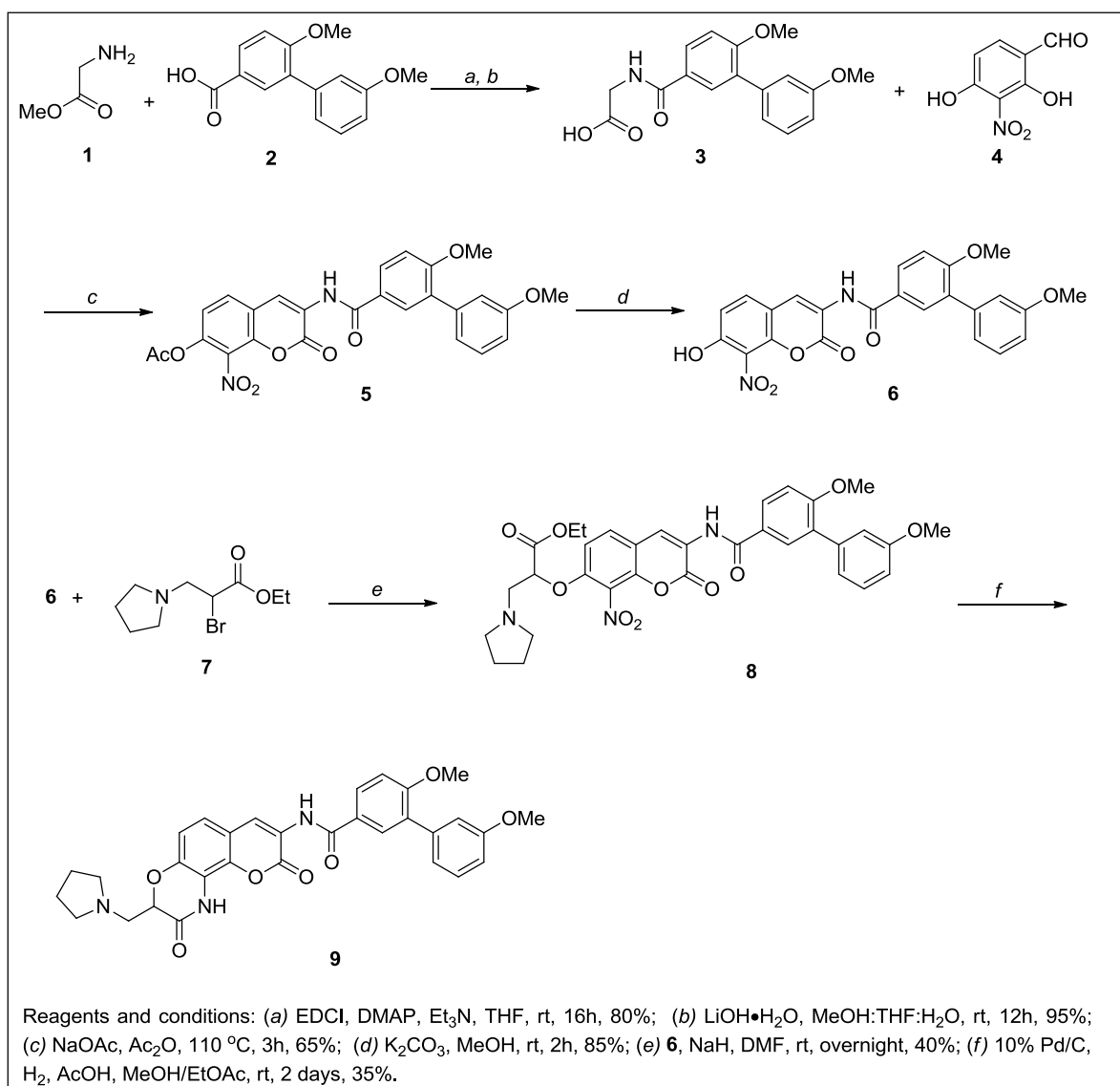


Scheme 2.1. Retrosynthetic analysis of lactamized novobiocin analogue **9**.

As shown in Scheme 2.2 the synthesis of compound **9** began via an amide coupling reaction between amine **1** and biaryl acid **2** to afford amide **3**, which underwent an Aldol

condensation with benzaldehyde **4** to give acetylated-coumarin, **5**. Subsequent deacetylation of **5** gave the coumarin intermediate, **6**, in high yield. Phenol **6** was *O*-alkylated with the previously reported α -bromo ester, **7**,²⁵ to yield the coumarin ether, **8**. Pd-catalyzed reduction of **8** resulted in generation of the amine, which subsequently underwent an acid-catalyzed cyclization to afford lactam **9**.

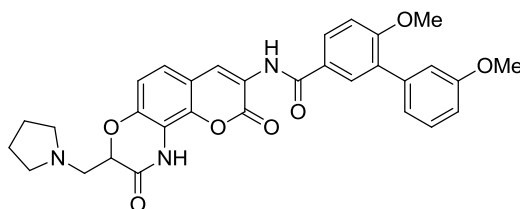
Scheme 2.2. Synthesis of pyrrolidine-containing lactam **9**.



Upon completion of its synthesis, lactam **9** was evaluated for anti-proliferative activity against SKBr3 (estrogen receptor negative, Her2 over-expressing breast cancer cells)

and MCF-7 (estrogen receptor positive breast cancer cells) cell lines (Table 2.1). The anti-proliferative data suggested that it manifested comparable activity to KU174.

Table 2.1. Anti-proliferative activity of pyrrolidine-containing lactam **9**.



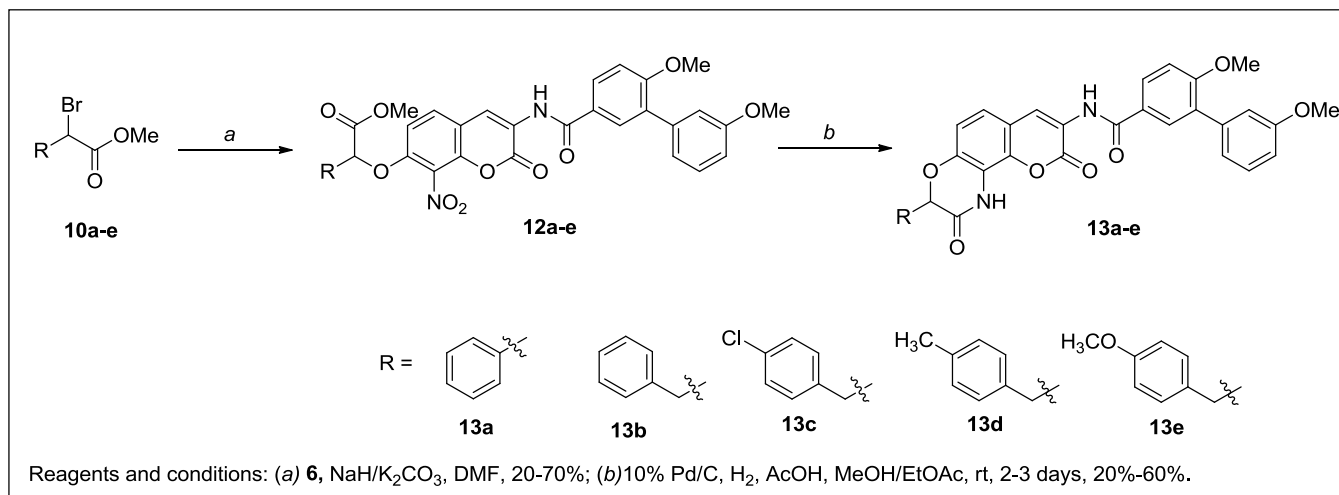
Entry	SKBr3 (IC ₅₀ , μM)	MCF-7 (IC ₅₀ , μM)
9	14.97 ± 4.3 ^a	22.90 ± 0.96
KU174	13.9 ± 0.15	9.0 ± 0.33

^a Values represent mean ± standard deviation for at least two separate experiments performed in triplicate.

The anti-proliferative activity manifested by compound **9** promoted additional investigations into the optimal substitutions that could be appended to the lactam core to produce more potent inhibitors. Since no co-crystal structure of Hsp90 bound to C-terminal inhibitors has been solved, there is limited knowledge about the size and nature of this binding pocket. Therefore, lactams containing various substituents, such as hydrophobic, rigid, ionizable and non-ionizable were pursued to elucidate potential interactions with the binding pocket.

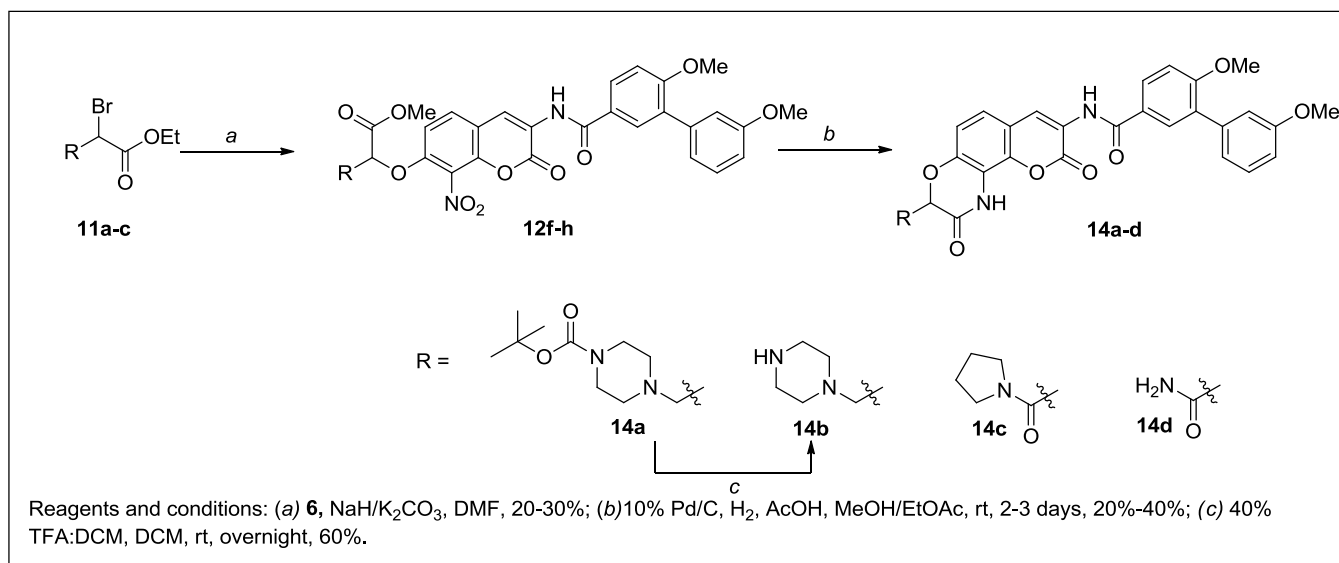
To elucidate these structure-activity relationships, a small library of aromatic- and amine-containing analogues was synthesized first. As shown in Scheme 2.3, the syntheses of aromatic analogues commenced by *O*-alkylation of phenol **6** with α -bromo esters **10a-e**²⁶⁻²⁸ to afford coumarin ethers **12a-e** in moderate yield. The resulting coumarin ethers **12a-e** were then reduced with Pd/C under a hydrogen atmosphere to furnish the free amines, which underwent an acid-catalyzed cyclization to afford lactams **13a-e**.

Scheme 2.3. Synthesis of aromatic-containing lactams.



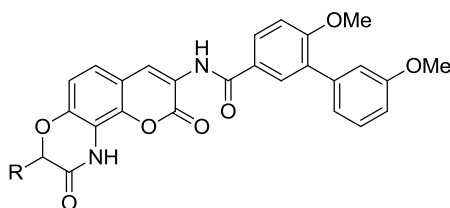
In parallel, the syntheses of amine-containing lactams (Scheme 2.4) were pursued by nucleophilic substitution of α -bromo esters **11a-c**²⁵ by phenol **6** to yield coumarin ethers **12f-h**, which in turn were subjected to a tandem reduction/intramolecular cyclization reaction, enlisting a Pd/C catalyst under hydrogen atmosphere to afford cyclic compounds **14a, 14c-d**. Compound **14b** was obtained by deprotection of the boc on amine **14a** using 40% trifluoroacetic acid in dichloromethane.

Scheme 2.4. Synthesis of amine-containing lactams.

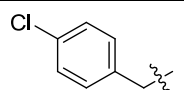
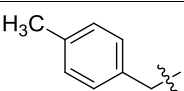
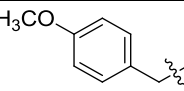
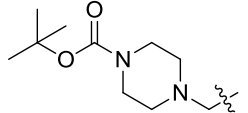
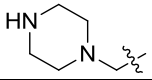
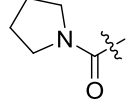
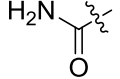


Upon their construction, the lactams were evaluated for anti-proliferative activity against SKBr3 and MCF-7 breast cancer cell lines (Table 2.2). In general, the aromatic-containing lactams were less effective than their amino counterparts, suggesting rigid moieties are not favorable. However, direct attachment of the aromatic moiety to the lactam core was found detrimental, as compound **13a** exhibited an IC_{50} value of $\sim 50 \mu M$. Although, the benzyl analogue (**13b**) manifested comparable activity to compound **9**, compounds **13c** and **13d** were inactive up to $50 \mu M$ against both cell lines. Interestingly, inclusion of a polar group onto the aromatic ring resulted in improved activity, as analogue **13e** exhibited 3~4 fold greater inhibitory activity than **13b**. These results suggest that a polar moiety attached to a more flexible linker may be beneficial. Consistent with the inhibitory data observed for aromatic-containing analogues, compound **14b** manifested improved inhibitory activity over compound **9**, while compound **14a** was inactive, suggesting that the polar moiety is necessary for activity, but a bulky group is not tolerable. Interestingly, replacement of the amino substituent with an amide resulted in inactive analogues (**9** vs **14c** and **14d**). This data suggest that the physiologically ionizable amine forms key interactions with the cognate protein and that these are critical for the manifestation of anti-proliferative activity.

Table 2.2. Anti-proliferative activity of aromatic- and amine-containing lactams.



Entry	R	SKBr3 (IC_{50} , μM)	MCF-7 (IC_{50} , μM)
13a		48.18 ± 2.28	>50
13b		21.49 ± 0.70	22.11 ± 0.64

13c		>50	>50
13d		>50	>50
13e		8.37 ± 1.41	6.12 ± 0.26
14a		>50	>50
14b		5.78 ± 0.91	5.27 ± 0.29
14c		>50	>50
14d		>50	33.35 ± 0.97

As mentioned earlier, preliminary structure-activity relationships suggest an amine and a flexible linker are important for inhibitory activity. To gain further insight into this region of the binding site, amino analogue **17a** (Figure 2.5B) that contains the pyrrolidine moiety tethered to the lactam core through a flexible linker was designed and docked into the Hsp90 C-terminal homology model. As shown in Figure 2.5A, the amine in pyrrolidine provides a hydrogen bonding interaction with Gln682 in the binding pocket. Interestingly, this pyrrolidine ring projects into a hydrophobic subpocket that allow for the inclusion of other substituents. Docking studies suggest there is ample space and further extension is possible. Therefore, it was hypothesized that incorporation of a two- or three-carbon tethered amine would project into the hydrophobic subpocket, while maintaining essential interactions between the ammonium group and complementary amino acids in the binding pocket. Towards this objective, several amines containing analogues with an ethylene or propylene linker were designed for elucidation of new structure-activity relationships. Amines were selected based on potential hydrogen bond interactions, ring size and sterics.

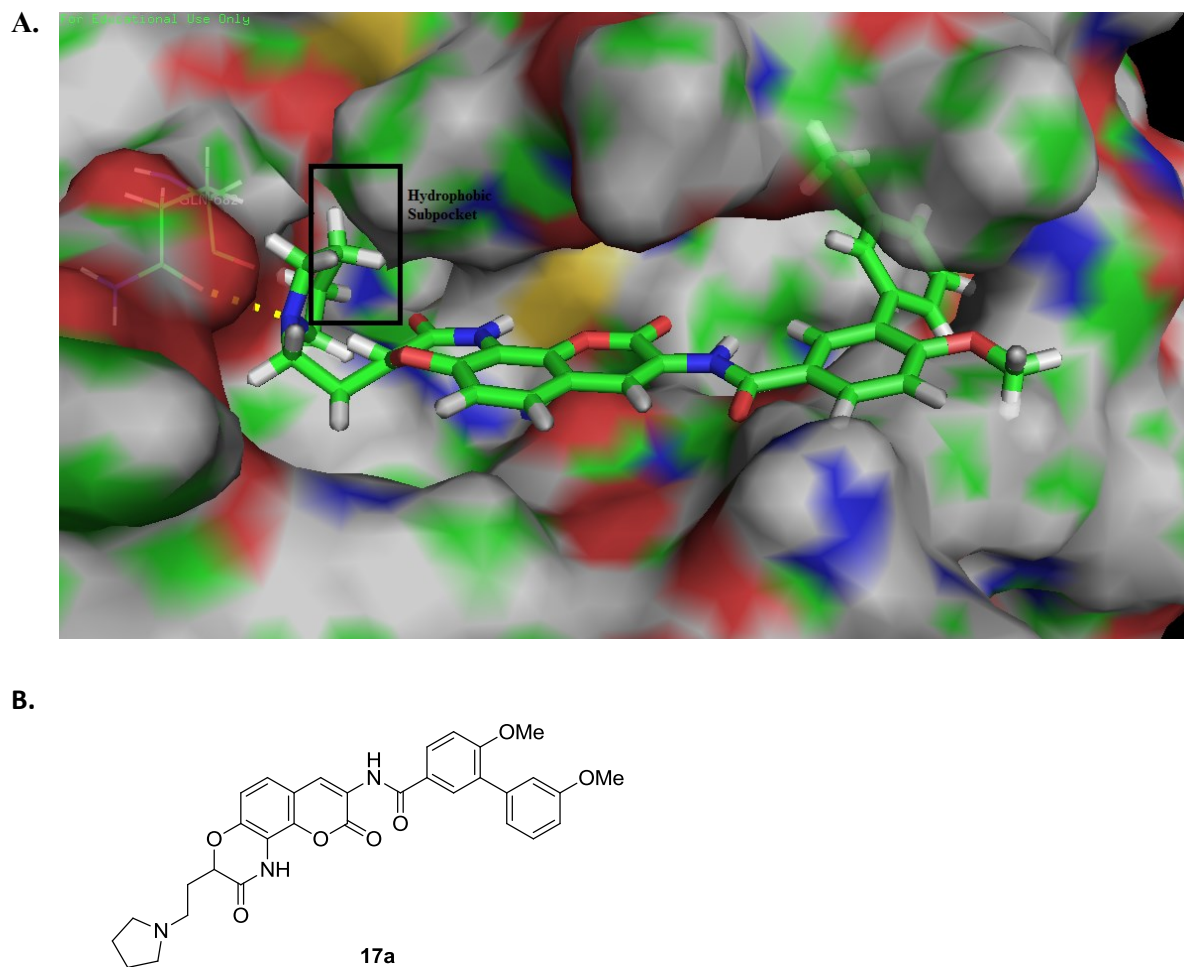
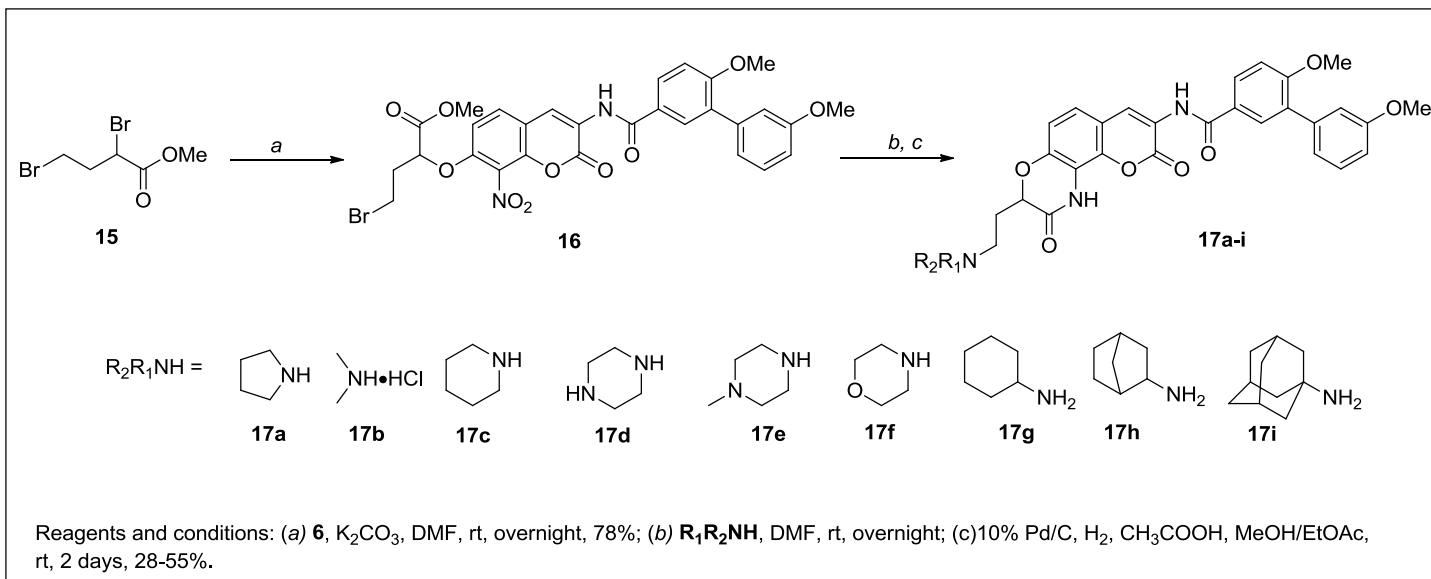


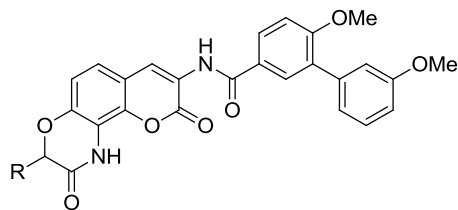
Figure 2.5. A. Docked structures of compound **17a** in the putative Hsp90 C-terminal binding site; B. structure of compound **17a**.

As shown in Scheme 2.5, the syntheses of ethylene-containing lactams was initiated by *O*-alkylation of phenol **6** with 2,4-dibromo ether **15** to give coumarin ether **16** in high yield. The resulting coumarin ether, **16**, was then treated with primary or secondary amines to give the corresponding products, which were then subjected to a tandem reduction/intramolecular ring closing, using a Pd/C catalyst under hydrogen atmosphere to furnish compounds **17a-i**.

Scheme 2.5. Synthesis of ethylene-containing lactams.



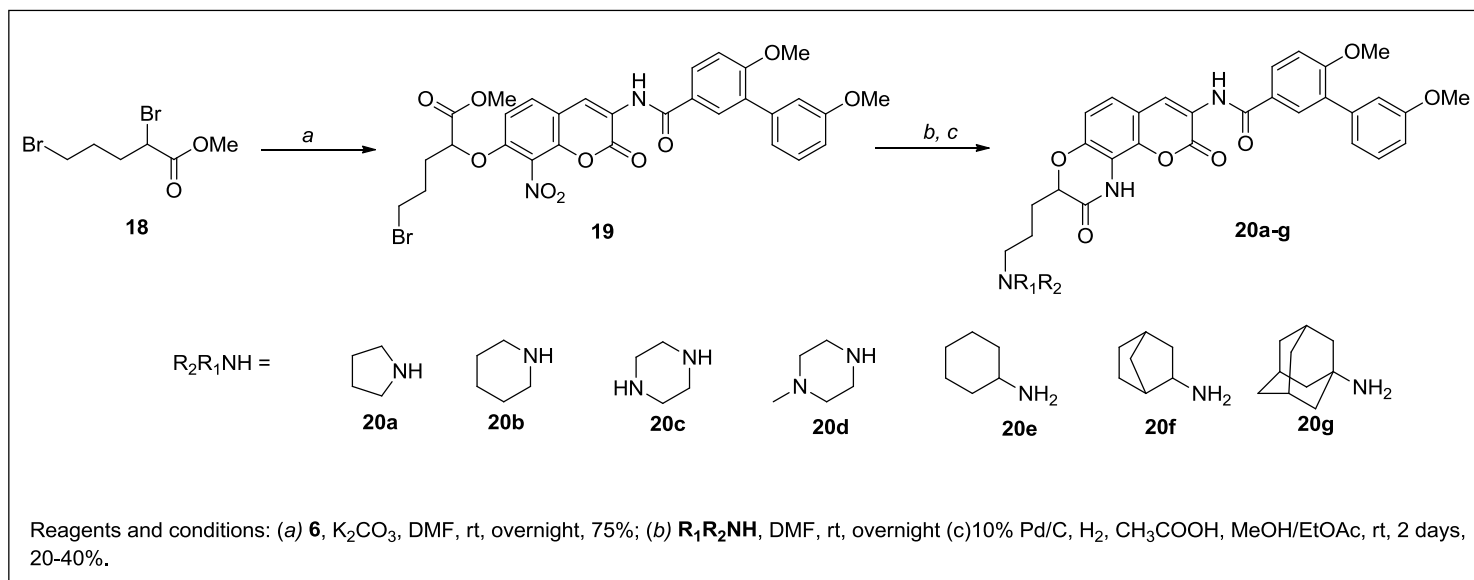
Upon completion of these ethylene-containing lactams, they were evaluated for anti-proliferative activity against SKBr3 and MCF-7 cell lines (Table 2.3). Consistent with docking studies, ethylene-containing lactams exhibited better inhibitory activity compared to their methylene-containing counterparts (**14** vs **17a**). Introduction of acyclic amine (**17b**) resulted in decreased potency, emphasizing a constrained ring system (entropy penalty) is important for activity. Increasing the ring to six atoms (**17c**) maintained activity, indicating various ring structures could be accommodated within the binding pocket. It was found that inclusion of a second hydrogen bond donor/acceptor (**17d**, **17e** and **17f**) decreased activity, suggesting the subpocket is hydrophobic in nature. Interestingly, the secondary amino analogues manifested better inhibitory activity than tertiary amino derivatives (**17g**, **17h** and **17i**). These data also suggest that bulky groups are tolerated in the binding pocket.

Table 2.3. Anti-proliferative activity of ethylene-containing lactams.

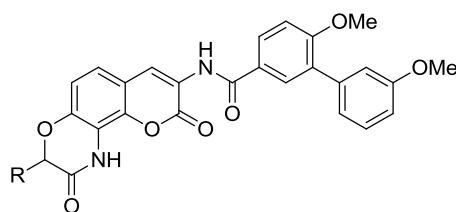
Entry	R	SKBr3 (IC ₅₀ , μM)	MCF-7 (IC ₅₀ , μM)
17a		3.49 ± 0.20	5.2 ± 0.38
17b		8.06 ± 0.82	11.40 ± 0.16
17c		1.03 ± 0.07	1.04 ± 0.01
17d		5.44 ± 0.12	7.63 ± 0.10
17e		4.1 ± 0.07	5.68 ± 0.37
17f		6.66 ± 0.47	7.44 ± 0.86
17g		0.78 ± 0.07	1.16 ± 0.04
17h		0.68 ± 0.04	1.22 ± 0.14
17i		0.88 ± 0.02	1.09 ± 0.17

With the SAR data from ethylene-containing lactams in hand, we next decided to investigate whether a two-carbon spacer is better. As discussed previously, docking studies suggested that analogues containing a three-carbon linker may maintain interactions with the binding pocket, but project deeper into the subpocket and therefore, manifest better affinity. Thus, a series of three carbon tethers were synthesized for comparison to their ethylene-containing counterparts. Following the scheme provided for the ethylene-containing lactams, the amino analogues containing a propylene linker were synthesized as shown in Scheme 2.6.

Scheme 2.6. Synthesis of propylene-containing lactams.



After completion of their syntheses, the propyl-amine lactams were evaluated for anti-proliferative activity against both cancer cell lines. As shown in Table 2.4, the analogues containing a propane linker exhibited better inhibitory activity than the corresponding ethylene-containing lactams, suggesting a three-carbon spacer is better at producing favorable interactions with the binding pocket. Similar to the trend observed with the ethylene-containing analogues, the piperidine (**20b**) analogue manifested improved anti-proliferative activity, while the piperazine (**20c**) and *N*-methylpiperazine (**20d**) resulted in decreased inhibitory activity. Interestingly, cyclohexylamino analog (**20e**) manifested the most potent inhibitory activity, validating that the propane linker is best at maintaining interactions with the binding pocket. Bicycloalkyl and tricyclic amino analogues (**20f**, **20g**) exhibited decreased activity, indicating a limited hydrophobic space within the binding pocket.

Table 2.4. Anti-proliferative activity of propylene-containing lactams.

Entry	R	SKBr3 (IC ₅₀ , μM)	MCF-7 (IC ₅₀ , μM)
20a		1.02 ± 0.19	1.49 ± 0.02
20b		0.78 ± 0.14	0.85 ± 0.05
20c		9.08 ± 0.02	12.85 ± 0.13
20d		1.76 ± 0.39	2.43 ± 0.45
20e		0.20 ± 0.08	0.35 ± 0.01
20f		1.26 ± 0.01	1.34 ± 0.11
20g		0.62 ± 0.01	0.72 ± 0.01

To confirm that the anti-proliferative activity observed exhibited by these lactams resulted from Hsp90 inhibition, Western blot analysis was performed on lysates treated with **17i**, **20b** and **20g**. Actin, an Hsp90-independent protein, was used as a negative control. As shown in Figure 2.6A, incubation with these compounds induced the degradation of Hsp90-dependent client proteins Her2, Raf-1, CDK6 and Akt, confirming these analogues manifest their cellular activity through Hsp90 inhibition. In addition, treatment of MCF-7 cells with **20b** induced the degradation of the Hsp90-dependent client proteins Her2, Raf-1, CDK6, and AKt in a concentration-dependent manner (Figure 2.6B). Actin levels remained unaffected, indicating selective degradation of Hsp90 client proteins. Additionally, Hsp90 levels were not changed, which is a hallmark manifested by Hsp90 C-terminal inhibitors.

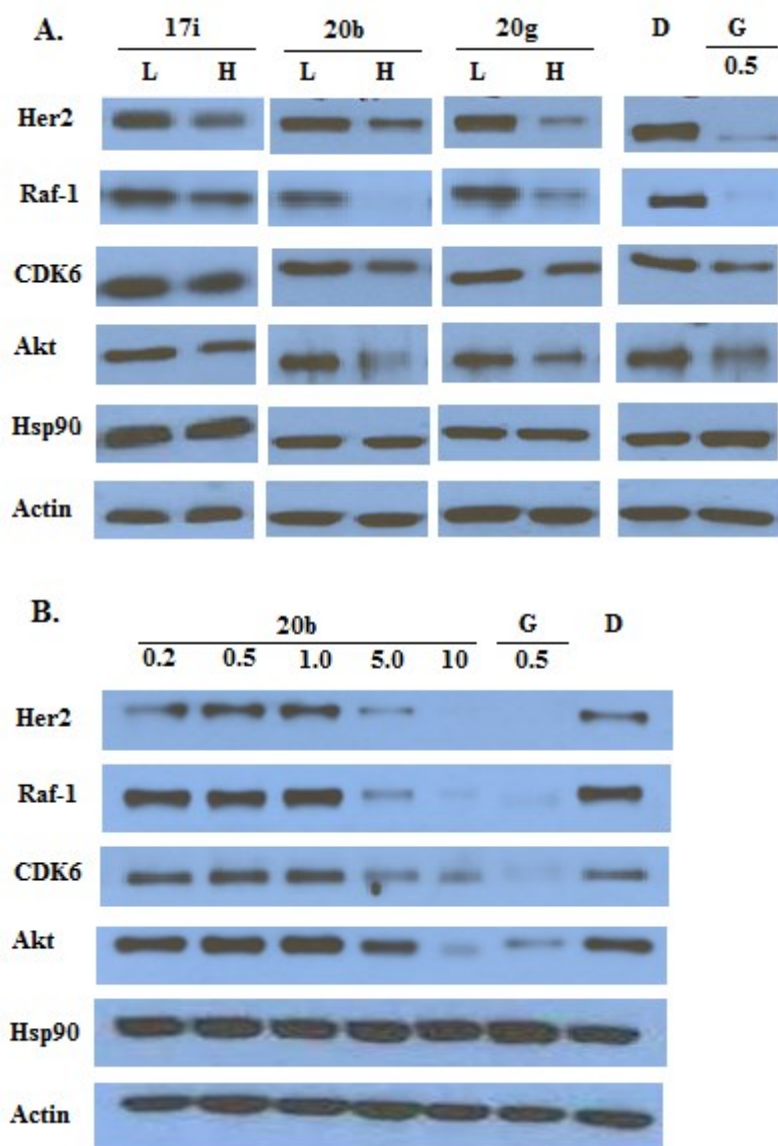


Figure 2.6. Western blot analyses of lactams after incubation with MCF-7 breast cancer cells for 24 h. Concentrations (in μM) are indicated above each lane. L represents a concentration $\frac{1}{2}$ of the anti-proliferative activity. H represents a concentration equal to 5-fold of the anti-proliferative activity. Geldanamycin (G, 0.5 μM) and dimethylsulfoxide (D, 100%) serve as positive and negative controls respectively.

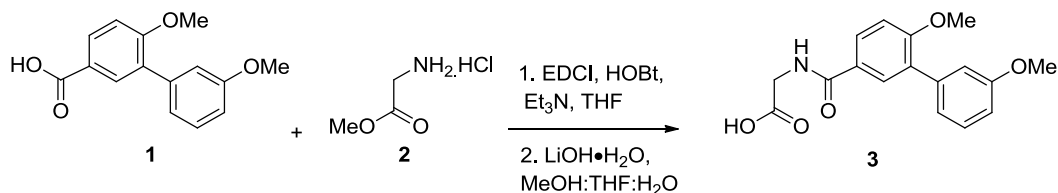
3. Conclusion and Future Directions

In summary, a series of ring-constrained novobiocin analogs was designed, synthesized and evaluated against MCF-7 and SKBr3 breast cancer cell lines. Incorporation of ring-constrained analogs led to the development of molecules that manifest sub micromolar to mid nanomolar inhibitory activity. SAR studies revealed that amines attached to a flexible linker manifested superior activity. In addition, it was determined that a three-

carbon spacer represents the optimal length for interactions with the binding pocket. Furthermore, studies showed that the inclusion of a bulky substituent is tolerated. The most active analogue **20e** manifests ~70 fold greater potency than KU174 and can serve as a lead compound for future analogue development.

4. Experimental Section

General procedure A: Amide coupling

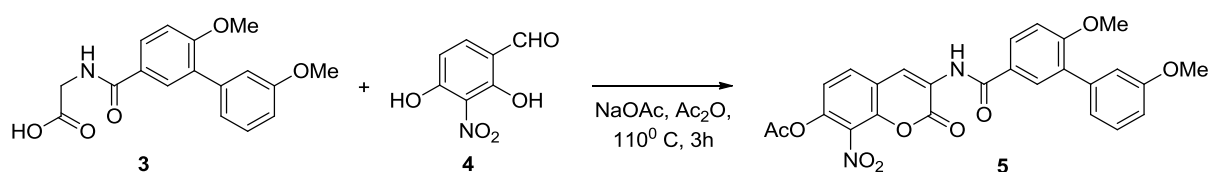


2-(3',6-Dimethoxy-[1,1'-biphenyl]-3-ylcarboxamido)acetic acid (3) A mixture of acid **1** (1.0 g, 3.87 mmol), glycine ester hydrochloride **2** (1.05 g, 4.65 mmol) and DMAP (10 mg, cat.) was dissolved in anhydrous THF (5ml) and treated with triethylamine (1.58 mL, 11.5 mmol). The reaction mixture (RM) was then cooled to 0 °C and EDCI.HCl (1.12 g, 5.78 mmol) was added to it. The resulting solution was allowed to stir at rt for 12 h. After 12 h, the RM was diluted with water (10 ml), pH adjusted to 7-8 with saturated sodium bicarbonate and extracted with EtOAc (3 X 15 ml). The organic layers were combined, dried (over Na₂SO₄) and concentrated under reduced pressure to residue. The residue was purified by column chromatography (SiO₂, 1:10, Methanol:DCM) to afford an ester as a colorless liquid (960 mg, 75%). ¹H NMR (500 MHz, Chloroform-d) δ 7.86 (dd, *J* = 8.6, 2.4 Hz, 1H), 7.83 (d, *J* = 2.4 Hz, 1H), 7.39 – 7.33 (m, 1H), 7.15 – 7.09 (m, 2H), 7.02 (dd, *J* = 8.7, 1.8 Hz, 1H), 6.93 (ddd, *J* = 8.3, 2.7, 1.1 Hz, 1H), 4.22 (s, 2H), 3.87 (s, 3H), 3.86 (s, 3H), 3.79 (s, 1H), 2.76 (s, 1H). ¹³C NMR (126 MHz, CDCl₃) δ 170.82, 167.42, 159.25, 159.19, 138.86, 130.40, 129.81, 129.05, 128.32, 125.74, 121.97, 115.21, 112.85, 110.83, 55.73, 55.26, 52.38, 41.56. HRMS (ESI⁺) *m/z*: [M + Na⁺] calcd for C₁₈H₁₉NO₅Na 352.1161; found 352.1165.

Lithium hydroxide (477.83 mg, 11.388 mmol) was added to the ester (750 mg, 2.28) in a solution of MeOH:THF:H₂O (2:2:1, 5 ml) and the resulting suspension was stirred at rt for 12 h. After 12 h, the RM was concentrated under reduced pressure to remove solvents. The residue was diluted with water (10 ml), pH adjusted to 3-5 and extracted with EtOAc (3 X 25 ml). The organic layers were combined, dried and concentrated to afford **3** as white

solid (675 mg, 94%). ^1H NMR (500 MHz, Chloroform-d) δ 7.84 – 7.80 (m, 1H), 7.76 (dd, J = 2.5, 1.1 Hz, 1H), 7.34 – 7.28 (m, 1H), 7.09 – 7.02 (m, 2H), 6.99 (d, J = 8.6 Hz, 1H), 6.88 (ddd, J = 8.3, 2.6, 1.0 Hz, 1H), 4.16 (s, 2H), 3.84 (s, 3H), 3.82 (s, 3H), 2.63 (s, 3H). ^{13}C NMR (126 MHz, CDCl_3) δ 170.90, 167.45, 159.41, 159.30, 138.94, 130.60, 129.86, 129.16, 128.42, 125.85, 122.08, 115.31, 112.99, 110.95, 55.86, 55.39, 52.56, 41.69. HRMS (ESI^+) m/z : $[\text{M} - \text{H}^+]$ calcd for $\text{C}_{17}\text{H}_{16}\text{NO}_5$ 314.1028; found 314.1022.

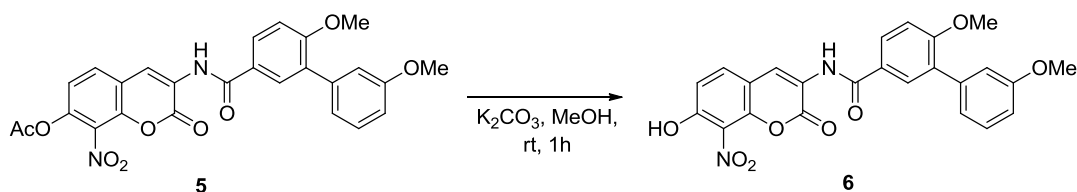
General procedure B: Aldol Condensation



3-(3',6-Dimethoxy-[1,1'-biphenyl]-3-ylcarboxamido)-8-nitro-2-oxo-2H-chromen-7-yl

acetate (5) A mixture of acid (300 mg, 0.951 mmol), nitro resorcinol (209 mg, 1.142 mmol), sodium acetate (312.04 mg, 3.804 mmol) and acetic anhydride (0.179 ml, 1.902 mmol) was heated at 110 °C for 3 h. After 3 h, the RM was allowed to cool to room temperature. The RM was diluted with water, pH adjusted to 5-6 with dilute HCl solution and extracted with EtOAc. The organic layer was collected, dried (over Na_2SO_4) and concentrated to residue. The residue was purified by column chromatography (SiO_2 , 1:99, Acetone:DCM) to afford desired product as a brownish amorphous solid (325 mg, 68 %). ^1H NMR (500 MHz, Chloroform-d) δ 8.90 (s, 1H), 8.76 (s, 1H), 7.96 – 7.86 (m, 2H), 7.71 (d, J = 8.7 Hz, 1H), 7.42 – 7.37 (m, 1H), 7.29 (d, J = 1.6 Hz, 1H), 7.16 – 7.08 (m, 3H), 6.96 (ddd, J = 8.3, 2.6, 1.0 Hz, 1H), 3.93 (s, 3H), 3.88 (s, 3H), 2.38 (s, 3H). ^{13}C NMR (126 MHz, CDCl_3) δ 166.86, 164.81, 159.32, 158.45, 155.65, 141.95, 140.60, 137.48, 130.31, 129.19, 128.81, 128.35, 128.33, 127.41, 124.33, 124.13, 121.05, 120.16, 119.67, 118.17, 114.42, 112.23, 110.21,

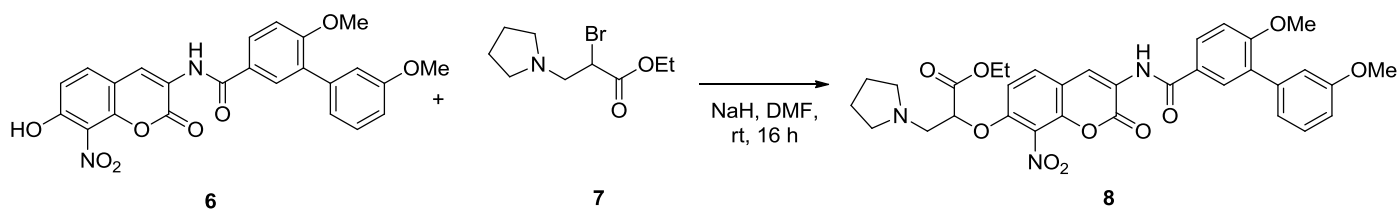
55.05, 54.44, 19.74. HRMS (ESI⁺) m/z: [M - H⁺] calcd for C₂₆H₁₉N₂O₉ 503.1091; found 503.0685.



N-(7-hydroxy-8-nitro-2-oxo-2H-chromen-3-yl)-3',6-dimethoxy-[1,1'-biphenyl]-3-

carboxamide (6) Potassium carbonate (0.267 g, 1.935 mmol) was added to a solution of **5** (0.32 g, 0.645 mmol) in anhydrous THF (2 ml) and the suspension was stirred at room temperature for 1 h. After 1 h, the RM was concentrated under reduced pressure to dryness and the residue was purified by column chromatography (SiO₂, 5:95 Acetone:DCM) to afford a yellow amorphous solid (280 mg, 96%). ¹H NMR (500 MHz, Chloroform-d) δ 10.69 (s, 1H), 8.85 (s, 1H), 8.68 (s, 1H), 7.95 – 7.88 (m, 2H), 7.70 (d, *J* = 8.9 Hz, 1H), 7.41 – 7.36 (m, 1H), 7.16 – 7.07 (m, 4H), 6.95 (ddd, *J* = 8.3, 2.6, 1.0 Hz, 1H), 3.92 (s, 3H), 3.87 (s, 3H). ¹³C NMR (126 MHz, CDCl₃) δ 165.91, 160.26, 159.49, 157.29, 156.42, 144.43, 138.56, 134.75, 131.36, 130.20, 129.38, 128.39, 125.56, 123.21, 122.74, 122.10, 116.58, 115.45, 113.73, 113.28, 111.22, 56.09, 55.48. HRMS (ESI⁺) m/z: [M - H⁺] calcd for C₂₄H₁₇N₂O₈ 461.0985; found 461.0980.

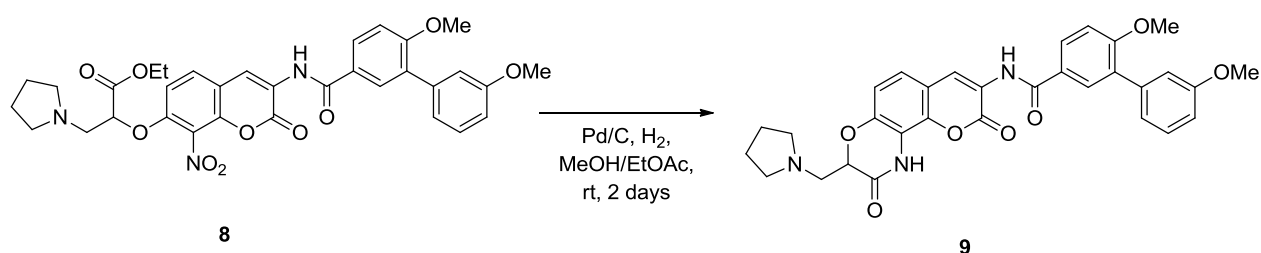
General procedure C: *O*-Alkylation



Ethyl 2-((3-(3',6-dimethoxy-[1,1'-biphenyl]-3-ylcarboxamido)-8-nitro-2-oxo-2H-chromen-7-yl)oxy)-3-(pyrrolidin-1-yl)propanoate (8) Sodium hydride (60%, 18.17 mg,

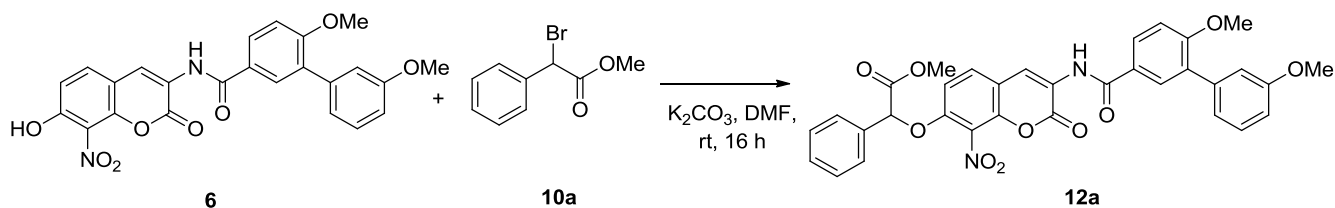
0.45 mmol) was added to a solution of **6** (100 mg, 0.2163 mmol) in anhydrous DMF (0.5 ml) and stirred at rt for 15 min. After 15 min, the solution was cooled to 0 °C and a solution of **7**²⁵ (162.33 mg, 0.649 mmol) in DMF (0.2 ml) was added. The solution was then allowed to stir at rt for 16 h. After 16 h, the RM was concentrated under reduced pressure to dryness. The resultant solid was diluted with water and extracted with EtOAc. The organic layer was collected, dried (over Na₂SO₄) and concentrated to residue. The residue was purified by column chromatography (SiO₂, 1:9, Methanol:DCM) to afford desired product as a brownish amorphous solid (65 mg, 48%). ¹H NMR (500 MHz, Chloroform-d) δ 8.81 (s, 1H), 8.67 (s, 1H), 7.90 – 7.80 (m, 2H), 7.54 (d, *J* = 8.9 Hz, 1H), 7.35 (t, *J* = 7.9 Hz, 1H), 7.12 – 7.01 (m, 4H), 6.92 (ddd, *J* = 8.4, 3.4, 2.3 Hz, 2H), 5.07 (dd, *J* = 6.5, 3.5 Hz, 1H), 4.22 (qt, *J* = 7.6, 3.8 Hz, 2H), 3.88 (s, 3H), 3.84 (s, 3H), 3.15 (dd, *J* = 9.2, 5.0 Hz, 2H), 2.75 – 2.64 (m, 4H), 1.83 – 1.71 (m, 4H), 1.32 – 1.18 (t, 3H). ¹³C NMR (126 MHz, CDCl₃) δ 168.41, 165.68, 160.11, 159.38, 157.02, 150.19, 141.90, 138.50, 131.14, 130.09, 129.92, 129.54, 129.26, 128.28, 125.50, 123.49, 122.06, 122.00, 115.34, 114.69, 113.15, 111.12, 110.92, 78.69, 62.02, 56.87, 55.98, 55.38, 54.95, 23.81, 14.15. HRMS (ESI⁺) *m/z*: [M - H⁺] calcd for C₃₃H₃₂N₃O₁₀ 630.2088; found 630.2103.

General procedure D: Tandem Reduction/Intramolecular Cyclization



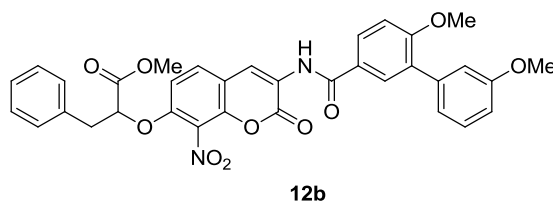
N-(2,9-dioxo-3-(pyrrolidin-1-ylmethyl)-1,2,3,9-tetrahydrochromeno[7,8-b][1,4]oxazin-8-yl)-3',6-dimethoxy-[1,1'-biphenyl]-3-carboxamide (9) Pd/C was added to a solution of **8** (50 mg, 0.016 mmol) in MeOH/EtOAc (1:1, 0.5 ml) and stirred at room temperature under hydrogen atmosphere for 2 days. After 2 days, RM was filtered through celite and filtrate was

concentrated under reduced pressure to get residue. The residue was purified by column chromatography (SiO₂, 5:95 MeOH:DCM) to afford a yellow amorphous solid (10 mg, 23%). ¹H NMR (400 MHz, Chloroform-d) δ 8.85 (s, 1H), 8.68 (s, 1H), 7.98 – 7.85 (m, 2H), 7.38 (t, *J* = 7.9 Hz, 1H), 7.22 – 7.06 (m, 5H), 7.03 (d, *J* = 8.5 Hz, 1H), 6.94 (ddd, *J* = 8.3, 2.6, 0.9 Hz, 1H), 4.90 (dd, *J* = 7.9, 2.9 Hz, 1H), 3.91 (s, 3H), 3.87 (s, 3H), 3.20 (dd, *J* = 13.7, 2.9 Hz, 1H), 3.07 (dd, *J* = 13.8, 7.9 Hz, 1H), 2.77 – 2.63 (m, 4H), 1.85 – 1.77 (m, 4H). ¹³C NMR (126 MHz, CDCl₃) δ 165.69, 164.43, 160.08, 159.46, 158.11, 144.03, 138.64, 136.95, 131.24, 130.07, 129.35, 128.39, 125.86, 124.03, 122.68, 122.11, 115.46, 114.74, 114.54, 114.49, 113.22, 111.20, 77.97, 56.07, 56.05, 55.47, 55.20, 23.82. HRMS (ESI⁺) *m/z*: [M + H⁺] calcd for C₃₁H₃₀N₃O₇ 556.2084; found 556.2103.

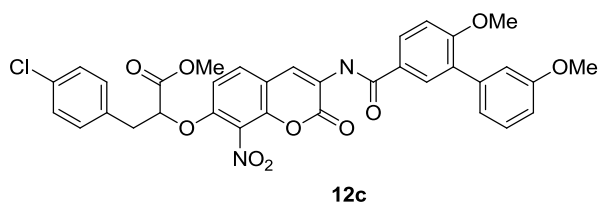


Methyl 2-((3-(3',6-dimethoxy-[1,1'-biphenyl]-3-ylcarboxamido)-8-nitro-2-oxo-2H-chromen-7-yl)oxy)-2-phenylacetate (12a) Potassium carbonate (59.70 mg, 0.433 mmol) was added to a solution of **6** (100 mg, 0.2163 mmol) in anhydrous DMF (0.5 ml) and stirred at rt for 15 min. After 15 min, the solution was cooled to 0 °C and a solution of **10a**²⁶ (148.63 mg, 0.649 mmol) in DMF (0.2 ml) was added. The solution was then allowed to stir at rt for 16 h. After 16 h, the RM was concentrated under reduced pressure to dryness. The resultant solid was diluted with water, pH adjusted to 6-7 and extracted with EtOAc (3 X 15 ml). The organic layer was collected, dried (over Na₂SO₄) and concentrated to residue. The residue was purified by column chromatography (SiO₂, 1:99, Acetone:DCM) to afford desired product as a brownish amorphous solid (280 mg, 96%). ¹H NMR (500 MHz, Chloroform-d) δ 8.83 (s, 1H), 8.69 (s, 1H), 7.95 – 7.84 (m, 2H), 7.58 – 7.51 (m, 3H), 7.45 – 7.41 (m, 3H), 7.41 – 7.35 (m, 1H), 7.15 – 7.06 (m, 3H), 6.98 – 6.89 (m,

2H), 5.80 (s, 1H), 3.91 (s, 3H), 3.87 (s, 3H), 3.76 (s, 3H). ^{13}C NMR (126 MHz, CDCl_3) δ 168.66, 165.80, 160.24, 159.47, 157.01, 149.58, 142.11, 138.55, 133.48, 131.34, 130.31, 130.17, 129.82, 129.66, 129.36, 129.21, 128.36, 127.11, 125.54, 123.76, 122.08, 121.91, 115.43, 115.15, 113.27, 111.22, 111.20, 79.97, 56.07, 55.47, 53.26. HRMS (ESI^+) m/z : $[\text{M} - \text{H}^+]$ calcd for $\text{C}_{33}\text{H}_{25}\text{N}_2\text{O}_{10}$ 609.1509; found 609.1432.

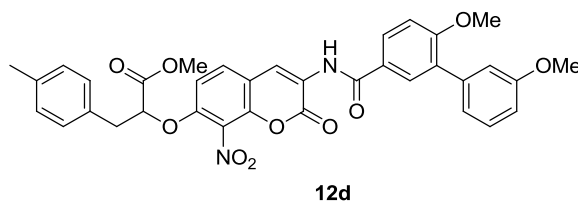


Methyl 2-((3-(3',6-dimethoxy-[1,1'-biphenyl]-3-ylcarboxamido)-8-nitro-2-oxo-2H-chromen-7-yl)oxy)-3-phenylpropanoate (12b) Compound **12b** was prepared from **6** using general procedure C and **10b**²⁷ to afford a brownish amorphous solid (15 mg, 28%). ^1H NMR (500 MHz, Chloroform- d) δ 8.81 (s, 1H), 8.67 (s, 1H), 7.94 – 7.83 (m, 2H), 7.49 (d, $J = 8.9$ Hz, 1H), 7.41 – 7.31 (m, 3H), 7.30 – 7.25 (m, 3H), 7.15 – 7.03 (m, 3H), 6.94 (ddd, $J = 8.2, 2.6, 0.9$ Hz, 1H), 6.73 (d, $J = 8.9$ Hz, 1H), 4.94 (dd, $J = 8.1, 4.4$ Hz, 1H), 3.91 (s, 3H), 3.86 (s, 3H), 3.76 (s, 3H), 3.38 – 3.22 (m, 2H). ^{13}C NMR (126 MHz, CDCl_3) δ 169.66, 165.79, 160.22, 159.47, 157.05, 150.20, 142.01, 138.55, 135.27, 131.33, 130.16, 129.99, 129.67, 129.53, 129.36, 128.82, 128.35, 127.54, 125.57, 123.61, 122.08, 121.96, 115.42, 114.86, 113.27, 111.20, 110.75, 79.50, 56.07, 55.47, 52.93, 38.87. HRMS (ESI^+) m/z : $[\text{M} - \text{H}^+]$ calcd for $\text{C}_{34}\text{H}_{27}\text{N}_2\text{O}_{10}$ 623.1741; found 623.1692.

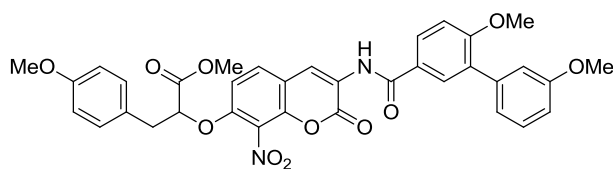


Methyl 3-(4-chlorophenyl)-2-((3-(3',6-dimethoxy-[1,1'-biphenyl]-3-ylcarboxamido)-8-nitro-2-oxo-2H-chromen-7-yl)oxy)propanoate (12c) Compound **12c** was prepared from **6** using general procedure C and **10c**²⁸ to afford a brownish amorphous solid (22 mg, 28%). ^1H

NMR (500 MHz, Chloroform-d) δ 8.82 (s, 1H), 8.67 (s, 1H), 7.93 – 7.85 (m, 2H), 7.51 (d, J = 8.9 Hz, 1H), 7.37 (t, J = 7.9 Hz, 1H), 7.34 – 7.28 (m, 2H), 7.23 – 7.16 (m, 2H), 7.14 – 7.06 (m, 3H), 6.94 (ddd, J = 8.3, 2.6, 0.9 Hz, 1H), 6.74 (d, J = 8.9 Hz, 1H), 4.91 (dd, J = 7.9, 4.2 Hz, 1H), 3.91 (s, 3H), 3.86 (s, 3H), 3.76 (s, 3H), 3.29 – 3.24 (m, 2H). ^{13}C NMR (126 MHz, CDCl_3) δ 169.52, 165.93, 160.36, 159.59, 157.12, 150.12, 142.13, 138.66, 133.77, 133.68, 131.46, 131.17, 130.28, 130.07, 129.69, 129.48, 129.09, 128.80, 128.47, 125.66, 123.81, 122.20, 122.00, 115.54, 115.13, 113.39, 111.32, 110.73, 79.16, 56.19, 55.58, 53.12, 38.27. HRMS (ESI⁺) m/z : $[\text{M} - \text{H}^+]$ calcd for $\text{C}_{34}\text{H}_{26}\text{ClN}_2\text{O}_{10}$ 657.1276; found 657.1305.

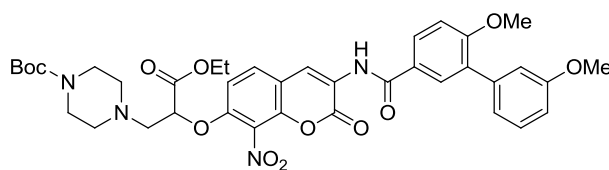


Methyl 2-((3-(3',6-dimethoxy-[1,1'-biphenyl]-3-yl)carboxamido)-8-nitro-2-oxo-2H-chromen-7-yl)oxy)-3-(p-tolyl)propanoate (12d) Compound **12d** was prepared from **6** using general procedure C and **10d**²⁸ to afford a brownish amorphous solid (35 mg, 38%). ^1H NMR (500 MHz, Chloroform-d) δ 8.81 (s, 1H), 8.67 (s, 1H), 7.92 – 7.84 (m, 2H), 7.49 (d, J = 8.9 Hz, 1H), 7.37 (t, J = 7.9 Hz, 1H), 7.14 (s, 4H), 7.11 (ddd, J = 7.6, 1.6, 1.0 Hz, 1H), 7.09 – 7.06 (m, 2H), 6.94 (ddd, J = 8.3, 2.6, 0.9 Hz, 1H), 6.74 (d, J = 8.9 Hz, 1H), 4.91 (dd, J = 7.9, 4.5 Hz, 1H), 3.91 (s, 3H), 3.86 (s, 3H), 3.76 (s, 3H), 3.29 – 3.21 (m, 2H), 2.33 (s, 3H). ^{13}C NMR (126 MHz, CDCl_3) δ 169.75, 165.82, 160.24, 159.48, 157.08, 150.28, 142.03, 138.57, 137.17, 132.17, 131.34, 130.18, 129.98, 129.55, 129.51, 129.38, 128.37, 125.59, 123.60, 122.10, 122.02, 115.44, 114.82, 113.29, 111.22, 110.77, 79.63, 56.08, 55.49, 52.92, 38.48, 21.27. HRMS (ESI⁺) m/z : $[\text{M} - \text{H}^+]$ calcd for $\text{C}_{35}\text{H}_{29}\text{N}_2\text{O}_{10}$ 637.1822; found 637.1802.



12e

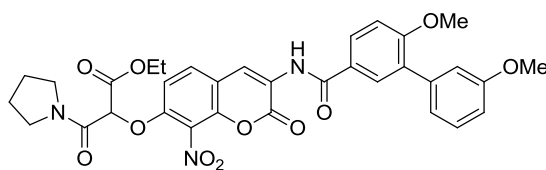
Methyl 2-((3-(3',6-dimethoxy-[1,1'-biphenyl]-3-yl)carboxamido)-8-nitro-2-oxo-2H-chromen-7-yl)oxy)-3-(4-methoxyphenyl)propanoate (12e) Compound **12e** was prepared from **6** using general procedure C and **10e**²⁸ to afford a brownish yellow amorphous solid (26 mg, 32%). ¹H NMR (500 MHz, Chloroform-d) δ 8.81 (s, 1H), 8.67 (s, 1H), 7.95 – 7.82 (m, 2H), 7.49 (d, J = 8.9 Hz, 1H), 7.37 (t, J = 7.9 Hz, 1H), 7.18 (d, J = 2.1 Hz, 1H), 7.15 – 7.10 (m, 2H), 7.09 – 7.06 (m, 2H), 6.94 (ddd, J = 8.3, 2.6, 1.0 Hz, 1H), 6.87 (d, J = 8.7 Hz, 2H), 6.74 (d, J = 9.0 Hz, 1H), 4.90 (dd, J = 7.8, 4.5 Hz, 1H), 3.91 (s, 3H), 3.86 (s, 3H), 3.80 (s, 4H), 3.75 (s, 3H), 3.27 – 3.21 (m, 2H). ¹³C NMR (126 MHz, CDCl₃) δ 169.59, 165.67, 160.09, 159.33, 158.87, 156.93, 150.14, 141.88, 138.42, 131.20, 130.61, 130.47, 130.03, 129.41, 129.23, 128.22, 127.06, 123.46, 121.95, 121.86, 115.29, 114.68, 114.05, 113.88, 113.14, 111.07, 110.61, 79.51, 55.93, 55.33, 55.24, 52.76, 37.90. HRMS (ESI⁺) m/z : [M - H⁺] calcd for C₃₅H₂₉N₂O₁₁ 653.1771; found 653.1692.



12f

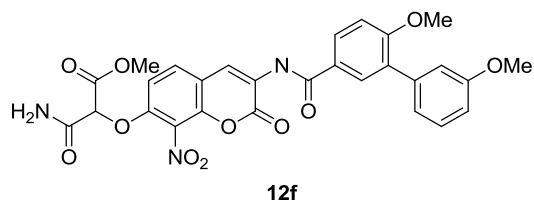
tert-butyl 4-(2-((3-(3',6-dimethoxy-[1,1'-biphenyl]-3-yl)carboxamido)-8-nitro-2-oxo-2H-chromen-7-yl)oxy)-3-ethoxy-3-oxopropyl)piperazine-1-carboxylate (12f) Compound **12f** was prepared from **6** using general procedure C and **11a**²⁵ to afford a brownish yellow amorphous solid (60 mg, 30%). ¹H NMR (500 MHz, Chloroform-d) δ 8.84 (s, 1H), 8.68 (s, 1H), 7.95 – 7.79 (m, 2H), 7.56 (d, J = 8.9 Hz, 1H), 7.37 (t, J = 7.9 Hz, 1H), 7.16 – 7.05 (m, 3H), 6.97 – 6.93 (m, 1H), 6.90 (d, J = 7.6 Hz, 1H), 4.34 – 4.15 (m, 1H), 3.91 (s, 3H), 3.86 (s,

3H), 3.49 – 3.28 (m, 3H), 3.13 – 2.97 (m, 2H), 2.71 – 2.42 (m, 4H), 1.27 (t, $J = 7.1$ Hz, 4H). ^{13}C NMR (126 MHz, CDCl_3) δ 168.50, 165.82, 160.24, 159.47, 157.06, 154.82, 150.23, 142.00, 138.55, 131.33, 130.17, 130.09, 129.60, 129.36, 128.36, 125.55, 123.70, 122.08, 121.99, 115.43, 114.98, 113.26, 111.21, 111.01, 79.90, 78.59, 59.30, 56.07, 55.47, 53.77, 28.55, 14.33. HRMS (ESI⁺) m/z : $[\text{M} - \text{H}^+]$ calcd for $\text{C}_{38}\text{H}_{41}\text{N}_4\text{O}_{12}$ 745.2721; found 745.2815.

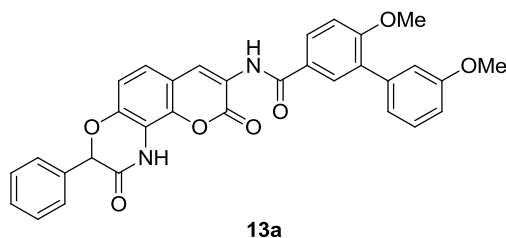


12g

Ethyl 2-((3-(3',6-dimethoxy-[1,1'-biphenyl]-3-yl)carboxamido)-8-nitro-2-oxo-2H-chromen-7-yl)oxy)-3-oxo-3-(pyrrolidin-1-yl)propanoate (12g) Compound **12g** was prepared from **6** using general procedure C and **11b** to afford a brownish amorphous solid (60 mg, 30%). ^1H NMR (500 MHz, Chloroform- d) δ 8.84 (s, 1H), 8.68 (s, 1H), 7.95 – 7.79 (m, 2H), 7.56 (d, $J = 8.9$ Hz, 1H), 7.37 (t, $J = 7.9$ Hz, 1H), 7.16 – 7.05 (m, 3H), 6.97 – 6.93 (m, 1H), 6.90 (d, $J = 7.6$ Hz, 1H), 4.34 – 4.15 (m, 1H), 3.91 (s, 3H), 3.86 (s, 3H), 3.49 – 3.28 (m, 3H), 3.13 – 2.97 (m, 2H), 2.71 – 2.42 (m, 4H), 1.27 (t, $J = 7.1$ Hz, 4H). ^{13}C NMR (126 MHz, CDCl_3) δ 168.50, 165.82, 160.24, 159.47, 157.06, 154.82, 150.23, 142.00, 138.55, 131.33, 130.17, 130.09, 129.60, 129.36, 128.36, 125.55, 123.70, 122.08, 121.99, 115.43, 114.98, 113.26, 111.21, 111.01, 79.90, 78.59, 59.30, 56.07, 55.47, 53.77, 28.55, 14.33. HRMS (ESI⁺) m/z : $[\text{M} - \text{H}^+]$ calcd for $\text{C}_{38}\text{H}_{41}\text{N}_4\text{O}_{12}$ 745.2721; found 745.2815.

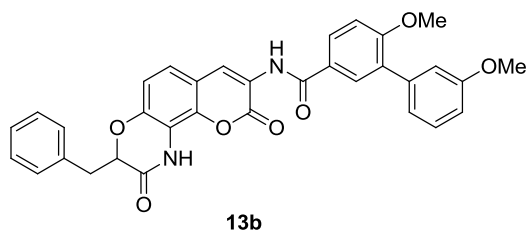


Ethyl 3-amino-2-(((3-(3',6-dimethoxy-[1,1'-biphenyl]-3-yl)carboxamido)-8-nitro-2-oxo-2H-chromen-7-yl)oxy)-3-oxopropanoate (12f) Compound **12f** was prepared from **6** using general procedure C and **11c** to afford a brownish amorphous solid (75 mg, 59%). ¹H NMR (500 MHz, Chloroform-d) δ 8.90 – 8.83 (m, 1H), 8.75 – 8.69 (m, 1H), 7.94 – 7.84 (m, 2H), 7.69 – 7.63 (m, 1H), 7.42 – 7.35 (m, 1H), 7.16 – 7.04 (m, 3H), 7.01 – 6.89 (m, 2H), 6.69 (s, 2H), 5.34 – 5.22 (m, 1H), 3.92 (s, 3H), 3.89 (s, 3H), 3.87 (s, 3H). ¹³C NMR (126 MHz, CDCl₃) δ 165.86, 165.20, 164.84, 160.35, 159.49, 156.76, 148.61, 142.39, 138.51, 131.41, 130.58, 130.18, 129.39, 128.43, 125.40, 124.31, 122.08, 121.42, 116.35, 115.48, 113.26, 111.25, 110.74, 78.14, 56.09, 55.48, 54.01. HRMS (ESI⁺) m/z: [M - H⁺] calcd for C₂₉H₂₄N₃O₁₁ 590.1411; found 590.1437.

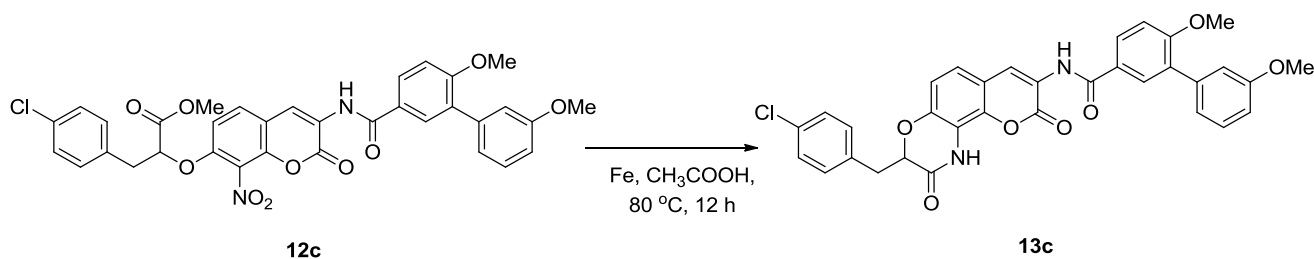


N-(2,9-dioxo-3-phenyl-1,2,3,9-tetrahydrochromeno[7,8-b][1,4]oxazin-8-yl)-3',6-dimethoxy-[1,1'-biphenyl]-3-carboxamide (13a) Compound **13a** was prepared from **12a** using general procedure D to afford a white amorphous solid (5 mg, 56%). ¹H NMR (500 MHz, Chloroform-d) δ 8.84 (s, 1H), 8.67 (s, 1H), 8.18 (s, 1H), 7.91 (dd, *J* = 8.6, 2.5 Hz, 1H), 7.88 (d, *J* = 2.4 Hz, 1H), 7.49 – 7.42 (m, 2H), 7.40 – 7.34 (m, 4H), 7.18 (d, *J* = 8.6 Hz, 1H), 7.14 – 7.02 (m, 4H), 6.94 (ddd, *J* = 8.3, 2.6, 1.0 Hz, 1H), 5.81 (s, 1H), 3.90 (s, 3H), 3.86 (s, 3H). ¹³C NMR (126 MHz, CDCl₃) δ 165.68, 163.67, 160.11, 159.47, 158.02, 143.85, 138.64,

137.05, 134.50, 131.26, 130.07, 129.37, 129.36, 129.01, 128.40, 126.96, 125.83, 123.88, 122.83, 122.33, 122.11, 115.46, 114.96, 114.68, 114.30, 113.23, 111.21, 79.11, 56.06, 55.48. HRMS (ESI⁺) m/z: [M + H⁺] calcd for C₃₂H₂₅N₂O₇ 549.1662 ; found 549.1698.



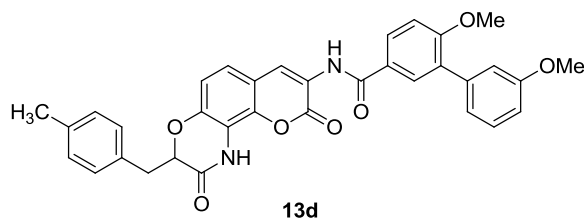
N-(3-benzyl-2,9-dioxo-1,2,3,9-tetrahydrochromeno[7,8-b][1,4]oxazin-8-yl)-3',6-dimethoxy-[1,1'-biphenyl]-3-carboxamide (13b) Compound **13b** was prepared from **12b** using general procedure D to afford a white amorphous solid (5 mg, 36%). ¹H NMR (500 MHz, Chloroform-d) δ 8.78 (d, *J* = 2.3 Hz, 1H), 7.87 (dd, *J* = 8.6, 2.5 Hz, 1H), 7.82 (d, *J* = 2.4 Hz, 1H), 7.32 (t, *J* = 7.9 Hz, 1H), 7.26 – 7.15 (m, 5H), 7.12 (dd, *J* = 8.5, 3.6 Hz, 1H), 7.07 (dt, *J* = 7.7, 1.2 Hz, 1H), 7.06 – 7.02 (m, 2H), 6.93 – 6.85 (m, 2H), 4.84 (ddd, *J* = 22.1, 8.8, 3.6 Hz, 1H), 3.86 (s, 3H), 3.82 (s, 3H), 3.25 (ddd, *J* = 14.7, 8.2, 3.6 Hz, 1H), 3.10 (dd, *J* = 14.6, 8.7 Hz, 1H). ¹³C NMR (126 MHz, CDCl₃) δ 164.51, 163.57, 158.92, 158.30, 156.88, 142.57, 137.47, 135.72, 134.67, 130.08, 128.98, 128.88, 128.70, 128.61, 128.18, 127.42, 127.21, 126.03, 124.68, 122.77, 121.53, 120.99, 120.93, 114.29, 113.53, 113.42, 113.15, 112.05, 110.03, 77.34, 54.88, 54.30, 36.06. HRMS (ESI⁺) m/z: [M + H⁺] calcd for C₃₃H₂₇N₂O₇ 563.1818; found 563.1901.



N-(3-(4-chlorobenzyl)-2,9-dioxo-1,2,3,9-tetrahydrochromeno[7,8-b][1,4]oxazin-8-yl)-

3',6-dimethoxy-[1,1'-biphenyl]-3-carboxamide (13c)

A suspension of **12c** (25 mg, 0.037 mmol) and iron metal (10.24 mg, 0.186 mmol) was heated at 80 °C for 12 h. After 12 h, the RM was concentrated, filtered through celite and extracted with EtOAc (3 X 5 ml). The organic layers were combined, dried (over Na₂SO₄) and concentrated to residue. The residue was purified by column chromatography (SiO₂, 2:98, Acetone:DCM) to afford desired product as a white amorphous solid (14 mg, 61%). ¹H NMR (500 MHz, Chloroform-d) δ 8.77 (s, 1H), 7.90 – 7.84 (m, 1H), 7.81 (t, *J* = 2.4 Hz, 1H), 7.32 (dd, *J* = 9.0, 6.9 Hz, 1H), 7.24 – 7.18 (m, 2H), 7.18 – 7.10 (m, 3H), 7.08 – 7.03 (m, 3H), 6.90 – 6.85 (m, 2H), 4.80 (ddd, *J* = 8.7, 3.8, 2.2 Hz, 1H), 3.85 (s, 3H), 3.81 (s, 3H), 3.23 (dt, *J* = 14.8, 3.0 Hz, 1H), 3.15 – 3.04 (m, 1H). ¹³C NMR (126 MHz, CDCl₃) δ 165.86, 165.18, 160.05, 159.34, 158.30, 143.81, 138.58, 137.20, 134.39, 132.97, 131.12, 131.06, 129.94, 129.27, 128.60, 128.37, 125.68, 124.40, 122.39, 122.18, 122.03, 115.36, 114.75, 114.59, 114.49, 113.12, 111.18, 77.97, 55.95, 55.38, 36.26. HRMS (ESI⁺) *m/z*: [M + H⁺] calcd for C₃₃H₂₆N₂O₇ 597.1429; found 597.3356.

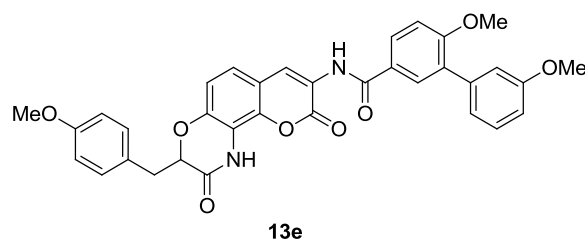


3',6-Dimethoxy-N-(3-(4-methylbenzyl)-2,9-dioxo-1,2,3,9-tetrahydrochromeno[7,8-

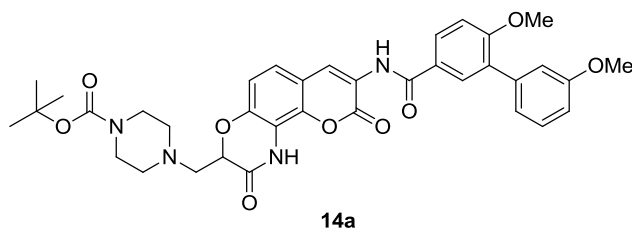
b][1,4]oxazin-8-yl)-[1,1'-biphenyl]-3-carboxamide (13d)

Compound **13d** was prepared from **12d** using general procedure D to afford a white amorphous solid (12 mg, 55%). ¹H

NMR (500 MHz, Chloroform-d) δ 8.84 (d, $J = 2.9$ Hz, 1H), 8.67 (d, $J = 2.9$ Hz, 1H), 8.05 (d, $J = 4.2$ Hz, 1H), 7.95 – 7.83 (m, 2H), 7.37 (td, $J = 7.9, 2.8$ Hz, 1H), 7.20 – 7.03 (m, 8H), 6.97 – 6.89 (m, 2H), 4.90 (dt, $J = 8.5, 3.2$ Hz, 1H), 3.90 (d, $J = 2.8$ Hz, 3H), 3.86 (d, $J = 2.9$ Hz, 3H), 3.28 (dt, $J = 14.8, 3.2$ Hz, 1H), 3.13 (ddd, $J = 14.4, 8.8, 2.7$ Hz, 1H), 2.31 (d, $J = 2.7$ Hz, 3H). ^{13}C NMR (126 MHz, CDCl_3) δ 165.70, 164.85, 160.10, 159.48, 158.09, 143.75, 138.65, 136.92, 136.83, 132.76, 131.26, 130.07, 129.63, 129.36, 129.32, 128.40, 125.86, 124.00, 122.68, 122.16, 122.11, 115.47, 114.70, 114.66, 114.40, 113.23, 111.21, 78.67, 56.06, 55.48, 36.77, 21.24. HRMS (ESI^+) m/z : $[\text{M} + \text{Na}^+]$ calcd for $\text{C}_{34}\text{H}_{28}\text{N}_2\text{O}_7\text{Na}$ 599.1794; found 599.1805.



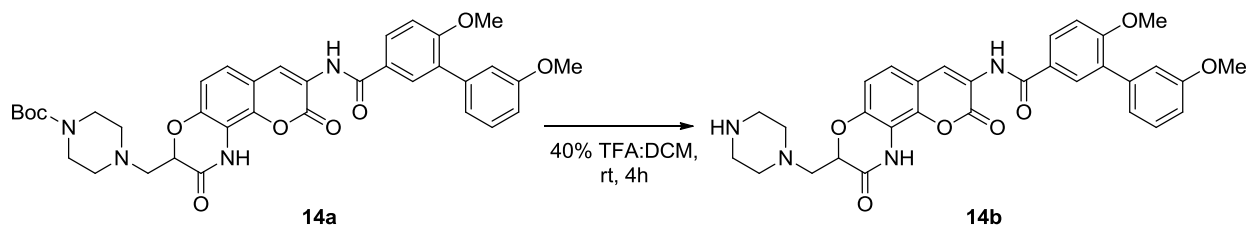
3',6-Dimethoxy-N-(3-(4-methoxybenzyl)-2,9-dioxo-1,2,3,9-tetrahydrochromeno[7,8-b][1,4]oxazin-8-yl)-[1,1'-biphenyl]-3-carboxamide (13e) Compound **13e** was prepared from **12e** using general procedure D to afford a white amorphous solid (20 mg, 80%). ^1H NMR (500 MHz, Chloroform-d) δ 8.84 (s, 1H), 8.68 (s, 1H), 8.12 (s, 1H), 7.95 – 7.83 (m, 2H), 7.36 (t, $J = 7.9$ Hz, 1H), 7.21 – 7.04 (m, 7H), 6.93 (dd, $J = 8.0, 2.7$ Hz, 2H), 6.85 – 6.80 (m, 2H), 4.88 (dd, $J = 8.5, 3.7$ Hz, 1H), 3.90 (s, 3H), 3.86 (s, 3H), 3.77 (s, 3H), 3.25 (dd, $J = 14.7, 3.7$ Hz, 1H), 3.13 (dd, $J = 14.7, 8.5$ Hz, 1H). ^{13}C NMR (126 MHz, CDCl_3) δ 165.94, 165.12, 160.34, 159.72, 159.04, 158.34, 144.03, 138.90, 137.17, 131.48, 131.08, 130.33, 129.60, 128.65, 128.02, 126.10, 124.25, 122.92, 122.39, 122.36, 115.72, 114.93, 114.82, 114.61, 114.24, 113.46, 111.45, 78.93, 56.30, 55.72, 55.63, 36.63. HRMS (ESI^+) m/z : $[\text{M} + \text{H}^+]$ calcd for $\text{C}_{34}\text{H}_{29}\text{N}_2\text{O}_8$ 593.1924; found 593.3711.



tert-butyl 4-((8-(3',6-dimethoxy-[1,1'-biphenyl]-3-ylcarboxamido)-2,9-dioxo-1,2,3,9-tetrahydrochromeno[7,8-b][1,4]oxazin-3-yl)methyl)piperazine-1-carboxylate (14a)

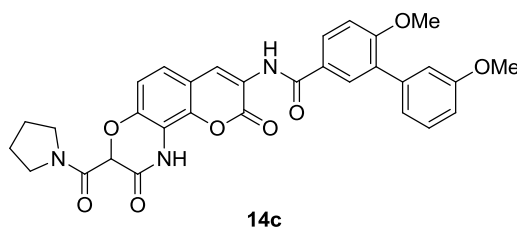
Compound **14a** was prepared from **12f** using general procedure D to afford a white amorphous solid (22 mg, 31%). ¹H NMR (500 MHz, Chloroform-d + CD₃OD) δ 8.78 (s, 1H), 8.62 (s, 1H), 7.91 – 7.81 (m, 2H), 7.34 (t, *J* = 7.9 Hz, 1H), 7.22 (d, *J* = 8.5 Hz, 1H), 7.14 – 7.01 (m, 3H), 6.98 (d, *J* = 8.5 Hz, 1H), 6.91 (dd, *J* = 8.1, 2.6 Hz, 1H), 4.99 (dd, *J* = 7.0, 3.1 Hz, 1H), 3.87 (s, 3H), 3.84 (s, 3H), 3.41 (q, *J* = 5.8 Hz, 4H), 3.21 (dd, *J* = 14.4, 3.1 Hz, 1H), 2.92 (dd, *J* = 14.4, 7.1 Hz, 1H), 2.65 – 2.54 (m, 4H), 1.44 (s, 9H). ¹³C NMR (126 MHz, CDCl₃) δ 165.86, 161.65, 160.07, 159.35, 158.54, 154.86, 146.81, 139.18, 138.57, 131.13, 129.97, 129.28, 128.38, 125.65, 124.54, 124.45, 122.41, 122.04, 118.11, 116.17, 115.36, 114.25, 113.13, 111.18, 80.13, 78.57, 57.34, 57.31, 55.96, 55.39, 53.47, 28.40. HRMS (ESI⁺) *m/z*: [M - Boc] calcd for C₃₁H₃₀N₄O₇ 570.2114; found 570.3211.

General procedure E: Boc-deprotection



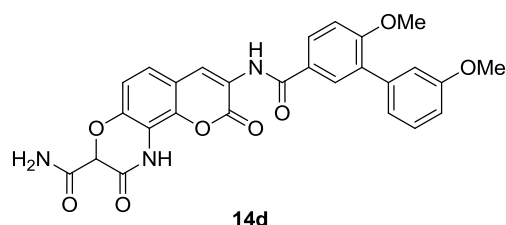
N-(2,9-dioxo-3-(piperazin-1-ylmethyl)-1,2,3,9-tetrahydrochromeno[7,8-b][1,4] oxazin-8-yl)-3',6-dimethoxy-[1,1'-biphenyl]-3-carboxamide (14b) A solution of **14a** (15 mg, 0.022 mmol) in 40% TFA:DCM was stirred at rt for 4 h. After 4 h, the RM was concentrated, pH

adjusted to 8, and extracted with EtOAc (3 X 5 ml). The organic layers were combined, dried (over Na₂SO₄) and concentrated to residue. The residue was purified by column chromatography (SiO₂, 1:9, Methanol:DCM) to afford desired product as a white amorphous solid (5 mg, 42%). ¹H NMR (500 MHz, Chloroform-d) δ 8.74 (s, 1H), 7.85 (dd, *J* = 8.6, 2.5 Hz, 1H), 7.80 (d, *J* = 2.4 Hz, 1H), 7.30 (t, *J* = 8.0 Hz, 1H), 7.21 (d, *J* = 8.6 Hz, 1H), 7.06 – 7.01 (m, 3H), 6.94 (d, *J* = 8.5 Hz, 1H), 6.87 (ddd, *J* = 8.2, 2.6, 0.9 Hz, 1H), 4.79 (dd, *J* = 6.6, 3.3 Hz, 1H), 3.84 (s, 3H), 3.79 (s, 3H), 3.09 – 2.92 (m, 6H), 2.83 – 2.69 (m, 4H). ¹³C NMR (126 MHz, CDCl₃+CH₃OH) δ 166.10, 161.68, 160.15, 159.39, 158.50, 146.67, 139.21, 138.64, 131.17, 130.04, 129.32, 128.46, 125.66, 124.62, 124.56, 122.56, 122.09, 118.06, 116.39, 115.40, 114.18, 113.17, 111.27, 78.63, 56.97, 55.99, 55.41, 51.06, 43.89, 29.78. HRMS (ESI⁺) *m/z*: [M + H⁺] calcd for C₃₁H₃₁N₄O₇ 571.2193; found 571.3309.



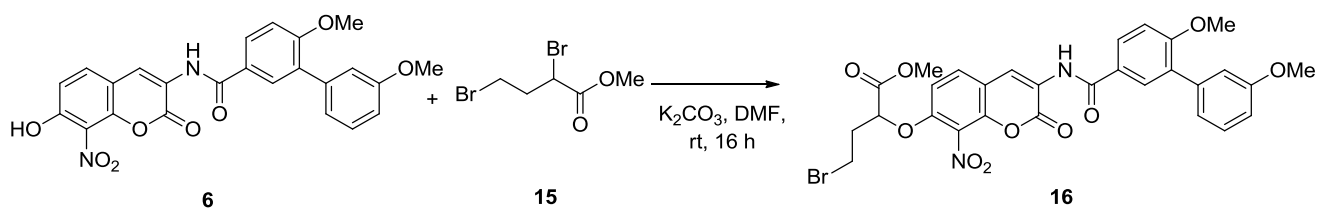
N-(2,9-dioxo-3-(pyrrolidine-1-carbonyl)-1,2,3,9-tetrahydrochromeno[7,8-b][1,4]oxazin-8-yl)-3',6-dimethoxy-[1,1'-biphenyl]-3-carboxamide (14c) Compound **14c** was prepared from **12g** using general procedure D to afford a white amorphous solid (8 mg, 47%). ¹H NMR (500 MHz, Chloroform-d) δ 8.82 (s, 1H), 8.68 (s, 1H), 8.48 (s, 1H), 7.94 – 7.87 (m, 2H), 7.36 (t, *J* = 7.9 Hz, 1H), 7.16 (d, *J* = 8.6 Hz, 1H), 7.14 – 6.98 (m, 4H), 6.93 (ddd, *J* = 8.3, 2.6, 0.9 Hz, 1H), 5.48 (s, 1H), 3.93 (dt, *J* = 10.4, 7.0 Hz, 1H), 3.88 (s, 3H), 3.85 (s, 3H), 3.64 (dt, *J* = 10.3, 7.0 Hz, 1H), 3.48 (qt, *J* = 12.4, 7.0 Hz, 2H), 2.01 (ddd, *J* = 13.2, 9.3, 6.6 Hz, 2H), 1.89 (q, *J* = 6.9 Hz, 2H). ¹³C NMR (126 MHz, CDCl₃) δ 165.65, 163.61, 161.02, 160.00, 159.44, 158.09, 144.21, 138.67, 137.09, 131.14, 130.11, 129.31, 128.40, 125.91, 124.04, 122.60, 122.37, 122.12, 115.43, 114.82, 113.94, 113.62, 113.20, 111.14, 75.60,

56.01, 55.46, 47.20, 46.65, 26.23, 24.15. HRMS (ESI⁺) m/z: [M + H⁺] calcd for C₃₁H₂₇N₃O₈ 569.1798; found 569.1801.



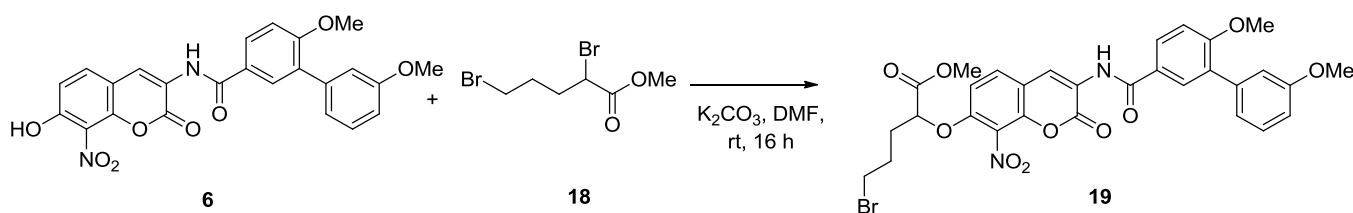
8-(3',6-Dimethoxy-[1,1'-biphenyl]-3-ylcarboxamido)-2,9-dioxo-1,2,3,9-tetrahydrochromeno[7,8-b][1,4]oxazine-3-carboxamide (14d) Compound **14c** was prepared from **12h** using general procedure D to afford a white amorphous solid (15 mg, 47%). ¹H NMR (500 MHz, DMSO-d₆) δ 8.52 (p, *J* = 1.3 Hz, 1H), 8.33 – 8.21 (m, 1H), 8.03 – 7.95 (m, 1H), 7.95 – 7.90 (m, 1H), 7.36 (td, *J* = 9.0, 1.9 Hz, 2H), 7.28 – 7.22 (m, 1H), 7.15 – 7.05 (m, 3H), 6.94 (ddd, *J* = 8.3, 2.7, 1.5 Hz, 1H), 5.21 (q, *J* = 1.2 Hz, 1H), 3.87 (q, *J* = 1.2 Hz, 3H), 3.84 – 3.78 (m, 3H). ¹³C NMR (126 MHz, DMSO) δ 164.79, 163.35, 159.75, 157.41, 157.20, 155.36, 142.41, 136.92, 136.34, 128.22, 127.66, 127.36, 127.31, 126.72, 123.87, 120.32, 119.94, 113.46, 112.65, 112.48, 111.81, 110.78, 109.74, 74.64, 54.09, 53.29. HRMS (ESI⁺) m/z: [M + H⁺] calcd for C₂₇H₂₂N₃O₈ 516.1407; found 516.1425.

General procedure F: *O*-alkylation



Methyl 4-bromo-2-((3-(3',6-dimethoxy-[1,1'-biphenyl]-3-ylcarboxamido)-8-nitro-2-oxo-2H-chromen-7-yl)oxy)butanoate (14d) Potassium carbonate (59.70 mg, 0.433 mmol) was

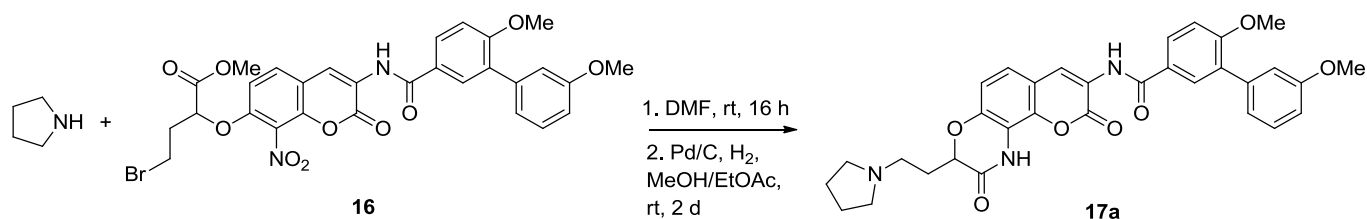
to a solution of **6** (100 mg, 0.2163 mmol) in anhydrous DMF (0.5 ml) and stirred at rt for 15 min. After 15 min, the solution was cooled to 0 °C and a solution of **15** (0.036 ml, 0.260 mmol) in DMF (0.1 ml) was added dropwise. The solution was then allowed to stir at rt for 16 h. After 16 h, the RM was concentrated under reduced pressure to dryness. The resultant solid was diluted with water, pH adjusted to 6-7 and extracted with EtOAc (3 X 15 ml). The organic layer was collected, dried (over Na₂SO₄) and concentrated to residue. The residue was purified by column chromatography (SiO₂, 1:99, Acetone:DCM) to afford desired product as a yellow amorphous solid (90 mg, 65%). ¹H NMR (500 MHz, Chloroform-d) δ 8.86 (s, 1H), 8.69 (s, 1H), 7.95 – 7.85 (m, 2H), 7.59 (d, *J* = 8.9 Hz, 1H), 7.38 (t, *J* = 7.9 Hz, 1H), 7.16 – 7.04 (m, 3H), 7.01 – 6.93 (m, 2H), 5.11 (dd, *J* = 9.2, 3.8 Hz, 1H), 3.91 (s, 3H), 3.87 (s, 3H), 3.81 (s, 3H), 3.66 – 3.58 (m, 2H), 2.62 – 2.44 (m, 2H). ¹³C NMR (126 MHz, CDCl₃) δ 169.67, 165.80, 160.24, 159.47, 157.01, 150.07, 142.03, 138.55, 131.33, 130.17, 130.08, 129.79, 129.36, 128.37, 125.54, 123.78, 122.08, 121.89, 115.43, 115.21, 113.26, 111.21, 111.01, 76.01, 56.07, 55.47, 53.17, 35.08, 28.40. HRMS (ESI⁺) *m/z*: [M - H⁺] calcd for C₂₉H₂₄BrN₂O₁₀ 639.0614; found 639.2997.



Methyl 5-bromo-2-((3-(3',6-dimethoxy-[1,1'-biphenyl]-3-yl)carboxamido)-8-nitro-2-oxo-2H-chromen-7-yl)oxy)pentanoate (19) Compound **19** was prepared from **6** using general procedure F and **15** to afford a white amorphous solid (90 mg, 65%). ¹H NMR (400 MHz, Chloroform-d) δ 8.85 (s, 1H), 8.69 (s, 1H), 7.95 – 7.84 (m, 2H), 7.57 (d, *J* = 8.9 Hz, 1H), 7.38 (t, *J* = 7.9 Hz, 1H), 7.15 – 7.06 (m, 4H), 6.97 – 6.92 (m, 1H), 6.85 (d, *J* = 8.9 Hz, 1H),

4.85 (dd, $J = 7.6, 4.4$ Hz, 1H), 3.92 (s, 3H), 3.87 (s, 3H), 3.80 (s, 3H), 3.57 – 3.38 (m, 2H), 2.30 – 2.00 (m, 2H), 1.36 – 1.16 (m, 2H). ^{13}C NMR (126 MHz, CDCl_3) δ 169.72, 165.86, 160.29, 159.52, 157.06, 150.12, 142.08, 138.59, 131.39, 130.21, 129.82, 129.41, 128.42, 125.59, 123.83, 122.13, 121.93, 115.47, 115.25, 113.32, 111.25, 111.05, 76.05, 56.12, 55.52, 53.21, 35.11, 32.46, 28.45. HRMS (ESI^+) m/z : $[\text{M} - \text{H}^+]$ calcd for $\text{C}_{30}\text{H}_{26}\text{BrN}_2\text{O}_{10}$ 653.0771; found 653.0794.

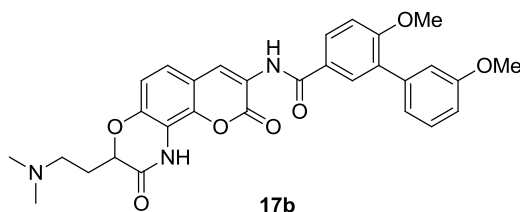
General procedure G: Nucleophilic substitution and cyclization



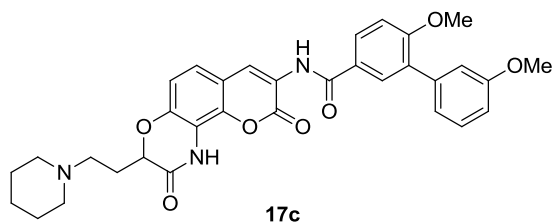
N-(2,9-dioxo-3-(2-(pyrrolidin-1-yl)ethyl)-1,2,3,9-tetrahydrochromeno[7,8-b][1,4]oxazin-8-yl)-3',6-dimethoxy-[1,1'-biphenyl]-3-carboxamide (17a) A solution of **16** (100 mg, 0.156 mmol) in dry DMF (0.5 ml) was treated with pyrrolidine (0.064 ml, 0.780 mmol) and stirred at rt for 16 h. After 16h, the RM was concentrated under reduced pressure to dryness. The resultant solid was filtered through a pad of silica gel column and used without further purification in the next step (65 mg mixture).

Pd/C was added to a solution of the coumarin ether (65 mg, obtained from previous step) in MeOH/EtOAc (1:1, 0.5 ml) and stirred at room temperature under hydrogen atmosphere for 2 days. After 2 days, RM was filtered through celite and concentrated under reduced pressure to residue. The residue was purified by column chromatography (SiO_2 , 5:95 MeOH:DCM) to afford a white amorphous solid (12 mg, 10%). ^1H NMR (500 MHz, Chloroform- d + CD_3OD) δ 8.84 (d, $J = 0.9$ Hz, 1H), 7.96 – 7.83 (m, 2H), 7.36 (t, $J = 7.9$ Hz,

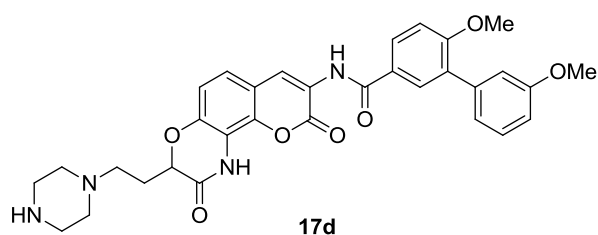
1H), 7.18 (d, $J = 8.6$ Hz, 1H), 7.15 – 7.04 (m, 3H), 7.00 (d, $J = 8.5$ Hz, 1H), 6.93 (ddd, $J = 8.3, 2.6, 0.9$ Hz, 1H), 4.80 (dd, $J = 6.3, 5.1$ Hz, 1H), 3.89 (s, 3H), 3.85 (s, 3H), 3.39 – 3.08 (m, 4H), 2.57 (d, $J = 63.0$ Hz, 2H), 2.38 – 2.15 (m, 2H), 1.68 – 1.28 (m, 4H). ^{13}C NMR (126 MHz, CDCl_3) δ 165.69, 164.97, 160.04, 159.37, 158.18, 144.21, 138.58, 137.19, 131.12, 129.95, 129.28, 128.38, 125.70, 124.14, 122.59, 122.22, 122.03, 115.39, 115.05, 114.78, 114.41, 113.12, 111.18, 75.00, 55.98, 55.40, 54.12, 51.37, 29.76, 23.47. HRMS (ESI⁺) m/z : [M^+] calcd for $\text{C}_{32}\text{H}_{31}\text{N}_3\text{O}_7$ 569.2162; found 569.2102.



N-(3-(2-(dimethylamino)ethyl)-2,9-dioxo-1,2,3,9-tetrahydrochromeno[7,8-b][1,4]oxazin-8-yl)-3',6-dimethoxy-[1,1'-biphenyl]-3-carboxamide (17b) Compound **17b** was prepared from **16** using general procedure G and dimethylamine hydrochloride and potassium carbonate to afford a white amorphous solid (22 mg, 18%). ^1H NMR (500 MHz, Chloroform-*d*) δ 8.80 (s, 1H), 7.89 (dd, $J = 8.6, 2.5$ Hz, 1H), 7.84 (d, $J = 2.4$ Hz, 1H), 7.34 (t, $J = 7.9$ Hz, 1H), 7.17 (d, $J = 8.6$ Hz, 1H), 7.12 – 7.03 (m, 3H), 6.96 (d, $J = 8.5$ Hz, 1H), 6.91 (ddd, $J = 8.3, 2.6, 1.0$ Hz, 1H), 4.72 (dd, $J = 6.8, 4.7$ Hz, 1H), 3.87 (s, 3H), 3.83 (s, 3H), 3.21 – 3.07 (m, 2H), 2.71 (s, 6H), 2.53 – 2.31 (m, 2H). ^{13}C NMR (126 MHz, $\text{CDCl}_3 + \text{CH}_3\text{OH}$) δ 165.78, 165.07, 160.06, 159.36, 158.20, 144.16, 138.58, 137.33, 131.13, 129.95, 129.28, 128.38, 125.67, 124.15, 122.66, 122.39, 122.04, 115.38, 115.19, 114.70, 114.35, 113.12, 111.19, 74.76, 55.97, 55.39, 53.98, 43.56, 29.76. HRMS (ESI⁺) m/z : [$\text{M} + \text{Na}^+$] calcd for $\text{C}_{30}\text{H}_{29}\text{N}_3\text{O}_7\text{Na}$ 566.1903; found 566.2942.

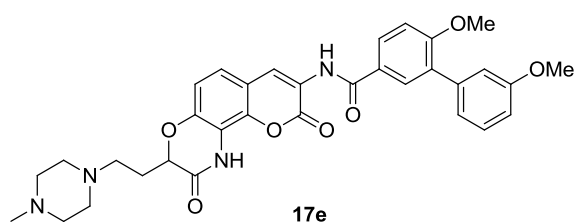


N-(2,9-dioxo-3-(2-(piperidin-1-yl)ethyl)-1,2,3,9-tetrahydrochromeno[7,8-b][1,4] oxazin-8-yl)-3',6-dimethoxy-[1,1'-biphenyl]-3-carboxamide (17c) Compound **17c** was prepared from **6** using general procedure B and piperidine to afford a white amorphous solid (25 mg, 36%). ^1H NMR (400 MHz, Chloroform- d) δ 8.84 (s, 1H), 8.68 (s, NH), 8.36 (s, NH), 7.94 – 7.87 (m, 2H), 7.35 (t, $J = 7.9$ Hz, 1H), 7.18 – 7.04 (m, 4H), 7.00 – 6.88 (m, 2H), 4.83 (dd, $J = 6.9, 4.9$ Hz, 1H), 3.89 (s, 3H), 3.85 (s, 3H), 2.81 – 2.69 (m, 2H), 2.68 – 2.40 (m, 4H), 2.40 – 2.20 (m, 2H), 1.76 – 1.52 (m, 4H), 1.50 – 1.33 (m, 2H). ^{13}C NMR (126 MHz, CDCl_3) δ 165.70, 164.71, 160.03, 159.34, 158.21, 144.23, 138.55, 137.21, 131.09, 129.93, 129.26, 128.37, 125.64, 124.16, 122.61, 122.30, 122.01, 115.38, 115.15, 114.76, 114.44, 113.08, 111.16, 74.80, 55.95, 55.38, 53.54, 53.23, 24.92, 22.96, 22.23. HRMS (ESI $^+$) m/z [$\text{M} + \text{H}^+$] calcd for $\text{C}_{33}\text{H}_{34}\text{N}_3\text{O}_7$ 584.2397; found 584.4839.

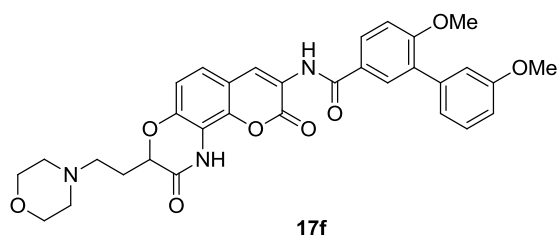


N-(2,9-dioxo-3-(2-(piperazin-1-yl)ethyl)-1,2,3,9-tetrahydrochromeno[7,8-b][1,4] oxazin-8-yl)-3',6-dimethoxy-[1,1'-biphenyl]-3-carboxamide (17d) Compound **17d** was prepared from Boc-protected **17d** using general procedure E to afford a white amorphous solid (20 mg, 95%). ^1H NMR (400 MHz, Chloroform- d) δ 8.84 (s, 1H), 8.68 (s, 1H), 8.36 (s, 1H), 7.94 – 7.87 (m, 2H), 7.35 (t, $J = 7.9$ Hz, 1H), 7.18 – 7.04 (m, 4H), 7.00 – 6.88 (m, 2H), 4.83 (dd, $J =$

6.9, 4.9 Hz, 1H), 3.89 (s, 3H), 3.85 (s, 3H), 2.81 – 2.69 (m, 2H), 2.68 – 2.40 (m, 4H), 2.40 – 2.20 2.30 (m, 2H), 1.76 – 1.52 (m, 4H), 1.50 – 1.33 (m, 2H). ^{13}C NMR (126 MHz, CDCl_3) δ 165.70, 164.71, 160.03, 159.34, 158.21, 144.23, 138.55, 137.21, 131.09, 129.93, 129.26, 128.37, 125.64, 124.16, 122.61, 122.30, 122.01, 115.38, 115.15, 114.76, 114.44, 113.08, 111.16, 74.80, 55.95, 55.38, 53.54, 53.23, 24.92, 22.96, 22.23. HRMS (ESI $^+$) m/z : $[\text{M} + \text{H}^+]$ calcd for $\text{C}_{32}\text{H}_{33}\text{N}_4\text{O}_7$ 585.2349; found 585.4844.

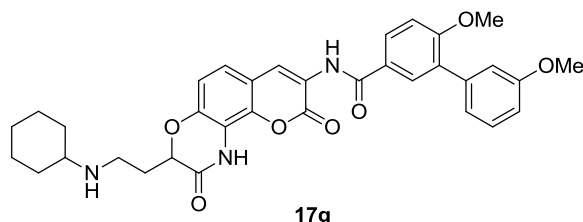


3',6-Dimethoxy-N-(3-(2-(4-methylpiperazin-1-yl)ethyl)-2,9-dioxo-1,2,3,9-tetrahydrochromeno[7,8-b][1,4]oxazin-8-yl)-[1,1'-biphenyl]-3-carboxamide (17e) Compound 17e was prepared from 16 using general procedure G and *N*-methyl piperazine to afford a white amorphous solid (14 mg, 36%). ^1H NMR (500 MHz, Chloroform- d + CD_3OD) δ 8.86 (s, 1H), 8.68 (s, 1H), 8.01 (s, 1H), 7.96 – 7.87 (m, 2H), 7.41 – 7.34 (m, 1H), 7.19 – 7.06 (m, 4H), 6.98 – 6.91 (m, 2H), 4.86 (dd, J = 6.8, 4.9 Hz, 1H), 3.91 (s, 3H), 3.87 (s, 3H), 2.59 (dt, J = 11.1, 6.6 Hz, 2H), 2.52 – 2.36 (m, 4H), 2.35 – 2.25 (m, 4H), 2.24 – 2.10 (m, 2H). ^{13}C NMR (126 MHz, CDCl_3) δ 165.71, 165.70, 160.10, 159.47, 158.12, 144.14, 138.65, 136.89, 131.26, 130.05, 129.36, 128.39, 125.86, 124.04, 122.61, 122.10, 122.00, 115.47, 114.60, 114.52, 114.23, 113.22, 111.21, 75.84, 56.06, 56.04, 55.48, 55.05, 53.03, 45.94, 28.47. HRMS (ESI $^+$) m/z : $[\text{M}^+]$ calcd for $\text{C}_{33}\text{H}_{34}\text{N}_4\text{O}_7$ 598.2428; found 598.2501.



17f

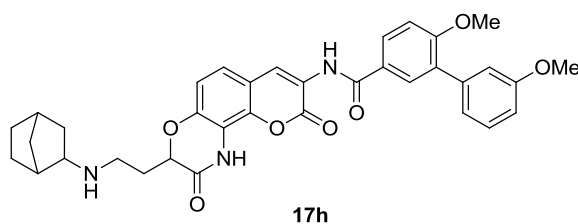
3',6-Dimethoxy-N-(3-(2-morpholinoethyl)-2,9-dioxo-1,2,3,9-tetrahydrochromeno[7,8-b][1,4]oxazin-8-yl)-[1,1'-biphenyl]-3-carboxamide (17f) Compound 17f was prepared from 16 using general procedure G and morpholine to afford a white amorphous solid (25 mg, 36%). ¹H NMR (400 MHz, Chloroform-d + CD₃OD) δ 8.85 (s, 1H), 8.67 (s, NH), 8.05 (s, NH), 7.95 – 7.86 (m, 2H), 7.37 (t, *J* = 7.9 Hz, 1H), 7.18 – 7.05 (m, 4H), 7.00 – 6.90 (m, 2H), 4.87 (dd, *J* = 7.0, 4.7 Hz, 1H), 3.90 (s, 3H), 3.86 (s, 3H), 3.69 – 3.59 (m, 4H), 2.62 – 2.56 (s, 2H), 2.54 – 2.32 (m, 4H), 2.22 – 2.14 (s, 2H). ¹³C NMR (126 MHz, CDCl₃) δ 165.71, 160.10, 159.47, 158.09, 144.11, 138.64, 136.92, 131.26, 130.07, 129.36, 128.38, 125.85, 123.98, 122.66, 122.10, 122.03, 115.46, 114.66, 114.52, 114.22, 113.23, 111.21, 75.72, 67.00, 56.06, 55.48, 53.60, 45.44, 27.81. HRMS (ESI⁺) *m/z*: [M⁺] calcd for C₃₃H₃₃N₃O₈ 599.2268; found 599.2290.



17g

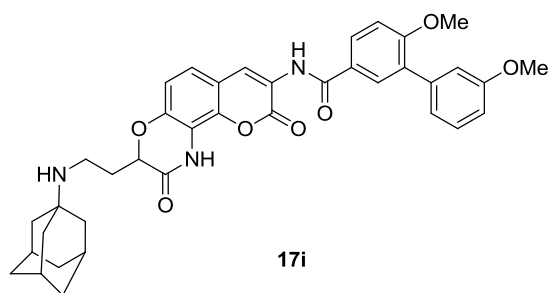
N-(3-(2-(cyclohexylamino)ethyl)-2,9-dioxo-1,2,3,9-tetrahydrochromeno[7,8-b][1,4]oxazin-8-yl)-[1,1'-biphenyl]-3-carboxamide (17g) Compound 17g was prepared from 16 using general procedure G and cyclohexylamine to afford a white amorphous solid (6 mg, 9%). ¹H NMR (500 MHz, Chloroform-d + CD₃OD) δ 8.80 (s, 1H), 7.90 – 7.83 (m, 2H), 7.35 (d, *J* = 7.9 Hz, 1H), 7.19 – 6.96 (m, 4H), 6.93 – 6.88 (m, 2H), 4.64 (dd, *J* = 7.2, 3.9 Hz, 1H), 3.87 (s, 3H), 3.83 (s, 3H), 3.31 – 3.11 (m, 1H), 2.99 (ddd, *J* = 14.4, 8.1, 4.5 Hz, 2H), 2.18 – 2.05 (m, 2H), 1.95 – 1.77 (m, 4H), 1.75 – 1.62 (m, 4H), 1.54 – 1.41

(m, 2H). ^{13}C NMR (126 MHz, CDCl_3) δ 165.69, 165.58, 159.97, 159.29, 158.22, 144.14, 138.51, 137.16, 131.05, 129.89, 129.22, 128.31, 125.61, 124.24, 122.43, 122.25, 121.97, 115.32, 114.90, 114.62, 114.45, 113.06, 111.10, 76.33, 57.27, 55.89, 55.33, 43.85, 29.70, 29.08, 24.81, 24.45. HRMS (ESI^+) m/z [M^+] calcd for $\text{C}_{34}\text{H}_{35}\text{N}_3\text{O}_7$ 597.2475; found 597.3386.



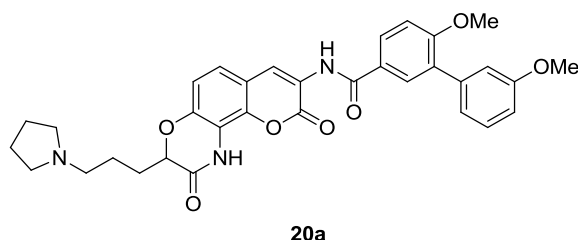
N-(3-(2-(bicyclo[2.2.1]heptan-2-ylamino)ethyl)-2,9-dioxo-1,2,3,9-tetrahydrochromeno[7,8-b][1,4]oxazin-8-yl)-3',6-dimethoxy-[1,1'-biphenyl]-3-carboxamide (17i)

Compound **17h** was prepared from **16** using general procedure G and bicyclo[2.2.1]heptan-2-amine hydrochloride and potassium carbonate to afford a white amorphous solid (14 mg, 13%). ^1H NMR (400 MHz, Chloroform- d + CD_3OD) δ 8.78 (d, $J = 3.4$ Hz, 1H), 7.92 – 7.80 (m, 2H), 7.36 – 7.28 (m, 1H), 7.14 (dd, $J = 8.6, 3.3$ Hz, 1H), 7.11 – 7.02 (m, 3H), 6.93 (ddd, $J = 21.7, 8.4, 3.1$ Hz, 2H), 4.75 (d, $J = 6.2$ Hz, 1H), 3.86 (s, 3H), 3.82 (s, 3H), 3.32 – 3.26 (m, 1H), 3.12 – 3.03 (m, 2H), 2.50 (s, 2H), 2.26 (s, 1H), 2.04 – 1.93 (m, 2H), 1.69 – 1.47 (m, 1H), 1.38 (s, 3H), 1.21 (s, 3H). ^{13}C NMR (126 MHz, CDCl_3) δ 165.79, 160.03, 159.33, 158.27, 144.35, 138.55, 137.32, 131.09, 129.93, 129.26, 128.36, 125.62, 124.28, 122.55, 122.33, 122.02, 115.36, 115.11, 114.81, 114.79, 114.38, 113.09, 111.16, 75.08, 59.57, 55.93, 55.37, 43.27, 38.56, 38.28, 36.39, 34.34, 30.95, 29.74, 29.20. HRMS (ESI^+) m/z [$\text{M} + \text{H}^+$] calcd for $\text{C}_{35}\text{H}_{36}\text{N}_3\text{O}_7$ 610.2553; found 610.2540.



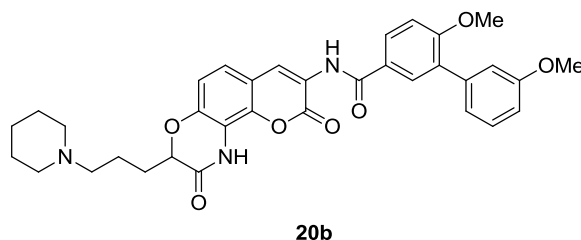
N-(3-(2-((3s,5s,7s)-adamantan-1-ylamino)ethyl)-2,9-dioxo-1,2,3,9-tetrahydrochromeno[7,8-b][1,4]oxazin-8-yl)-3',6-dimethoxy-[1,1'-biphenyl]-3-carboxamide (17i)

Compound **17i** was prepared from **16** using general procedure G and adamantan-1-amine to afford a white amorphous solid (22 mg, 16%). ¹H NMR (400 MHz, Chloroform-d) δ 8.77 (s, 1H), 7.89 – 7.80 (m, 2H), 7.32 (t, *J* = 7.9 Hz, 1H), 7.14 (d, *J* = 8.5 Hz, 1H), 7.10 – 6.99 (m, 3H), 6.96 (d, *J* = 8.5 Hz, 1H), 6.89 (dd, *J* = 8.3, 2.6 Hz, 1H), 4.74 (t, *J* = 5.9 Hz, 1H), 3.85 (s, 3H), 3.81 (s, 3H), 3.19 – 3.12 (m, 2H), 2.65 – 2.54 (m, 1H), 2.50 (dt, *J* = 14.4, 6.9 Hz, 1H), 2.17 (s, 3H), 1.97 – 1.93 (m, 6H), 1.67 (d, *J* = 8.5 Hz, 6H). ¹³C NMR (126 MHz, CDCl₃) δ 165.78, 165.36, 160.05, 159.34, 158.28, 144.45, 138.56, 137.34, 131.10, 129.95, 129.27, 128.36, 125.63, 124.27, 122.58, 122.37, 122.03, 115.37, 115.14, 114.79, 114.42, 113.10, 111.17, 75.12, 57.50, 55.95, 55.38, 38.72, 35.74, 35.59, 29.05, 27.51. HRMS (ESI⁺) *m/z*: [M⁺] calcd for C₃₈H₃₉N₃O₇ 649.2788; found 649.2803.



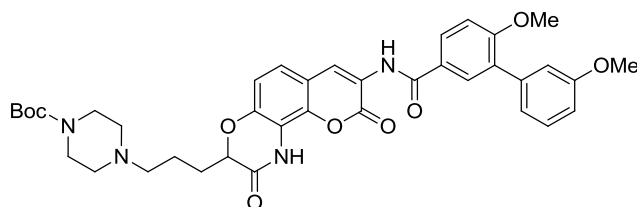
N-(2,9-dioxo-3-(3-(pyrrolidin-1-yl)propyl)-1,2,3,9-tetrahydrochromeno[7,8-b][1,4]oxazin-8-yl)-3',6-dimethoxy-[1,1'-biphenyl]-3-carboxamide (20a) Compound **20a** was prepared from **19** using general procedure G and pyrrolidine to afford a light yellowish

amorphous solid (28 mg, 42%). ¹H NMR (400 MHz, Chloroform-d + CD₃OD) δ 8.80 (s, 1H), 7.93 – 7.80 (m, 2H), 7.34 (t, *J* = 7.9 Hz, 1H), 7.15 (d, *J* = 8.7 Hz, 1H), 7.11 – 7.03 (m, 3H), 6.98 (d, *J* = 8.6 Hz, 1H), 6.90 (ddd, *J* = 8.3, 2.6, 1.0 Hz, 1H), 4.62 (dd, *J* = 6.9, 3.6 Hz, 1H), 3.87 (s, 3H), 3.83 (s, 3H), 2.75 – 2.45 (m, 6H), 2.02 (dt, *J* = 10.7, 5.9 Hz, 2H), 1.85 – 1.72 (m, 4H), 1.62 – 1.48 (m, 2H). ¹³C NMR (126 MHz, CDCl₃) δ 165.72, 165.25, 160.02, 159.35, 158.25, 144.15, 138.58, 137.18, 131.08, 129.97, 129.27, 128.37, 125.68, 124.25, 122.53, 122.25, 122.03, 115.39, 114.99, 114.75, 114.50, 113.10, 111.17, 76.32, 55.96, 55.40, 54.97, 53.83, 27.49, 23.39, 21.41. HRMS (ESI⁺) *m/z* [M + H⁺] calcd for C₃₃H₃₄N₃O₇ 584.2397, found 584.2417.



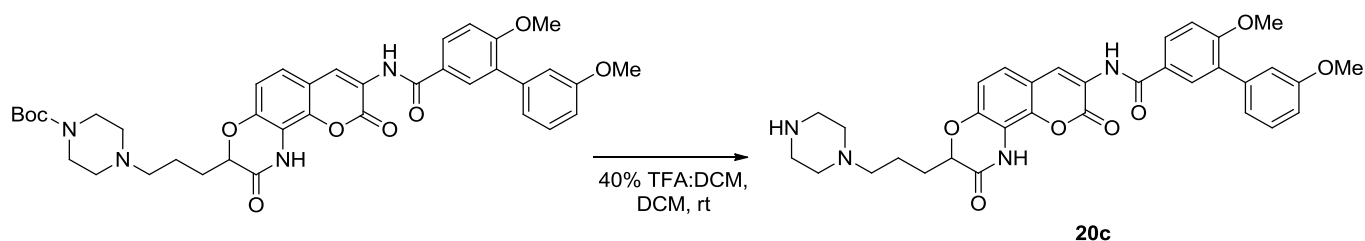
N-(2,9-dioxo-3-(3-(piperidin-1-yl)propyl)-1,2,3,9-tetrahydrochromeno[7,8-b][1,4]

oxazin-8-yl)-3',6-dimethoxy-[1,1'-biphenyl]-3-carboxamide (20b) Compound **20b** was prepared from **19** using general procedure G and piperidine to afford a light yellowish amorphous solid (15 mg, 21%). ¹H NMR (500 MHz, Chloroform-d + CD₃OD) δ 8.77 (d, *J* = 2.0 Hz, 1H), 7.89 – 7.80 (m, 2H), 7.31 (t, *J* = 7.9 Hz, 1H), 7.16 – 7.09 (m, 1H), 7.10 – 7.01 (m, 3H), 6.97 (d, *J* = 8.5 Hz, 1H), 6.88 (dd, *J* = 8.1, 2.5 Hz, 1H), 4.62 (dd, *J* = 7.2, 4.3 Hz, 1H), 3.84 (s, 2H), 3.81 (s, 2H), 3.10 – 3.00 (m, 2H), 2.72 (dt, *J* = 15.2, 4.8 Hz, 4H), 2.25 – 2.04 (m, 6H), 1.98 (dd, *J* = 14.2, 7.0 Hz, 1H), 1.41 (ddq, *J* = 13.7, 9.7, 5.6, 4.2 Hz, 1H). ¹³C NMR (126 MHz, CDCl₃) δ 165.77, 165.36, 160.03, 159.34, 158.29, 144.18, 138.58, 137.23, 131.06, 129.97, 129.28, 128.38, 125.66, 124.36, 122.49, 122.26, 122.04, 115.39, 114.98, 114.79, 114.53, 113.09, 111.18, 76.37, 56.75, 55.96, 55.40, 27.50, 22.63, 21.96, 19.40. HRMS (ESI⁺) *m/z* [M + H⁺] calcd for C₃₃H₃₄N₃O₇ 584.2397, found 584.2407.



tert-butyl 4-(3-(8-(3',6-dimethoxy-[1,1'-biphenyl]-3-yl)carboxamido)-2,9-dioxo-1,2,3,9-tetrahydrochromeno[7,8-b][1,4]oxazin-3-yl)propyl)piperazine-1-carboxylate Compound

Boc-protected amine **20** was prepared from **19** using general procedure G and N-boc piperazine to afford a light yellowish amorphous solid (45 mg, 42%). ¹H NMR (500 MHz, Chloroform-d) δ 8.84 (s, 1H), 8.68 (s, 1H), 8.33 (s, 1H), 7.94 – 7.86 (m, 2H), 7.35 (t, *J* = 7.9 Hz, 1H), 7.16 – 7.03 (m, 4H), 6.97 – 6.90 (m, 2H), 4.71 (dd, *J* = 8.3, 4.4 Hz, 1H), 3.89 (s, 3H), 3.85 (s, 3H), 3.41 (t, *J* = 5.0 Hz, 4H), 2.44 – 2.34 (m, 6H), 2.08 – 1.91 (m, 1H), 1.87 – 1.67 (m, 1H), 1.45 (s, 10H). ¹³C NMR (126 MHz, CDCl₃) δ 165.66, 165.45, 160.05, 159.44, 158.11, 154.84, 144.00, 138.63, 136.98, 131.18, 130.08, 129.31, 128.38, 125.82, 123.99, 122.70, 122.08, 122.07, 115.46, 114.77, 114.61, 114.38, 113.16, 111.16, 79.74, 77.55, 57.97, 56.02, 55.44, 53.05, 28.75, 28.55, 22.03. HRMS (ESI⁺) *m/z* [M - Boc] calcd for C₃₃H₃₅N₄O₇ 599.2506, found 599.2578.

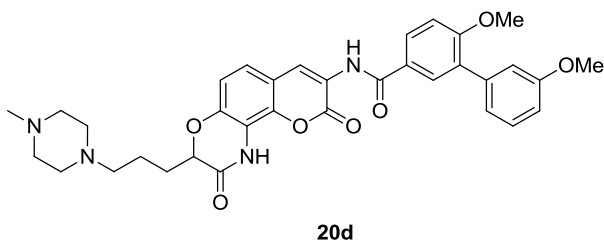


N-(2,9-dioxo-3-(3-(piperazin-1-yl)propyl)-1,2,3,9-tetrahydrochromeno[7,8-

b][1,4]oxazin-8-yl)-3',6-dimethoxy-[1,1'-biphenyl]-3-carboxamide (20c) Compound **20c**

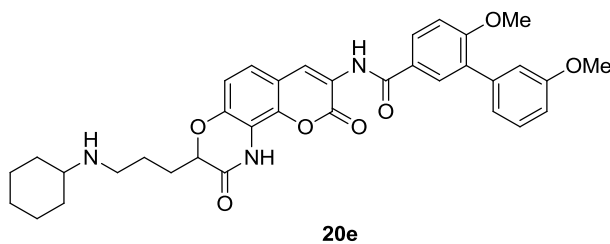
was prepared from Boc-amine (obtained from previous step) using general procedure E to afford a light yellowish amorphous solid (13 mg, 76%). ¹H NMR (500 MHz, Chloroform-d

+ CD₃OD) δ 8.77 (s, 1H), 7.89 – 7.76 (m, 2H), 7.31 (t, J = 7.9 Hz, 1H), 7.13 (d, J = 8.5 Hz, 1H), 7.09 – 7.01 (m, 3H), 6.94 – 6.85 (m, 2H), 4.62 (dd, J = 7.9, 4.6 Hz, 1H), 3.85 (s, 3H), 3.81 (d, J = 1.4 Hz, 3H), 3.12 (t, J = 5.1 Hz, 4H), 2.62 (d, J = 8.7 Hz, 4H), 2.48 – 2.41 (m, 2H), 1.94 (dt, J = 7.6, 3.8 Hz, 2H), 1.69 (ddt, J = 22.9, 15.6, 7.3 Hz, 2H). ¹³C NMR (126 MHz, CDCl₃) δ 166.11, 165.88, 159.99, 159.26, 158.31, 144.13, 138.52, 137.24, 131.04, 129.88, 129.20, 128.30, 125.58, 124.53, 122.30, 122.15, 121.96, 115.29, 114.72, 114.63, 114.28, 113.03, 111.12, 76.96, 60.60, 57.15, 55.86, 55.29, 43.33, 28.06, 22.30. HRMS (ESI⁺) m/z [M + H⁺] calcd for C₃₃H₃₅N₄O₇ 599.2506; found 599.2556.

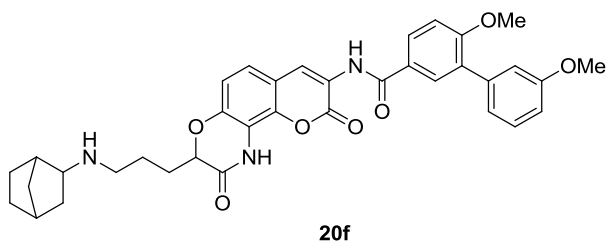


3',6-Dimethoxy-N-(3-(3-(4-methylpiperazin-1-yl)propyl)-2,9-dioxo-1,2,3,9-tetrahydrochromeno[7,8-b][1,4]oxazin-8-yl)-[1,1'-biphenyl]-3-carboxamide (20d)

Compound **20d** was prepared from **19** using general procedure G and N-methyl piperazine to afford a light yellowish amorphous solid (18 mg, 25%). ¹H NMR (400 MHz, Chloroform-d + CD₃OD) δ 8.81 (s, 1H), 7.93 – 7.82 (m, 2H), 7.34 (t, J = 8.0 Hz, 1H), 7.16 – 7.03 (m, 4H), 6.97 – 6.87 (m, 2H), 4.65 (dd, J = 8.2, 4.4 Hz, 1H), 3.88 (s, 3H), 3.84 (s, 3H), 2.70 – 2.25 (m, 8H), 2.36 (s, 3H), 2.04 – 1.87 (m, 2H), 1.75 (dd, J = 15.2, 7.8 Hz, 2H), 1.32 – 1.12 (m, 2H). ¹³C NMR (126 MHz, CDCl₃) δ 165.53, 165.54, 159.79, 159.11, 158.02, 143.85, 138.33, 136.90, 130.89, 129.71, 129.03, 128.11, 125.46, 124.09, 122.14, 121.83, 121.79, 121.77, 115.12, 114.48, 114.17, 112.88, 110.93, 77.02, 57.32, 55.72, 55.15, 54.27, 51.89, 28.27, 21.61. HRMS (ESI⁺) m/z [M + H⁺] calcd for C₃₄H₃₇N₃O₇ 613.2662; found 613.2672.

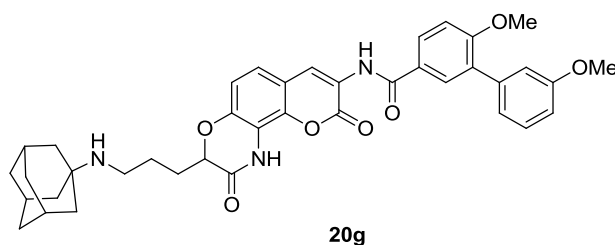


N-(3-(3-(cyclohexylamino)propyl)-2,9-dioxo-1,2,3,9-tetrahydrochromeno[7,8-b][1,4]oxazin-8-yl)-3',6-dimethoxy-[1,1'-biphenyl]-3-carboxamide (20e) Compound **20e** was prepared from **19** using general procedure G and cyclohexylamine to afford a white amorphous solid (15 mg, 21%). ^1H NMR (500 MHz, Chloroform- d + CD_3OD) δ 8.78 (s, 1H), 8.67 (s, 1H), 7.89 – 7.81 (m, 2H), 7.37 – 7.29 (m, 1H), 7.14 (dd, $J = 8.6, 1.0$ Hz, 1H), 7.11 – 7.00 (m, 3H), 6.98 (dd, $J = 8.5, 1.0$ Hz, 1H), 6.90 (ddt, $J = 8.3, 2.5, 1.0$ Hz, 1H), 4.63 (dd, $J = 7.5, 3.4$ Hz, 1H), 3.85 (s, 3H), 3.82 (s, 3H), 3.01 (qd, $J = 7.1, 4.6, 3.7$ Hz, 3H), 2.14 – 2.08 (m, 3H), 1.90 – 1.81 (m, 4H), 1.66 (dd, $J = 11.8, 4.1$ Hz, 2H), 1.52 (qd, $J = 12.5, 8.1$ Hz, 4H), 1.33 – 1.24 (m, 2H). ^{13}C NMR (126 MHz, CDCl_3) δ 165.82, 165.70, 159.92, 159.19, 158.23, 144.15, 138.45, 137.24, 130.93, 129.81, 129.12, 128.26, 125.49, 124.46, 122.29, 122.17, 121.90, 115.22, 114.81, 114.69, 114.35, 112.94, 111.06, 76.23, 57.21, 55.78, 55.21, 43.84, 28.97, 27.23, 24.73, 24.33, 21.56. HRMS (ESI $^+$) m/z $[\text{M} + \text{H}^+]$ calcd for $\text{C}_{35}\text{H}_{38}\text{N}_3\text{O}_7$ 612.2710, found 612.2710.



N-(3-(3-(bicyclo[2.2.1]heptan-2-ylamino)propyl)-2,9-dioxo-1,2,3,9-tetrahydrochromeno[7,8-b][1,4]oxazin-8-yl)-3',6-dimethoxy-[1,1'-biphenyl]-3-carboxamide (20f) Compound **20f** was prepared from **19** using general procedure G and bicyclo[2.2.1]heptan-2-amine hydrochloride and potassium carbonate to afford a white amorphous solid (11 mg,

16%). ¹H NMR (400 MHz, Chloroform-d) δ 8.78 (d, *J* = 3.4 Hz, 1H), 7.91 – 7.80 (m, 2H), 7.36 – 7.29 (m, 1H), 7.14 (dd, *J* = 8.6, 3.3 Hz, 1H), 7.11 – 7.01 (m, 3H), 6.93 (ddd, *J* = 21.7, 8.4, 3.1 Hz, 2H), 4.75 (d, *J* = 6.2 Hz, 1H), 3.86 (s, 3H), 3.82 (s, 3H), 2.50 (s, 2H), 2.26 (s, 1H), 2.08 – 1.89 (m, 2H), 1.73 – 1.46 (m, 3H), 1.46 – 1.02 (m, 8H). ¹³C NMR (126 MHz, CDCl₃) δ 165.79, 165.55, 160.04, 159.34, 158.28, 144.29, 144.27, 138.56, 137.28, 131.11, 129.94, 129.27, 129.24, 128.36, 125.65, 124.30, 122.51, 122.25, 122.03, 115.36, 114.99, 114.79, 114.38, 113.11, 111.17, 75.38, 59.44, 55.95, 55.38, 43.40, 43.28, 38.78, 38.25, 36.44, 35.45, 29.74, 29.49, 28.41. HRMS (ESI⁺) *m/z* [M + H⁺] calcd for C₃₆H₃₈N₃O₇ 624.2710, found 624.2740.



N-(3-(3-((1s,3s)-adamantan-1-ylamino)propyl)-2,9-dioxo-1,2,3,9-tetrahydrochromeno[7,8-b][1,4]oxazin-8-yl)-3',6-dimethoxy-[1,1'-biphenyl]-3-carboxamide (20g)

Compound **20g** was prepared from **19** using general procedure G and (1s,3s)-adamantan-1-amine to afford a white amorphous solid (22 mg, 31%). ¹H NMR (500 MHz, Chloroform-d) δ 8.77 (d, *J* = 1.0 Hz, 1H), 7.88 – 7.82 (m, 2H), 7.32 (t, *J* = 7.9 Hz, 1H), 7.13 (d, *J* = 1.0 Hz, 0H), 7.11 – 6.95 (m, 4H), 6.90 (ddd, *J* = 8.3, 2.5, 1.1 Hz, 1H), 4.63 (dd, *J* = 7.7, 4.5 Hz, 1H), 3.84 (s, 3H), 3.82 (s, 3H), 3.03 – 2.90 (m, 2H), 2.20 – 2.16 (m, 5H), 2.02 – 2.00 (m, 6H), 1.75 – 1.61 (m, 6H), 1.24 – 1.20 (m, 2H). ¹³C NMR (126 MHz, CDCl₃) δ 165.64, 165.64, 159.95, 159.31, 158.22, 144.07, 138.53, 137.14, 131.01, 129.98, 129.22, 128.28, 125.62, 124.20, 122.42, 122.24, 121.99, 115.36, 114.85, 114.62, 114.52, 113.04, 111.07, 76.55, 57.79, 55.93, 55.29, 39.24, 38.47, 35.47, 29.02, 27.68, 22.16. HRMS (ESI⁺) *m/z* [M + H⁺] calcd for C₃₉H₄₂N₃O₇ 664.3023, found 664.3070.

5. Reference:

1. Taipale, M.; Jarosz, D. F.; Lindquist, S., HSP90 at the hub of protein homeostasis: emerging mechanistic insights. *Nat. Rev. Mol. Cell Biol.* **2010**, *11*, 515-528.
2. Neckers, L.; Workman, P., Hsp90 Molecular Chaperone Inhibitors: Are We There Yet? *Clin. Cancer Res.* **2012**, *18*, 64-76.
3. Pearl, L. H.; Prodromou, C.; Workman, P., The Hsp90 molecular chaperone: an open and shut case for treatment. *Biochem. J.* **2008**, *410*, 439-453.
4. Blagg, B. S. J.; Kerr, T. D., Hsp90 inhibitors: Small molecules that transform the Hsp90 protein folding machinery into a catalyst for protein degradation. *Med. Res. Rev.* **2006**, *26*, 310-338.
5. Whitesell, L.; Lindquist, S. L., HSP90 and the chaperoning of cancer. *Nat. Rev. Cancer* **2005**, *5*, 761-772.
6. Hanahan, D.; Weinberg, R. A., The Hallmarks of Cancer. *Cell* **2000**, *100*, 57-70.
7. Miyata, Y.; Nakamoto, H.; Neckers, L., The therapeutic target Hsp90 and cancer hallmarks. *Curr. pharmaceu. design* **2013**, *19*, 347-65.
8. Sreedhar, A. S.; So"ti, C.; Csermely, P., Inhibition of Hsp90: a new strategy for inhibiting protein kinases. *Biochimica et Biophysica Acta (BBA) - Prot. Proteo.* **2004**, *1697*, 233-242.
9. Bagatell, R.; Whitesell, L., Altered Hsp90 function in cancer: A unique therapeutic opportunity. *Mol. Cancer Ther.* **2004**, *3*, 1021-1030.
10. Marcu, M. G.; Schulte, T. W.; Neckers, L., Novobiocin and Related Coumarins and Depletion of Heat Shock Protein 90-Dependent Signaling Proteins. *J. Natl. Cancer Inst.* **2000**, *92*, 242-248.
11. Marcu, M. G.; Chadli, A.; Bouhouche, I.; Catelli, M.; Neckers, L. M., The Heat Shock Protein 90 Antagonist Novobiocin Interacts with a Previously Unrecognized ATP-binding Domain in the Carboxyl Terminus of the Chaperone. *J. Biol. Chem.* **2000**, *275*, 37181-37186.
12. Yu, X. M.; Shen, G.; Neckers, L.; Blake, H.; Holzbeierlein, J.; Cronk, B.; Blagg, B. S. J., Hsp90 Inhibitors Identified from a Library of Novobiocin Analogues. *J. Am. Chem. Soc.* **2005**, *127*, 12778-12779.
13. Burlison, J. A.; Neckers, L.; Smith, A. B.; Maxwell, A.; Blagg, B. S. J., Novobiocin: Redesigning a DNA Gyrase Inhibitor for Selective Inhibition of Hsp90. *J. Am. Chem. Soc.* **2006**, *128*, 15529-15536.
14. Donnelly, A. C.; Mays, J. R.; Burlison, J. A.; Nelson, J. T.; Vielhauer, G.; Holzbeierlein, J.; Blagg, B. S. J., The Design, Synthesis, and Evaluation of Coumarin Ring Derivatives of the Novobiocin Scaffold that Exhibit Antiproliferative Activity. *J. Org. Chem.* **2008**, *73*, 8901-8920.
15. Burlison, J. A.; Blagg, B. S. J., Synthesis and Evaluation of Coumermycin A1 Analogues that Inhibit the Hsp90 Protein Folding Machinery. *Org. Lett.* **2006**, *8*, 4855-4858.
16. Eskew, J.; Sadikot, T.; Morales, P.; Duren, A.; Dunwiddie, I.; Swink, M.; Zhang, X.; Hembruff, S.; Donnelly, A.; Rajewski, R.; Blagg, B.; Manjarrez, J.; Matts, R.; Holzbeierlein, J.; Vielhauer, G., Development and characterization of a novel C-terminal inhibitor of Hsp90 in androgen dependent and independent prostate cancer cells. *BMC Cancer* **2011**, *11*, 1-16.
17. Donnelly, A. C.; Zhao, H.; Reddy Kusuma, B.; Blagg, B. S. J., Cytotoxic sugar analogues of an optimized novobiocin scaffold. *MedChemComm* **2010**, *1*, 165-170.
18. Shelton, S. N.; Shawgo, M. E.; Matthews, S. B.; Lu, Y.; Donnelly, A. C.; Szabla, K.; Tanol, M.; Vielhauer, G. A.; Rajewski, R. A.; Matts, R. L.; Blagg, B. S. J.; Robertson, J. D., KU135, a Novel Novobiocin-Derived C-Terminal Inhibitor of the 90-kDa Heat

- Shock Protein, Exerts Potent Antiproliferative Effects in Human Leukemic Cells. *Mol. Pharmacol.* **2009**, *76*, 1314-1322.
19. Zhao, H.; Donnelly, A. C.; Kusuma, B. R.; Brandt, G. E. L.; Brown, D.; Rajewski, R. A.; Vielhauer, G.; Holzbeierlein, J.; Cohen, M. S.; Blagg, B. S. J., Engineering an Antibiotic to Fight Cancer: Optimization of the Novobiocin Scaffold to Produce Anti-proliferative Agents. *J. Med. Chem.* **2011**, *54*, 3839-3853.
 20. Huang, X. Y.; Shan, Z. J.; Zhai, H. L.; Li, L. N.; Zhang, X. Y., Molecular Design of Anticancer Drug Leads Based on Three-Dimensional Quantitative Structure–Activity Relationship. *J. Chem. Info. Mod.* **2011**, *51*, 1999-2006.
 21. Zhao, H.; Blagg, B. S. J., Novobiocin analogues with second-generation noviose surrogates. *Bioorg. Med. Chem. Lett.* **2013**, *23*, 552-557.
 22. Zhao, H.; Moroni, E.; Yan, B.; Colombo, G.; Blagg, B. S., 3D-QSAR-Assisted Design, Synthesis, and Evaluation of Novobiocin Analogues. *ACS med. chem. lett.* **2012**, *4*, 57-62.
 23. Fkyerat, A.; Dubin, G.-M.; Tabacchi, R., The Synthesis of Natural Acetylenic Compounds from *Stereum hirsutum*. *Helv. Chim. Acta* **1999**, *82*, 1418-1422.
 24. Burlison, J. A.; Avila, C.; Vielhauer, G.; Lubbers, D. J.; Holzbeierlein, J.; Blagg, B. S. J., Development of Novobiocin Analogues That Manifest Anti-proliferative Activity against Several Cancer Cell Lines. *J. Org. Chem.* **2008**, *73*, 2130-2137.
 25. Hekking, K. F. W.; Moelands, M. A. H.; van Delft, F. L.; Rutjes, F. P. J. T., An In-Depth Study on Ring-Closing Metathesis of Carbohydrate-Derived α -Alkoxyacrylates: Efficient Syntheses of DAH, KDO, and 2-Deoxy- β -KDO. *J. Org. Chem.* **2006**, *71*, 6444-6450.
 26. Epstein, J. W.; Brabander, H. J.; Fanshawe, W. J.; Hofmann, C. M.; McKenzie, T. C.; Safir, S. R.; Osterberg, A. C.; Cosulich, D. B.; Lovell, F. M., 1-Aryl-3-azabicyclo[3.1.0]hexanes, a new series of nonnarcotic analgesic agents. *J. Med. Chem.* **1981**, *24*, 481-490.
 27. Moumne, R.; Lavielle, S.; Karoyan, P., Efficient Synthesis of β 2-Amino Acid by Homologation of α -Amino Acids Involving the Reformatsky Reaction and Mannich-Type Imminium Electrophile. *J. Org. Chem.* **2006**, *71*, 3332-3334.
 28. Matiichuk, V. S.; Obushak, N. D.; Tsyalkovskii, V. M., Synthesis of Heterocycles from Arylation Products of Unsaturated Compounds: XIII. 5-R1-Benzyl-2-(R2-2-pyridylimino)thiazolidin-4-ones. *Russ. J. Org. Chem.* **2005**, *41*, 1050-1054.

**Identification of Arylbiphenylamide as a Novel
Scaffold for Hsp90 Inhibition**

Chapter 3

Identification of Arylbiphenylamides as Hsp90 C-Terminal Inhibitors

1. Introduction

Hsp90 is a molecular chaperone that plays a crucial role in normal homeostatic processes as well as adaptive responses to cellular stress.^{1, 2} Hsp90 regulates the conformational maturation, activation, and integrity of a wide range of client proteins, many of which are critical for cell signaling, proliferation and survival.^{3, 4} However, in cancer, several of these client proteins are often mutated and/or over-expressed and therefore become highly dependent upon the Hsp90 folding machinery for their maturation and stability.^{5, 6} In fact, oncogenic proteins (e.g. Her2, Raf1, Akt, CDK4 etc.) associated with all six hallmarks of cancer have been found to be dependent upon Hsp90 for their function.⁷ Consequently, Hsp90 has emerged as an attractive therapeutic drug target for the development of cancer chemotherapeutics.

Hsp90 exists as a homodimer with each monomer consisting of three domains: (1) N-terminal ATP-binding domain, (2) middle domain, and (3) C-terminal dimerization domain. However, the majority of research to date has been focused on the development of Hsp90 N-terminal inhibitors. In fact, all Hsp90 inhibitors in clinical trials belong to this class.⁴ Although, significant progress has been made towards the identification of potent inhibitors, concomitant induction of the pro-survival response and poor toxicity profiles of N-terminal inhibitors have remained obstacles to their clinical success.

In 2000, Neckers and co-workers identified a second druggable site at the C-terminus of Hsp90.⁸ Using affinity chromatography, they demonstrated the coumarin

antibiotics, such as novobiocin (NB), bound to a previously unrecognized Hsp90 C-terminal domain and induced Hsp90 client protein degradation in a concentration-dependent manner. In addition, it was observed that inhibitors bound to the Hsp90 C-terminus allosterically modulate the binding of ligands to the N-terminus. Interestingly, NB did not induce the pro-survival heat shock response, one of the major drawbacks associated with N-terminal inhibitors. However, NB manifests poor anti-proliferative activity against cancer cell lines (e.g. SKBr3, $IC_{50} \sim 700 \mu M$), thus exhibits a limit for use as a chemotherapeutic agent.

Following this pioneering work by Neckers, attempts were made to improve the efficacy and selectivity of NB. In 2005, SAR studies by Blagg and co-workers led to the development of the first selective and potent Hsp90 C-terminal inhibitors (DHN1, DHN2).⁹ Subsequent structural modification led to identification of several analogues that manifest efficacy similar to N-terminal inhibitors.¹⁰ In addition, SAR studies revealed a unique class of C-terminal inhibitors (A4, KU32) that induce Hsp90 levels at much lower concentration (1000-10000 fold) than that required for client protein degradation. These compounds are currently under investigation for the treatment of neurodegenerative diseases.^{11, 12} In light of these findings, it is desired to further explore C-terminal inhibitors to obtain additional insight into the unique mechanism exhibited by such compounds and to produce more efficacious modulators of the Hsp90 protein folding machine.

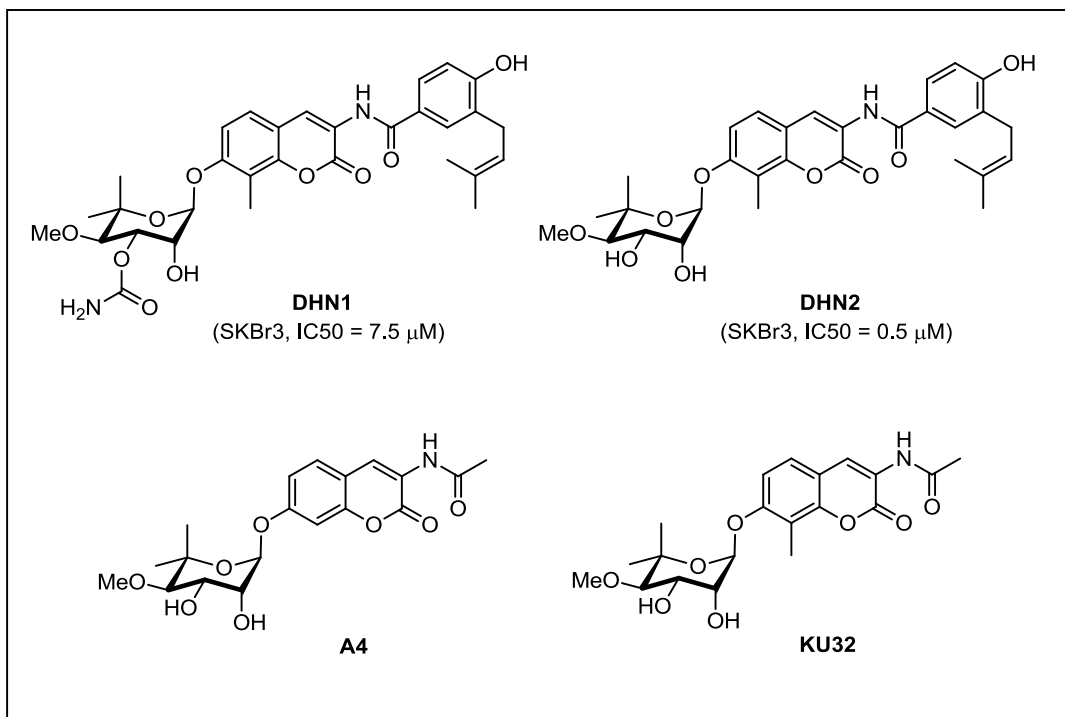


Figure 3.1. Structures of DHN1, DHN2, A4 and KU32.

2. Design, Synthesis and Biological Evaluation of Arylbiphenylamides

Since identification of the Hsp90 C-terminal binding site, the majority of research efforts have been focused on the coumarin-containing natural products (Figure 3.2) for elucidation of the Hsp90 C-terminal nucleotide-binding pocket and development of more potent inhibitors.^{11, 13-15} Although, significant progress has been made towards the development of more potent analogues,^{10, 13} access to diversified novobiocin analogues has remained a challenge. Therefore, the identification of new chemical scaffolds that can be modified in an expeditious manner and can produce compounds with enhanced activities are actively sought.

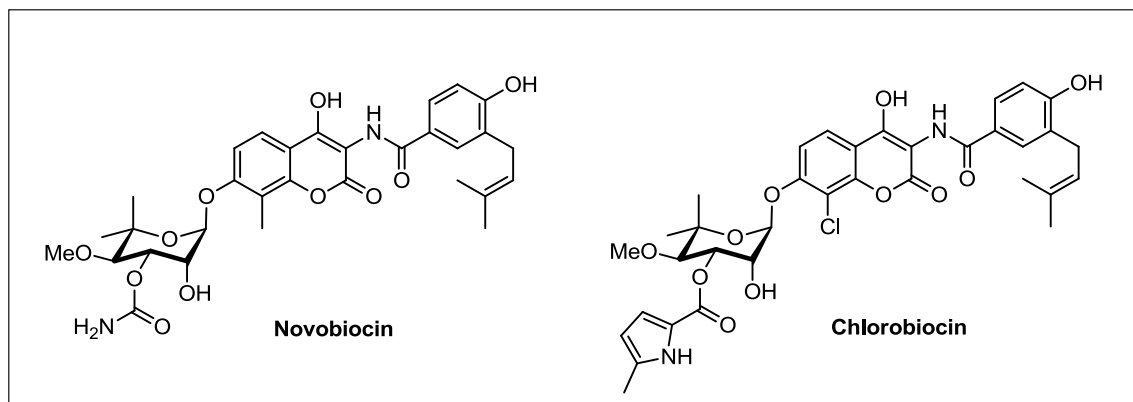


Figure 3.2. Hsp90 C-terminus inhibitors-containing coumarin scaffold.

A. Rationale for design of Arylbiphenylamides

Earlier SAR studies, focused on the modification of NB, unveiled key structural features of NB required for anti-proliferative activity and several potent analogues such as compound **4** were identified (Figure 3.3).^{11, 13, 14} These studies led to elucidation of the following structure-activity-relationships: 1) the sugar (or its surrogate) and benzamide side chain are critical for activity and removal of either decreases activity, 2) the coumarin core serves as an anchor for orientation of the side chains within the binding pocket and can be replaced without compromising activity¹³, 3) the amide linker provides additional hydrogen bonding interactions with the binding pocket. Furthermore, recent SAR studies revealed that replacement of the amide linker with a urea further improved inhibitory activity and lead candidate **5** was identified (manuscript in preparation, Figure 3.3). As a consequence of these observations, it was proposed that replacement of the coumarin core with other scaffolds that incorporated an optimized sugar surrogate and the benzamide side chain could produce new compounds that exhibit improved inhibitory activities.

In an effort to find a suitable replacement for the coumarin core, several scaffolds were screened (*in silico*) based on their ease of accessibility and inclusion of points for diversification. Initial screening suggested the biphenyl ring system could serve as a replacement for the coumarin core. The biphenyl moiety is a privileged structure that could be easily modified to produce diverse analogues for development of more potent inhibitors. Furthermore, the biphenyl ring system is a flexible structure compared to the rigid coumarin scaffold and could therefore adopt different conformations within the binding pocket and serve to provide additional interactions with the protein.

Since there is no co-crystal of Hsp90 bound to a C-terminal inhibitor, prior SAR studies and computational models were used to design new inhibitors. Earlier SAR studies demonstrated that replacement of the noisise sugar with ionizable amines such as *N*-methylpiperidine, enhance anti-proliferative activity (Figure 3.3).^{10, 16} Therefore, *N*-methylpiperidine was selected as a sugar surrogate for analog development. In addition, studies have shown that biaryl side chain containing inhibitors manifest improved activity compared to other analogues, thus the biaryl side chain was chosen for initial SAR studies.¹⁰ Recently it was observed that the optimum distance between the nitrogen atoms on the piperidine ring and the amide/urea is critical for Hsp90 C-terminal inhibition.¹⁷ Consequently, it was proposed that the biphenyl ring system that contains different substitution patterns (e.g., *para-meta*, *meta-meta* and *para-para*) could provide an optimized ring system for replacement of the coumarin core. In addition, we hypothesized that incorporation of different substitutions on the biphenyl system could elucidate additional interactions with the protein. Lastly, different benzamide side chains were explored to identify the most potent analogues.

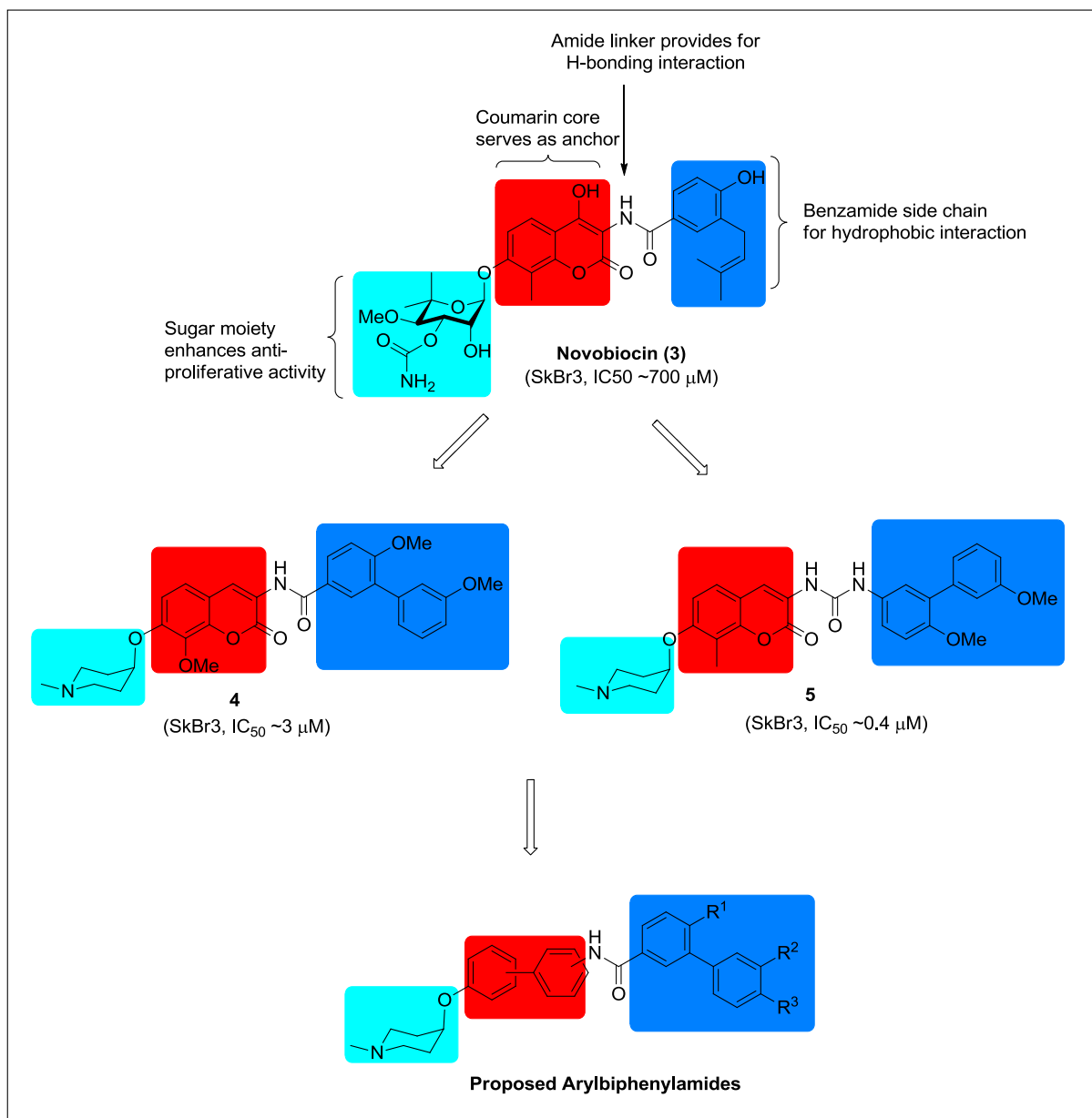
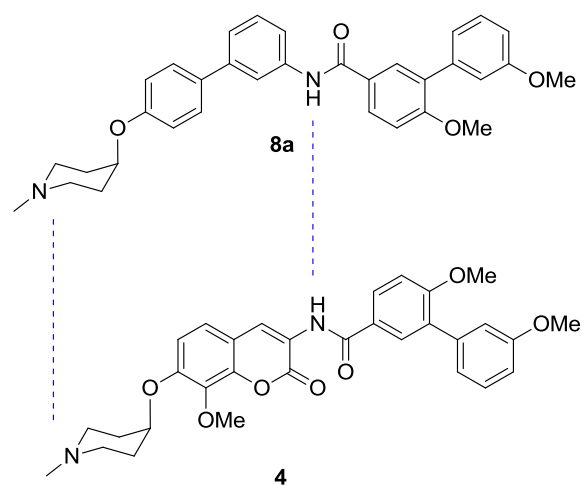
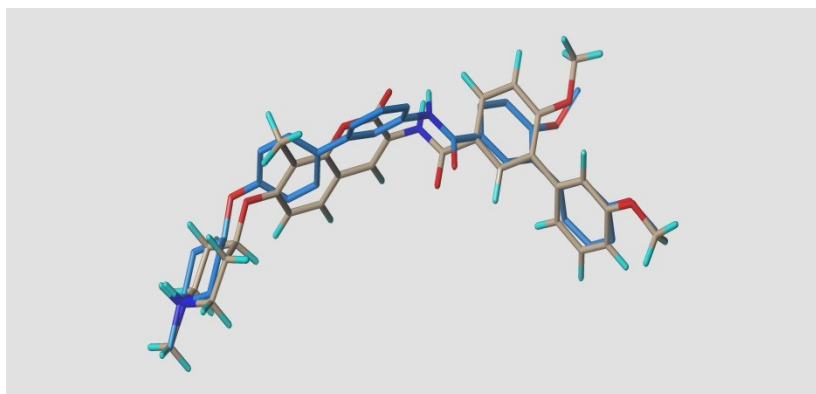


Figure 3.3. Rationale for proposed arylbiphenylamides

To support our hypothesis, the proposed biphenyl derivatives were docked into our homology model as illustrated in Figure 3.4. Molecular docking studies suggested that compound **8a**, which contains a *para-meta* substitution showed the best structural alignment with lead molecule **4**, while compound **8c**, which contains a *para-para* substitution overlaid with lead molecule **5**.

A.



B.

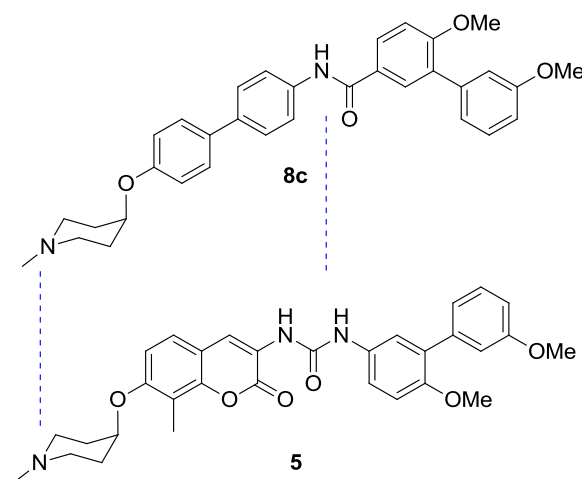
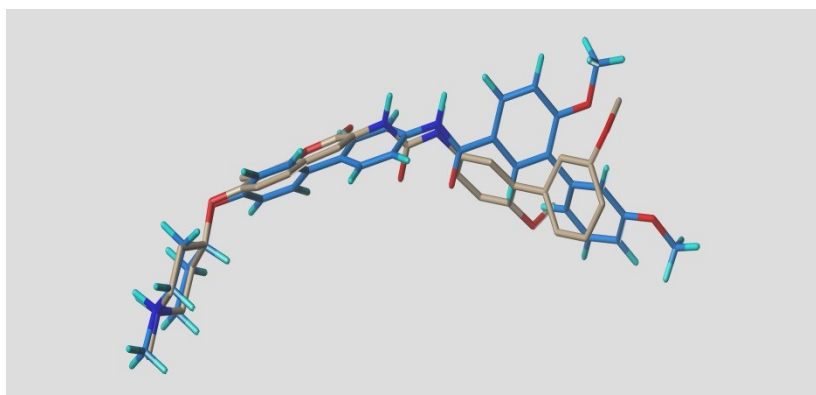


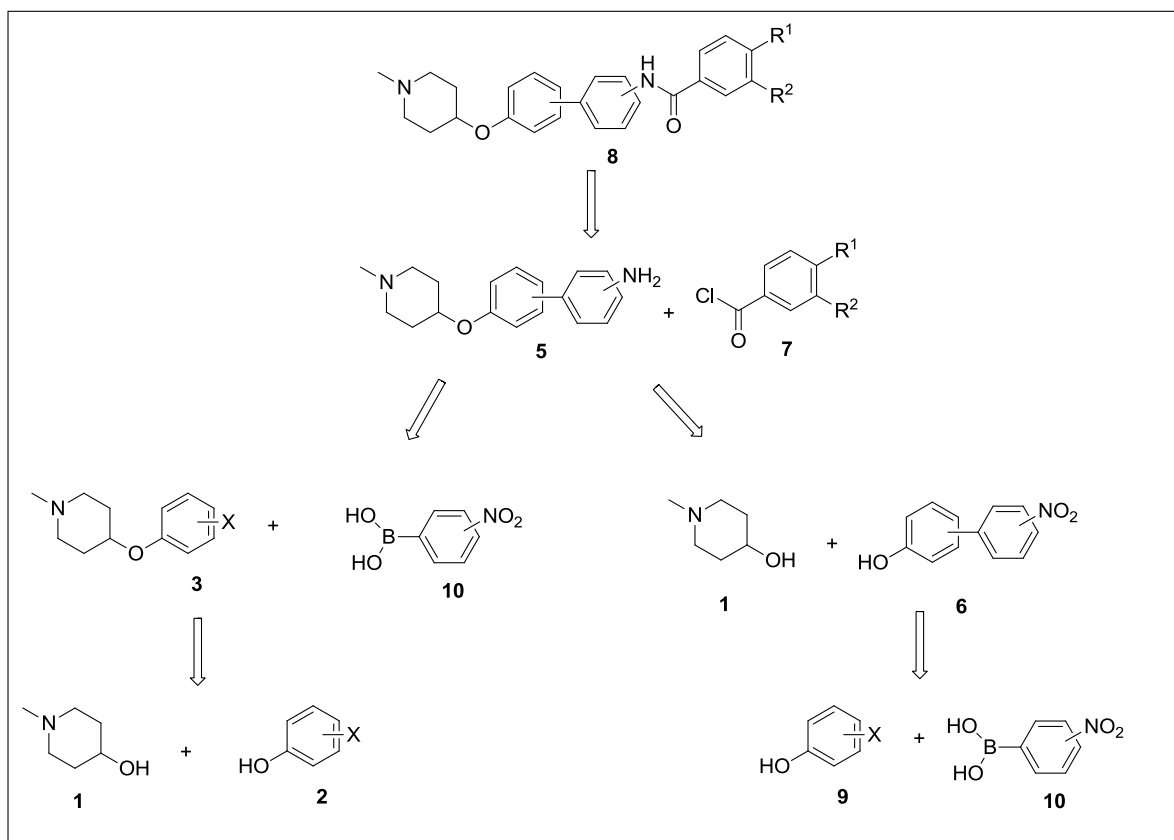
Figure 3.4. Molecular overlay of arylbiphenylamides to coumarin derivatives in the putative Hsp90 C-terminal binding site. (A) Compound 4 (grey) overlaid with proposed para-meta substituted arylbiphenylamide 8a (blue); (B) Compound 5 (grey) overlaid with proposed para-para substituted arylbiphenylamide 8c (blue).

B. Synthesis and Evaluation of Arylbiphenylamides

To elucidate initial SARs, a small library of biphenyl derivatives containing *para-meta*, *meta-meta* and *para-para* substitution patterns was synthesized and evaluated.

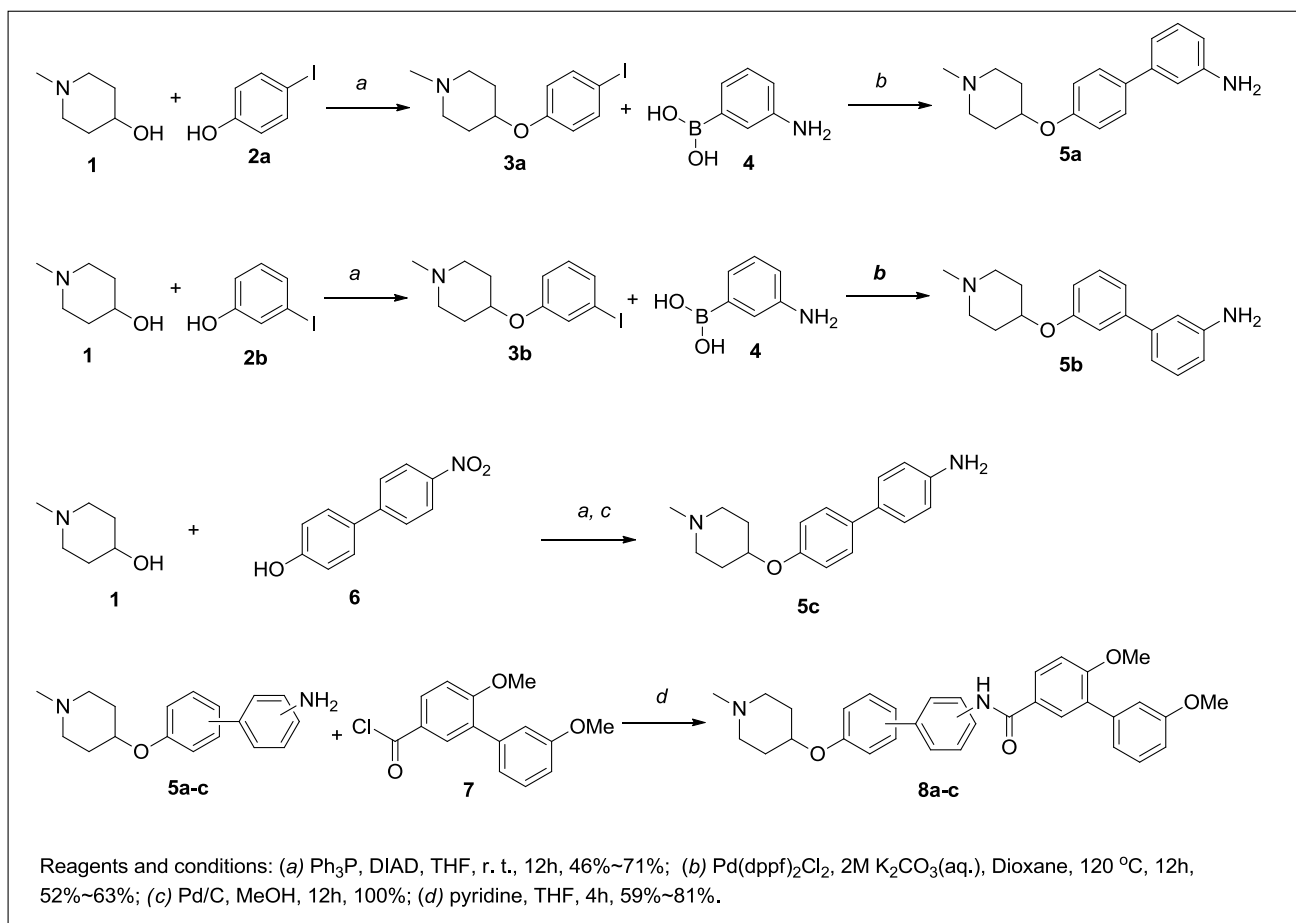
Retrosynthetically, we envisioned the construction of arylbiphenylamides via an amide coupling between amine **5** and acid chloride **7** (Scheme 3.1). The intermediate **5** could be obtained either from a Suzuki coupling between arylhalide **3** and phenylboronic acid **10** or a Mitsunobu etherification between 1-methyl-4-hydroxyperiperidine (**1**) and phenol **6**, followed by reduction via a Pd-catalyzed hydrogenation. Arylhalide **3** was proposed to come from a Mitsunobu etherification between 1-methyl-4-hydroxyperiperidine (**1**) and phenol **2**. Phenol **6** could be then prepared from a Suzuki coupling between arylhalide **3** and phenylboronic acid **4**.

Scheme 3.1. Retrosynthetic analysis of arylbiphenylamides.



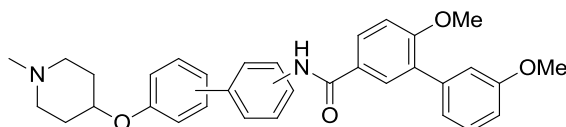
As shown in Scheme 3.2, synthesis of the biphenyl analogues began with Mitsunobu etherification of 1-methyl-4-hydroxyperiperidine (**1**) with iodophenols **2a-b** to give aryl iodides **3a** and **3b** respectively. The resulting aryl iodides **3a-b** were then coupled with aryl boronic acid **4** under standard Suzuki coupling conditions to afford the corresponding amines **5a** and **5b**. Amine **5c** was obtained by Mitsunobu etherification of phenol **6** with 1-methyl-4-hydroxyperiperidine **1**, followed by reduction with Pd/C under a hydrogen atmosphere. Finally, amines **5a-c** were coupled with acid chloride **7** via an amide coupling procedure to afford the requisite amides **8a-c** in moderate to high yields.

Scheme 3.2. Synthesis of biphenyl analogues.



After completion of the syntheses, the arylbiphenylamides **5a-c** were evaluated for anti-proliferative activity against SKBr3 and MCF-7 breast cancer cell lines. As shown in Table 3.1, all the biphenyl analogues showed low micromolar activity in these anti-proliferative assays. Consistent with our docking studies, the *para-para* (**8c**) biphenyl analogue was found 2~3-fold more active than the *para-meta* and *meta-meta* derivatives, suggesting that it represents the optimal distance between the nitrogen atoms on piperidine and amide for activity.

Table 3.1. Anti-proliferative activity of novobiocin mimics.



Entry	Biphenyl	SKBr3	MCF-7
8a	<i>para-meta</i>	3.65 ± 0.14 ^a	1.25 ± 0.02
8b	<i>meta-meta</i>	1.62 ± 0.07	2.00 ± 0.07
8c	<i>para-para</i>	0.47 ± 0.06	0.71 ± 0.02

^aValues represent mean ± standard deviation for at least two separate experiments performed in triplicate.

To verify that the anti-proliferative activity manifested by the biphenyl analogues was the result of Hsp90 inhibition, compounds **8a** and **8c** were evaluated for their ability to induce the degradation of Hsp90-dependent client proteins by Western blot analyses. MCF-7 breast cancer cells were treated with high-low concentrations of compounds **8a** or **8c** for 24 h. Actin, an Hsp90-independent protein, was used as a negative control to confirm that all protein levels were not affected by these analogues. As shown in Figure 3.5, administration of both compounds **8a** and **8c** resulted in the degradation of Hsp90-

dependent client proteins Her2, Raf, and Akt. Since actin levels remained unaffected, the inhibition of cell growth was directly linked to the degradation of Hsp90-dependent client proteins. Additionally, Hsp90 levels were not changed, which is consistent with inhibition of the Hsp90 C-terminus.

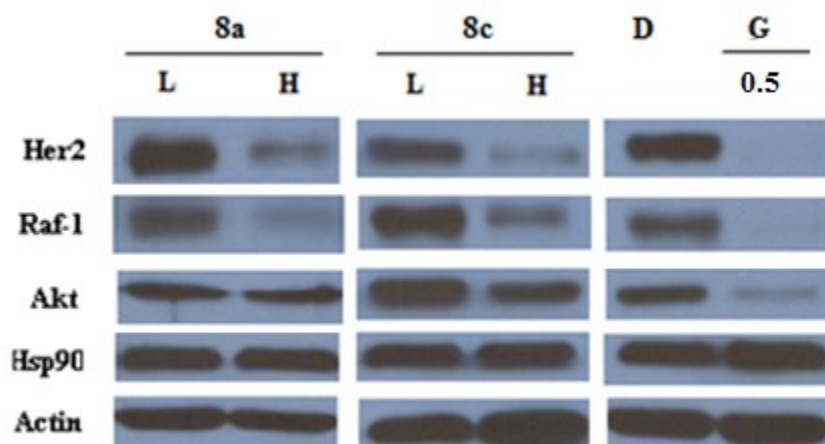
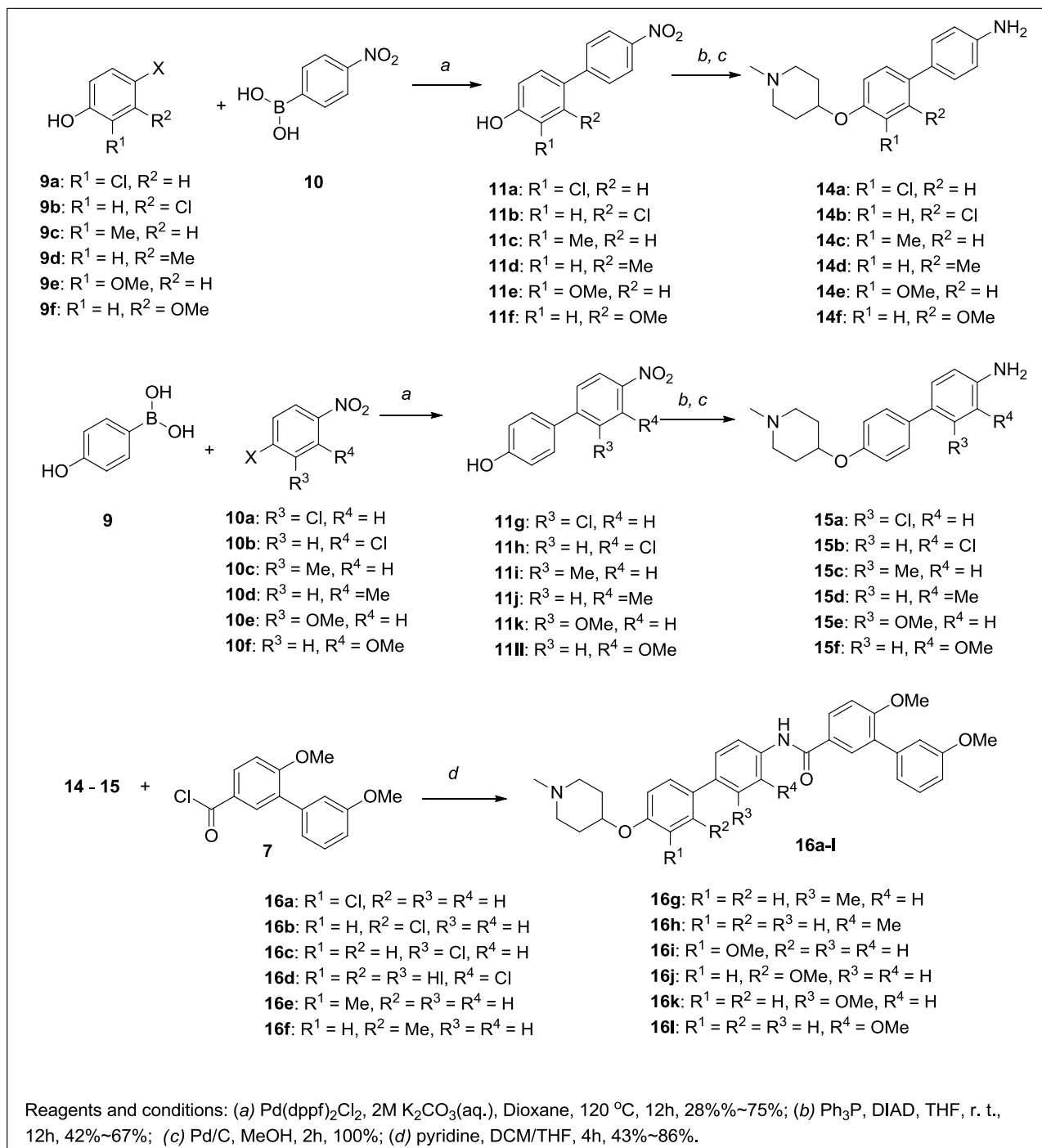


Figure 3.5. Western blot analyses of biphenyl analogues **8a** and **8c** after incubation with MCF-7 breast cancer cells for 24 h. Concentrations (in μM) are indicated above each lane. L represents a concentration $\frac{1}{2}$ of the anti-proliferative activity. H represents a concentration equal to 5-fold of the anti-proliferative activity. Geldanamycin (G, $0.5 \mu\text{M}$) and dimethylsulfoxide (D, 100%) serve as positive and negative controls respectively.

Preliminary anti-proliferative data suggested that the *para-para* substituted biphenyl system is a good replacement for the coumarin core, and was thus chosen for further development of structure-activity relationships. Prior SAR studies on the coumarin scaffold have demonstrated that introduction of substituents at appropriate positions could enhance activity.¹³ Consequently, we directed our efforts toward identification of substituent(s) on the biphenyl system to explore structural surrounding of this molecule. Towards this objective, substituents containing differing electronic properties, such as nitro, chloro, methyl, methoxy and amine were systemically

incorporated at all four positions of the biphenyl system. Following the scheme provided for the *para-para* biphenyl system, biphenyl derivatives containing chloro, methyl and methoxy were synthesized. As shown in Scheme 3.3, Suzuki coupling of compounds **9a-g** with **10a-g** afforded nitrophenols **11a-l** in moderate yields. Nitrophenols **11a-l** were coupled with 1-methyl-4-hydroxypeperidine via a Mitsunobu etherification, followed by reduction with Pd/C under a hydrogen atmosphere to give the corresponding amines, **14a-f** and **15a-f**. Amines **14a-f** and **15a-f** were then coupled with acid chloride **7** to afford amides **16a-l**, respectively.

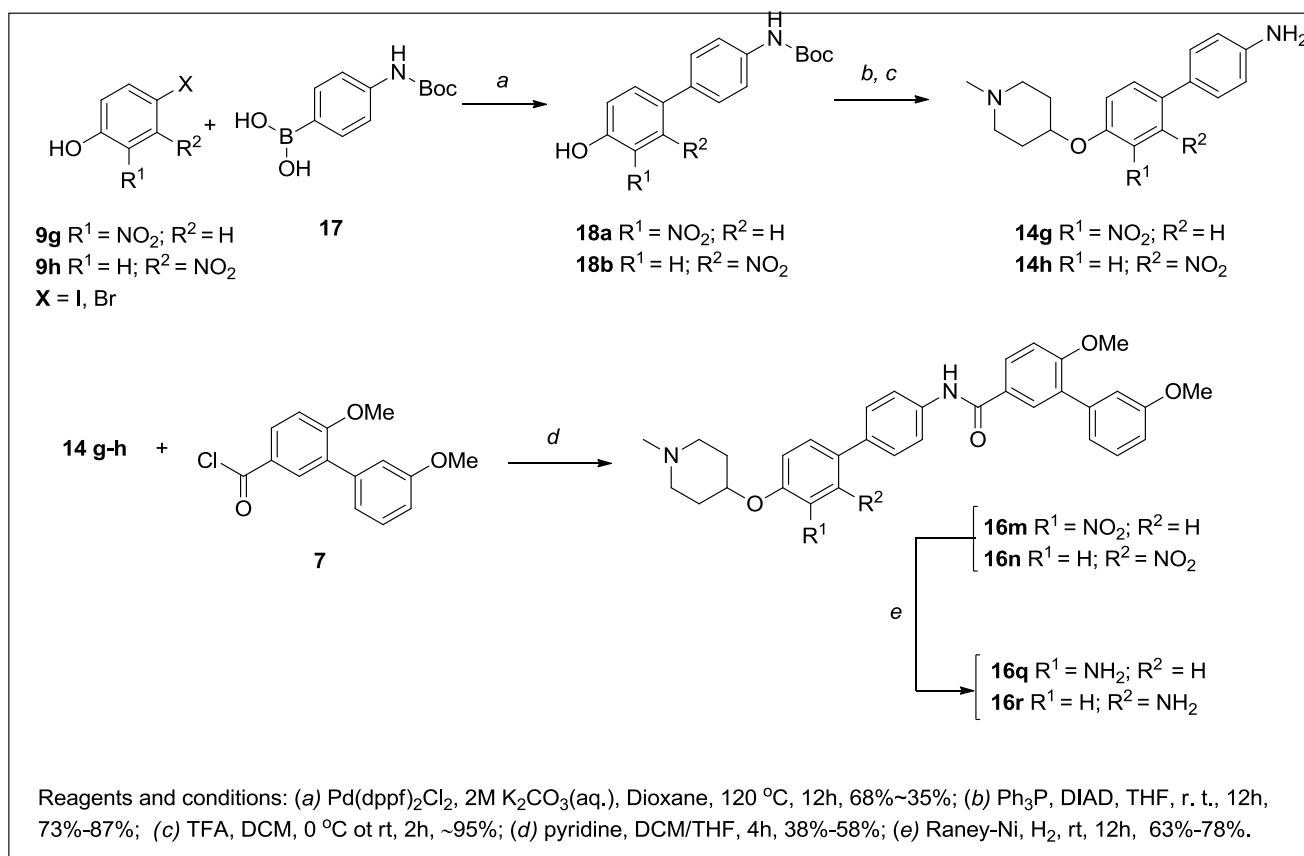
Scheme 3.3. Synthesis of substituted biphenyl analogues.



As shown in Scheme 3.4, biphenyl analogues **16m-n** that contain nitro substituents were prepared by a slightly modified synthetic route. Arylhalides **9g-h** were

coupled with boc-protected aminophenylboronic acid **17** via Suzuki coupling to afford phenols **18a-b**. The resulting phenols (**18a-b**) underwent Mitsunobu etherification, followed by boc-deprotection in the presence of trifluoroacetic acid to furnish the free amines, **14g-h**. Amines **14g-h** were coupled with acid chloride **7** to give amides **16m-n**. The reduction of **16m-n** with a Raney-Nickel catalyzed hydrogenation afforded the corresponding amines **16q-r**, respectively.

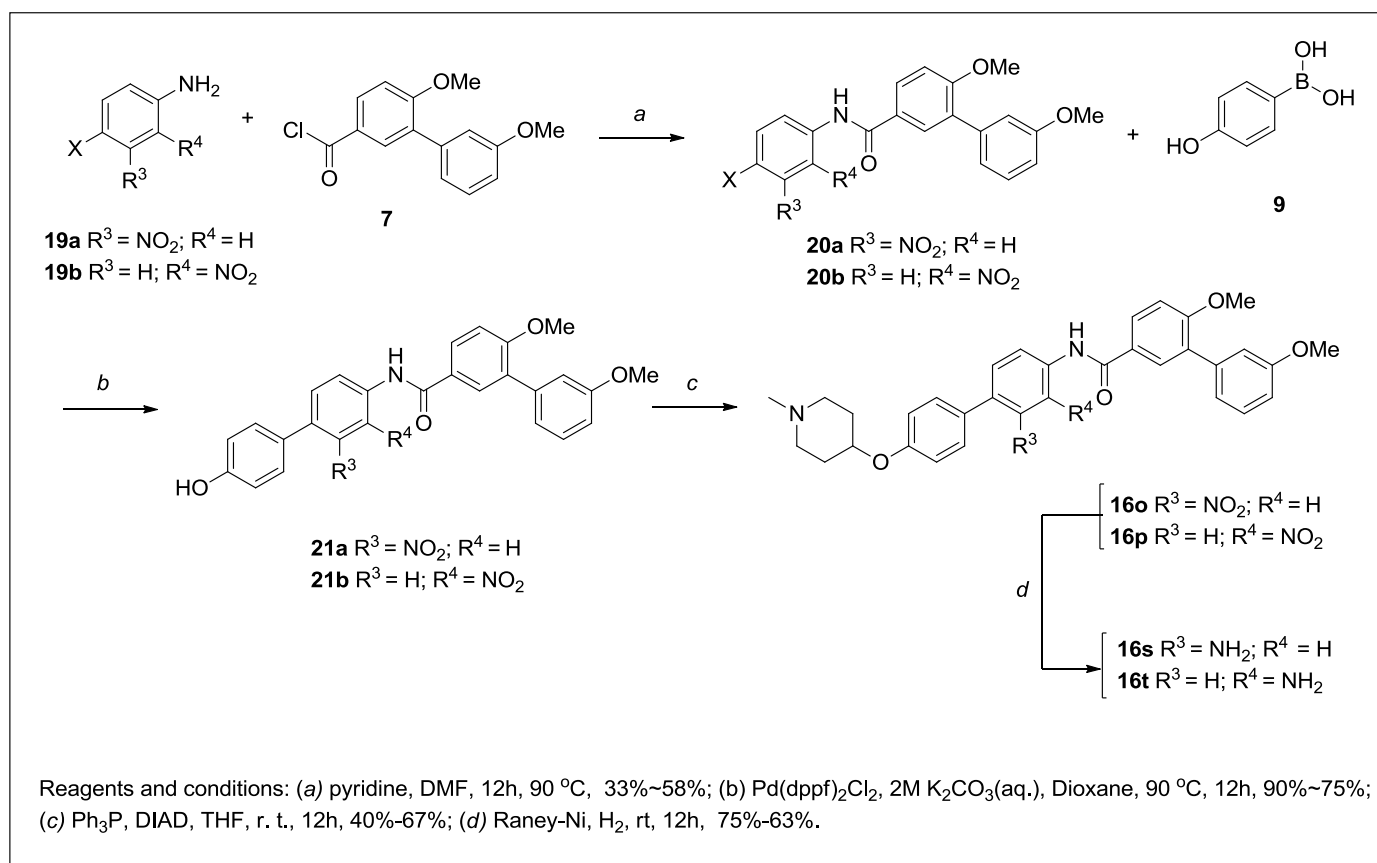
Scheme 3.4. Synthesis of substituted biphenyl analogues.



Biphenyl analogues **16o-p** were proposed for assembly by the same synthetic route. However, attempts to couple the amines with an acid chloride failed, due to the low nucleophilicity exhibited by these anilines. Therefore, syntheses of **16o-p** were

accomplished by the synthetic route depicted in Scheme 3.5. Anilines **19a-b** were coupled with acid chloride **7** to give amides **20a-b**, which were then subjected to Suzuki coupling conditions containing boronic acid **9** to afford the phenols, **21a-b**. The resulting phenols (**21a-b**) were treated with 1-methyl-4-hydroxypiperidine under Mitsunobu conditions to furnish **16o-p**, followed by reduction with Raney-Nickel catalyzed hydrogenation to give compounds **16s-t**.

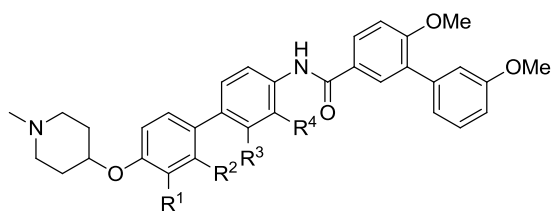
Scheme 3.5. Synthesis of substituted biphenyl analogues.



Upon construction of the biphenyl analogues, **16a-t**, they were evaluated for anti-proliferative activity against SKBr3 and MCF-7 breast cancer cells (Table 3.2). In general, the substituted biphenyl analogues were less active than unsubstituted analogue **8c**,

suggesting that any substitution on this molecule is not tolerated and the flexible biphenyl ring system is necessary for optimal interactions with the binding pocket. However, substitution close in proximity to the amide linker was found highly detrimental to activity, as compounds **16d**, **16h**, **16l**, **16p** and **16t** manifested 5~10 fold decreased activity compared to the unsubstituted analogue **8c**. Overall, structural modifications to the biphenyl moiety exhibited a relatively flat SAR, suggesting that like the coumarin core, it acts as backbone for orientation of the sugar and benzamide side chain.

Table 3.2. Anti-proliferative activity of substituted biphenyl analogues.

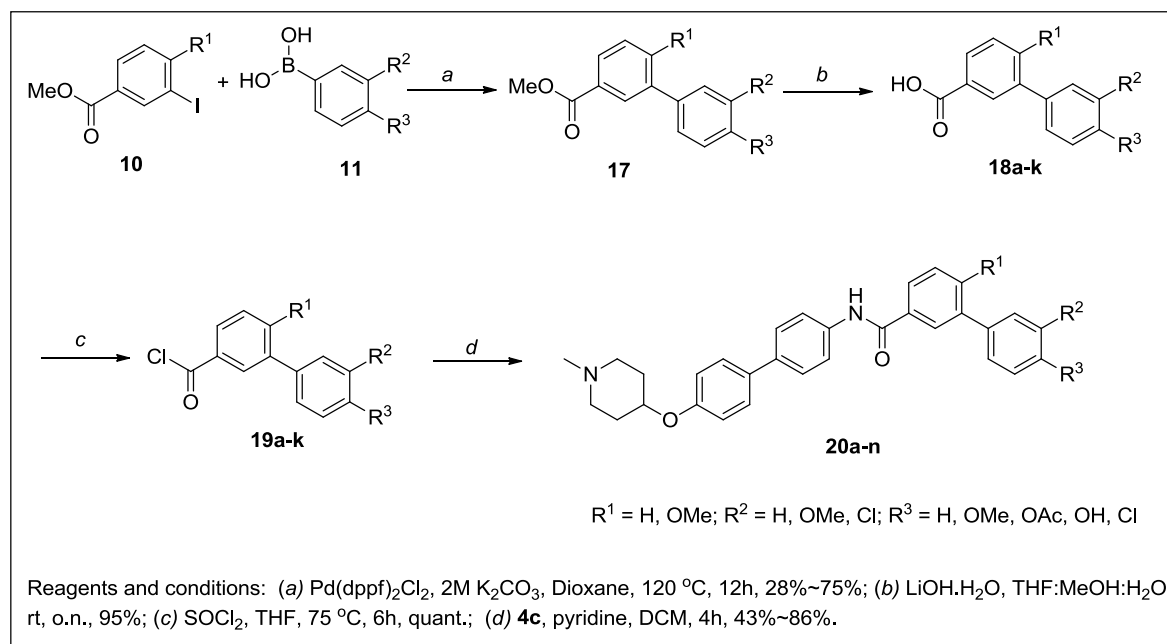


Entry	R ¹	R ²	R ³	R ⁴	SKBr3 (IC ₅₀ , μM)	MCF-7 (IC ₅₀ , μM)
8c	H	H	H	H	0.47 ± 0.06	0.71 ± 0.02
16a	Cl	H	H	H	1.84 ± 0.57	1.48 ± 0.12
16b	H	Cl	H	H	1.28 ± 0.14	1.48 ± 0.33
16c	H	H	Cl	H	2.21 ± 0.18	3.44 ± 0.21
16d	H	H	H	Cl	4.29 ± 0.65	1.80 ± 0.19
16e	Me	H	H	H	0.83 ± 0.03	1.69 ± 0.08
16f	H	Me	H	H	1.18 ± 0.11	1.21 ± 0.03
16g	H	H	Me	H	0.97 ± 0.01	1.57 ± 0.56
16h	H	H	H	Me	2.47 ± 0.39	1.43 ± 0.35
16i	OMe	H	H	H	0.68 ± 0.13	1.32 ± 0.08
16j	H	OMe	H	H	1.41 ± 0.35	1.35 ± 0.16
16k	H	H	OMe	H	0.90 ± 0.08	1.50 ± 0.08
16l	H	H	H	OMe	3.92 ± 0.21	1.22 ± 0.04

16m	NO ₂	H	H	H	2.07 ± 0.17	1.23 ± 0.25
16n	H	NO ₂	H	H	1.18 ± 0.15	1.30 ± 0.12
16o	H	H	NO ₂	H	2.48 ± 0.77	3.32 ± 0.25
16p	H	H	H	NO ₂	3.40 ± 0.14	1.15 ± 0.01
16q	NH ₂	H	H	H	2.23 ± 0.49	5.95 ± 1.22
16r	H	NH ₂	H	H	2.13 ± 0.06	1.76 ± 0.37
16s	H	H	NH ₂	H	3.90 ± 0.18	2.07 ± 0.23
16t	H	H	H	NH ₂	3.21 ± 0.45	2.25 ± 0.49

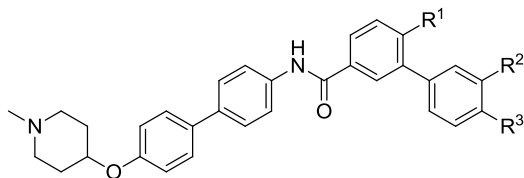
Earlier studies suggested that modification of the benzamide side chain in novobiocin analogues could improve anti-proliferative activity. To investigate this effect on the biphenyl scaffold, aromatic rings bearing various functionalities were installed onto the biphenyl amide. As shown in Scheme 3.6, substituted biaryl acids **18a-i** were prepared by Suzuki coupling of aryl iodide **10** with boronic acid **11**, followed by ester hydrolysis. Biaryl acids **18a-k** were then converted to acid chlorides **19a-k** via thionyl chloride and subsequently coupled with amine **4c** to generate the corresponding biphenyl analogues that contain substituted benzamide ring system.

Scheme 3.6. Synthesis of biphenyl analogues with a modified benzamide side chain.



Anti-proliferative activity of biphenyl analogues **20a-n** against SKBr3 and MCF-7 cells lines are summarized in Table 3.3. The data suggest that 4-methoxy substitution in **8c** is necessary for activity, as **20a** and **20b** exhibited decreased activity. In addition, the data suggest that a hydrogen bond acceptor at the *para*-position is beneficial for activity, as replacement of the methoxy group with acetoxy or hydroxy groups resulted in decreased activity. Concerning the structural requirements of the B ring on the benzamide side chain, we found that electron withdrawing groups such as acetoxy, nitro and chloro substituents at the 3'-position, were more active than the electron donating groups such as hydroxy and amine, suggesting that lipophilic interactions may be important in this region of the binding pocket. Decreased activity manifested by **20k** compared to **20j** suggested that the 4'-substituent is either in close proximity to polar residues or solvent exposed. Consistent with this observation, installation of polar substituents at the 4'-position as in **20l**, **20m** and **20n** improved inhibitory activity.

Table 3.3. Anti-proliferative activity of biphenyl analogues with a modified benzamide side chain.



Entry	R ¹	R ²	R ³	SKBr3 (IC ₅₀ , μM)	MCF-7 (IC ₅₀ , μM)
8c	OMe	OMe	H	0.47 ± 0.06	0.71 ± 0.02
20a	H	H	H	0.73 ± 0.07	1.15 ± 0.18
20b	H	OMe	H	0.81 ± 0.14	1.02 ± 0.08
20c	OMe	H	H	0.51 ± 0.11	0.84 ± 0.01
20d	OAc	OMe	H	1.90 ± 0.47	1.62 ± 0.04
20e	OH	OMe	H	2.78 ± 0.35	2.71 ± 0.45
20f	OMe	OH	H	1.56 ± 0.35	1.08 ± 0.34
20g	OMe	OAc	H	0.27 ± 0.05	0.62 ± 0.07
20h	OMe	NO ₂	H	0.40 ± 0.07	1.09 ± 0.28
20i	OMe	NH ₂	H	1.52 ± 0.55	1.67 ± 0.68
20j	OMe	Cl	H	0.33 ± 0.03	0.32 ± 0.09
20k	OMe	H	Cl	1.06 ± 0.05	0.82 ± 0.13
20l	OMe	H	OMe	0.63 ± 0.04	0.79 ± 0.13
20m	OMe	H	OAc	0.14 ± 0.01	0.64 ± 0.08
20n	OMe	H	OH	0.13 ± 0.02	0.50 ± 0.01

To verify these biphenyl analogues exhibited their anti-proliferative activity via Hsp90 inhibition, Western blot analysis was performed for compounds **20c**, **20j** and **20m**. As shown in Figure 3.6, incubation with these compounds resulted in the degradation of Hsp90 client proteins Her2, Raf-1, and Akt, suggesting these analogues manifest their activity through Hsp90 inhibition. Actin and Hsp90 levels remained unchanged, which is consistent with observations made for earlier Hsp90 C-terminal inhibitors.

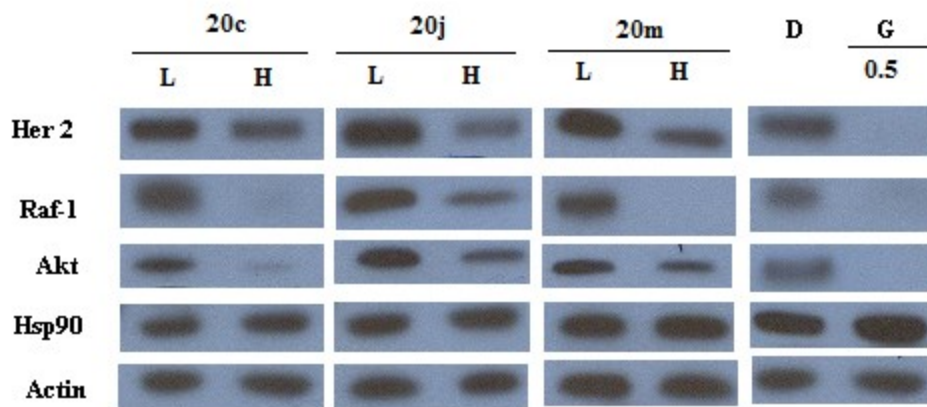


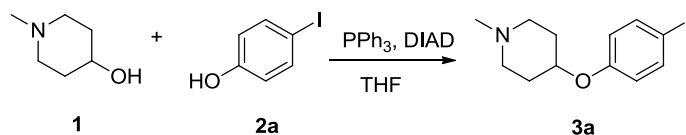
Figure 3.6. Western blot analyses of biphenyl analogues **20c**, **20j**, and **20m** after incubation with MCF-7 breast cancer cells for 24 h. Concentrations (in μM) are indicated above each lane. L represents a concentration $\frac{1}{2}$ of the anti-proliferative activity. H represents a concentration equal to 5-fold of the anti-proliferative activity. Geldanamycin (G, $0.5 \mu\text{M}$) and dimethylsulfoxide (D, 100%) serve as positive and negative controls respectively.

3. Conclusion and Future Directions

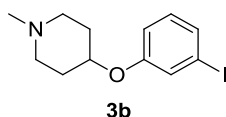
In summary, our studies demonstrated that a flexible biphenyl ring system could serve as a replacement for the rigid coumarin core in novobiocin analogues. Based on prior SAR studies and molecular modeling, a small library of biphenyl derivatives was designed, synthesized, and evaluated for anti-proliferative activity. SAR studies revealed that the unsubstituted *para-para* biphenyl ring system provides for the optimal conformation for maximum interactions with the binding pocket. In addition, incorporation of an optimized benzamide side chain onto the biphenyl moiety led to identification of several analogues that manifest low nanomolar activity. Identification of the arylbiphenylamide represents a novel class of Hsp90 C-terminal inhibitors and has opened the doors for development of future Hsp90 inhibitors, which could be made in an expeditious manner and could concurrently unravel interesting biological consequences of Hsp90 C-terminal inhibition.

4. Experimental Section

General procedure A: Mitsunobo etherification



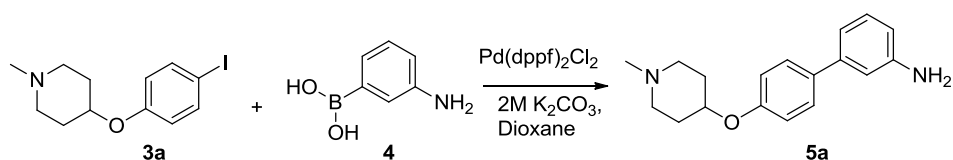
4-(4-Iodophenoxy)-1-methylpiperidine (3a) Diisopropylazodicarboxylate (1.89 g, 9.36 mmol) was added to an ice-cooled solution of 4-iodophenol (0.92 g, 4.18 mmol), N-methyl-4-hydroxy-piperidine (480 mg, 4.18 mmol) and triphenylphosphine (2.46 g, 9.36 mmol) in anhydrous THF (50 mL). The reaction mixture (RM) was then allowed to stir at room temperature for 12h. After 12 h, the RM was concentrated under reduced pressure and the residue was purified by column chromatography (SiO₂, 1:10, Methanol:DCM) to afford desired product as a colorless amorphous solid (1.02 g, 77 %). ¹H NMR (500 MHz, Chloroform-*d*) δ 7.54 (d, *J* = 8.9 Hz, 2H), 6.69 (d, *J* = 2.0 Hz, 2H), 4.27 (m, 1H), 2.73 – 2.59 (m, 2H), 2.31 (s, 3H), 2.30 (m, 2H), 1.98 (m, 2H), 1.82 (m, 2H). ¹³C NMR (101 MHz, CDCl₃) δ 157.34, 138.34, 118.50, 82.91, 72.18, 52.61, 46.28, 30.71. HRMS (ESI⁺) *m/z*: [M + H⁺] calcd for C₁₂H₁₇INO 318.0355; found 318.0357.



4-(3-Iodophenoxy)-1-methylpiperidine (3b) Compound **3b** was prepared following the general procedure A with N-methyl-4-hydroxy-piperidine **1** (557.10 mg, 4.18 mmol) and 4-iodophenol **2a** (0.92 g, 4.18 mmol) and was purified by column chromatography (SiO₂, 5:95 Methanol:DCM) to afford a yellow amorphous solid (611.1 mg, 46%). ¹H NMR

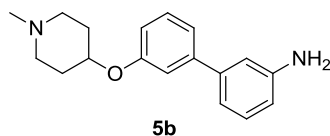
(500 MHz, Chloroform-*d*) δ 7.26 (m, 2H), 6.98 (t, $J = 9.3$ Hz, 1H), 6.87 (dd, $J = 7.8, 2.3$ Hz, 1H), 4.39 – 4.20 (m, 1H), 2.75 – 2.58 (m, 2H), 2.35 – 2.30 (m, 2H), 2.32 (s, 3H), 1.99 (m, 2H), 1.84 (m, 2H). ^{13}C NMR (126 MHz, CDCl_3) δ 158.22, 131.03, 130.11, 125.39, 115.72, 94.61, 72.37, 52.67, 46.36, 30.81. HRMS (ESI⁺) m/z : [M + H⁺] calcd for $\text{C}_{12}\text{H}_{17}\text{INO}$ 318.0355; found 318.0356.

General procedure B: Suzuki coupling

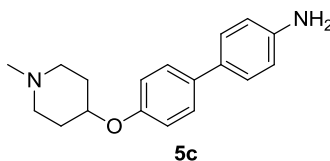


4'-((1-Methylpiperidin-4-yl)oxy)-[1,1'-biphenyl]-3-amine (5a) A mixture of iodide 3a (250 mg, 0.79 mmol) and boronic acid 4 (216 mg, 1.58 mmol) and potassium carbonate solution (2M, 100 μL) was suspended in dioxane (15 mL) and purged with argon for 15 min. After 15 min, [1,1'-Bis(diphenylphosphino)ferrocene]dichloropalladium(II) (57 mg, 0.08 mmol) was added to the suspension and the RM was heated in a sealed tube at 110 $^{\circ}\text{C}$ for 12 hours. The RM was concentrated to dryness and the brown residue was purified by column chromatography (SiO_2 , 1:10, Methanol:DCM) to afford desired product as a brown amorphous solid (149 mg, 67 %). ^1H NMR (500 MHz, Chloroform-*d*) δ 7.50 (d, $J = 8.7$ Hz, 2H), 7.22 (t, $J = 7.8$ Hz, 1H), 6.99 – 6.92 (m, 3H), 6.88 (s, 1H), 6.66 (dd, $J = 7.9, 2.3$ Hz, 1H), 4.45 – 4.34 (m, 1H), 3.74 (s, 2H), 2.79 (ddd, $J = 11.8, 7.8, 3.8$ Hz, 2H), 2.48 – 2.42 (m, 2H), 2.39 (s, 3H), 2.11 (ddt, $J = 11.5, 7.3, 3.6$ Hz, 2H), 1.94 (ddt, $J = 14.0, 7.9, 3.7$ Hz, 2H). ^{13}C NMR (126 MHz, CDCl_3) δ 156.77, 146.69, 141.94, 134.13, 129.65,

128.16, 117.28, 116.15, 113.60, 113.49, 71.45, 52.37, 45.96, 30.42. HRMS (ESI⁺) m/z: [M + H⁺] calcd for C₁₈H₂₃N₂O 283.1810; found, 283.1808.



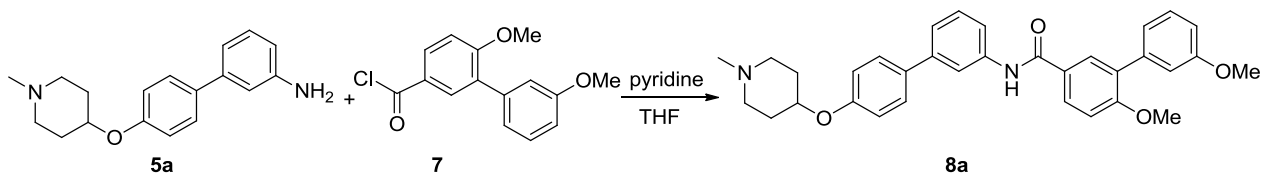
3'-((1-Methylpiperidin-4-yl)oxy)-[1,1'-biphenyl]-3-amine (5b) Compound **5b** was prepared following the general procedure B with iodide **3b** (250 mg, 0.79 mmol) and boronic acid **4** (216 mg, 1.58 mmol) and was purified by column chromatography (SiO₂, 5:95 MeOH:DCM) to afford a brownish amorphous solid (116 mg, 52%). ¹H NMR (500 MHz, Chloroform-*d*) δ 7.19 (t, *J* = 7.9 Hz, 1H), 7.09 (t, *J* = 7.8 Hz, 1H), 7.03 (m, 2H, NH₂), 6.98 – 6.96 (m, 1H), 6.86 – 6.83 (m, 1H), 6.80 (t, *J* = 2.0 Hz, 1H), 6.77 – 6.73 (m, 1H), 6.68 – 6.64 (m, 1H), 6.59 (dd, *J* = 8.1, 2.3 Hz, 1H), 4.36 (m, 1H), 2.66 (m, 2H), 2.37 (m, 2H), 2.25 (s, 3H), 1.92 (s, 2H), 1.80 (m, 2H). ¹³C NMR (126 MHz, CDCl₃+CH₃OH) δ 157.29, 146.62, 143.06, 142.03, 129.70, 129.59, 119.98, 117.78, 115.03, 114.74, 114.64, 114.14, 72.15, 54.63, 45.46, 29.85. HRMS (ESI⁺) m/z: [M + H⁺] calcd for C₁₈H₂₃N₂O 283.1810; found, 283.18108.



4'-((1-Methylpiperidin-4-yl)oxy)-[1,1'-biphenyl]-4-amine (5c) Compound **5c** was prepared using the general procedure A with N-methyl-4-hydroxy-piperidine **1** (535.17 mg, 4.65 mmol) and nitrophenol **6** (1.0 g, 4.65 mmol) to give yellow amorphous solid (855.4 mg, 65%). The yellow solid (850 mg, 3.01 mmol) was dissolved in methanol

(10ml) and 10% w/w Pd/C (10 mg) was added. The resulting mixture was stirred at room temperature under hydrogen atmosphere for 4h. After 4h, RM was filtered through celite and filtrate was concentrated to dryness to afford a brownish amorphous solid (765 mg, 100%). ¹H NMR (500 MHz, Chloroform-*d*) δ 7.89 (d, *J* = 4.3 Hz, 2H), 7.57 (d, *J* = 8.8 Hz, 2H), 7.14 (d, *J* = 4.3 Hz, 2H), 6.97 (d, *J* = 8.8 Hz, 2H), 4.42 (m, 1H), 2.79 – 2.61 (m, 2H), 2.39 (m, 2H), 2.36 (s, 3H), 2.08 (m, 2H), 1.91 (m, 2H). ¹³C NMR (126 MHz, CDCl₃) δ 159.13, 152.41, 149.27, 129.99, 127.82, 124.74, 121.22, 116.52, 72.02, 52.41, 46.08, 30.53. HRMS (ESI⁺) *m/z*: [M + H⁺] calcd for C₁₈H₂₃N₂O 283.1810; found, 283.1811.

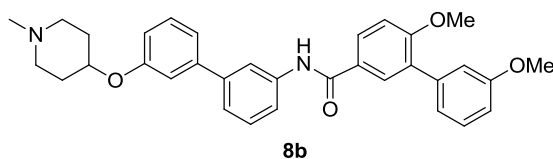
General procedure C: Amide coupling



3',6-Dimethoxy-N-(4'-((1-methylpiperidin-4-yl)oxy)-[1,1'-biphenyl]-3-yl)-[1,1'-

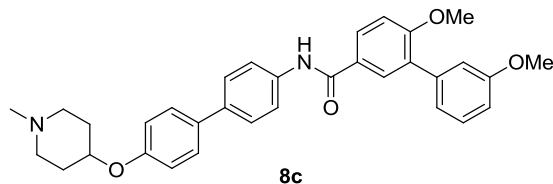
biphenyl]-3-carboxamide (8a) A solution of acid chloride **7** (75 mg, 0.27 mmol) in anhydrous THF (1ml) was cooled to 0 °C and treated with anhydrous pyridine (0.04 mL, 0.54 mmol) and a solution of 4'-((1-methylpiperidin-4-yl)oxy)-[1,1'-biphenyl]-3-amine **5a** (75 mg, 0.18 mmol) in anhydrous THF (2 mL). The resulting solution was allowed to stir at rt for 4 h. After 4 h, the solvent was removed and the residue was purified by column chromatography (SiO₂, 1:10, Methanol:DCM) to afford product as a colorless amorphous solid (48 mg, 52%). ¹H NMR (500 MHz, Chloroform-*d*) δ 7.97 (s, 1H), 7.90 – 7.82 (m, 2H), 7.78 (s, 1H), 7.52 – 7.44 (m, 3H), 7.36 – 7.21 (m, 3H), 7.09 – 6.92 (m, 3H), 6.90 –

6.79 (m, 3H), 4.47 (s, 1H), 2.93 (ddd, $J = 13.3, 10.4, 3.4$ Hz, 2H), 2.84 – 2.73 (m, 2H), 2.26 (td, $J = 10.5, 4.9$ Hz, 2H), 2.04 – 1.91 (m, 2H). ^{13}C NMR (126 MHz, CDCl_3) δ 165.26, 159.37, 159.32, 156.30, 141.41, 138.81, 138.61, 133.98, 130.67, 129.62, 129.43, 129.16, 128.47, 127.02, 122.66, 121.99, 118.63, 118.58, 116.15, 115.34, 112.93, 111.08, 68.68, 55.87, 55.35, 51.03, 44.81, 28.52. HRMS (ESI^+) m/z : $[\text{M} + \text{H}^+]$ calcd for $\text{C}_{33}\text{H}_{35}\text{N}_2\text{O}_4$ 523.2597; found 523.2599.



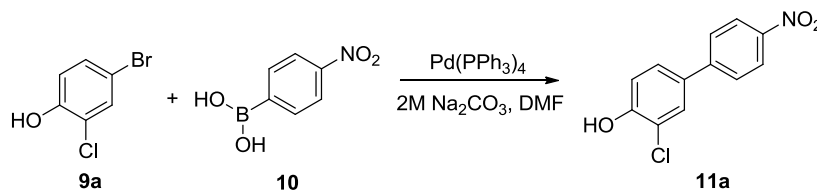
3',6-Dimethoxy-N-(3'-((1-methylpiperidin-4-yl)oxy)-[1,1'-biphenyl]-3-yl)-[1,1'-

biphenyl]-3-carboxamide (8b) Compound **8b** was prepared following the general procedure C with amine **5b** (100 mg, 0.36 mmol) and acid chloride **7** (150 mg, 0.54 mmol) and was purified by column chromatography (SiO_2 , 1:10 MeOH:DCM) to afford a white amorphous solid (114.7 mg, 62%). ^1H NMR (500 MHz, Chloroform-*d*) δ 8.54 (s, 1H, NH), 7.98 (s, 1H), 7.89 – 7.81 (m, 2H), 7.77 (s, 1H), 7.65 – 7.53 (m, 1H), 7.34 (t, $J = 7.8$ Hz, 1H), 7.30 – 7.22 (m, 2H), 7.13 (dd, $J = 7.7, 1.7$ Hz, 1H), 7.08 (d, $J = 2.5$ Hz, 1H), 7.08 – 6.92 (m, 3H), 6.83 (m, 2H), 4.41 (m, 1H), 3.81 (s, 3H), 3.77 (s, 3H), 2.77 (m, 2H), 2.57 – 2.47 (m, 2H), 2.37 (s, 3H), 2.08 (m, 2H), 1.90 (m, 2H). ^{13}C NMR (126 MHz, CDCl_3) δ 165.47, 159.57, 159.51, 157.58, 150.01, 142.61, 142.01, 138.99, 130.87, 130.08, 129.79, 129.63, 129.36, 128.65, 127.21, 123.32, 122.16, 120.32, 119.43, 119.14, 115.52, 115.42, 114.94, 113.13, 111.27, 70.53, 56.05, 55.53, 51.96, 45.72, 29.91. HRMS (ESI^+) m/z : $[\text{M} + \text{H}^+]$ calcd for $\text{C}_{33}\text{H}_{35}\text{N}_2\text{O}_4$ 523.2597; found 523.2593.



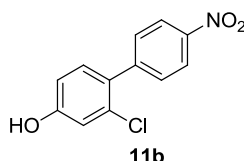
3',6-Dimethoxy-N-(4'-((1-methylpiperidin-4-yl)oxy)-[1,1'-biphenyl]-4-yl)-[1,1'-

biphenyl]-3-carboxamide (8c) Compound **8c** was prepared following the general procedure C with amine **5c** (750 mg, 2.68 mmol) and acid chloride **7** (1.11 g, 4.02 mmol) and was purified by column chromatography (SiO₂, 1:10 MeOH:DCM) to afford a white amorphous solid (1.10 g, 78%). ¹H NMR (500 MHz, Chloroform-*d*) δ 7.93 (dd, *J* = 8.6, 2.4 Hz, 1H), 7.89 (d, *J* = 2.4 Hz, 1H), 7.71 (d, *J* = 8.6 Hz, 2H), 7.51 (d, *J* = 7.2 Hz, 2H), 7.49 (d, *J* = 7.2 Hz, 2H), 7.32 (t, *J* = 7.9 Hz, 1H), 7.12 (dt, *J* = 7.6, 1.3 Hz, 1H), 7.09 (dd, *J* = 2.6, 1.6 Hz, 1H), 7.04 (d, *J* = 8.7 Hz, 1H), 6.95 (d, *J* = 8.8 Hz, 2H), 6.89 (ddd, *J* = 8.3, 2.6, 1.0 Hz, 1H), 4.57 (m, 1H), 3.86 (s, 3H), 3.82 (s, 3H), 3.05 (m, 2H), 2.99 (m, 2H), 2.63 (s, 3H), 2.20 (ddt, *J* = 14.3, 10.4, 3.4 Hz, 2H), 2.12 – 1.98 (m, 2H). ¹³C NMR (126 MHz, CDCl₃+CH₃OH) δ 166.41, 159.27, 159.17, 155.86, 148.91, 138.93, 137.31, 136.39, 134.01, 130.38, 130.07, 129.04, 128.58, 128.00, 126.91, 122.01, 121.08, 116.23, 115.26, 112.75, 110.88, 68.10, 55.69, 55.21, 50.60, 44.10, 28.06. HRMS (ESI⁺) *m/z*: [M + H⁺] calcd for C₃₃H₃₅N₂O₄ 523.2597; found 523.2561.

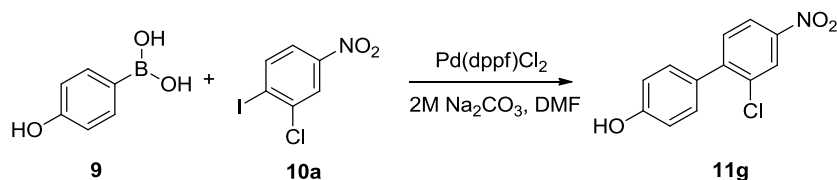


3-Chloro-4'-nitro-[1,1'-biphenyl]-4-ol (10a) Compound **11a** was prepared following the general procedure B with bromide **9a** (300 mg, 1.45 mmol) and 4-nitrophenylboronic

acid **10** (255.5 mg, 1.52 mmol). The residue was purified by column chromatography (SiO₂, 10:1, EtOAc:Hexane) to afford a yellow amorphous solid (200 mg, 56%). ¹H NMR (500 MHz, CDCl₃) δ 8.34 – 8.23 (m, 2H), 7.71 – 7.64 (m, 2H), 7.62 (d, *J* = 2.3 Hz, 1H), 7.48 (dd, *J* = 8.5, 2.3 Hz, 1H), 7.15 (d, *J* = 8.5 Hz, 1H), 5.74 (s, 1H). ¹³C NMR (126 MHz, CDCl₃) δ 152.10, 146.93, 145.83, 132.28, 127.88, 127.50, 127.24 (2C), 124.24 (2C), 120.75, 116.95. HRMS (ESI⁺) *m/z* [M-H⁺] calcd for C₁₂H₈ClNO₃ 248.0114, found 248.0117.

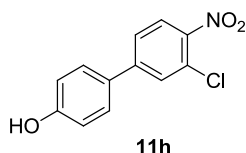


2-Chloro-4'-nitro-[1,1'-biphenyl]-4-ol (11b) Compound **11a** was prepared following the general procedure B with bromide **9a** (300 mg, 1.45 mmol) and 4-nitrophenylboronic acid **10** (290 mg, 1.74 mmol). The residue was purified by column chromatography (SiO₂, 10:1, EtOAc:Hexane) to afford a yellow amorphous solid (160 mg, 44%). ¹H NMR (500 MHz, Chloroform-d) δ 8.25 – 8.14 (m, 2H), 7.58 – 7.43 (m, 2H), 7.11 (dt, *J* = 8.4, 1.8 Hz, 1H), 6.92 (t, *J* = 2.4 Hz, 1H), 6.80 – 6.71 (m, 1H). ¹³C NMR (126 MHz, CDCl₃) δ 158.21, 146.82, 146.34, 132.64, 131.88, 130.64, 129.48, 123.32, 117.12, 114.74. HRMS (ESI⁺) *m/z* [M+K]⁺ calcd for C₁₂H₈ClNO₃ 288.0214, found 288.2896.

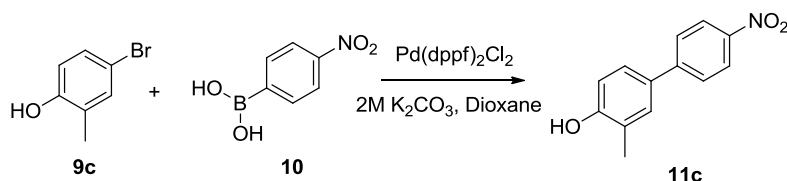


2'-Chloro-4'-nitro-[1,1'-biphenyl]-4-ol (11g) Compound **11g** was prepared following the general procedure B with 4-hydroxyphenylboronic acid **9** (300 mg, 2.18 mmol) and

iodide **10a** (616 mg, 2.18 mmol). The residue was purified by column chromatography (SiO₂, 10:1, EtOAc:Hexane) to afford a yellow amorphous solid (300 mg, 59%). ¹H NMR (500 MHz, CDCl₃) δ 8.36 (d, *J* = 2.4 Hz, 1H), 8.16 (dd, *J* = 8.5, 2.3 Hz, 1H), 7.51 (d, *J* = 8.5 Hz, 1H), 7.44 – 7.31 (m, 2H), 6.99 – 6.91 (m, 2H), 4.91 (s, 1H). ¹³C NMR (126 MHz, CDCl₃) δ 156.08, 147.01, 146.55, 133.51, 131.81, 130.77 (2C), 129.87, 125.33, 121.83, 115.35 (2C). HRMS (ESI⁺) *m/z* [M-H⁺] calcd for C₁₂H₈ClNO₃ 248.0114, found 248.0118.

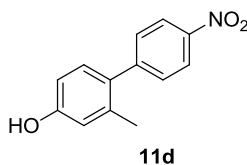


3'-Chloro-4'-nitro-[1,1'-biphenyl]-4-ol (11h) Compound **11h** was prepared following the general procedure B with 4-hydroxyphenylboronic acid **9** (300 mg, 2.18 mmol) and iodide **10b** (616 mg, 2.18 mmol). The residue was purified by column chromatography (SiO₂, 10:1, EtOAc:Hexane) to afford a yellow amorphous solid (259 mg, 42%). ¹H NMR (500 MHz, Chloroform-d) δ 7.95 (d, *J* = 8.5 Hz, 1H), 7.67 (d, *J* = 1.9 Hz, 1H), 7.52 (dd, *J* = 8.5, 2.0 Hz, 1H), 7.47 – 7.41 (m, 2H), 6.95 – 6.86 (m, 2H). ¹³C NMR (126 MHz, CDCl₃+CH₃OH) δ 154.32, 142.77, 141.49, 125.48, 124.80, 124.64, 123.86, 122.46, 121.13, 112.19. HRMS (ESI⁺) *m/z* [M-H⁺] calcd for C₁₂H₈ClNO₃ 248.0114, found 248.0108.

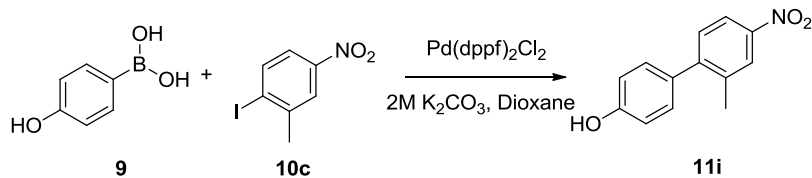


3-Methyl-4'-nitro-[1,1'-biphenyl]-4-ol (11c) Compound **11c** was prepared following the general procedure B with bromide **9c** (187 mg, 1.00 mmol) and 4-nitrophenylboronic

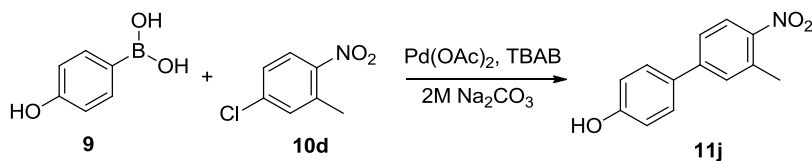
acid **10** (249 mg, 1.50 mmol) and was purified via column chromatography (SiO₂, 10:1, EtOAc:Hexane) to afford desired product as a yellow amorphous solid (134 mg, 59%). ¹H NMR (400 MHz, Chloroform-d + CD₃OD) δ 8.28 (d, *J* = 8.9 Hz, 2H), 7.70 (d, *J* = 8.9 Hz, 2H), 7.44 (s, 1H), 7.42 – 7.36 (m, 1H), 6.91 (d, *J* = 8.3 Hz, 1H), 2.36 (s, 3H). ¹³C NMR (126 MHz, CDCl₃) δ 154.94, 146.75, 145.29, 129.30, 129.07, 125.97, 125.05, 123.15, 122.42, 114.36, 15.18. HRMS (ESI⁺) *m/z*: [M + H⁺] calcd for C₁₃H₁₂NO₃: 230.0817; found 230.0815.



2-Methyl-4'-nitro-[1,1'-biphenyl]-4-ol (11d) Compound **11d** was prepared following the general procedure B with bromide **9d** (374 mg, 2.0 mmol) and 4-nitrophenylboronic acid **10** (688 mg, 4.0 mmol). The residue was purified by column chromatography (SiO₂, 10:1, EtOAc:Hexane) to afford desired product as a yellow amorphous solid (185 mg, 40%). ¹H NMR (400 MHz, Chloroform-d) δ 8.13 (d, *J* = 2.4 Hz, 1H), 8.06 (dd, *J* = 8.4, 2.5 Hz, 1H), 7.35 (d, *J* = 8.4 Hz, 1H), 7.26 - 7.14 (m, 2H), 7.00 - 6.91 (m, 2H), 2.37 (s, 3H). ¹³C NMR (126 MHz, CDCl₃) δ 155.57, 148.36, 146.85, 137.40, 132.38, 130.81, 130.34, 125.35, 121.08, 115.49, 20.90. HRMS (ESI⁺) *m/z*: [M + H⁺] calcd for C₁₃H₁₂NO₃: 230.0817; found 230.0822.

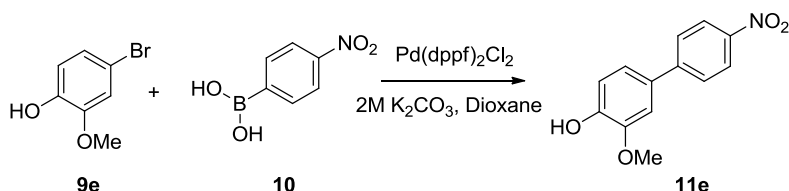


2'-Methyl-4'-nitro-[1,1'-biphenyl]-4-ol (11i) Compound **11i** was prepared following the general procedure B with 4-hydroxyphenylboronic acid **9** (326 mg, 2.36 mmol) and iodide **10c** (621 mg, 2.36 mmol). The residue was purified by column chromatography (SiO₂, 10:1, EtOAc:Hexane) to afford desired product as a yellow amorphous solid (120 mg, 22%). ¹H NMR (500 MHz, Chloroform-*d*) δ 8.14 (s, 1H), 8.08 (dd, *J* = 8.4, 2.4 Hz, 1H), 7.36 (d, *J* = 8.4 Hz, 1H), 7.21 (d, *J* = 8.5 Hz, 2H), 6.94 (d, *J* = 8.6 Hz, 2H), 5.03 (s, 1H, OH), 2.38 (s, 3H). ¹³C NMR (126 MHz, CDCl₃) δ 155.63, 148.42, 146.92, 137.46, 132.45, 130.88, 130.41, 125.42, 121.14, 115.56, 20.97. HRMS (ESI⁺) *m/z*: [M + H⁺] calcd for C₁₃H₁₂NO₃: 230.0817; found 230.0819.

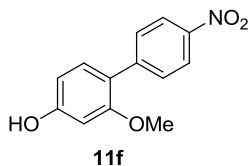


3'-Methyl-4'-nitro-[1,1'-biphenyl]-4-ol (11j) A mixture of boronic acid (300 mg, 2.175 mmol), 4-chloro-2-methyl-1-nitrobenzene (373 mg, 2.175 mmol), Pd(OAc)₂ (5 mg, 0.022 mmol), TBAB (723 mg, 2.175 mmol) and 2M Na₂CO₃ was irradiated by microwave at 175° C for 10 min. The reaction mixture was then extracted by ethyl acetate. The organic layer was collected, dried (over Na₂SO₄) and concentrated under reduced pressure. The brown residue was purified by flash column chromatography (SiO₂, 10:1, EtOAc:Hexane) to afford desired product as a yellowish amorphous solid (80 mg, 17%). ¹H NMR (500 MHz, Chloroform-*d*) δ 8.09 (d, *J* = 9.0 Hz, 1H), 7.62 – 7.40 (m, 4H), 7.03 – 6.85 (m, 2H),

4.89 (s, 1H), 2.69 (s, 3H). ^{13}C NMR (126 MHz, CDCl_3) δ 155.97, 147.51, 145.34, 144.15, 134.24, 133.92, 131.29, 130.48, 128.50, 125.32, 124.59, 115.74, 20.87. HRMS (ESI^+) m/z $[\text{M}^+]$ calcd for $\text{C}_{13}\text{H}_{11}\text{NO}_3$ 229.0739, found 229.0742.

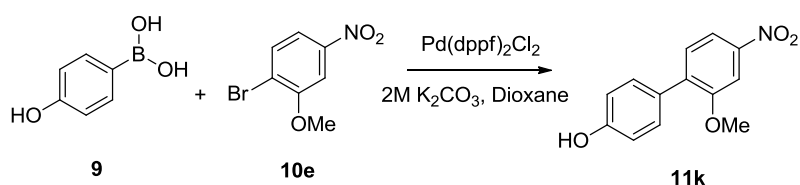


3-Methoxy-4'-nitro-[1,1'-biphenyl]-4-ol (11e) Compound **11e** was prepared following the general procedure B with bromide **9e** (200 mg, 0.98 mmol) and 4-nitrophenylboronic acid **10** (240 mg, 1.45 mmol). The residue was purified by column chromatography (SiO_2 , 10:1, EtOAc:Hexane) to afford desired product as a yellow amorphous solid (180mg 74% yield). ^1H NMR (400 MHz, Chloroform- d) δ 8.27 (d, $J = 8.9$ Hz, 2H), 7.68 (d, $J = 8.9$ Hz, 2H), 7.17 (dd, $J = 8.2, 2.1$ Hz, 1H), 7.10 (d, $J = 2.1$ Hz, 1H), 7.03 (d, $J = 8.2$ Hz, 1H), 5.78 (s, 1H, OH), 3.99 (s, 3H). ^{13}C NMR (126 MHz, CDCl_3) δ 147.70, 147.16, 146.86, 131.21, 127.37, 124.28, 120.99, 115.22, 109.76, 56.23. HRMS (ESI^+) m/z : $[\text{M} + \text{H}^+]$ calcd for $\text{C}_{13}\text{H}_{12}\text{NO}_4$: 246.0766; found 246.0762.

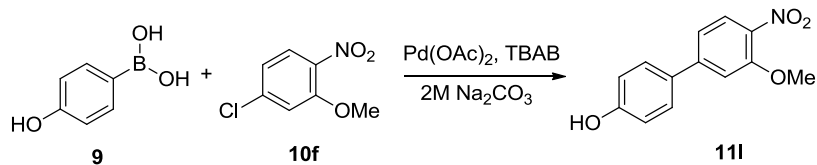


2-Methoxy-4'-nitro-[1,1'-biphenyl]-4-ol (11f) Compound **11f** was prepared following the general procedure B with bromide **9f** (200 mg, 0.98 mmol) and 4-nitrophenylboronic acid **10** (240 mg, 1.45 mmol). The crude product was purified by flash column

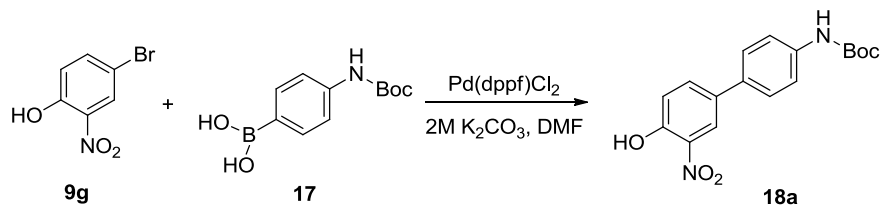
chromatography (SiO₂, 10:1, EtOAc:Hexane) to afford desired product as a yellow amorphous solid (180mg 74% yield). ¹H NMR (500 MHz, Chloroform-*d*) δ 8.23 (d, *J* = 8.8 Hz, 2H), 7.66 (d, *J* = 8.8 Hz, 2H), 7.21 (d, *J* = 8.2 Hz, 1H), 6.62 – 6.45 (m, 2H), 4.96 (s, 1H, OH), 3.82 (s, 3H). ¹³C NMR (126 MHz, CDCl₃) δ 157.18, 156.88, 145.60, 144.69, 130.92, 129.41, 122.65, 120.40, 107.07, 98.88, 55.01. HRMS (ESI+) *m/z*: [M + H⁺] calcd for C₁₃H₁₂NO₄: 246.0766; found 246.0769.



2'-Methoxy-4'-nitro-[1,1'-biphenyl]-4-ol (11k) Compound **11k** was prepared following the general procedure B with bromide **10e** (538mg, 2.32 mmol) and 4-hydroxyphenylboronic acid **9** (320 mg, 2.32 mmol). The crude product was purified by flash column chromatography (SiO₂, 10:1, EtOAc:Hexane) to afford desired product as a yellow amorphous solid (152 mg, 27%). ¹H NMR (500 MHz, Chloroform-*d*) δ 7.91 (dd, *J* = 8.4, 2.2 Hz, 1H), 7.82 (d, *J* = 2.2 Hz, 1H), 7.46 (d, *J* = 8.6 Hz, 1H), 7.45 (s, 1H), 6.93 (d, *J* = 8.6 Hz, 2H), 3.93 (s, 3H). ¹³C NMR (126 MHz, CDCl₃) δ 156.87, 155.93, 147.77, 137.21, 131.11, 130.84, 129.03, 116.38, 115.45, 106.37, 56.29. HRMS (ESI+) *m/z*: [M + H⁺] calcd for C₁₃H₁₂NO₄: 246.0766; found 246.0763.

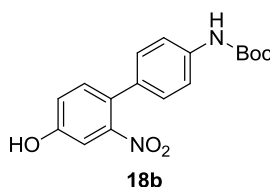


3'-Methoxy-4'-nitro-[1,1'-biphenyl]-4-ol (11I) A mixture of boronic acid (300 mg, 2.18 mmol), 4-chloro-2-methoxy-1-nitrobenzene (408 mg, 2.18 mmol), Pd(OAc)₂ (5 mg, 0.022 mmol), TBAB (723 mg, 2.18 mmol) and 2M Na₂CO₃ (3.27 ml, 6.54 mmol) was irradiated by microwave at 175° C for 10 min. The reaction mixture was then extracted by ethyl acetate. The organic layer was collected, dried (over Na₂SO₄) and concentrated under reduced pressure. The brown residue was purified by column chromatography (SiO₂, 10:1, EtOAc:Hexane) to afford desired product as a yellowish amorphous solid (95 mg, 18 %). ¹H NMR (400 MHz, Chloroform-d) δ 7.93 (d, *J* = 8.5 Hz, 1H), 7.48 – 7.42 (m, 2H), 7.19 – 7.11 (m, 2H), 6.95 – 6.87 (m, 2H), 4.00 (s, 3H). ¹³C NMR (126 MHz, CDCl₃) δ 156.80, 152.76, 146.98, 136.59, 129.71, 127.71, 125.69, 117.48, 115.07, 110.41, 55.59. HRMS (ESI+) *m/z*: [M + H⁺] calcd for C₁₃H₁₁NO₄ (M-H): 244.0546; found (M-H): 244.0542.

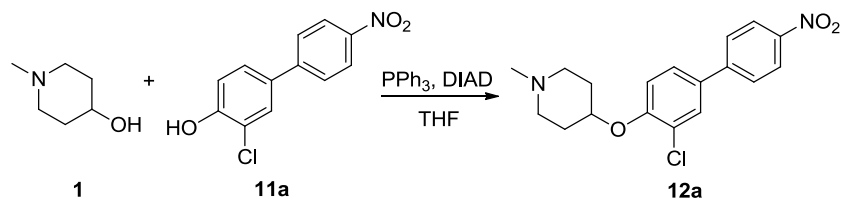


tert-butyl (4'-hydroxy-3'-nitro-[1,1'-biphenyl]-4-yl)carbamate (18a) Compound **18a** was prepared following the general procedure B with bromide **9g** (150 mg, 0.69 mmol) and boronic acid **17** (300 mg, 0.82 mmol). The residue was purified by column chromatography (SiO₂, 10:1, EtOAc:Hexane) to afford desired product as a yellow

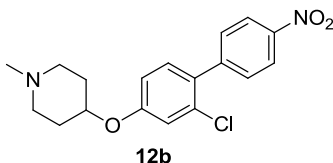
amorphous solid (136 mg, 60%). ^1H NMR (500 MHz, Chloroform-*d*) δ 10.58 (s, 1H), 8.29 (d, $J = 2.3$ Hz, 1H), 7.81 (dd, $J = 8.7, 2.4$ Hz, 1H), 7.61 – 7.37 (m, 4H), 7.25 – 7.21 (m, 1H), 6.55 (s, 1H), 1.55 (s, 9H). ^{13}C NMR (126 MHz, CDCl_3) δ 154.11, 151.21, 138.75, 138.34, 136.01, 135.15, 132.82, 127.25, 122.26, 120.39, 118.90, 81.15, 28.35. HRMS (ESI) m/z $[\text{M}-\text{H}^+]$ calcd for $\text{C}_{17}\text{H}_{18}\text{N}_2\text{O}_5$ 329.1137, found 329.1133.



tert-butyl (4'-hydroxy-2'-nitro-[1,1'-biphenyl]-4-yl)carbamate (18b)) Compound **18b** was prepared following the general procedure B with bromide **9h** (500 mg, 2.29 mmol) and boronic acid **17** (781.6 mg, 2.75 mmol). The residue was purified by column chromatography (SiO_2 , 10:1, EtOAc:Hexane) to afford desired product as a yellow amorphous solid (210 mg, 72%). ^1H NMR (500 MHz, Chloroform-*d*) δ 7.40 (d, $J = 8.3$ Hz, 2H), 7.32 (d, $J = 2.6$ Hz, 1H), 7.28 (d, $J = 5.0$ Hz, 1H), 7.23 – 7.17 (m, 2H), 7.07 (dd, $J = 8.4, 2.6$ Hz, 1H), 6.53 (s, 1H), 5.47 (s, 1H), 1.54 (s, 9H). ^{13}C NMR (126 MHz, CDCl_3) δ 155.35, 153.00, 149.83, 138.39, 133.34, 132.05, 129.00, 128.64, 119.86, 118.99, 111.40, 81.16, 28.64. HRMS (ESI) m/z $[\text{M}-\text{H}^+]$ calcd for $\text{C}_{17}\text{H}_{18}\text{N}_2\text{O}_5$ 329.1137, found 329.1132.

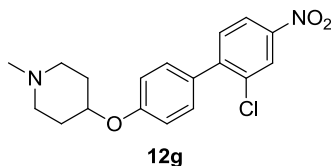


4-((3-Chloro-4'-nitro-[1,1'-biphenyl]-4-yl)oxy)-1-methylpiperidine (12a) Compound **12a** was prepared following the general procedure A with phenol (175 mg, 0.70 mmol) and N-methyl-4-hydroxy-piperidine (96.9 mg, 0.84 mmol). The residue was purified by column chromatography (SiO₂, 5:95, Methanol:DCM) to afford desired product as a yellow amorphous solid (200 mg, 83%). ¹H NMR (500 MHz, CDCl₃) δ 8.22 (d, *J* = 8.8 Hz, 2H), 7.77 – 7.52 (m, 3H), 7.46 (dd, *J* = 8.5, 2.4 Hz, 1H), 7.06 (d, *J* = 8.6 Hz, 1H), 4.81 (m, 1H), 3.49 – 3.37 (m, 2H), 3.23 (m, 2H), 2.87 (s, 3H), 2.32 (m, 2H), 2.24 – 2.10 (m, 2H). ¹³C NMR (126 MHz, CDCl₃+CH₃OH) δ 147.99, 142.90, 141.28, 129.32, 125.35, 123.24, 123.19, 122.97, 120.71, 120.08, 120.04, 111.82, 67.46, 54.11, 44.12, 26.76. HRMS (ESI⁺) *m/z* [M+H⁺] calcd for C₁₈H₁₉ClN₂O₃ 347.1163, found 347.1159.

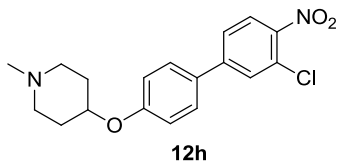


4-((2-Chloro-4'-nitro-[1,1'-biphenyl]-4-yl)oxy)-1-methylpiperidine (12b) Compound **12b** was prepared following the general procedure A with phenol (150 mg, 0.60 mmol) and N-methyl-4-hydroxy-piperidine (83.12 mg, 0.72 mmol). The residue was purified by column chromatography (SiO₂, 5:95, Methanol:DCM) to afford desired product as a yellow amorphous solid (150 mg, 78%). ¹H NMR (500 MHz, Chloroform-*d*) δ 8.28 (d, *J* = 8.7 Hz, 2H), 7.60 (d, *J* = 8.7 Hz, 2H), 7.27 (d, *J* = 0.7 Hz, 1H), 7.07 (d, *J* = 2.5 Hz, 1H),

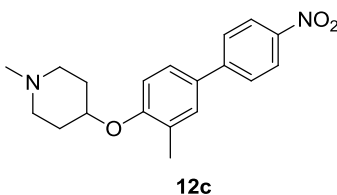
6.92 (dd, $J = 8.5, 2.5$ Hz, 1H), 4.42 (m, 1H), 2.76 (m, 2H), 2.42 (m, 2H), 2.39 (s, 3H), 2.11 (m, 2H), 1.93 (m, 2H). ^{13}C NMR (126 MHz, $\text{CDCl}_3 + \text{CH}_3\text{OH}$) δ 158.30, 147.19, 145.92, 133.15, 131.99, 130.72, 126.23, 123.55, 117.64, 115.13, 72.44, 52.65, 46.15, 30.40. HRMS (ESI^+) m/z [$\text{M} + \text{H}^+$] calcd for $\text{C}_{18}\text{H}_{19}\text{ClN}_2\text{O}_3$ 347.1163, found 347.1158.



4-((2'-Chloro-4'-nitro-[1,1'-biphenyl]-4-yl)oxy)-1-methylpiperidine (12g) Compound **12g** was prepared following the general procedure A with phenol **11g** (200 mg, 0.80 mmol) and N-methyl-4-hydroxy-piperidine (110.72 mg, 0.96 mmol). The residue was purified by column chromatography (SiO_2 , 5:95, Methanol:DCM) to afford desired product as a yellow amorphous solid (225 mg, 81%). ^1H NMR (500 MHz, Chloroform- d) δ 8.35 (d, $J = 2.3$ Hz, 1H), 8.15 (dt, $J = 8.4, 2.2$ Hz, 1H), 7.51 (d, $J = 8.5$ Hz, 1H), 7.43 – 7.34 (m, 2H), 7.05 – 6.94 (m, 2H), 4.41 (dt, $J = 7.2, 3.7$ Hz, 1H), 2.83 – 2.65 (m, 2H), 2.34 (s, 3H), 2.07 (ddd, $J = 13.9, 7.1, 3.5$ Hz, 2H), 1.92 (ddd, $J = 13.2, 7.9, 3.7$ Hz, 2H). ^{13}C NMR (126 MHz, CDCl_3) δ 158.01, 146.90, 146.62, 133.42, 131.78, 130.57, 129.47, 125.32, 121.80, 115.58, 71.98, 52.60, 46.17, 30.74. HRMS (ESI^+) m/z [$\text{M} + \text{H}^+$] calcd for $\text{C}_{18}\text{H}_{19}\text{ClN}_2\text{O}_3$ 347.1163, found 347.1136.

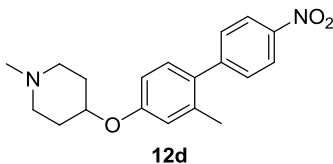


4-((3'-Chloro-4'-nitro-[1,1'-biphenyl]-4-yl)oxy)-1-methylpiperidine (12h) Compound **12h** was prepared following the general procedure A with phenol **11h** (125 mg, 0.50 mmol) and N-methyl-4-hydroxy-piperidine (69.10 mg, 0.60 mmol). The residue was purified by column chromatography (SiO₂, 5:95, Methanol:DCM) to afford desired product as a yellow amorphous solid (110 mg, 63%). ¹H NMR (500 MHz, Chloroform-*d*) δ 7.99 (d, *J* = 8.5 Hz, 1H), 7.71 (d, *J* = 1.9 Hz, 1H), 7.62 – 7.47 (m, 3H), 7.02 (d, *J* = 8.7 Hz, 2H), 4.44 (m, 1H), 2.76 (m, 2H), 2.42 (m, 2H), 2.38 (s, 3H), 2.10 (m, 2H), 1.93 (m, 2H). ¹³C NMR (126 MHz, CDCl₃) δ 158.71, 146.52, 145.96, 130.06, 129.83, 128.80, 128.10, 126.65, 125.45, 116.72, 71.93, 52.54, 46.21, 30.62. HRMS (ESI⁺) *m/z* [M+H⁺] calcd for C₁₈H₁₉ClN₂O₃ 347.1163, found 347.1159.

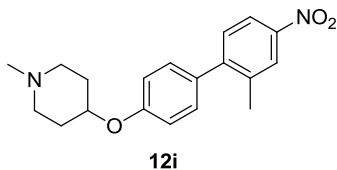


1-Methyl-4-((3-methyl-4'-nitro-[1,1'-biphenyl]-4-yl)oxy)piperidine (12c) Compound **12c** was prepared following the general procedure A with phenol **11c** (280 mg, 1.20 mmol) and N-methyl-4-hydroxy-piperidine (280 mg, 2.40 mmol). The residue was purified by column chromatography (SiO₂, 5:95, Methanol:DCM) to afford desired product as a yellow amorphous solid (180 mg, 46%). ¹H NMR (500 MHz, Chloroform-*d*) δ 8.35-8.18 (m, 2H), 7.75-7.62 (m, 2H), 7.49-7.36 (m, 2H), 6.92 (d, *J* = 8.4 Hz, 1H), 4.45

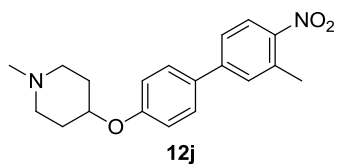
(s, 1H), 2.66 (s, 2H), 2.44-2.34 (m, 2H), 2.33 (s, 3H), 2.31 (s, 3H), 2.11-1.86 (m, 4H). ^{13}C NMR (126 MHz, CDCl_3) δ 156.59, 147.57, 146.54, 130.70, 130.04, 128.86, 127.15, 124.23, 113.06, 52.57, 46.47, 30.92, 29.85, 16.80. HRMS (ESI^+) m/z [$\text{M}+\text{H}^+$] calcd for $\text{C}_{19}\text{H}_{23}\text{N}_2\text{O}_3$ 327.1709, found 327.1724.



1-Methyl-4-((2-methyl-4'-nitro-[1,1'-biphenyl]-4-yl)oxy)piperidine (12d) Compound **12d** was prepared following the general procedure A with phenol **11d** (230 mg, 1.50 mmol) and N-methyl-4-hydroxy-piperidine (230 mg, 3.10 mmol). The residue was purified by column chromatography (SiO_2 , 5:95, Methanol:DCM) to afford desired product as a yellow amorphous solid (300 mg, 61%). ^1H NMR (500 MHz, Chloroform- d) δ 8.26 (d, $J = 8.9$ Hz, 2H), 7.68 (d, $J = 8.9$ Hz, 2H), 7.47 - 7.37 (m, 2H), 6.92 (d, $J = 8.5$ Hz, 1H), 4.49 (s, 1H), 2.77 - 2.68 (m, 2H), 2.50 (s, 2H), 2.39 (s, 3H), 2.31 (s, 3H), 2.15 - 2.08 (m, 2H), 2.02 - 1.92 (m, 2H). ^{13}C NMR (126 MHz, CDCl_3) δ 156.51, 147.61, 146.68, 130.96, 130.20, 127.28, 124.35, 113.11, 52.42, 46.27, 30.57, 16.90. IR 2954, 2923, 2852, 2358, 2341, 1593, 1514, 1485, 1340, 1307, 1274, 1247, 1135, 1108, 1039 cm^{-1} . HRMS (ESI^+) m/z [$\text{M}+\text{Na}^+$] calcd for $\text{C}_{19}\text{H}_{22}\text{N}_2\text{O}_3$ 349.1528, found 349.1528.

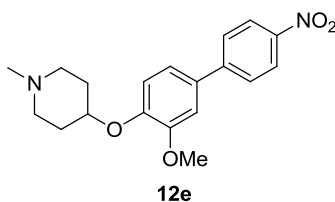


1-Methyl-4-((2'-methyl-4'-nitro-[1,1'-biphenyl]-4-yl)oxy)piperidine (12i) Compound **12i** was prepared following the general procedure A with phenol **11i** (116 mg, 0.50 mmol) and N-methyl-4-hydroxy-piperidine (116 mg, 2.02 mmol). The residue was purified by column chromatography (SiO₂, 5:95, Methanol:DCM) to afford desired product as a yellow amorphous solid (120 mg, 73%). ¹H NMR (500 MHz, Methanol-d₄) δ 8.14 (d, *J* = 2.4 Hz, 1H), 8.09 - 8.02 (m, 1H), 7.39 (d, *J* = 8.4 Hz, 1H), 7.31 - 7.24 (m, 2H), 7.03 (d, *J* = 8.7 Hz, 2H), 4.49 (q, *J* = 5.1, 4.6 Hz, 1H), 2.76 (s, 2H), 2.50 - 2.40 (m, 2H), 2.37 (s, 3H), 2.33 (s, 3H), 2.05 (ddd, *J* = 12.7, 6.5, 3.1 Hz, 2H), 1.91 - 1.81 (m, 2H). ¹³C NMR (126 MHz, MeOD) δ 158.59, 149.66, 148.08, 138.64, 133.53, 131.82, 131.22, 126.00, 124.48, 121.80, 116.90, 112.62, 79.50, 53.25, 46.10, 31.30, 20.88, 16.60. HRMS (ESI⁺) *m/z* [M+Na⁺] calcd for C₁₉H₂₂N₂O₄ 365.1477, found 365.1481.

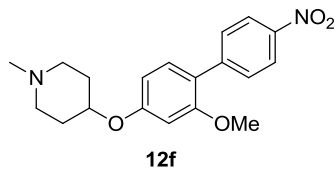


1-Methyl-4-((3'-methyl-4'-nitro-[1,1'-biphenyl]-4-yl)oxy)piperidine (12j) Compound **12j** was prepared following the general procedure A with phenol **11j** (75 mg, 0.33 mmol) and N-methyl-4-hydroxy-piperidine (45.4 mg, 0.39 mmol). The residue was purified by column chromatography (SiO₂, 5:95, Methanol:DCM) to afford desired product as a yellow amorphous solid (80.3 mg, 75%). ¹H NMR (500 MHz, Chloroform-*d*) δ 8.08 (d, *J*

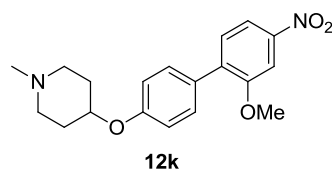
= 9.1 Hz, 1H), 7.55 (d, $J = 8.7$ Hz, 2H), 7.52 – 7.46 (m, 2H), 7.01 (d, $J = 8.8$ Hz, 2H), 4.46 (s, 1H), 2.83 – 2.79 (m, 2H), 2.69 (s, 3H), 2.56 – 2.48 (m, 2H), 2.42 (s, 3H), 2.18 – 2.14 (m, 2H), 1.98 – 1.94 (m, 2H). ^{13}C NMR (126 MHz, CDCl_3) δ 158.10, 147.64, 145.77, 134.69, 131.60, 130.90, 128.79, 125.78, 125.02, 116.59, 71.39, 52.31, 45.99, 30.29, 21.34. (ESI⁺) m/z $[\text{M}+\text{H}^+]$ calcd for $\text{C}_{19}\text{H}_{22}\text{N}_2\text{O}_4$ 327.1709; found 327.1721.



4-((3-Methoxy-4'-nitro-[1,1'-biphenyl]-4-yl)oxy)-1-methylpiperidine (12e) Compound **12e** was prepared following the general procedure A with phenol **11e** (180 mg, 0.73 mmol) and N-methyl-4-hydroxy-piperidine (160 mg, 1.46 mmol). The residue was purified by column chromatography (SiO_2 , 5:95, Methanol:DCM) to afford desired product as a yellow amorphous solid (200 mg, 80%). ^1H NMR (500 MHz, Chloroform- d : Acetone d_6 (10:1)) δ 8.25 (d, $J = 8.9$ Hz, 2H), 7.67 (d, $J = 8.8$ Hz, 2H), 7.18 - 7.08 (m, 2H), 7.00 (d, $J = 8.4$ Hz, 1H), 4.44 (dp, $J = 6.9, 3.4$ Hz, 1H), 3.92 (s, 3H), 2.90 (ddd, $J = 11.9, 8.6, 3.4$ Hz, 2H), 2.70 - 2.60 (m, 1H), 2.43 (s, 3H), 2.11 (ddd, $J = 12.5, 8.5, 3.8$ Hz, 2H), 1.99 (s, 3H). ^{13}C NMR (126 MHz, CDCl_3 : Acetone d_6 (10:1)) δ 176.70, 151.31, 146.78, 132.86, 127.43, 124.20, 120.20, 117.41, 111.54, 56.26, 44.99, 22.83. (ESI⁺) m/z $[\text{M}+\text{Na}^+]$ calcd for $\text{C}_{19}\text{H}_{22}\text{N}_2\text{O}_4$ 365.1477, found 365.1473.



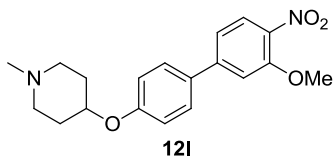
4-((2-Methoxy-4'-nitro-[1,1'-biphenyl]-4-yl)oxy)-1-methylpiperidine (12f) Compound **12f** was prepared following the general procedure A with phenol **11f** (175 mg, 0.72 mmol) and N-methyl-4-hydroxy-piperidine (124.2 mg, 1.08 mmol). The residue was purified by column chromatography (SiO₂, 5:95, Methanol:DCM) to afford desired product as a yellow amorphous solid (191 mg, 78%). ¹H NMR (500 MHz, Chloroform-*d*) δ 8.23 (d, *J* = 8.9 Hz, 2H), 7.67 (d, *J* = 8.8 Hz, 2H), 7.25 (d, *J* = 8.8 Hz, 1H), 6.59 (m, 2H), 4.41 (m, 1H), 3.82 (s, 3H), 2.75 (m, 2H), 2.38 (m, 2H), 2.36 (s, 3H), 2.06 (m, 2H), 2.00 – 1.82 (m, 2H). ¹³C NMR (126 MHz, CDCl₃) δ 159.53, 157.90, 146.38, 145.52, 131.49, 130.18, 123.45, 121.25, 106.92, 101.09, 70.09, 55.80, 52.72, 46.31, 30.88. (ESI⁺) *m/z* [M+Na⁺] calcd for C₁₉H₂₂N₂O₄ 365.1477, found 365.1493.



4-((2'-Methoxy-4'-nitro-[1,1'-biphenyl]-4-yl)oxy)-1-methylpiperidine(12k)

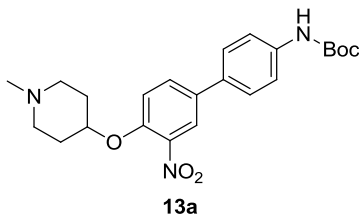
Compound **12k** was prepared following the general procedure A with phenol **11k** (125 mg, 0.51 mmol) and N-methyl-4-hydroxy-piperidine (88 mg, 0.77 mmol). The residue was purified by column chromatography (SiO₂, 5:95, Methanol:DCM) to afford desired product as a yellow amorphous solid (113.5 mg, 65%). ¹H NMR (400 MHz, Chloroform-*d*) δ 7.96 – 7.87 (m, 1H), 7.82 (d, *J* = 2.2 Hz, 1H), 7.49 (d, *J* = 8.8 Hz, 2H), 7.44 (d, *J* = 8.4 Hz, 1H), 6.98 (d, *J* = 8.8 Hz, 2H), 4.41 (m, 1H), 3.93 (s, 3H), 2.82 – 2.63 (m, 2H),

2.39 (m, 2H), 2.36 (s, 3H), 2.09 (m, 2H), 1.92 (m, 2H). ^{13}C NMR (126 MHz, CDCl_3) δ 157.69, 156.87, 147.77, 137.20, 130.97, 130.83, 128.90, 116.39, 115.79, 106.37, 70.23, 56.30, 52.29, 45.98, 30.45. (ESI^+) m/z $[\text{M}+\text{Na}^+]$ calcd for $\text{C}_{19}\text{H}_{22}\text{N}_2\text{O}_4$ 365.1477; found 365.1483.

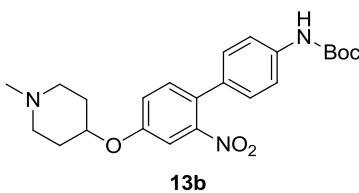


4-((3'-Methoxy-4'-nitro-[1,1'-biphenyl]-4-yl)oxy)-1-methylpiperidine (121)

Compound **121** was prepared following the general procedure A with phenol **111** (100 mg, 0.41 mmol) and N-methyl-4-hydroxy-piperidine (57 mg, 0.49 mmol). The residue was purified by column chromatography (SiO_2 , 5:95, Methanol:DCM) to afford desired product as a yellow amorphous semi-solid (85 mg, 60 %). ^1H NMR (400 MHz, Chloroform- d) δ 7.96 (d, $J = 8.3$ Hz, 1H), 7.53 (d, $J = 8.7$ Hz, 2H), 7.22 – 7.14 (m, 2H), 7.01 (d, $J = 8.7$ Hz, 2H), 4.45 (s, 1H), 4.03 (s, 3H), 2.89 – 2.69 (m, 2H), 2.52 – 2.42 (m, 2H), 2.37 (s, 3H), 2.15 (d, $J = 16.9$ Hz, 2H), 1.94 (s, 2H). ^{13}C NMR (126 MHz, CDCl_3) δ 158.23, 153.75, 147.55, 137.94, 131.76, 128.73, 126.72, 118.62, 116.53, 111.59, 56.67, 52.30, 45.99, 30.34. IR 3392, 2945, 2358, 2331, 1276, 1263 cm^{-1} . (ESI^+) m/z $[\text{M}+\text{H}^+]$ calcd for $\text{C}_{19}\text{H}_{22}\text{N}_2\text{O}_4$ 343.1658, found 343.1658.



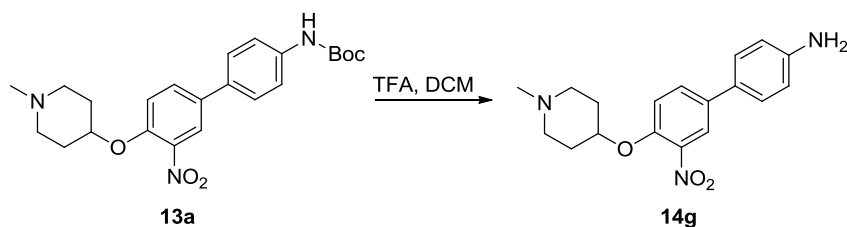
tert-butyl (4'-((1-methylpiperidin-4-yl)oxy)-3'-nitro-[1,1'-biphenyl]-4-yl)carbamate (13a) Compound **13a** was prepared following the general procedure A with phenol **18a** (75 mg, 0.23 mmol) and N-methyl-4-hydroxy-piperidine (31.5 mg, 0.27 mmol). The residue was purified by column chromatography (SiO₂, 5:95, Methanol:DCM) to afford desired product as a yellow amorphous semi-solid (80 mg, 82%). ¹H NMR (500 MHz, Chloroform-d) δ 8.01 (d, *J* = 2.4 Hz, 1H), 7.70 (dd, *J* = 8.7, 2.4 Hz, 1H), 7.51 – 7.41 (m, 4H), 7.13 (d, *J* = 8.8 Hz, 1H), 6.57 (s, 1NH), 4.70 (s, 1H), 2.85 (s, 2H), 2.70 (s, 2H), 2.48 (s, 3H), 2.24 (s, 2H), 2.06 (ddd, *J* = 15.0, 7.7, 3.9 Hz, 2H), 1.54 (s, 9H). ¹³C NMR (126 MHz, CDCl₃) δ 153.49, 150.08, 141.99, 139.23, 134.69, 133.72, 132.74, 128.15, 124.54, 119.81, 117.21, 81.78, 51.83, 46.40, 30.62, 30.18, 29.24. (ESI⁺) *m/z* [M+H⁺] calcd for C₂₃H₂₉N₃O₅ 428.2186, found 428.2177.



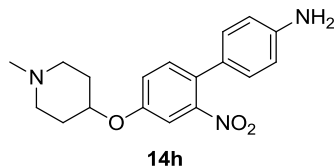
tert-butyl (4'-((1-methylpiperidin-4-yl)oxy)-2'-nitro-[1,1'-biphenyl]-4-yl)carbamate (13b) Compound **13b** was prepared following the general procedure A with phenol **18b** (150 mg, 0.46 mmol) and N-methyl-4-hydroxy-piperidine (63 mg, 0.54 mmol). The residue was purified by column chromatography (SiO₂, 5:95, Methanol:DCM) to afford desired product as a yellow amorphous semi-solid (175 mg, 89%). ¹H NMR (500 MHz,

Chloroform-d) δ 7.41 (d, $J = 8.2$ Hz, 2H), 7.34 (d, $J = 2.6$ Hz, 1H), 7.29 (d, $J = 33.1$ Hz, 1H), 7.23 – 7.19 (m, 2H), 7.13 (dd, $J = 8.6, 2.6$ Hz, 1H), 6.53 (s, NH), 4.42 (s, 1H), 2.73 (s, 2H), 2.36 (s, 3H), 2.15 – 2.01 (m, 2H), 1.91 (d, $J = 11.4$ Hz, 2H), 1.65 – 1.54 (m, 2H), 1.54 (s, 9H). ^{13}C NMR (126 MHz, CDCl_3) δ 156.95, 152.90, 149.98, 138.48, 133.18, 131.97, 128.97, 128.51, 120.36, 118.84, 111.29, 81.09, 52.25, 46.19, 30.42, 30.03, 28.63. HRMS (ESI⁺) m/z [$\text{M}+\text{H}^+$] calcd for $\text{C}_{23}\text{H}_{29}\text{N}_3\text{O}_5$ 428.2186, found 428.2182.

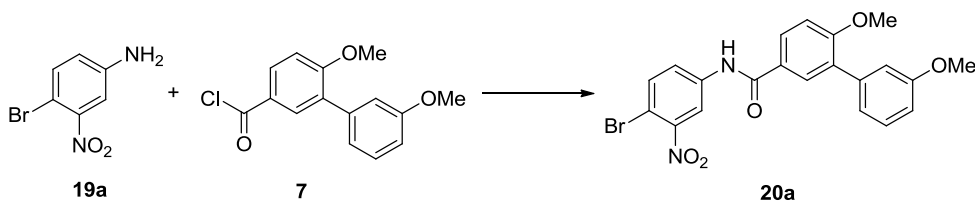
General Procedure D: TFA mediated boc-deprotection



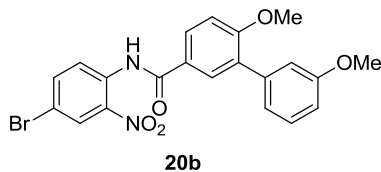
4'-((1-Methylpiperidin-4-yl)oxy)-3'-nitro-[1,1'-biphenyl]-4-amine (14g) A solution of TFA (0.5 ml) in dry DCM (0.5 ml) was added to an ice-cooled solution of boc-protected aniline (65mg, 0.15 mmol) in dry DCM (0.5 ml) and allowed to stir at rt for 2h. After 2h, the RM was concentrated under high vacuum to afford a brownish amorphous semi-solid (48 mg, 98%), which was used as such without further purification in the next step. HRMS (ESI⁺) m/z [$\text{M}+\text{H}^+$] calcd for $\text{C}_{18}\text{H}_{21}\text{N}_3\text{O}_3$ 328.1662, found 328.1667.



4'-((1-Methylpiperidin-4-yl)oxy)-2'-nitro-[1,1'-biphenyl]-4-amine (14h) Compound **14h** was obtained following the general procedure D as a brownish amorphous solid (160 mg, 90%), which was used as such without further purification in the next step. HRMS (ESI⁺) *m/z* [M+H⁺] calcd for C₁₈H₂₁N₃O₃ 328.1662, found 328.1653.

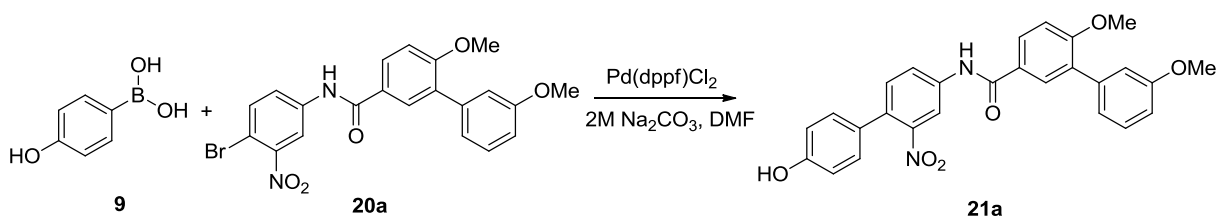


N-(4-bromo-3-nitrophenyl)-3',6-dimethoxy-[1,1'-biphenyl]-3-carboxamide (20a) Compound **20a** was prepared following the general procedure C with amine **19a** (150 mg, 0.69 mmol) and acid chloride **7** (200 mg, 0.72 mmol). The residue was purified by column chromatography (SiO₂, 1:100, Acetone:DCM) to afford desired product as a light brown solid (283 mg, 90%). ¹H NMR (400 MHz, Chloroform-*d*) δ 8.28 (d, *J* = 2.5 Hz, 1H), 7.97 (broad, 1H, NH), 7.90 (dd, *J* = 8.6, 2.4 Hz, 1H), 7.79 (d, *J* = 2.4 Hz, 1H), 7.76 (d, *J* = 2.5 Hz, 1H), 7.70 (d, *J* = 8.8 Hz, 1H), 7.37 (t, *J* = 7.9 Hz, 1H), 7.13 – 7.05 (m, 3H), 6.94 (dd, *J* = 8.3, 2.7 Hz, 1H), 3.91 (s, 3H), 3.86 (s, 3H). ¹³C NMR (126 MHz, CDCl₃) δ 165.35, 160.13, 159.57, 150.09, 138.71, 138.57, 135.53, 131.18, 129.76, 129.45, 128.81, 125.97, 124.32, 122.10, 116.92, 115.61, 113.18, 111.45, 108.40, 56.14, 55.56. HRMS (ESI⁺) *m/z* [M+H⁺] calcd for C₂₁H₁₈BrN₂O₅ 457.0399, found 457.0402.



N-(4-bromo-2-nitrophenyl)-3',6-dimethoxy-[1,1'-biphenyl]-3-carboxamide (20b)

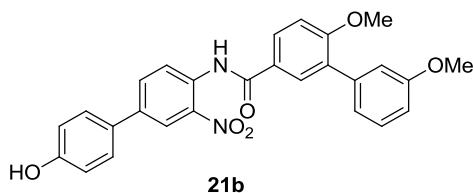
Compound **20b** was prepared following the general procedure C with amine **19b** (200 mg, 0.75 mmol) and acid chloride **7** (242.3 mg, 0.91 mmol). The residue was purified by column chromatography (SiO₂, 1:10, EtOAc:Hexane) to afford desired product as a light yellowish amorphous solid (80 mg, 43%). ¹H NMR (500 MHz, Chloroform-d) δ 11.30 (s, NH), 8.97 (d, *J* = 9.1 Hz, 1H), 8.43 (d, *J* = 2.4 Hz, 1H), 8.05 – 7.93 (m, 2H), 7.80 (dd, *J* = 9.1, 2.4 Hz, 1H), 7.38 (t, *J* = 7.9 Hz, 1H), 7.20 – 7.06 (m, 3H), 6.94 (ddd, *J* = 8.3, 2.6, 1.0 Hz, 1H), 3.93 (s, 3H), 3.87 (s, 3H). ¹³C NMR (126 MHz, CDCl₃) δ 165.81, 160.78, 159.94, 139.61, 139.05, 137.11, 135.41, 131.81, 130.97, 129.82, 128.99, 126.57, 124.11, 122.53, 115.78, 115.65, 113.81, 111.79, 56.54, 55.92. HRMS (ESI⁺) *m/z* [M+H⁺] calcd for C₂₁H₁₇BrN₂O₅ 457.0399, found 457.0402.



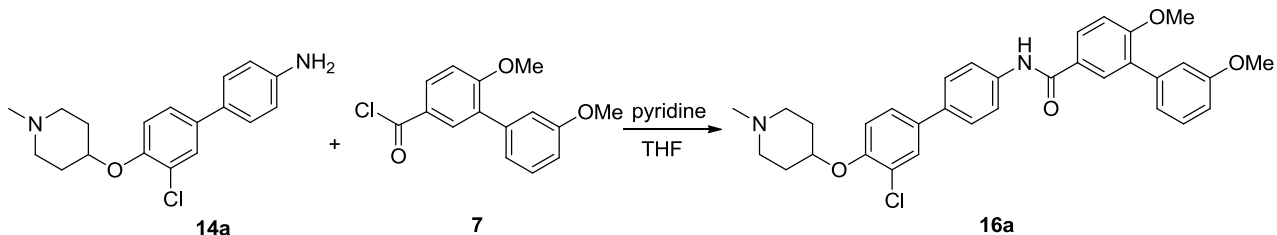
N-(4'-hydroxy-2-nitro-[1,1'-biphenyl]-4-yl)-3',6-dimethoxy-[1,1'-biphenyl]-3-

carboxamide (21a) Compound **21a** was prepared following the general procedure B with 4-hydroxyphenylboronic acid **9** (72 mg, 0.52 mmol) and bromide **20a** (120 mg, 0.26 mmol). The residue was purified by column chromatography (SiO₂, 1:100, Acetone:DCM) to afford desired product as a brown amorphous solid (52 mg, 43 %). ¹H

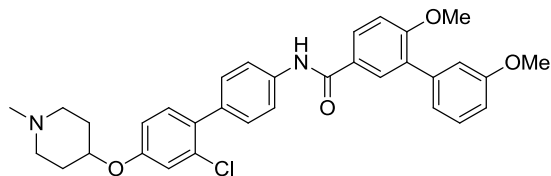
NMR (400 MHz, Chloroform-*d*) δ 9.83 (s, 1H, NH), 8.16 (t, $J = 1.8$ Hz, 1H), 7.91 – 7.83 (m, 3H), 7.29 (d, $J = 8.3$ Hz, 1H), 7.25 – 7.22 (m, 1H), 7.05 (m, 3H), 7.03 – 6.97 (m, 2H), 6.82 (dd, $J = 8.3, 2.6$ Hz, 1H), 6.79 – 6.72 (m, 2H), 3.80 (s, 3H), 3.76 (s, 3H). ^{13}C NMR (126 MHz, CDCl_3) δ 166.66, 159.52, 159.17, 156.95, 149.16, 138.84, 138.32, 131.98, 131.09, 130.42, 130.24, 129.07, 129.02, 128.78, 128.18, 127.52, 126.35, 123.76, 121.98, 115.52, 115.24, 112.74, 110.87, 55.67, 55.18. HRMS (ESI⁺) m/z [M+Na⁺] calcd for $\text{C}_{27}\text{H}_{22}\text{N}_2\text{O}_6\text{Na}$ 493.1376, found 493.1371.



N-(4'-hydroxy-3-nitro-[1,1'-biphenyl]-4-yl)-3',6-dimethoxy-[1,1'-biphenyl]-3-carboxamide (21b) Compound **21b** was prepared following the general procedure B with 4-hydroxyphenylboronic acid **9** (102.3 mg, 0.36 mmol) and bromide **20a** (110 mg, 0.24 mmol). The residue was purified by column chromatography (SiO_2 , 1:100, Acetone:DCM) to afford desired product as a light yellowish amorphous solid (110 mg, 92%). ^1H NMR (500 MHz, Chloroform-*d*) δ 11.35 (s, OH), 9.05 (d, $J = 8.8$ Hz, 1H), 8.45 (d, $J = 2.3$ Hz, 1H), 8.09 – 7.95 (m, 2H), 7.90 (dd, $J = 8.8, 2.3$ Hz, 1H), 7.59 – 7.47 (m, 2H), 7.38 (t, $J = 7.9$ Hz, 1H), 7.21 – 7.05 (m, 3H), 6.98 – 6.89 (m, 3H), 3.93 (s, 3H), 3.88 (s, 3H). ^{13}C NMR (126 MHz, CDCl_3) δ 165.90, 160.62, 159.94, 156.48, 139.16, 137.21, 136.56, 134.72, 134.65, 131.73, 131.41, 130.97, 129.81, 128.96, 128.75, 126.96, 123.77, 123.11, 122.58, 116.65, 115.77, 113.82, 111.76, 56.53, 55.93. HRMS (ESI⁺) m/z [M+Na]⁺ calcd for $\text{C}_{27}\text{H}_{22}\text{N}_2\text{O}_6$ 493.1376, found 493.3180.

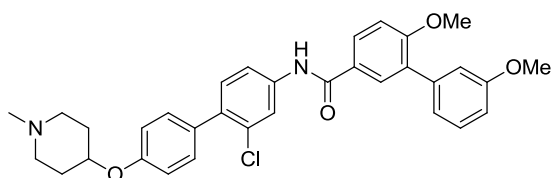


N-(3'-chloro-4'-((1-methylpiperidin-4-yl)oxy)-[1,1'-biphenyl]-4-yl)-3',6-dimethoxy-[1,1'-biphenyl]-3-carboxamide (16a) Compound **16a** was prepared following the general procedure C with amine **14a** (25 mg, 0.08 mmol) and acid chloride **7** (21.37 mg, 0.08 mmol) and was purified by column chromatography (SiO₂, 1:10 MeOH:DCM) to afford a white amorphous solid (20 mg, 47%). ¹H NMR (500 MHz, Chloroform-d) δ 8.08 (s, 1H), 7.94 (dd, *J* = 8.6, 2.4 Hz, 1H), 7.85 (d, *J* = 2.4 Hz, 1H), 7.76 – 7.69 (m, 2H), 7.61 (d, *J* = 2.3 Hz, 1H), 7.51 (d, *J* = 8.6 Hz, 2H), 7.41 (dd, *J* = 8.5, 2.3 Hz, 1H), 7.36 (t, *J* = 7.9 Hz, 1H), 7.13 (dt, *J* = 7.6, 1.2 Hz, 1H), 7.10 (dd, *J* = 2.6, 1.6 Hz, 1H), 7.05 (d, *J* = 8.7 Hz, 1H), 7.00 (d, *J* = 8.6 Hz, 1H), 6.92 (ddd, *J* = 8.2, 2.6, 1.0 Hz, 1H), 4.55 (s, 1H), 3.89 (s, 3H), 3.85 (s, 3H), 3.05 – 2.87 (m, 2H), 2.78 (d, *J* = 16.2 Hz, 2H), 2.52 (s, 3H), 2.32 – 2.18 (m, 2H), 2.05 (dq, *J* = 14.6, 4.6 Hz, 2H). ¹³C NMR (126 MHz, CDCl₃) δ 165.19, 159.35, 159.30, 151.60, 138.78, 137.59, 135.18, 134.98, 130.64, 129.63, 129.14, 128.77, 128.46, 127.18, 126.97, 125.98, 124.76, 121.96, 120.57, 116.34, 115.32, 112.91, 111.03, 55.84, 55.32, 51.08, 45.24, 29.69, 29.06. HRMS (ESI⁺) *m/z* [M+H⁺] calcd for C₃₃H₃₃ClN₂O₄ 557.2207, found 557.2215.



16b

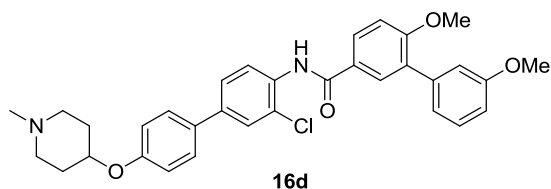
N-(2'-chloro-4'-((1-methylpiperidin-4-yl)oxy)-[1,1'-biphenyl]-4-yl)-3',6-dimethoxy-[1,1'-biphenyl]-3-carboxamide (16b) Compound **16a** was prepared following the general procedure C with amine **14b** (50 mg, 0.16 mmol) and acid chloride **7** (42.3 mg, 0.16 mmol) and was purified by column chromatography (SiO₂, 1:10 MeOH:DCM) to afford a white amorphous solid (90 mg, 87%). ¹H NMR (400 MHz, Chloroform-d) δ 8.56 (s, 1H), 7.99 (dd, *J* = 8.6, 2.4 Hz, 1H), 7.91 (d, *J* = 2.3 Hz, 1H), 7.83 – 7.72 (m, 2H), 7.41 – 7.30 (m, 3H), 7.22 (d, *J* = 8.4 Hz, 1H), 7.17 – 7.09 (m, 2H), 7.03 (d, *J* = 8.6 Hz, 1H), 6.98 (d, *J* = 2.5 Hz, 1H), 6.94 – 6.87 (m, 1H), 6.81 (dd, *J* = 8.5, 2.5 Hz, 1H), 4.52 (s, 1H), 3.85 (d, *J* = 11.2 Hz, 6H), 3.01 (d, *J* = 8.7 Hz, 4H), 2.62 (s, 3H), 2.36 (d, *J* = 7.4 Hz, 2H), 2.12 – 1.98 (m, 2H). ¹³C NMR (126 MHz, CDCl₃) δ 165.20, 159.35, 159.31, 149.80, 138.79, 137.31, 135.06, 133.06, 132.06, 131.96, 130.69, 130.22, 130.15, 129.60, 129.15, 128.41, 127.04, 121.97, 119.69, 117.24, 115.29, 114.70, 112.97, 111.03, 67.62, 55.85, 55.33, 50.82, 45.61, 29.86. HRMS (ESI⁺) *m/z* [M⁺] calcd for C₃₃H₃₃ClN₂O₄ 557.2207, found 557.2209.



16c

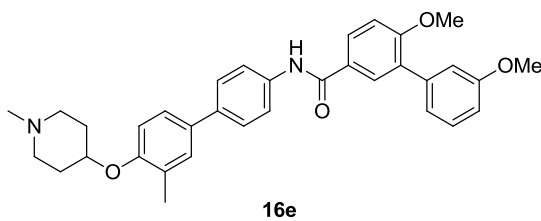
N-(2-chloro-4'-((1-methylpiperidin-4-yl)oxy)-[1,1'-biphenyl]-4-yl)-3',6-dimethoxy-[1,1'-biphenyl]-3-carboxamide (16c) Compound **16a** was prepared following the

general procedure C with amine **15a** (50 mg, 0.16 mmol) and acid chloride **7** (42.3 mg, 0.16 mmol) and was purified by column chromatography (SiO₂, 1:10 MeOH:DCM) to afford a white amorphous solid (35 mg, 39%). ¹H NMR (500 MHz, Chloroform-*d*) δ 7.77 (m, 3H), 7.32 – 7.20 (m, 1H), 7.11 (d, *J* = 8.6 Hz, 2H), 7.07 (t, *J* = 7.9 Hz, 1H), 7.00 (d, *J* = 8.5 Hz, 1H), 6.88 (d, *J* = 7.6 Hz, 1H), 6.86 (s, 1H), 6.84 (d, *J* = 9.2 Hz, 1H), 6.72 (d, *J* = 8.2 Hz, 2H), 6.62 (dd, *J* = 8.3, 2.7 Hz, 1H), 4.45 (m, 1H), 3.63 (s, 3H), 3.57 (s, 3H), 3.11 – 2.90 (m, 4H), 2.54 (s, 3H), 2.02 (m, 2H), 1.89 (m, 2H). ¹³C NMR (126 MHz, CDCl₃+CH₃OH) δ 166.39, 160.09, 159.95, 140.43, 139.92, 135.32, 132.62, 131.98, 131.70, 131.14, 130.57, 130.25, 129.89, 127.79, 127.40, 122.88, 122.30, 119.94, 117.34, 116.36, 116.31, 113.42, 111.78, 69.59, 56.68, 56.10, 50.37, 44.39, 27.88. HRMS (ESI⁺) *m/z* [M+H⁺] calcd for C₃₃H₃₃ClN₂O₄ 557.2207, found 557.2211.



N-(3-chloro-4'-((1-methylpiperidin-4-yl)oxy)-[1,1'-biphenyl]-4-yl)-3',6-dimethoxy-[1,1'-biphenyl]-3-carboxamide (16d) Compound **16a** was prepared following the general procedure C with amine **15b** (60 mg, 0.19 mmol) and acid chloride **7** (60.43 mg, 0.23 mmol) and was purified by column chromatography (SiO₂, 1:10 MeOH:DCM) to afford a white amorphous solid (92 mg, 86%) ¹H NMR (500 MHz, Chloroform-*d*) δ 8.61 (d, *J* = 8.6 Hz, 1H), 8.43 (s, NH), 7.95 (dd, *J* = 8.5, 2.4 Hz, 1H), 7.91 (d, *J* = 2.4 Hz, 1H), 7.60 (d, *J* = 2.1 Hz, 1H), 7.55 – 7.48 (m, 3H), 7.38 (t, *J* = 7.9 Hz, 1H), 7.17 – 7.08 (m, 4H), 6.98 (d, *J* = 8.8 Hz, 2H), 4.72 (s, 1H), 3.92 (s, 3H), 3.87 (s, 3H), 3.35 – 3.25 (m,

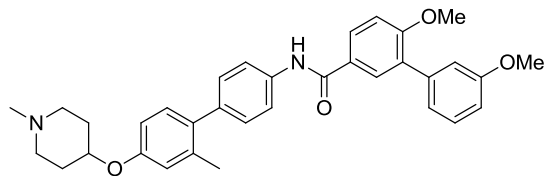
2H), 3.24 – 3.10 (m, 2H), 2.78 (s, 3H), 2.65 – 2.55 (m, 2H), 2.26 – 2.15 (m, 2H). ¹³C NMR (126 MHz, CDCl₃) δ 164.78, 159.68, 159.34, 138.69, 136.88, 133.72, 131.00, 129.84, 129.20, 128.26, 128.20, 127.27, 126.94, 126.79, 126.02, 123.38, 121.98, 121.69, 120.48, 116.24, 115.31, 113.06, 111.12, 71.59, 55.91, 55.34, 50.01, 43.62, 29.95. HRMS (ESI⁺) m/z [M⁺] calcd for C₃₃H₃₃ClN₂O₄ 557.2207, found 557.2189.



3',6-Dimethoxy-N-(3'-methyl-4'-((1-methylpiperidin-4-yl)oxy)-[1,1'-biphenyl]-4-yl)-

[1,1'-biphenyl]-3-carboxamide (16e) Compound **16e** was prepared from **14c** using general procedure C and acid chloride **7** to afford a white amorphous solid (55 mg, 78%).

¹H NMR (500 MHz, Chloroform-*d*) δ 8.20 (s, 1H), 7.98 (dd, *J* = 8.6, 2.4 Hz, 1H), 7.89 (d, *J* = 2.4 Hz, 1H), 7.75 (d, *J* = 8.6 Hz, 1H), 7.54 (d, *J* = 8.6 Hz, 1H), 7.42 – 7.40 (m, 1H), 7.37 – 7.32 (m, 2H), 7.17 – 7.14 (m, 1H), 7.12 (dd, *J* = 2.6, 1.5 Hz, 1H), 7.07 (d, *J* = 8.7 Hz, 1H), 6.93 (dd, *J* = 8.3, 2.6 Hz, 1H), 6.84 (d, *J* = 8.5 Hz, 1H), 4.58 (m, 1H), 3.90 (s, 3H), 3.86 (s, 3H), 3.00 (m, 4H), 2.64 (s, 3H), 2.45 – 2.34 (m, 2H), 2.30 (s, 3H), 2.17 – 2.06 (m, 2H). ¹³C NMR (126 MHz, CDCl₃) δ 165.23, 159.32, 154.02, 149.81, 138.84, 137.10, 136.60, 133.49, 130.61, 129.75, 129.69, 129.15, 128.51, 127.79, 127.14, 127.08, 125.22, 122.01, 120.66, 115.33, 112.94, 112.83, 111.03, 67.89, 55.85, 55.35, 50.88, 44.64, 28.28, 16.63. HRMS (ESI⁺) m/z [M+H⁺] calcd for C₃₄H₃₇N₂O₄ 537.2753; found 537.2758.



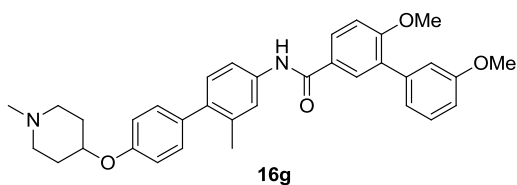
16f

3',6-Dimethoxy-N-(2'-methyl-4'-((1-methylpiperidin-4-yl)oxy)-[1,1'-biphenyl]-4-yl)-

[1,1'-biphenyl]-3-carboxamide (16f) Compound **16f** was prepared from **14d** using

general procedure C and acid chloride **7** to afford a white amorphous solid (45 mg, 81%).

^1H NMR (500 MHz, Chloroform-*d*) δ 7.89 (s, 1H), 7.87 (dd, $J = 8.6, 2.4$ Hz, 1H), 7.77 (d, $J = 2.4$ Hz, 1H), 7.63 (d, $J = 8.6$ Hz, 2H), 7.47 (d, $J = 8.6$ Hz, 2H), 7.34 – 7.33 (m, 1H), 7.31 – 7.26 (m, 2H), 7.06 (dt, $J = 7.6, 1.3$ Hz, 1H), 7.03 (dd, $J = 2.7, 1.6$ Hz, 1H), 6.99 (d, $J = 8.6$ Hz, 1H), 6.86 (dd, $J = 8.3, 2.7$ Hz, 1H), 6.79 (d, $J = 8.5$ Hz, 1H), 4.50 (s, 1H), 3.82 (s, 3H), 3.78 (s, 3H), 2.94 – 2.74 (m, 4H), 2.52 (s, 3H), 2.33 – 2.25 (m, 3H), 2.23 (m, 2H), 2.06 – 1.98 (m, 2H). ^{13}C NMR (126 MHz, CDCl_3) δ 165.12, 159.34, 154.16, 138.83, 136.97, 136.71, 133.41, 130.69, 129.69, 129.60, 129.17, 128.45, 127.85, 127.61, 127.20, 127.10, 125.20, 121.99, 120.50, 115.33, 112.96, 112.87, 111.07, 68.06, 55.87, 55.35, 50.99, 44.88, 28.84, 16.64. HRMS (ESI $^+$) m/z $[\text{M}+\text{H}^+]$ calcd for $\text{C}_{34}\text{H}_{37}\text{N}_2\text{O}_4$ 537.2753; found 537.2758.



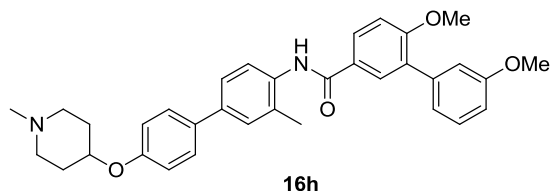
16g

3',6-Dimethoxy-N-(2-methyl-4'-((1-methylpiperidin-4-yl)oxy)-[1,1'-biphenyl]-4-yl)-

[1,1'-biphenyl]-3-carboxamide (16g) Compound **16g** was prepared from **15c** using

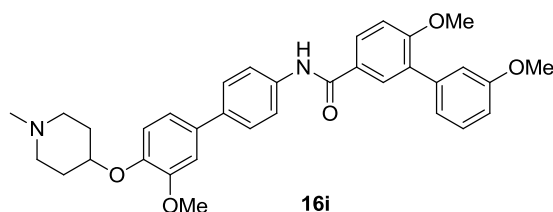
general procedure C and acid chloride **7** to afford a white amorphous solid (25 mg, 76%).

^1H NMR (500 MHz, Chloroform-*d*) δ 7.91 (s, 1H), 7.87 (dd, $J = 8.6, 2.4$ Hz, 1H), 7.77 (d, $J = 2.3$ Hz, 1H), 7.50 (d, $J = 2.3$ Hz, 1H), 7.44 (dd, $J = 8.3, 2.3$ Hz, 1H), 7.28 (t, $J = 7.9$ Hz, 1H), 7.16 (d, $J = 8.6$ Hz, 2H), 7.12 (d, $J = 8.3$ Hz, 1H), 7.06 (dt, $J = 7.8, 1.2$ Hz, 1H), 7.03 (dd, $J = 2.7, 1.5$ Hz, 1H), 6.99 (d, $J = 8.6$ Hz, 1H), 6.87 – 6.83 (m, 3H), 4.46 (m, 1H), 3.81 (s, 3H), 3.78 (s, 3H), 2.92 (m, 2H), 2.82 – 2.67 (m, 2H), 2.51 (s, 3H), 2.30 – 2.22 (m, 2H), 2.21 (s, 3H), 1.99 (m, 2H). ^{13}C NMR (126 MHz, CDCl_3) δ 165.17, 159.33, 159.31, 155.62, 149.82, 138.85, 137.48, 137.01, 136.26, 134.56, 130.64, 130.56, 130.41, 129.62, 129.16, 128.44, 127.14, 122.00, 117.77, 115.46, 115.32, 112.95, 111.05, 69.02, 55.86, 55.35, 51.35, 44.89, 28.70, 20.75. HRMS (ESI $^+$) m/z [M+H $^+$] calcd for $\text{C}_{34}\text{H}_{37}\text{N}_2\text{O}_4$ 537.2753; found 537.2762.

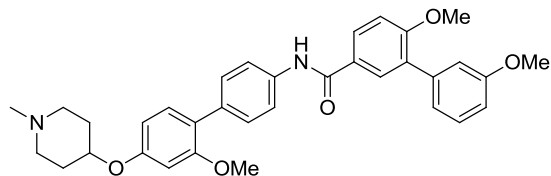


3',6-Dimethoxy-N-(3-methyl-4'-((1-methylpiperidin-4-yl)oxy)-[1,1'-biphenyl]-4-yl)-[1,1'-biphenyl]-3-carboxamide (16h) Compound **16h** was prepared from **15d** using general procedure C and acid chloride **7** to afford a white amorphous solid (13 mg, 58%). ^1H NMR (500 MHz, Chloroform-*d*) δ 8.01 (s, NH), 7.90 (dd, $J = 8.5, 2.4$ Hz, 1H), 7.85 – 7.78 (m, 2H), 7.48 (dd, $J = 8.4, 1.4$ Hz, 2H), 7.39 (d, $J = 8.6$ Hz, 2H), 7.35 – 7.30 (m, 1H), 7.12 – 7.08 (m, 1H), 7.08 – 7.03 (m, 2H), 6.93 (dd, $J = 8.5, 1.4$ Hz, 2H), 6.91 – 6.87 (m, 1H), 4.52 – 4.38 (m, 1H), 3.86 (d, $J = 1.2$ Hz, 3H), 3.82 (d, $J = 1.3$ Hz, 3H), 2.92 – 2.54 (m, 4H), 2.44 (s, 3H), 2.34 (s, 3H), 2.11 (d, $J = 10.8$ Hz, 2H), 1.96 (s, 2H). ^{13}C NMR (126 MHz, CDCl_3) δ 165.91, 159.56, 159.44, 156.55, 139.02, 138.03, 134.74, 133.89,

130.88, 130.78, 129.94, 129.33, 128.98, 128.58, 128.29 (2C), 127.10, 125.16, 124.33, 122.17, 116.44 (2C), 115.43, 113.08, 111.25, 69.95, 55.97, 55.37, 51.73, 45.43, 29.44, 18.24. HRMS (ESI⁺) m/z [M+H⁺] calcd for C₃₄H₃₆N₂O₄ 537.2753, found 537.2757.

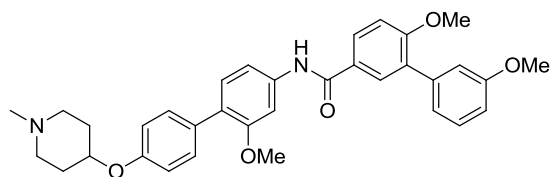


3',6-Dimethoxy-N-(3'-methoxy-4'-((1-methylpiperidin-4-yl)oxy)-[1,1'-biphenyl]-4-yl)-[1,1'-biphenyl]-3-carboxamide (16i) Compound **16i** was prepared from **14e** using general procedure C and acid chloride **7** to afford a white amorphous solid (33 mg, 68%). ¹H NMR (500 MHz, DMSO-*d*₆) δ 10.25 (s, 1H, NH), 8.03 (dd, *J* = 8.6, 2.4 Hz, 1H), 7.98 (d, *J* = 2.4 Hz, 1H), 7.85 (d, *J* = 8.4 Hz, 2H), 7.65 (d, *J* = 8.4 Hz, 2H), 7.37 (t, *J* = 7.9 Hz, 1H), 7.27 (s, 1H), 7.26 (d, *J* = 5.7 Hz, 1H), 7.18 (d, *J* = 9.0 Hz, 1H), 7.14 – 7.07 (m, 3H), 6.95 (dd, *J* = 8.3, 2.6 Hz, 1H), 4.51 – 4.39 (m, 1H), 3.87 (s, 3H), 3.86 (s, 3H), 3.80 (s, 3H), 3.09 (m, 2H), 2.83 (m, 2H), 2.57 (s, 3H), 2.05 (m, 2H), 1.83 (m, 2H). ¹³C NMR (126 MHz, DMSO) δ 164.74, 158.92, 158.71, 150.62, 149.53, 145.14, 138.77, 138.30, 134.92, 134.04, 129.80, 129.20, 129.14, 129.10, 126.80, 126.44, 121.73, 120.62, 118.41, 115.14, 112.54, 111.40, 110.68, 71.29, 55.84, 55.67, 55.07, 51.02, 43.45, 28.64. HRMS (ESI⁺) m/z [M+H⁺] calcd for C₃₄H₃₇N₂O₅ 553.2702, found 553.2757.



16j

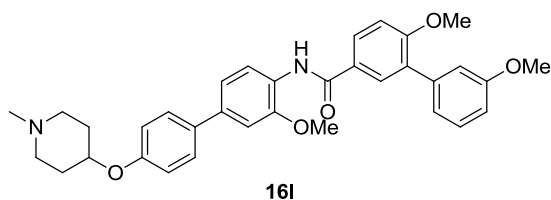
3',6-Dimethoxy-N-(2'-methoxy-4'-((1-methylpiperidin-4-yl)oxy)-[1,1'-biphenyl]-4-yl)-[1,1'-biphenyl]-3-carboxamide (16j) Compound **16j** was prepared from **14f** using general procedure C and acid chloride **7** to afford a white amorphous solid (31 mg, 72%). ¹H NMR (500 MHz, Chloroform-*d*) δ 7.86 (m, 2H), 7.77 (d, *J* = 2.4 Hz, 1H), 7.60 (d, *J* = 8.5 Hz, 2H), 7.42 (d, *J* = 8.6 Hz, 2H), 7.29 (t, *J* = 7.9 Hz, 1H), 7.15 (d, *J* = 9.0 Hz, 1H), 7.06 (dd, *J* = 7.6, 1.2 Hz, 1H), 7.03 (dd, *J* = 2.7, 1.6 Hz, 1H), 6.99 (d, *J* = 8.7 Hz, 1H), 6.85 (dd, *J* = 8.3, 2.7 Hz, 1H), 6.49 – 6.44 (m, 1H), 4.41 (m, 1H), 3.81 (s, 3H), 3.78 (s, 3H), 3.71 (s, 3H), 2.90 – 2.67 (m, 2H), 2.64 (m, 2H), 2.44 (s, 3H), 2.23 – 2.10 (m, 2H), 2.01 – 1.84 (m, 2H). ¹³C NMR (126 MHz, CDCl₃) δ 165.09, 159.33, 159.30, 157.64, 138.85, 136.68, 134.22, 131.15, 130.67, 129.99, 129.61, 129.16, 128.40, 127.21, 123.46, 122.00, 119.79, 115.29, 112.99, 111.05, 106.57, 102.55, 100.79, 69.99, 55.86, 55.60, 55.35, 51.55, 45.22, 29.31. HRMS (ESI⁺) *m/z* [M+H⁺] calcd for C₃₄H₃₇N₂O₅ 553.2702, found 553.2727.



16k

3',6-Dimethoxy-N-(2-methoxy-4'-((1-methylpiperidin-4-yl)oxy)-[1,1'-biphenyl]-4-yl)-[1,1'-biphenyl]-3-carboxamide (16k) Compound **16k** was prepared from **15e** using general procedure C and acid chloride **7** to afford a white amorphous solid (42 mg, 79%).

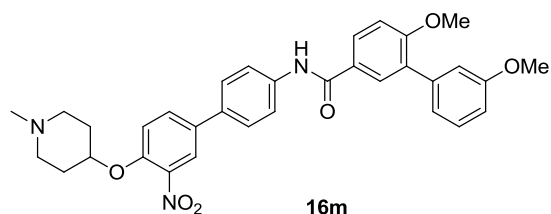
^1H NMR (500 MHz, Chloroform-*d*) δ 8.11 (s, 1H), 7.98 (dd, $J = 8.6, 2.4$ Hz, 1H), 7.88 (d, $J = 2.4$ Hz, 1H), 7.70 (d, $J = 2.1$ Hz, 1H), 7.48 (d, $J = 8.6$ Hz, 2H), 7.38 (t, $J = 7.9$ Hz, 1H), 7.27 (d, $J = 8.3$ Hz, 1H), 7.17 – 7.13 (m, 2H), 7.12 (s, 1H), 7.09 (d, $J = 8.6$ Hz, 1H), 6.96 – 6.91 (m, 3H), 4.55 (m, 1H), 3.91 (s, 3H), 3.87 (s, 6H), 3.01 (m, 2H), 2.90 (m, 2H), 2.61 (s, 3H), 2.41 – 2.27 (m, 2H), 2.10 – 2.00 (m, 2H). ^{13}C NMR (126 MHz, CDCl_3) δ 165.22, 159.39, 159.33, 156.73, 155.57, 149.83, 138.81, 138.52, 130.73, 130.68, 130.58, 129.61, 129.17, 128.48, 127.00, 125.88, 122.00, 115.44, 115.36, 112.93, 112.07, 111.09, 103.77, 68.43, 55.87, 55.67, 55.36, 50.95, 44.75, 28.50. HRMS (ESI $^+$) m/z $[\text{M}+\text{H}^+]$ calcd for $\text{C}_{34}\text{H}_{37}\text{N}_2\text{O}_5$ 553.2702, found 553.2707.



3',6-Dimethoxy-N-(3-methoxy-4'-((1-methylpiperidin-4-yl)oxy)-[1,1'-biphenyl]-4-yl)-[1,1'-biphenyl]-3-carboxamide (16l) Compound **16l** was prepared from **15f** using general procedure C and acid chloride **7** to afford a white amorphous solid (50 mg, 65%).

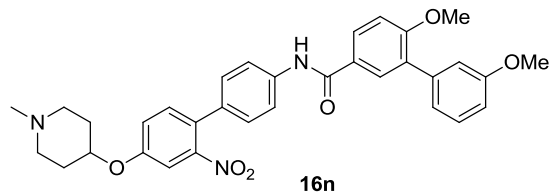
^1H NMR (500 MHz, Chloroform-*d*) δ 8.55 (d, $J = 8.4$ Hz, 1H), 8.51 (s, NH), 7.91 (dd, $J = 8.5, 2.4$ Hz, 1H), 7.87 (d, $J = 2.4$ Hz, 1H), 7.56 – 7.46 (m, 2H), 7.36 (t, $J = 7.9$ Hz, 1H), 7.27 (s, 1H), 7.19 (dd, $J = 8.4, 1.9$ Hz, 1H), 7.17 – 7.09 (m, 2H), 7.07 (dd, $J = 5.3, 3.4$ Hz, 2H), 6.99 – 6.95 (m, 2H), 6.93 (ddd, $J = 8.2, 2.6, 1.0$ Hz, 1H), 4.59 (s, 1H), 3.97 (s, 3H), 3.87 (d, $J = 15.2$ Hz, 6H), 3.11 – 2.89 (m, 5H), 2.64 (s, 3H), 2.43 – 2.31 (m, 2H), 2.11 (dt, $J = 14.3, 4.6$ Hz, 2H). ^{13}C NMR (126 MHz, CDCl_3) δ 164.67, 159.22, 159.18, 155.89, 148.34, 138.81, 136.12, 134.27, 130.58, 129.61, 129.05, 128.10, 127.43, 126.81, 121.92,

119.95, 119.32, 116.15, 115.21, 112.87, 110.92, 108.31, 68.19, 55.82, 55.76, 55.23, 50.61, 44.45, 27.93. HRMS (ESI⁺) m/z [M+H⁺] calcd for C₃₄H₃₆N₂O₅ 553.2702, found 553.2713.

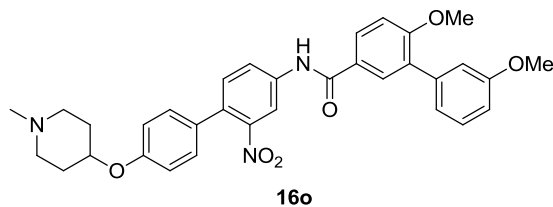


3',6-Dimethoxy-N-(4'-((1-methylpiperidin-4-yl)oxy)-3'-nitro-[1,1'-biphenyl]-4-yl)-

[1,1'-biphenyl]-3-carboxamide (16m) Compound **16m** was prepared from **14g** using general procedure C and acid chloride **7** to afford a yellow amorphous solid (30 mg, 63%). ¹H NMR (500 MHz, Chloroform-d) δ 8.28 (s, 1H), 8.05 (d, *J* = 2.4 Hz, 1H), 7.97 (dd, *J* = 8.6, 2.4 Hz, 1H), 7.89 (d, *J* = 2.4 Hz, 1H), 7.81 (d, *J* = 8.3 Hz, 2H), 7.75 (dd, *J* = 8.7, 2.4 Hz, 1H), 7.53 (d, *J* = 8.4 Hz, 2H), 7.36 (t, *J* = 7.9 Hz, 1H), 7.17 – 7.09 (m, 3H), 7.06 (d, *J* = 8.7 Hz, 1H), 6.92 (ddd, *J* = 8.3, 2.6, 1.0 Hz, 1H), 4.84 (s, 1H), 3.87 (d, *J* = 19.2 Hz, 6H), 3.30 – 2.89 (m, 4H), 2.67 (s, 3H), 2.54 – 2.37 (m, 2H), 2.16 – 2.09 (m, 2H). ¹³C NMR (126 MHz, CDCl₃) δ 165.28, 159.41, 159.29, 148.60, 140.80, 138.72, 138.34, 134.09, 133.66, 132.21, 130.59, 129.71, 129.13, 128.58, 127.17, 126.81, 123.85, 121.95, 120.77, 116.04, 115.35, 112.86, 111.03, 69.03, 55.84, 55.32, 49.78, 44.39, 27.82. HRMS (ESI⁺) m/z [M+H⁺] calcd for C₃₃H₃₃N₃O₆ 568.2448, found 568.2445.

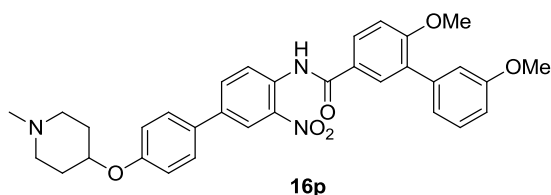


3',6-Dimethoxy-N-(4'-((1-methylpiperidin-4-yl)oxy)-2'-nitro-[1,1'-biphenyl]-4-yl)-[1,1'-biphenyl]-3-carboxamide (16n) Compound **16n** was prepared from **14h** using general procedure C and acid chloride **7** to afford a yellow amorphous solid (125 mg, 63%). ¹H NMR (500 MHz, Chloroform-*d*) δ 7.95 (s, 1H), 7.87 (dd, *J* = 8.5, 2.4 Hz, 1H), 7.78 (d, *J* = 2.4 Hz, 1H), 7.66 – 7.61 (m, 2H), 7.32 – 7.26 (m, 3H), 7.20 (d, *J* = 2.0 Hz, 1H), 7.06 (ddd, *J* = 9.0, 5.3, 1.9 Hz, 2H), 7.04 – 6.97 (m, 2H), 6.86 (ddd, *J* = 8.3, 2.7, 1.0 Hz, 1H), 4.50 (s, 1H), 3.80 (d, *J* = 18.6 Hz, 6H), 2.86 (t, *J* = 10.5 Hz, 2H), 2.48 (s, 3H), 2.23 (s, 3H), 2.04 – 1.88 (m, 2H). ¹³C NMR (126 MHz, CDCl₃) δ 165.20, 159.43, 159.33, 156.29, 149.67, 138.77, 138.05, 133.07, 132.82, 130.74, 129.68, 129.17, 128.71, 128.56, 128.43, 126.92, 121.98, 120.33, 119.86, 115.29, 113.01, 111.24, 111.08, 70.27, 55.87, 55.35, 51.14, 44.96, 29.71. HRMS (ESI⁺) *m/z* [M+H⁺] calcd for C₃₃H₃₃N₃O₆ 568.2448, found 568.2446.



3',6-Dimethoxy-N-(4'-((1-methylpiperidin-4-yl)oxy)-2-nitro-[1,1'-biphenyl]-4-yl)-[1,1'-biphenyl]-3-carboxamide (16o) Compound **16o** was prepared from **21a** using general procedure A and **1** to afford a yellow amorphous solid (85 mg, 65%). ¹H NMR (500 MHz, Chloroform-*d*) δ 8.15 (s, 1H), 7.93 (dd, *J* = 8.5, 2.5 Hz, 2H), 7.90 (d, *J* = 8.7

Hz, 1H), 7.85 (s, 1H), 7.31 (dd, $J = 8.4, 2.5$ Hz, 2H), 7.30 – 7.27 (m, 1H), 7.17 – 7.13 (m, 1H), 7.07 (d, $J = 7.7$ Hz, 1H), 7.03 (d, $J = 2.1$ Hz, 1H), 7.01 (dd, $J = 8.7, 2.4$ Hz, 1H), 6.85 (m, 3H), 4.35 (s, 1H), 3.82 (s, 3H), 3.78 (s, 3H), 2.70 (m, 2H), 2.52 – 2.40 (m, 2H), 2.30 (s, 3H), 1.99 (m, 2H), 1.85 (m, 2H). ^{13}C NMR (126 MHz, $\text{CDCl}_3 + \text{CH}_3\text{OH}$) δ 166.45, 159.66, 159.30, 157.16, 149.24, 138.93, 138.60, 132.22, 130.87, 130.58, 130.21, 129.71, 129.33, 129.18, 128.93, 126.43, 123.83, 122.11, 116.10, 115.66, 115.44, 112.86, 111.06, 70.57, 55.87, 55.39, 51.93, 45.64, 29.74. HRMS (ESI⁺) m/z $[\text{M} + \text{K}^+]$ calcd for $\text{C}_{33}\text{H}_{33}\text{N}_3\text{O}_6\text{K}$ 606.2006, found 606.2007.

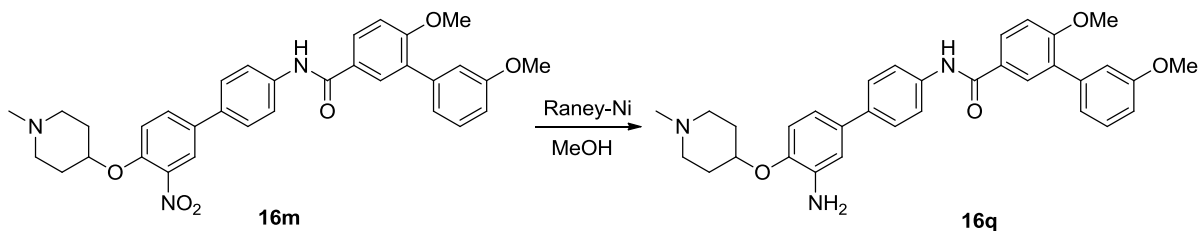


3',6-Dimethoxy-N-(4'-((1-methylpiperidin-4-yl)oxy)-3-nitro-[1,1'-biphenyl]-4-yl)-

[1,1'-biphenyl]-3-carboxamide (16p) Compound **16p** was prepared from **21b** using general procedure A and **1** to afford a yellow amorphous solid (25 mg, 39%). ^1H NMR (500 MHz, Chloroform- d) δ 11.34 (s, 1H), 9.05 (d, $J = 8.8$ Hz, 1H), 8.45 (d, $J = 2.3$ Hz, 1H), 8.00 (d, $J = 8.1$ Hz, 2H), 7.90 (dd, $J = 8.8, 2.3$ Hz, 1H), 7.58 – 7.52 (m, 2H), 7.37 (t, $J = 7.9$ Hz, 1H), 7.18 – 7.10 (m, 3H), 7.04 – 6.99 (m, 2H), 6.96 – 6.92 (m, 1H), 4.43 (s, 1H), 3.92 (s, 3H), 3.87 (s, 3H), 2.83 – 2.72 (m, 2H), 2.51 – 2.41 (m, 2H), 2.39 (s, 3H), 2.11 (ddd, $J = 11.3, 8.1, 3.7$ Hz, 2H), 1.93 (tdd, $J = 10.9, 7.2, 3.5$ Hz, 2H). ^{13}C NMR (126 MHz, CDCl_3) δ 165.23, 159.99, 159.32, 157.55, 138.55, 136.58, 135.90, 134.07, 134.03, 131.09, 130.67, 130.34, 129.19, 128.33, 127.95, 126.34, 123.12, 122.47, 121.95, 116.52,

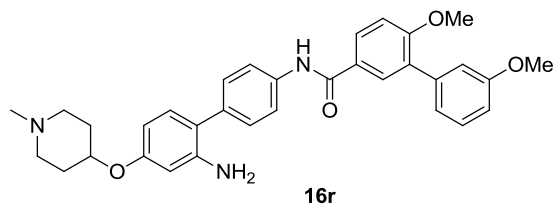
115.15, 113.19, 111.14, 71.62, 55.81, 55.36, 52.44, 45.84, 29.73. HRMS (ESI⁺) m/z [M⁺] calcd for C₃₃H₃₃N₃O₆ 567.2348, found 567.2339.

General procedure E: Raney-Nickel-catalyzed reduction

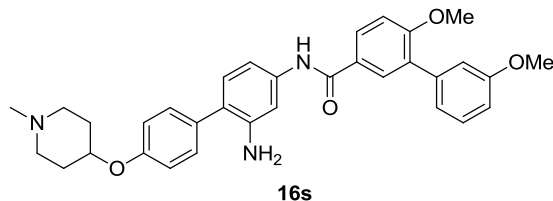


N-(3'-amino-4'-((1-methylpiperidin-4-yl)oxy)-[1,1'-biphenyl]-4-yl)-3',6-dimethoxy-[1,1'-biphenyl]-3-carboxamide (16q) Raney-Nickel was added to a solution of **16m** (25 mg, 0.044 mmol) in MeOH (1 ml) and stirred at room temperature under hydrogen atmosphere for 12 h. After 12 h, RM was filtered through celite and filtrate was concentrated under reduced pressure to residue. The residue was purified by column chromatography (SiO₂, 5:95 MeOH:DCM) to afford a white amorphous solid (10 mg, 44%). ¹H NMR (400 MHz, Chloroform-*d*) δ 7.94 (d, *J* = 8.7 Hz, 1H), 7.84 (d, *J* = 2.3 Hz, 1H), 7.69 (d, *J* = 8.2 Hz, 2H), 7.53 (d, *J* = 8.3 Hz, 2H), 7.37 (t, *J* = 7.9 Hz, 1H), 7.14 (d, *J* = 7.6 Hz, 1H), 7.10 (t, *J* = 2.1 Hz, 1H), 7.08 (d, *J* = 8.7 Hz, 1H), 7.00 (s, 1H), 6.97 – 6.91 (m, 2H), 6.85 – 6.81 (m, 1H), 4.63 (m, 1H), 3.90 (s, 3H), 3.87 (s, 3H), 3.16 (m, 4H), 2.72 (s, 3H), 2.42 (m, 2H), 2.20 (m, 2H). ¹³C NMR (126 MHz, CDCl₃) δ 165.31, 159.57, 159.54, 143.58, 139.02, 137.56, 137.24, 137.04, 135.04, 130.92, 129.77, 129.38, 128.63, 127.48, 127.28, 122.19, 120.62, 117.47, 115.54, 114.63, 114.31, 113.16, 111.29, 69.10,

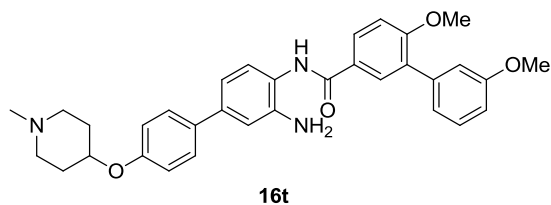
56.08, 55.56, 50.61, 44.37, 28.10. HRMS (ESI⁺) m/z [M+H⁺] calcd for C₃₃H₃₆N₃O₄ 538.2706, found 538.2707.



N-(2'-amino-4'-((1-methylpiperidin-4-yl)oxy)-[1,1'-biphenyl]-4-yl)-3',6-dimethoxy-[1,1'-biphenyl]-3-carboxamide (16r) Compound **16r** was prepared from **16n** using general procedure E to afford a white amorphous solid (28 mg, 39%). ¹H NMR (500 MHz, Chloroform-d) δ 8.03 (d, *J* = 2.9 Hz, 1H), 7.94 (dd, *J* = 8.5, 2.4 Hz, 1H), 7.86 (d, *J* = 2.5 Hz, 1H), 7.71 (dd, *J* = 8.5, 2.7 Hz, 2H), 7.42 (dd, *J* = 8.7, 2.6 Hz, 2H), 7.36 (td, *J* = 7.9, 2.8 Hz, 1H), 7.17 – 7.09 (m, 2H), 7.05 (ddd, *J* = 18.4, 8.5, 2.7 Hz, 2H), 6.93 (dd, *J* = 8.2, 2.6 Hz, 1H), 6.38 (dt, *J* = 8.5, 2.6 Hz, 1H), 6.33 (d, *J* = 2.5 Hz, 1H), 4.42 (s, 1H), 3.89 (s, 3H), 3.86 (s, 3H), 3.80 (s, NH₂), 2.95 – 2.81 (m, 2H), 2.67 (s, 2H), 2.49 (s, 3H), 2.29 – 2.14 (m, 2H), 1.99 (d, *J* = 14.2 Hz, 2H). ¹³C NMR (126 MHz, CDCl₃) δ 165.25, 159.34, 159.30, 157.35, 144.89, 138.79, 136.90, 135.13, 131.38, 130.65, 129.70, 129.63, 129.14, 128.45, 127.00, 121.96, 120.69, 120.60, 115.32, 112.91, 111.04, 106.02, 103.05, 69.81, 55.84, 55.32, 51.86, 45.30, 29.69. HRMS (ESI⁺) m/z [M+H⁺] calcd for C₃₃H₃₅N₃O₄ 538.2706, found 538.2704.

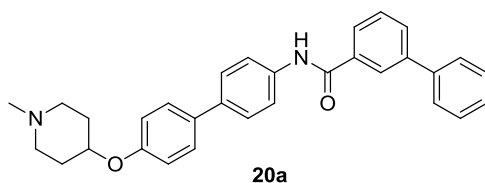


N-(2-amino-4'-((1-methylpiperidin-4-yl)oxy)-[1,1'-biphenyl]-4-yl)-3',6-dimethoxy-[1,1'-biphenyl]-3-carboxamide (16s) Compound **16s** was prepared from **16o** using general procedure E to afford a white amorphous solid (21 mg, 36%). ¹H NMR (400 MHz, Chloroform-*d*) δ 7.92 (dd, *J* = 8.5, 2.3 Hz, 1H), 7.82 (d, *J* = 2.4 Hz, 1H), 7.77 (s, 1H), 7.39 (d, *J* = 8.7 Hz, 3H), 7.14 (d, *J* = 7.9 Hz, 1H), 7.10 (d, *J* = 2.3 Hz, 1H), 7.07 (dd, *J* = 8.5, 2.2 Hz, 2H), 6.97 (d, *J* = 8.5 Hz, 2H), 6.94 (dd, *J* = 8.3, 2.7 Hz, 1H), 6.86 (dd, *J* = 8.2, 2.1 Hz, 1H), 4.58 (m, 1H), 3.90 (s, 3H), 3.87 (s, 3H), 3.02 (m, 4H), 2.63 (s, 3H), 2.37 (m, 2H), 2.10 (m, 2H). ¹³C NMR (126 MHz, CDCl₃) δ 165.05, 159.33, 159.30, 155.73, 144.29, 138.82, 138.19, 132.21, 130.79, 130.69, 130.45, 129.51, 129.16, 128.34, 127.24, 123.26, 121.97, 116.17, 115.30, 112.96, 111.05, 110.21, 107.01, 69.03, 55.86, 55.34, 50.67, 44.57, 28.34. HRMS (ESI⁺) *m/z* [M+H⁺] calcd for C₃₃H₃₆N₃O₄ 538.2706, found 538.2709.



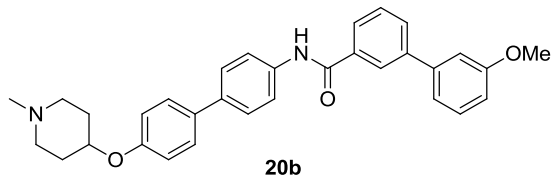
N-(3-amino-4'-((1-methylpiperidin-4-yl)oxy)-[1,1'-biphenyl]-4-yl)-3',6-dimethoxy-[1,1'-biphenyl]-3-carboxamide (16t) Compound **16s** was prepared from **16o** using general procedure E to afford a white amorphous solid (12 mg, 34%). ¹H NMR (400 MHz, Chloroform-*d*) δ 7.91 (dd, *J* = 9.0, 2.4 Hz, 1H), 7.87 (s, 1H), 7.43 (d, *J* = 8.7 Hz,

2H), 7.29 (t, $J = 7.9$ Hz, 1H), 7.24 (d, $J = 7.8$ Hz, 1H), 7.09 – 6.94 (m, 5H), 6.89 (d, $J = 8.8$ Hz, 2H), 6.85 (dd, $J = 8.3, 2.6$ Hz, 1H), 4.51 (m, 1H), 3.83 (s, 3H), 3.79 (s, 3H), 2.99 – 2.74 (m, 4H), 2.54 (s, 3H), 2.15 (m, 2H), 2.06 – 1.94 (m, 2H). ^{13}C NMR (126 MHz, CDCl_3) δ 159.52, 159.32, 156.19, 141.22, 139.75, 138.96, 134.13, 130.65, 130.31, 129.19, 128.84, 128.42, 128.27, 126.33, 126.25, 123.71, 122.11, 118.33, 116.42, 116.23, 115.37, 112.96, 111.03, 68.80, 55.88, 55.39, 50.92, 44.54, 28.39. HRMS (ESI^+) m/z [$\text{M}+\text{K}^+$] calcd for $\text{C}_{33}\text{H}_{35}\text{N}_3\text{O}_4\text{K}$ 576.2265, found 576.2264.

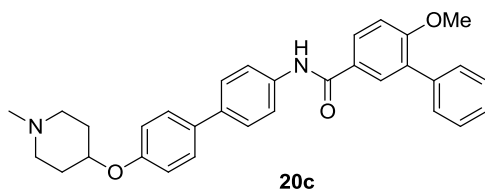


N-(4'-((1-methylpiperidin-4-yl)oxy)-[1,1'-biphenyl]-4-yl)-[1,1'-biphenyl]-3-

carboxamide (20a) Compound **20a** was prepared from **19a** using general procedure C and acid chloride **7** to afford a white amorphous solid (20 mg, 65%). ^1H NMR (500 MHz, $\text{DMSO}-d_6$) δ 10.24 (s, 1H, NH), 8.03 (dd, $J = 8.6, 2.4$ Hz, 1H), 7.97 (d, $J = 2.3$ Hz, 1H), 7.85 (d, $J = 8.4$ Hz, 2H), 7.61 (d, $J = 8.4$ Hz, 4H), 7.56 (d, $J = 7.4$ Hz, 2H), 7.46 (t, $J = 7.6$ Hz, 2H), 7.38 (t, $J = 7.4$ Hz, 1H), 7.27 (d, $J = 8.7$ Hz, 1H), 7.08 (d, $J = 8.5$ Hz, 2H), 4.63 (m, 1H), 3.15 (m, 2H), 2.96 (m, 2H), 2.64 (s, 3H), 2.11 (m, 2H), 1.96 – 1.78 (m, 2H). ^{13}C NMR (126 MHz, DMSO) δ 164.73, 158.69, 155.89, 138.17, 137.46, 134.70, 132.63, 129.87, 129.37, 129.34, 129.08, 128.08, 127.44, 127.19, 126.88, 126.18, 120.69, 116.38, 111.38, 68.81, 50.55, 43.04, 28.02. HRMS (ESI^+) m/z [$\text{M}+\text{H}^+$] calcd for $\text{C}_{31}\text{H}_{31}\text{N}_2\text{O}_2$ 463.2386, found 463.2387.

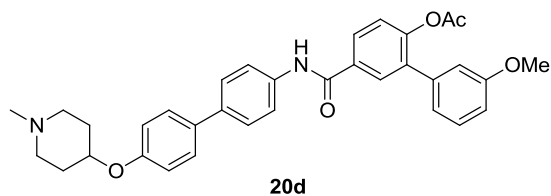


3'-Methoxy-N-(4'-((1-methylpiperidin-4-yl)oxy)-[1,1'-biphenyl]-4-yl)-[1,1'-biphenyl]-3-carboxamide (20b) Compound **20b** was prepared from **19b** using general procedure C and acid chloride **7** to afford a white amorphous solid (52 mg, 72%). ^1H NMR (500 MHz, DMSO- d_6) δ 10.44 (s, 1H, NH), 8.24 (s, 1H), 7.96 (dt, $J = 7.7, 1.4$ Hz, 1H), 7.93 – 7.84 (m, 3H), 7.68 – 7.57 (m, 4H), 7.44 (dd, $J = 8.6, 7.1$ Hz, 1H), 7.35 (dt, $J = 7.8, 1.2$ Hz, 1H), 7.33 (t, $J = 2.1$ Hz, 1H), 7.10 – 7.05 (m, 2H), 7.03 – 6.98 (m, 1H), 4.61 (m, 1H), 3.86 (s, 3H), 3.11 – 3.02 (m, 2H), 2.88 (s, 2H), 2.60 (s, 3H), 2.20 – 2.01 (m, 2H), 1.93 – 1.76 (m, 2H). ^{13}C NMR (126 MHz, DMSO) δ 165.34, 159.78, 156.00, 140.99, 140.15, 138.02, 135.52, 134.95, 132.54, 130.08, 129.88, 129.06, 127.46, 126.97, 126.24, 125.86, 120.72, 119.23, 116.36, 113.34, 112.49, 69.66, 55.20, 50.77, 43.33, 28.33. HRMS (ESI $^+$) m/z $[\text{M}+\text{H}^+]$ calcd for $\text{C}_{32}\text{H}_{33}\text{N}_2\text{O}_3$ 493.2491, found 493.2494.



6-Methoxy-N-(4'-((1-methylpiperidin-4-yl)oxy)-[1,1'-biphenyl]-4-yl)-[1,1'-biphenyl]-3-carboxamide(20c) Compound **20c** was prepared from **19c** using general procedure C and acid chloride **7** to afford a white amorphous solid (33 mg, 78%). ^1H NMR (500 MHz, DMSO- d_6) δ 10.25 (s, 1H, NH), 8.04 (dd, $J = 8.6, 2.4$ Hz, 1H), 7.98 (d, $J = 2.3$ Hz, 1H),

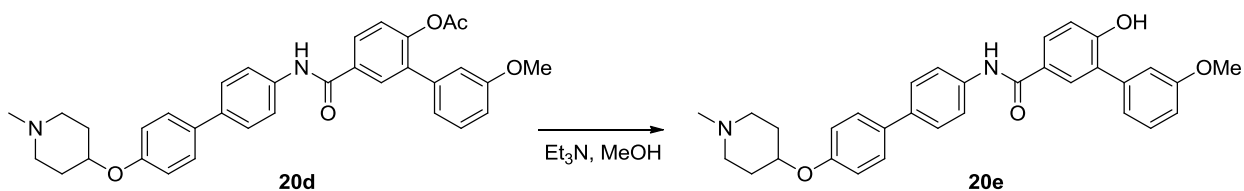
7.86 (d, $J = 8.6$ Hz, 2H), 7.60 (dd, $J = 8.6, 3.5$ Hz, 4H), 7.56 (d, $J = 7.3$ Hz, 2H), 7.45 (t, $J = 7.6$ Hz, 2H), 7.37 (t, $J = 7.4$ Hz, 1H), 7.26 (d, $J = 8.7$ Hz, 1H), 7.06 (d, $J = 8.5$ Hz, 2H), 4.58 (m, 1H), 3.86 (s, 3H), 3.11 – 2.93 (m, 2H), 2.78 (m, 2H), 2.52 (s, 3H), 2.08 (m, 2H), 1.85 (m, 2H). ^{13}C NMR (126 MHz, DMSO) δ 164.68, 158.68, 156.01, 138.20, 137.49, 134.70, 132.52, 129.90, 129.36, 129.09, 128.06, 127.41, 127.17, 126.93, 126.16, 120.66, 116.33, 111.36, 69.61, 55.85, 50.89, 43.61, 28.55. HRMS (ESI⁺) m/z [M+H⁺] calcd for C₃₂H₃₃N₂O₃ 493.2491, found 493.2495.



3'-Methoxy-5-((4'-((1-methylpiperidin-4-yl)oxy)-[1,1'-biphenyl]-4-yl)carbamoyl)-

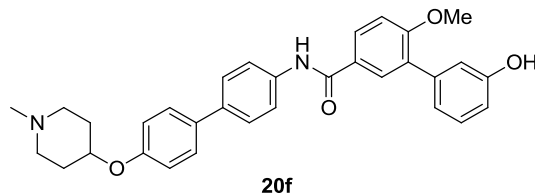
[1,1'-biphenyl]-2-yl acetate (20d) Compound **20d** was prepared from **19d** using general procedure C and acid chloride **7** to afford a white amorphous solid (35 mg, 76%). ^1H NMR (500 MHz, Chloroform-*d*) δ 8.13 (s, 1H), 7.87 (s, 1H), 7.83 (dd, $J = 8.3, 2.3$ Hz, 1H), 7.64 (d, $J = 8.6$ Hz, 2H), 7.46 (d, $J = 8.5$ Hz, 2H), 7.43 (d, $J = 8.7$ Hz, 2H), 7.26 (t, $J = 7.9$ Hz, 1H), 7.16 (d, $J = 8.3$ Hz, 1H), 7.00 – 6.77 (m, 5H), 4.40 (m, 1H), 3.76 (s, 3H), 2.82 (m, 2H), 2.63 (m, 2H), 2.41 (s, 3H), 2.12 (m, 2H), 2.06 (s, 3H), 1.97 – 1.86 (m, 2H). ^{13}C NMR (126 MHz, CDCl₃) δ 169.13, 164.90, 159.60, 156.36, 150.41, 137.88, 136.89, 136.80, 135.26, 133.58, 133.16, 129.94, 129.51, 128.05, 127.53, 127.20, 123.50, 121.19, 120.67, 116.27, 114.39, 113.66, 69.70, 55.35, 51.31, 45.08, 29.17, 20.91.

General procedure F: Base-catalyzed deacetylation



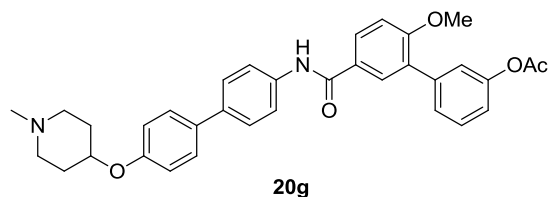
2'-Hydroxy-5'-((4'-((1-methylpiperidin-4-yl)oxy)-[1,1'-biphenyl]-4-yl)carbamoyl)-

[1,1'-biphenyl]-3-yl acetate (20e) A solution of **20d** (30 mg, 0.052 mmol) in MeOH (0.5 ml) was treated with triethylamine (0.020 ml, 0.156 mmol) and stirred for 4 h. After 4h, the RM was concentrated and residue was purified by column chromatography (SiO₂, 5:95 MeOH:DCM) to afford a white amorphous solid (14 mg, 49%). ¹H NMR (500 MHz, Chloroform-*d*) δ 7.86 (d, *J* = 2.4 Hz, 1H), 7.77 (dd, *J* = 8.5, 2.4 Hz, 1H), 7.69 (d, *J* = 8.6 Hz, 2H), 7.54 – 7.46 (m, 4H), 7.35 – 7.31 (m, 1H), 7.17 (d, *J* = 7.5 Hz, 1H), 7.14 (d, *J* = 2.6 Hz, 1H), 6.98 (d, *J* = 8.4 Hz, 1H), 6.95 (d, *J* = 8.7 Hz, 2H), 6.88 (dd, *J* = 8.4, 2.6 Hz, 1H), 4.52 (m, 1H), 3.83 (s, 3H), 3.03 – 2.86 (m, 2H), 2.81 (m, 2H), 2.53 (s, 3H), 2.26 – 2.09 (m, 2H), 2.09 – 1.92 (m, 2H). ¹³C NMR (126 MHz, CDCl₃+CH₃OH) δ 166.63, 159.37, 157.41, 156.02, 139.03, 137.26, 136.42, 133.88, 130.14, 129.26, 128.35, 128.34, 127.96, 126.93, 126.05, 121.74, 120.97, 116.26, 115.87, 114.92, 112.85, 68.65, 55.20, 51.11, 44.67, 28.69.



3'-Hydroxy-6-methoxy-N-(4'-((1-methylpiperidin-4-yl)oxy)-[1,1'-biphenyl]-4-yl)-

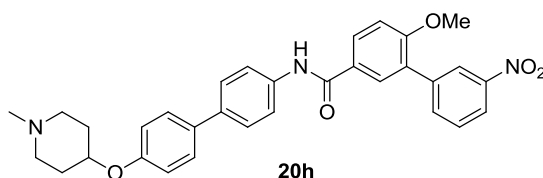
[1,1'-biphenyl]-3-carboxamide Compound **20f** was prepared from **120g** using general procedure F to afford a white amorphous solid (25 mg, 76%). ¹H NMR (500 MHz, Methanol-*d*₄) δ 7.95 (dd, *J* = 8.6, 2.5 Hz, 1H), 7.91 (d, *J* = 2.4 Hz, 1H), 7.74 (d, *J* = 8.5 Hz, 2H), 7.56 (d, *J* = 8.6 Hz, 2H), 7.53 (d, *J* = 8.7 Hz, 2H), 7.27 (t, *J* = 7.9 Hz, 1H), 7.08 (d, *J* = 8.6 Hz, 2H), 7.05 – 7.03 (m, 1H), 6.99 (d, *J* = 8.7 Hz, 2H), 6.84 (dd, *J* = 8.0, 2.5 Hz, 1H), 4.49 (m, 1H), 3.90 (s, 3H), 2.86 (m, 2H), 2.63 (m, 2H), 2.46 (s, 3H), 2.12 (m, 2H), 2.02 – 1.93 (m, 2H). ¹³C NMR (126 MHz, CDCl₃+CH₃OH) δ 166.57, 159.32, 156.47, 156.29, 138.87, 137.19, 136.60, 133.67, 130.54, 130.01, 129.01, 128.41, 127.90, 126.91, 126.88, 121.04, 120.98, 116.35, 116.31, 114.33, 110.87, 69.62, 55.62, 51.63, 45.18, 29.42. HRMS (ESI⁺) *m/z* [M+H⁺] calcd for C₃₂H₃₃N₂O₄ 509.2440, found 509.2442.



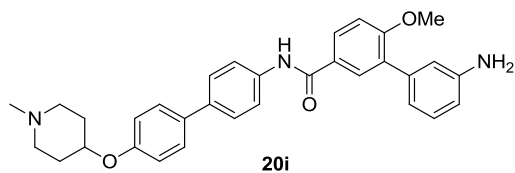
2'-Methoxy-5'-((4'-((1-methylpiperidin-4-yl)oxy)-[1,1'-biphenyl]-4-yl)carbamoyl)-

[1,1'-biphenyl]-3-yl acetate (20g) Compound **20g** was prepared from **19e** using general procedure C and acid chloride **7** to afford a white amorphous solid (32 mg, 76%). ¹H NMR (500 MHz, Chloroform-*d*) δ 7.93 (s, 1H), 7.86 (dd, *J* = 8.7, 2.4 Hz, 1H), 7.73 (d, *J*

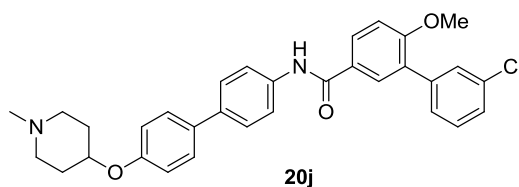
= 2.4 Hz, 1H), 7.63 (d, $J = 8.5$ Hz, 2H), 7.47 (d, $J = 8.7$ Hz, 2H), 7.45 (d, $J = 8.8$ Hz, 2H), 7.35 – 7.30 (m, 1H), 7.01 (d, $J = 7.4$ Hz, 1H), 6.98 (d, $J = 8.7$ Hz, 1H), 6.89 (d, $J = 8.7$ Hz, 2H), 4.43 (m, 1H), 3.81 (s, 3H), 2.90 – 2.79 (m, 2H), 2.66 (m, 2H), 2.45 (s, 3H), 2.25 (s, 3H), 2.19 (m, 2H), 1.95 (m, 2H). ^{13}C NMR (126 MHz, CDCl_3) δ 169.64, 165.09, 159.23, 156.27, 150.37, 138.92, 137.04, 136.58, 133.73, 129.62, 129.55, 129.12, 128.82, 128.05, 127.22, 127.18, 127.03, 122.77, 120.64, 120.51, 116.27, 111.11, 69.73, 55.86, 51.43, 45.19, 29.15, 21.21. HRMS (ESI^+) m/z [$\text{M}+\text{H}^+$] calcd for $\text{C}_{34}\text{H}_{35}\text{N}_2\text{O}_5$ 551.2546, found 551.2543.



6-Methoxy-N-(4'-((1-methylpiperidin-4-yl)oxy)-[1,1'-biphenyl]-4-yl)-3'-nitro-[1,1'-biphenyl]-3-carboxamide (20h) Compound **20h** was prepared from **19f** using general procedure C and acid chloride **7** to afford a yellow amorphous solid (23 mg, 72%). ^1H NMR (500 MHz, $\text{DMSO}-d_6$) δ 10.27 (s, 1H, NH), 8.42 (t, $J = 2.0$ Hz, 1H), 8.26 (dd, $J = 8.2, 2.4$ Hz, 1H), 8.11 (dd, $J = 8.6, 2.3$ Hz, 1H), 8.08 – 8.03 (m, 2H), 7.86 – 7.83 (m, 2H), 7.78 (t, $J = 8.0$ Hz, 1H), 7.65 – 7.57 (m, 4H), 7.34 (d, $J = 8.8$ Hz, 1H), 7.05 (d, $J = 8.7$ Hz, 2H), 4.52 (m, 1H), 3.91 (s, 3H), 2.91 (m, 2H), 2.66 – 2.56 (m, 2H), 2.44 (s, 3H), 2.09 – 1.96 (m, 2H), 1.85 – 1.66 (m, 2H). ^{13}C NMR (126 MHz, DMSO) δ 164.46, 158.58, 156.14, 147.68, 138.93, 138.06, 136.08, 134.82, 132.37, 130.15, 129.96, 129.71, 127.40, 127.21, 126.80, 126.18, 123.79, 122.14, 120.68, 116.27, 111.69, 69.71, 56.10, 51.67, 44.44, 29.14. HRMS (ESI^+) m/z [$\text{M}+\text{H}^+$] calcd for $\text{C}_{32}\text{H}_{32}\text{N}_3\text{O}_5$ 538.2342, found 538.2346.

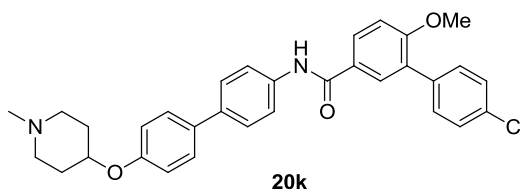


3'-Amino-6-methoxy-N-(4'-((1-methylpiperidin-4-yl)oxy)-[1,1'-biphenyl]-4-yl)-[1,1'-biphenyl]-3-carboxamide Compound **20i** was prepared from **20h** using general procedure D to afford a white amorphous solid (10 mg, 76%). ¹H NMR (400 MHz, Chloroform-*d*) δ 7.85 – 7.81 (m, 1H), 7.78 (s, 1H), 7.64 (d, *J* = 8.5 Hz, 2H), 7.43 (m, 4H), 7.11 (t, *J* = 7.8 Hz, 1H), 6.95 (d, *J* = 8.7 Hz, 1H), 6.87 (m, 3H), 6.81 (s, 1H), 6.64 – 6.62 (m, 1H), 4.54 (m, 1H), 3.77 (s, 3H), 3.13 – 2.99 (m, 4H), 2.63 (s, 3H), 2.25 – 2.15 (m, 2H), 2.08 – 2.00 (m, 2H). ¹³C NMR (126 MHz, CDCl₃+CH₃OH) δ 159.41, 156.00, 146.03, 138.68, 137.32, 136.51, 134.07, 130.83, 129.93, 128.98, 128.53, 128.09, 127.04, 126.93, 121.02, 120.98, 120.31, 116.69, 116.31, 114.71, 110.97, 68.71, 55.76, 50.83, 44.44, 28.31. HRMS (ESI⁺) *m/z* [M+H⁺] calcd for C₃₂H₃₄N₃O₃ 508.2600, found 508.2598.

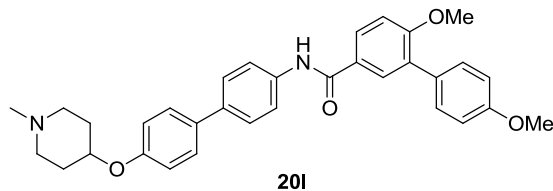


3'-Chloro-6-methoxy-N-(4'-((1-methylpiperidin-4-yl)oxy)-[1,1'-biphenyl]-4-yl)-[1,1'-biphenyl]-3-carboxamide (20j) Compound **20j** was prepared from **19g** using general procedure C and acid chloride **7** to afford a white amorphous solid (32 mg, 80%). ¹H NMR (500 MHz, DMSO-*d*₆) δ 10.21 (s, 1H), 8.06 (dd, *J* = 8.6, 2.4 Hz, 1H), 8.00 (d, *J* = 2.4 Hz, 1H), 7.84 (d, *J* = 8.6 Hz, 2H), 7.63 – 7.57 (m, 54H), 7.55 – 7.44 (m, 3H), 7.30 (d, *J* = 8.7 Hz, 1H), 7.02 (d, *J* = 8.7 Hz, 2H), 4.41 (m, 1H), 3.88 (s, 3H), 2.71 – 2.57 (m, 2H),

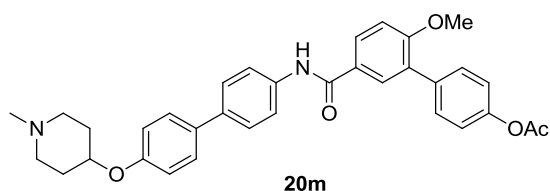
2.20 (m, 5H), 2.12 – 1.90 (m, 2H), 1.66 (m, 2H). ^{13}C NMR (126 MHz, DMSO) δ 164.50, 158.58, 156.38, 139.55, 138.04, 134.86, 132.73, 132.09, 129.95, 129.81, 129.71, 128.97, 128.13, 127.70, 127.35, 127.12, 127.01, 126.13, 120.67, 116.17, 111.55, 71.85, 55.98, 52.32, 45.74, 30.51. HRMS (ESI⁺) m/z [M+H⁺] calcd for C₃₂H₃₂ClN₂O₃ 527.2101, found 527.2100.



4'-Chloro-6-methoxy-N-(4'-((1-methylpiperidin-4-yl)oxy)-[1,1'-biphenyl]-4-yl)-[1,1'-biphenyl]-3-carboxamide (20k) Compound **20k** was prepared from **19i** using general procedure C and acid chloride **7** to afford a white amorphous solid (23 mg, 70%). ^1H NMR (500 MHz, DMSO-*d*₆) δ 10.23 (s, 1H, NH), 8.04 (dd, J = 8.6, 2.3 Hz, 1H), 7.97 (d, J = 2.3 Hz, 1H), 7.84 (d, J = 8.7 Hz, 2H), 7.60 (m, 5H), 7.52 (d, J = 8.5 Hz, 2H), 7.28 (d, J = 8.7 Hz, 1H), 7.06 (d, J = 8.7 Hz, 2H), 4.55 (m, 1H), 3.87 (s, 3H), 3.33 (s, 3H), 2.98 (m, 2H), 2.70 (m, 2H), 2.06 (m, 2H), 1.80 (m, 2H). ^{13}C NMR (126 MHz, DMSO) δ 164.60, 158.61, 156.07, 138.16, 136.26, 134.76, 132.48, 132.02, 131.18, 129.78, 129.44, 128.10, 127.98, 127.43, 127.04, 126.19, 120.66, 116.33, 111.51, 69.88, 55.96, 51.10, 43.86, 28.74. HRMS (ESI⁺) m/z [M+H⁺] calcd for C₃₂H₃₂ClN₂O₃ 527.2101, found 527.2105.

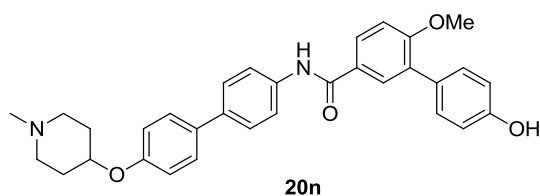


4',6-Dimethoxy-N-(4'-((1-methylpiperidin-4-yl)oxy)-[1,1'-biphenyl]-4-yl)-[1,1'-biphenyl]-3-carboxamide (20l) Compound **20l** was prepared from **19j** using general procedure C and acid chloride **7** to afford a white amorphous solid (23 mg, 56%). ¹H NMR (500 MHz, DMSO-*d*₆) δ 10.22 (s, 1H, NH), 7.99 (dd, *J* = 8.6, 2.4 Hz, 1H), 7.95 (d, *J* = 2.4 Hz, 1H), 7.85 (d, *J* = 8.7 Hz, 1H), 7.64 – 7.60 (m, 3H), 7.51 (d, *J* = 8.7 Hz, 1H), 7.24 (d, *J* = 8.7 Hz, 1H), 7.09 (d, *J* = 8.6 Hz, 2H), 7.02 (d, *J* = 8.8 Hz, 1H), 4.65 (m, 1H), 3.86 (s, 3H), 3.81 (s, 3H), 3.25 – 2.96 (m, 4H), 2.68 (s, 3H), 2.11 (m, 2H), 1.91 (m, 2H). ¹³C NMR (126 MHz, DMSO) δ 164.78, 158.67, 158.50, 155.86, 138.25, 134.63, 132.70, 130.48, 129.63, 129.04, 128.52, 127.44, 126.91, 126.18, 120.63, 116.40, 113.56, 113.52, 111.29, 66.97, 55.82, 55.12, 51.23, 42.74, 28.33. HRMS (ESI⁺) *m/z* [M+H⁺] calcd for C₃₃H₃₅N₂O₄ 523.2597, found 523.2602.



2'-Methoxy-5'-((4'-((1-methylpiperidin-4-yl)oxy)-[1,1'-biphenyl]-4-yl)carbamoyl)-[1,1'-biphenyl]-4-yl acetate (20m) Compound **20m** was prepared from **19k** using general procedure C and acid chloride **7** to afford a white amorphous solid (55 mg, 66%). ¹H NMR (500 MHz, Chloroform-*d*) δ 7.98 (s, 1H), 7.86 (dd, *J* = 8.6, 2.4 Hz, 1H), 7.74 (d, *J* = 2.4 Hz, 1H), 7.65 (d, *J* = 8.6 Hz, 1H), 7.46 (m, 5H), 7.06 (d, *J* = 8.6 Hz, 1H), 6.98 (d,

$J = 8.6$ Hz, 1H), 6.89 (d, $J = 8.7$ Hz, 2H), 4.43 (m, 1H), 3.81 (s, 3H), 2.93 – 2.78 (m, 2H), 2.66 (s, 2H), 2.45 (s, 3H), 2.26 (s, 3H), 2.26 – 2.10 (m, 2H), 1.95 (m, 2H). ^{13}C NMR (126 MHz, CDCl_3) δ 169.68, 165.08, 159.28, 156.27, 149.97, 137.10, 136.56, 135.14, 133.71, 130.58, 129.83, 129.63, 128.59, 128.04, 127.18, 127.15, 121.29, 120.51, 116.27, 111.06, 69.72, 55.81, 51.41, 45.17, 29.16, 21.21. HRMS (ESI^+) m/z $[\text{M}+\text{H}^+]$ calcd for $\text{C}_{34}\text{H}_{35}\text{N}_2\text{O}_5$ 551.2546, found 551.2545.



4'-Hydroxy-6-methoxy-N-(4'-((1-methylpiperidin-4-yl)oxy)-[1,1'-biphenyl]-4-yl)-

[1,1'-biphenyl]-3-carboxamide (20n) Compound **20n** was prepared from **19m** using general procedure F to afford a white amorphous solid (30 mg, 72%). ^1H NMR (500 MHz, Methanol- d_4) δ 7.90 (dd, $J = 8.5, 2.4$ Hz, 1H), 7.87 (d, $J = 2.4$ Hz, 1H), 7.73 (d, $J = 8.6$ Hz, 2H), 7.56 – 7.50 (m, 4H), 7.43 (d, $J = 8.6$ Hz, 1H), 7.06 (d, $J = 8.6$ Hz, 1H), 6.98 (d, $J = 8.7$ Hz, 2H), 6.90 (d, $J = 8.6$ Hz, 1H), 4.55 (m, 1H), 3.89 (s, 3H), 3.00 (m, 2H), 2.84 (m, 2H), 2.57 (s, 3H), 2.20 (m, 2H), 2.06 (m, 2H). ^{13}C NMR (126 MHz, $\text{CDCl}_3+\text{CH}_3\text{OH}$) δ 166.53, 159.30, 156.25, 156.03, 137.23, 136.47, 133.88, 130.59, 130.56, 129.76, 128.81, 127.96, 127.80, 126.93, 126.91, 121.00, 116.26, 114.96, 110.79, 68.82, 55.63, 51.12, 44.67, 28.69. HRMS (ESI^+) m/z $[\text{M}+\text{H}^+]$ calcd for $\text{C}_{32}\text{H}_{33}\text{N}_2\text{O}_4$ 509.2440, found 509.2441.

5. Reference

1. Taipale, M.; Jarosz, D. F.; Lindquist, S., HSP90 at the hub of protein homeostasis: emerging mechanistic insights. *Nat. Rev. Mol. Cell Biol.* **2010**, *11*, 515-528.
2. Whitesell, L.; Lindquist, S. L., HSP90 and the chaperoning of cancer. *Nat. Rev. Cancer* **2005**, *5*, 761-772.
3. Pearl, L. H.; Prodromou, C.; Workman, P., The Hsp90 molecular chaperone: an open and shut case for treatment. *Biochem. J.* **2008**, *410*, 439-453.
4. Neckers, L.; Workman, P., Hsp90 Molecular Chaperone Inhibitors: Are We There Yet? *Clin. Cancer Res.* **2012**, *18*, 64-76.
5. Xu, W.; Neckers, L., Targeting the Molecular Chaperone Heat Shock Protein 90 Provides a Multifaceted Effect on Diverse Cell Signaling Pathways of Cancer Cells. *Clin. Cancer Res.* **2007**, *13*, 1625-1629.
6. Isaacs, J. S.; Xu, W.; Neckers, L., Heat shock protein 90 as a molecular target for cancer therapeutics. *Cancer cell* **2003**, *3*, 213-217.
7. Hanahan, D.; Weinberg, R. A., The Hallmarks of Cancer. *Cell* **2000**, *100*, 57-70.
8. Marcu, M. G.; Schulte, T. W.; Neckers, L., Novobiocin and Related Coumarins and Depletion of Heat Shock Protein 90-Dependent Signaling Proteins. *J. Natl. Cancer Inst.* **2000**, *92*, 242-248.
9. Burlison, J. A.; Neckers, L.; Smith, A. B.; Maxwell, A.; Blagg, B. S. J., Novobiocin: Redesigning a DNA Gyrase Inhibitor for Selective Inhibition of Hsp90. *J. Am. Chem. Soc.* **2006**, *128*, 15529-15536.
10. Zhao, H.; Donnelly, A. C.; Kusuma, B. R.; Brandt, G. E. L.; Brown, D.; Rajewski, R. A.; Vielhauer, G.; Holzbeierlein, J.; Cohen, M. S.; Blagg, B. S. J., Engineering an Antibiotic to Fight Cancer: Optimization of the Novobiocin Scaffold to Produce Anti-proliferative Agents. *J. Med. Chem.* **2011**, *54*, 3839-3853.
11. Yu, X. M.; Shen, G.; Neckers, L.; Blake, H.; Holzbeierlein, J.; Cronk, B.; Blagg, B. S. J., Hsp90 Inhibitors Identified from a Library of Novobiocin Analogues. *J. Am. Chem. Soc.* **2005**, *127*, 12778-12779.
12. Ansar, S.; Burlison, J. A.; Hadden, M. K.; Yu, X. M.; Desino, K. E.; Bean, J.; Neckers, L.; Audus, K. L.; Michaelis, M. L.; Blagg, B. S. J., A non-toxic Hsp90 inhibitor protects neurons from A β -induced toxicity. *Bioorg. Med. Chem. Lett.* **2007**, *17*, 1984-1990.
13. Donnelly, A. C.; Mays, J. R.; Burlison, J. A.; Nelson, J. T.; Vielhauer, G.; Holzbeierlein, J.; Blagg, B. S. J., The Design, Synthesis, and Evaluation of Coumarin Ring Derivatives of the Novobiocin Scaffold that Exhibit Antiproliferative Activity. *J. Org. Chem.* **2008**, *73*, 8901-8920.
14. Burlison, J. A.; Avila, C.; Vielhauer, G.; Lubbers, D. J.; Holzbeierlein, J.; Blagg, B. S. J., Development of Novobiocin Analogues That Manifest Anti-proliferative Activity against Several Cancer Cell Lines. *J. Org. Chem.* **2008**, *73*, 2130-2137.
15. Khandelwal, A.; Hall, J. A.; Blagg, B. S. J., Synthesis and Structure–Activity Relationships of EGCG Analogues, a Recently Identified Hsp90 Inhibitor. *J. Org. Chem.* **2013**, *78*, 7859-7884.
16. Zhao, H.; Moroni, E.; Colombo, G.; Blagg, B. S. J., Identification of a New Scaffold for Hsp90 C-Terminal Inhibition. *ACS Med. Chem. Lett.* **2013**, *5*, 84-88.

17. Zhao, H.; Moroni, E.; Yan, B.; Colombo, G.; Blagg, B. S. J., 3D-QSAR-Assisted Design, Synthesis, and Evaluation of Novobiocin Analogues. *ACS Med. Chem. Lett.* **2012**, *4*, 57-62.